Carnegie Mellon University

CARNEGIE INSTITUTE OF TECHNOLOGY

THESIS

SUBMITTED IN PARTIAL FULFILLMENT OF THE REQUIREMENTS

FOR THE DEGREE OF:

Doctor of Philosophy

TITLE: Network Topologies and Transmission Investment Under Electric-Industry Restructuring

PRESENTED BY: Seth Adam Blumsack

ACCEPTED BY THE DEPARTMENT: Engineering and Public Policy

_____ _____

ADVISOR, MAJOR PROFESSOR DATE

_____ _____

DEPARTMENT HEAD DATE

APPROVED BY THE COLLEGE COUNCIL

_____ _____

DEAN DATE

Carnegie Mellon University

Carnegie Institute of Technology

Network Topologies and Transmission Investment Under Electric-Industry Restructuring

A DISSERTATION

SUBMITTED TO THE GRADUATE SCHOOL
IN PARTIAL FULFILLMENT OF THE REQUIREMENTS

for the degree of

DOCTOR OF PHILOSOPHY

in

ENGINEERING AND PUBLIC POLICY

By

Seth Blumsack

Pittsburgh, Pennsylvania

May, 2006

Acknowledgements

Mine is the only name on this thesis, which gives me far more credit than I deserve for seeing the Ph.D. through to its completion. Credit first and foremost should go to my mentor and advisor, Lester Lave, who has truly been the Virgil guiding me through the many levels of graduate school. He has had far more patience with me than I deserve. Marija Ilić also deserves special mention for her good humor and patience in dealing with a rogue economist suddenly stumbling through an engineering education. I would like to thank Jay Apt and Sarosh Talukdar not only for their valuable input and joining my thesis committee on reasonably short notice, but also for their encouragement and precision of thought. I would also like to thank Granger Morgan for making room in EPP for a wayward economist.

The Ph.D. is all about intellectual ideas, but it can go nowhere unless someone pays for it. During my time at CMU, I have been fortunate enough to receive generous support from the Carnegie Mellon Electricity Industry Center, EPRI, the Alfred P. Sloan Foundation, the Green Design Institute, the Tennessee Valley Authority, and Florida Power and Light.

On a personal level, I would not have survived graduate school without a great group of people around me to "share" this intense experience. To Doug King, Marcus Louie, Kyle Meisterling, Rob Behrman, and Sean McCoy, if all the pierogie pizzas (especially during the Part B) and D's hot dogs didn't kill us, then who knows what will. Stacia Thompson, Costa Samaras, Tony Barrett, and Aimee Curtright have been responsible for probably 99% of all the time I spent procrastinating in the office, and they are all the more terrific

for it. Particularly special thanks go to Paul Hines, Sara “Club 12:11” Eggers, Ketra Schmitt, Elisabeth Gilmore, Dalia Patiño-Echeverri, and Dmitri Perekhodtsev for invaluably providing both friendship and intellectual support (and good-natured sparring).

On an even more personal note, a world of thanks and love go out to my parents and my brother, who have supported me no matter what, particularly when I did not deserve it. Sharon Goodman Lasher has secured herself infinite good karma by remaining my friend, even after years of non-stop kvetching. Thanks to Helgi Felixson for introducing me to the joys of long climbs with heinous approaches, big trucks, Depeche Mode, and lutefisk. Adam Speight, Pasha Mourachov, and Irina Shklovski forced me to get over (some of) my academic guilt and get out and have fun. To the girls, through all the barking, chasing bikes, chasing deer, rolling in who-knows-what, eating random things in the house, and crawling on my face at 6:30 every morning, you have made every day better.

To Erin: I have always said that if a relationship can survive graduate school, it can survive anything. Well, you did it. These years of adventures, travels, late nights, offensive Halloween costumes, manatees, scaring away bears, running from sheep, getting lost in the desert, getting lost in the woods, and Allenwood Motels have been the best. May there be many more. I love you.

Abstract

A number of factors, including the U.S. blackout of August, 2003, have convinced even some skeptics that the North American power grid is under increasing stress, and that restructuring has failed to attract sufficient transmission investment in areas controlled by regional transmission organizations (RTOs). The architects of electricity restructuring hoped that the energy markets run by RTOs would encourage a vibrant non-utility transmission segment of the industry. Analyses by Hogan (1992) and Bushnell and Stoft (1996) suggest compensating transmission investors by awarding them financial rights to a portion of the congestion rent along a given network path. An allocation of these financial rights that respects the physical constraints of the network will yield the proper incentives for market-based transmission planning.

This thesis addresses several issues in transmission planning and investment in the restructured electricity industry. In particular, the thesis exploits topological structures common in actual power networks to highlight some problems with market-based transmission planning.

The topological analysis of the power grid focuses on identifying and analyzing Wheatstone structures embedded in larger systems. In other networks (such as water or gas pipes, the internet, and even crowd control), the Wheatstone network is associated with the Braess Paradox, a phenomenon where adding links to a network increases congestion throughout the network. This thesis provides the first quantitative analysis of how the presence of a Wheatstone structure can affect the flow of power through electric

networks, and develops a fast heuristic algorithm to identify embedded Wheatstone structures, which are quite common in real networks.

In power systems that use locational pricing signals to manage congestion and promote investment, the presence of an embedded Wheatstone network drives a wedge between the price signal and the underlying physical state of the grid. Locational prices fail to identify the active system constraint; simply upgrading the transmission line with the highest congestion price fails to relieve physical congestion in the system. The thesis derives conditions under which this phenomenon occurs. One consequence is that even if financial congestion contracts are allocated according to the method suggested by Hogan (1992), investors can still profit from exploiting the Braess Paradox – that is, by constructing transmission lines that cause congestion rather than relieving congestion.

Wheatstone networks can cause congestion, but they may be justified on the grounds that they increase the reliability of the network, helping to reduce the frequency of blackouts. Models of market-based transmission investment labor under the assumption that congestion and reliability are independent attributes in power networks. New transmission links can be justified as providing either a reliability benefit or an economic (congestion-relief) benefit. The cost of investments made for reliability should be socialized, while market incentives will provide for economic investments. This thesis provides the first quantitative assessment of the claim that reliability and congestion are independent. The thesis develops metrics to decompose a line's reliability benefit from its impact on network congestion, and applies these metrics to four embedded

Wheatstone sub-networks in the IEEE 118-bus test system. While it is possible to account separately for a transmission line's effect on system reliability and congestion, the two are almost never independent quantities. Further, the benefit of a particular transmission line to the network varies highly with the level of demand and the topological state of the rest of the system.

From a policy standpoint, the analysis of Wheatstone networks in this thesis suggests that the debate over transmission investment, at least in areas that have undertaken restructuring, has been misguided. The principal problem is not with non-utility transmission, but in the way that RTOs have proposed to compensate non-utility transmission investments. RTOs should stop trying to attract transmission investment by offering financial contracts based on locational spot-market prices. RTOs and their regulators also need to realize that the network benefit of a given transmission project depends critically on identifying the relevant range of demand and the state of the system, both at the time of construction and into the future. Under restructuring, the transmission planning problem has been cast as a problem of encouraging competition under peak demand conditions. It should be re-cast as a problem in risk management. The question of who (utilities, non-utility transmission companies, or RTOs) should bear the responsibility for transmission investment is a matter of who can manage this risk at the lowest cost.

Table of Contents

List of Tables

List of Figures

Notation Used in the Thesis

The following notational definitions will be used consistently throughout the text. Additional notation will be introduced as necessary, but will not be inconsistent with the notation presented here.

NL = Number of lines in the network

NB = Number of buses in the network

S_{ij} = Transmission line connecting buses i and j

B_{ij} = Susceptance of the link connecting buses i and j

Y_{ij} = Complex admittance of the link connecting buses i and j

X_{ij} = Reactance of the link connecting buses i and j

θ_i = Phase angle at the ith bus

P_i = Net real power injection at the ith bus; positive for net generation and negative for net withdrawal

P_{Li} = Real power demand at the ith bus

P_{Gi} = Real power demand at the ith bus

δ_{ij} = Phase angle difference between buses i and j

F_{ij} = Real power flow between buses i and j

π_i = Nodal price at bus i

μ_{ij} = Shadow price of transmission between buses i and j

C_i = Total cost function at the ith bus.

MC_i = Marginal cost function at the ith bus, equal to dC_i/dP_i.

d_i = Number of buses connected to bus i (that is, the degree of bus i).

$\mathbf{B}$ = ($NB \times NB$) system susceptance matrix

$\mathbf{B}^{\mathbf{diag}}$ = ($NL \times NL$) diagonal matrix of line susceptances

$\mathbf{X}$ = ($NB \times NB$) system complex reactance matrix

Y = ($NB \times NB$) system complex admittance matrix

Z = ($NB \times NB$) system complex resistance matrix

$\mathbf{N}$ = ($NB \times NB$) node-node adjacency matrix

$\mathbf{A}$ = ($NB \times NL$) system node-line adjacency matrix

$\mathbf{P}$ = ($NB \times 1$) vector of bus injections

$\mathbf{F}$ = ($NL \times 1$) vector of line flows

$\boldsymbol{\theta}$ = ($NB \times 1$) vector of bus angles

$\boldsymbol{\delta}$ = ($NL \times 1$) vector of bus angle differences

$\mathbf{p}_k$ = ($NB \times 1$) vector of net bus injections by the kth grid participant

$\boldsymbol{\pi}$ = ($NB \times 1$) vector of nodal prices

Chapter 1: Electric-Industry Restructuring and Patterns in Transmission Utilization

On August 14, 2003, a cascading failure in the eastern portion of the North American electric transmission grid blacked out 50 million people in the United States and Canada. Outages occurred in an area stretching from roughly Chicago to New York. The blackout did not consist of a completely covered area, with many systems in between able to island themselves and avoid massive interruptions. A joint investigation of the blackout, undertaken with the cooperation of the U.S. and Canadian governments, placed the economic cost of the blackout at $6 billion (U.S.-Canada Power System Outage Task Force 2004).

The official report issued by the joint U.S.-Canadian task force avoided laying blame for the blackout at the feet of restructuring in the electric power sector. The task force concluded that the blackout resulted from the failure of a specific utility to follow industry reliability guidelines. Maintenance of rights-of-way was not performed properly, causing power lines to sag into tree branches. Control-center operators lacked situational awareness due to computer problems. Even if the control-center computers had been operating properly, the report also noted that the operators themselves lacked sufficient training to deal with emergencies (U.S.-Canada Power System Outage Task Force 2004).

Other observers are convinced that restructuring had at least some role to play in how the August 2003 blackout proceeded. Ilić (2003), Joskow (2003) and Joskow and Tirole (2005b) have been particularly vocal proponents of this view. Joskow and Tirole (2005b) argue that the current market institutions and vertical dis-integration that characterize restructuring in the U.S. do not provide the right incentives for reliability investment such as the construction of beneficial new transmission projects or the maintenance of existing transmission paths. Ilić (2003) argues that restructuring has upset the utility hierarchical control paradigm without a sufficient new operating regime to take its place. Further, the competitive aspect of restructuring has discouraged the sharing of information among control areas who may be potential competitors. While remaining agnostic regarding its cause, Hines, Apt, Liao, and Talukdar (2006) note that the frequency of large blackouts appears to be increasing.

1.1 Electricity Restructuring in the United States[1]

For years, the fundamental building block of the electric power sector was the vertically-integrated utility. Roughly speaking, the electric power supply chain has three links: generation, transmission, and distribution. Generators are electric power stations that produce electricity by various means, including the burning of fossil fuels or waste products, harnessing kinetic energy of water and wind, and nuclear fission. The various generators, which are often located large distances from consumption centers, connect to a high-voltage transmission network. Closer to the point of consumption, the transmission network is connected (through a series of step-down transformers) to a

[1] This section borrows heavily from Blumsack, Apt, and Lave (2005).

lower-voltage distribution network. A second series of transformers connects individual customers to the distribution network.

Most electric utility customers in the United States have never known anything except the vertically-integrated monopoly provider, regulated on a state-by-state basis. Up until restructuring laws took effect in the mid 1990s, the electric utility industry had not seen any radical changes in organization for over eighty years. As a result, the utility business could have been variously described as stable (if you were an investment manager choosing stocks for widows and orphans) or dull (if you were a recent business-school graduate looking for a high-flying career). Things were not always this way. The electric utility industry emerged in the late 1800s, alongside the oil industry. Far from being stable or dull, the early decades of the U.S. electric power industry were marked by intense competition, corruption, and monopolization.

Regulatory reform in the U.S. electricity industry was not primarily aimed at disrupting the existing industrial structure, although it did result in divestitures by many formerly vertically-integrated firms. First and foremost in the minds of policymakers was cost control (de Vries 2004). Figure 1.1 shows the retail price of electricity in the United States for the residential sector (primarily homes and apartment buildings) from the industry's beginnings in the 1800s through 2002. Up until the 1970s, power prices generally fell every year with few exceptions. The trend reversed itself beginning in the early 1970s; power prices in the U.S. have been rising ever since. The cost of electricity

to residential consumers in the United States is now, in real terms, roughly the same as it was in the 1920s.

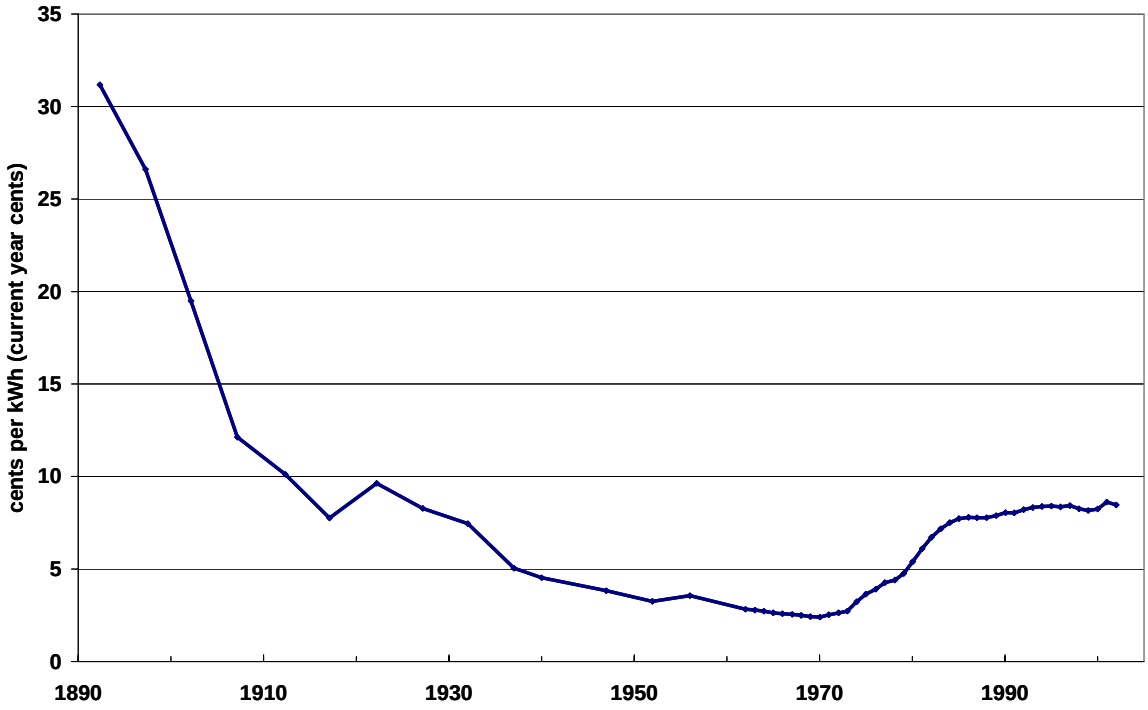

Figure 1.1. Residential Price of Electricity in the United States, in current-year cents per kilowatt-hour. Source: Morgan et. al. 2005.

The initial step in electric industry reform was the Public Utility Regulatory Policies Act (PURPA), passed by the U.S. Congress in 1978. The goals of PURPA were twofold. The first was to reduce the reliance of the electric power industry on crude oil, and the second was to introduce competition. Prior to PURPA, only regulated utilities could own and operate power plants. PURPA paved the way for unregulated independent power producers (IPPs) to begin operating in the United States and forced electric utilities to purchase energy from these IPPs under long-term contracts.

In 1992, Congress expanded the field of eligible players in the electric power industry with the passage of the Energy Policy Act (EPAct).[2] The 1992 EPAct allowed for unregulated IPPs that did not have long-term contracts. These generators would simply be allowed to generate electricity and sell it to traditional utilities at whatever price the market would bear. Hoping to promote risk management and competition in electricity the same way that it had developed in natural gas and crude oil (de Vany and Walls 1993, van Vactor 2004), the 1992 EPAct also allowed for the wholesale trading of electric power as a commodity. Brokers and marketers (who may or may not have owned any physical assets) were now allowed to buy and sell electricity. Bilateral trading for bulk power began in earnest, particularly in the Western U.S. (Lehr and van Vactor 1997).[3]

Although electricity reform in the U.S. happened largely on a state-by-state basis, nearly all restructuring plans have shared a number of common traits. Most electric-sector reforms at the state or regional level have included most, if not all, of the following components:

1. Vertical dis-integration of the generation, transmission, and distribution businesses of regulated utilities. In some places, dis-integration was brought about through explicit divestiture, while in other places a "Chinese Wall" has

[2] So as not to avoid confusion with the more recent Energy Policy Act, passed in 2005, we will refer to the Energy Policy Act of 1992 as the 1992 EPAct.
[3] Bilateral trading had been underway in the West for a number of years prior to EPAct. In 1987, the Federal Energy Regulatory Commission (FERC) approved the Western Systems Power Pool (WSPP), which allowed utilities in the Western Interconnect to trade surplus electric power at market-based rates. Its success paved the way for the EPAct (van Vactor 2004).

been erected, limiting flows of information between different parts of the business.

2. The creation of centralized hourly and day-ahead spot markets for wholesale electricity, ancillary services, and capacity.

3. The designation of a single entity to manage regional transmission grids and (often times) to operate the hourly spot market. These entities are known as Independent System Operators (ISO) or Regional Transmission Organizations (RTO).

4. Introduction of retail competition, where individual consumers are able to choose between the utility and a third-party supplier for their electric generation needs. Although the purchase of generation is open to competition, distribution (delivery to ultimate consumers) has typically remained regulated. In some states, retail competition has been limited to large industrial customers.

5. Utilities have been given some provision to recover "stranded costs" – debts incurred during the regulated era that would leave the utility unable to compete in the deregulated era. Debts remaining from investments in nuclear power plants and PURPA contracts are often included in a utility's stranded costs.

Individual states have not been entirely free to design their own reform programs. Order 888, passed by the Federal Energy Regulatory Commission (FERC) in 1996, required that all transmission owners provide non-discriminatory access to their transmission lines. FERC Order 2000, passed in 2000, required all transmission owners to form or join an RTO. While most areas appear to be compliant with the open-access directive under Order 888, the formation of RTOs has been somewhat slower. At this point, the entire northeastern U.S. and much of the Midwest have RTOs approved by the FERC.[4] These FERC-approved RTOs represent less than half of the geographic area of the United States (excluding Alaska and Hawaii), and approximately two-thirds of U.S. demand (Morgan et. al. 2005, Krellenstein 2004).

The primary effect of industry restructuring on the transmission grid has been to change the level of, and protocols regarding, access to the network. Prior to Order 888, bilateral transactions traversing a number of different control areas (known as "wheeling" contracts) required the purchase of some form of transmission service from each control area being traversed. At the most general level, transmission service was available in two varieties. Non-firm service was cheaper, but was the first to be revoked during contingencies (see the discussion of transmission loading relief events in Section 1.2). Firm service was more expensive and accordingly less risky.

Under restructuring, congestion in the grid has largely been managed using price signals rather than command-and-control procedures. Many centralized markets in restructured

[4] Texas and California have functioning institutions nearly identical to RTOs. Since the Texas electric grid does not cross any state lines, FERC has no jurisdiction over Texas. At the time of this writing, California was in the process of seeking FERC approval of its RTO.

areas generate a set of nodal prices through the operation of the spot energy auction. Differences in nodal prices indicate congestion on the network (Bohn, Caramanis, and Schweppe 1984, Hogan 1992), and the market operator collects these congestion payments from market participants in the network.

Electricity markets established by the major restructuring initiatives in the U.S. have largely been focused on the spot market, which includes contracts traded one day prior to delivery and sooner. This stands in contrast to many other commodity markets, such as crude oil, in which "spot" markets comprise contracts for delivery days to years ahead of time (van Vactor 2004). Many centralized RTO electricity markets have established longer-term markets for financial transmission rights (FTR), which essentially are swaps contracts defined over differences in nodal prices. But no RTO has established a long-term centralized spot market for electric energy. At the onset of electric restructuring, the New York Mercantile Exchange, the Chicago Board of Trade, and the Minnesota Grain Exchange all sought to capitalize on the industry enthusiasm for bulk power trading by offering electricity futures contracts; all have been dismal failures, achieving nowhere near the trading volumes seen in benchmark energy futures such as crude oil and natural gas.

1.2 Trends in Transmission Investment and Utilization

Prior to industry restructuring, transmission planning was largely performed at the level of the individual utility (Hirst and Kirby 2001). In the electric utility system, the transmission network fills two roles. First, it acts as a vehicle for delivering power from

the utility's generators to its distribution network (and on to individual end users). Second, it acts as a physical hedge against the possibility of outages at generating stations.

Thus, system reliability has been the main driver of traditional utility transmission plans. Reliability itself has always been somewhat poorly defined, but reflects the goal that the system should be redundant enough to avoid service interruptions even in the face of contingencies. Examples of some common reliability metrics are:

1. The $N - k$ criterion; whether the system can continue to provide uninterrupted service to customers in the face of a contingency in which k out of N pieces of equipment are lost, damaged, or otherwise disconnected from the network;
2. the Loss of Load Probability (LOLP), defined as the probability over some period of time that the network will fail to provide uninterrupted service to customers;
3. the Loss of Energy Expectation (LOEE) and Loss of Energy Probability (LOEP), defined as the expected amount and proportion of customer demand not served over some time frame.

For very large N, which can easily grow into the tens and hundreds of thousands in actual power systems, once k grows larger one, verifying that the network satisfies the $N - k$ criterion becomes computationally burdensome. While the optimal transmission planning problem may be easy to write down (see Section 1.3 for a mathematical formulation), it is very difficult to solve. Actual transmission planning studies consider

multiple scenarios involving peak demand, new investments, and contingencies. Thus, the correct characterization of the transmission planning process is a heuristic or (at best) local optimization problem rather than a global optimization problem.

The magnitude of the August 2003 blackout led Bill Richardson, former U.S. Secretary of Energy, to declare that the North American transmission infrastructure was more comparable to that of a poor, developing nation than a rich, industrialized nation. Although the comparison was made to drive home the point that more of society's time and wealth ought to be directed towards preventing large-scale electricity interruptions, the phrasing does question the adequacy of the North American transmission grid, and even "adequate" should be defined.

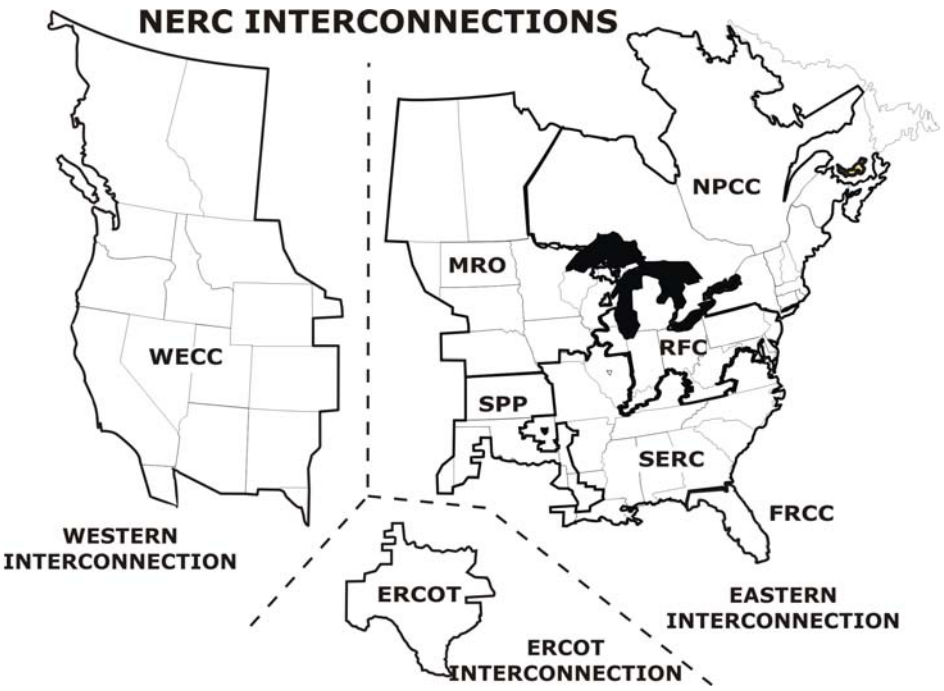

Figure 1.2. The North American transmission grid is divided into three separate pieces and multiple coordinating regions. Source: North American Electric Reliability Council (NERC).

According to the U.S. Energy Information Administration (EIA), the United States has 160,000 miles of high-voltage transmission infrastructure, apportioned among three reasonably independent regional networks.[5] These networks are shown in Figure 1.2. The Rocky Mountains divide the North American grid into its two major Western and Eastern components. Much of Texas is on its own system as well. Back-to-back DC Interconnections link the three independent grids, but power transfer between them is minimal, and it is reasonable to think of the systems as being completely separated.

Total transmission capacity on the grid amounts to approximately 140,000 gigawatt-miles (Hirst 2004), compared to a total peak generating capacity of 1,000 gigawatts. Thus, in the aggregate, enough transmission exists to transport many times more electric power than is currently produced. Resistive losses limit the amount of energy that can be transmitted over very long distances, but transmission capacity is generally not a scarce resource.

Problems in the transmission grid are not related to the amount of capacity, but rather the configuration of existing capacity, as shown in Figure 1.3. The original purpose of the transmission grid, as built and operated by vertically-integrated and regulated utilities, was to transport large volumes of power from central-station generation owned by the utility to the distribution network owned by the utility, for sale to the utility's ultimate consumers. With the advent of industry restructuring and the creation of centralized regional spot markets, owners of inexpensive generation have found new profit opportunities selling into new high-priced markets.

[5] EIA web site, http://www.eia.doe.gov/fuelelectric.html.

Figure 1.4 shows an order-of-magnitude summary of these profit opportunities (without transmission costs) for a utility in the Southeast looking to sell into the Pennsylvania-New Jersey-Maryland (PJM) spot market. In effect, the contract path for these transactions may cross multiple utility control areas; the real effect is to alter the inter-regional dispatch of power plants. The end result is to increase the amount of power that is "wheeled" between control areas, as shown in the right-hand panel of Figure 1.3.

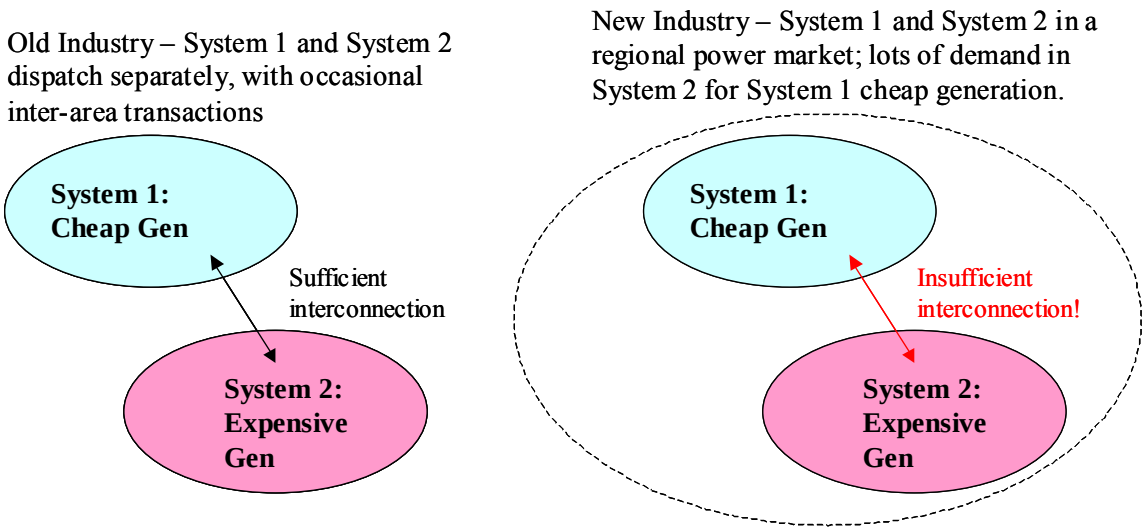

Figure 1.3. Electric-industry restructuring has increased the demand for long-distance transactions crossing multiple control-area boundaries.

The increase in demand for the transmission system to support such "economic" transactions can be measured in two different ways. In restructured areas, the increase in demand should be reflected in higher congestion revenues collected by the market operators. Table 1.1 shows the total and average congestion payment for the PJM system. Using the average congestion payment as a metric allows comparison across years for PJM, whose territory has been expanding. Congestion payments in PJM have

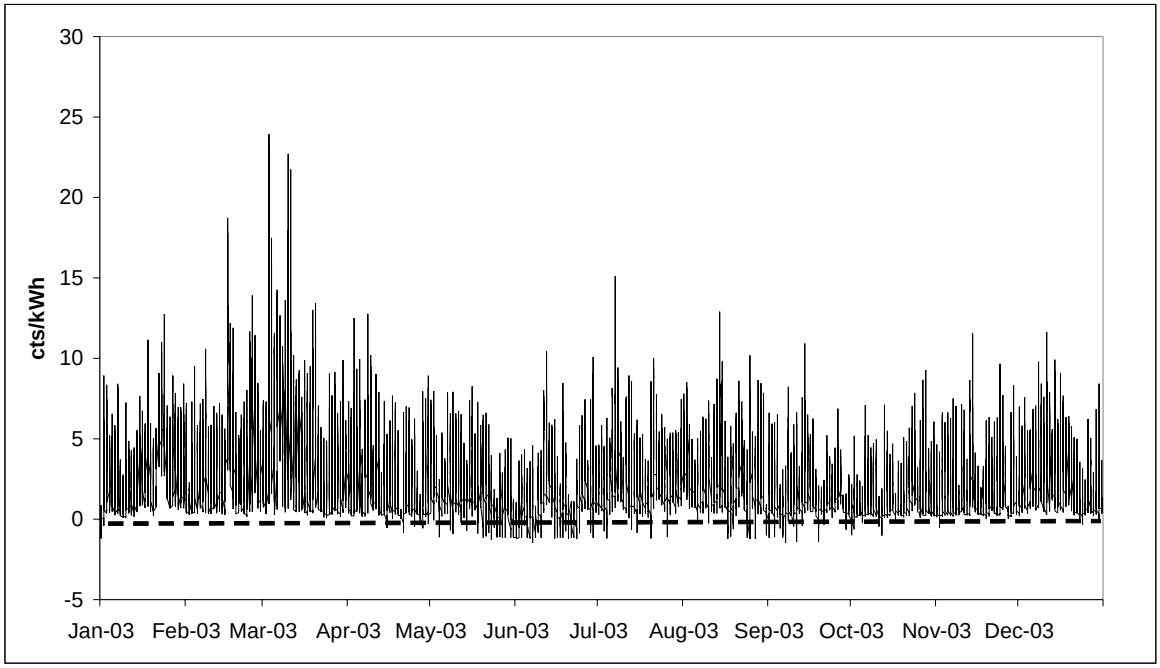

Figure 1.4. Generators in the Southeast could often make money selling into the PJM market. The figure plots the difference between the hourly market price in PJM and the marginal cost of generation in SERC (at the level of hourly demand in PJM). Marginal costs are calculated using average heat rates from the Environmental Protection Agency E-GRID database, and PJM load and market price data. The calculations assume a coal price of $25/ton, oil at $55/bbl, and natural gas at $5/mmbtu. The marginal costs of nuclear, hydro, and wood/waste facilities are assumed to be 3.5cts/kWh, 1.5cts/kWh, and 4cts/kWh.

	PJM Congestion Costs	
Year	Total ($M)	Average ($/MWh)
1999	53	0.20
2000	132	0.50
2001	271	1.02
2002	430	1.37
2003	499	1.52
2004	750	1.71
2005	2,090	3.05

Table 1.1. Congestion costs in PJM, 1999 – 2005. Source: PJM State of the Market Reports, available at http://www.pjm.com.

grown by a factor of nearly ten, increasing from $0.3 per MWh in 1999 to over $3 per MWh in 2005.[6]

TLR Level	System Operator Action
1	Inform neighboring system operators of possible operating limit violations.
2	Freeze interchange amounts; no new transmission service granted.
3	Curtailment of non-firm transmission customers, first on a pro rata basis and then on a priority basis.
4	Firm transmission allowed up to contingency operating limits.
5a	Pro rata curtailment of firm transmission service.
5b	Curtailment of firm transmission service on a priority basis.
6	Emergency measures, including load shedding.
0	End of TLR Event.

Table 1.2. TLR levels and procedures. Source: NERC.

Some areas of the U.S., particularly in the Southeast, have chosen not to go forward with restructuring as in the Northeast. These areas do not manage congestion using price signals, and so there is no publicly-available congestion cost for these areas. Traditional utilities use a command-and-control procedure known as transmission loading relief (TLR) to manage congestion.[7] TLR relieves congestion in a hierarchical fashion. If a

[6] The congestion payment only includes congestion revenue collected by the grid operator. It does not reflect the social cost associated with having to dispatch generation out of merit order due to congestion in the transmission network. This issue will be discussed further in Chapter 2.

[7] TLRs are still used to some degree in restructured areas. It is interesting to note that for the period between 2000 and 2005, no TLRs were issued in the Western Interconnect. See ftp://www.nerc.com/pub/sys/all_updl/oc/scs/logs/trends.htm.

transmission-owning utility is forced to call a TLR event, the holders of non-firm transmission service rights are told first that their access to the transmission system will be restricted or eliminated for the duration of the event, followed by holders of firm transmission service. Thus, a utility calling a TLR event essentially voids the purchase/sale contract held by the generator or load involved in the wheeling transaction. The TLR procedure is summarized in Table 1.2.

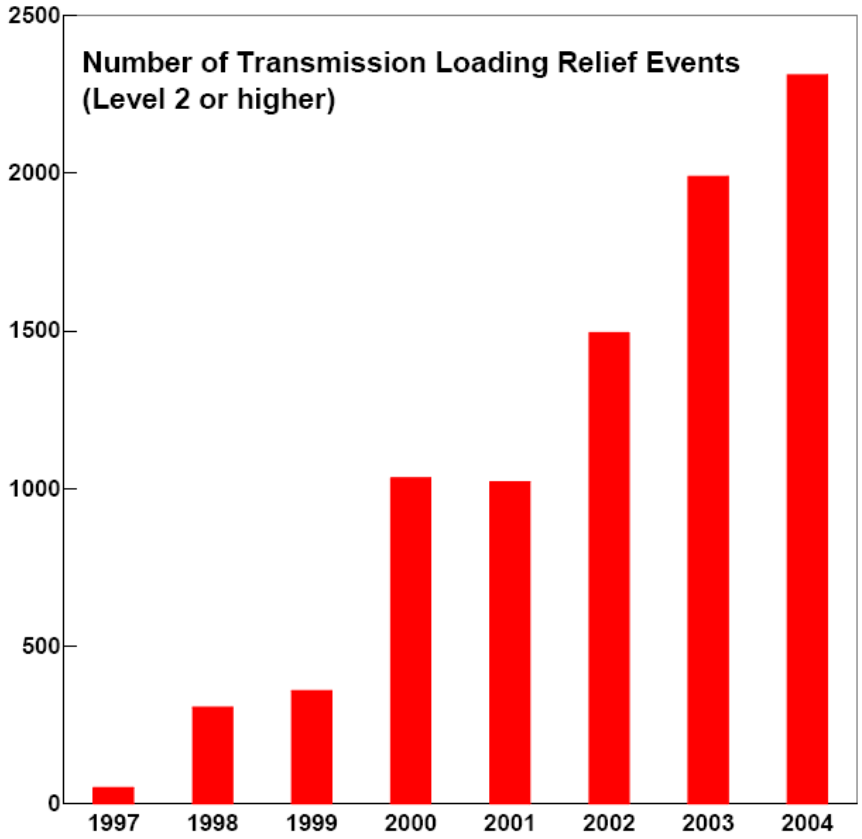

Figure 1.5. Transmission Loading Relief Events, 1997 – 2004. Source: NERC.

The number of annual TLR events called (of at least Level 2, when no incremental requests for transmission service can be honored) is shown in Figure 1.5. The frequency of TLR events has increased by several orders of magnitude since NERC records began

in 1997. Not reflected in Figure 1.5 is the geographic or magnitude distribution of TLR events over time. Aggregate data collected by NERC indicate that most TLR events are called in the Midwestern and Mid-Atlantic portions of the Eastern Interconnect, indicating that transmission bottlenecks tend to occur at the upstream end of a given transaction, rather than in intermediate control areas or areas closer to generators.

Whether TLRs or congestion payments are the metric of choice, the data indicate that certain portions of the transmission system are in very high demand. Economists usually expect that high prices encourage entry and new sources of supply, but this has largely not happened in the North American transmission grid. Hirst (2004) discusses the decline in transmission investment since the mid-1970s. On average, transmission investment has fallen by $50 million per year during this period. However, transmission investment has actually risen since 2000; Hirst (2004) does not discuss any possible reason. Joskow (2005a) claims that this investment largely represents incremental upgrades to low-voltage lines and should not be seen as representative of investment in the transmission grid as a whole.

The U.S. experience has shown that in the restructured electricity environment, investments in needed transmission will only occur with the aid of political will. Transmission projects with clear social benefits have taken years to complete or gain approval, if they have gotten approval at all. Success stories include the Path 15 expansion linking Northern and Southern California (Awad et. al. 2004) or the Cross-Sound transmission line linking Southeastern Connecticut with Long Island

(Krellenstein 2004). Notable failures include a proposed line linking New York City with generators in upstate New York. Krellenstein (2004) reports that although the project was demonstrably beneficial, already had rights-of-way, and faced little opposition, it did not go forth due to lack of funding. Perhaps learning from the experience of New York, the governors of four Western states have recently put their political muscle behind the Pioneer Line linking coal-fired generation in Montana and Wyoming with demand centers in California.

1.3 The Transmission Planning Problem

In the regulated electric utility industry, the primary function of transmission planning is to identify the least-cost set of investments necessary to support a defined level of system reliability. Models of transmission planning can be static, in which the problem is formulated for a single state of the electric network, or dynamic, in which certain state variables (particularly demand) are allowed to vary over time. Either way, the key feature of these models is that they link the investment problem with the operations problem.

This coupling is particularly simple for the static transmission-planning problem since the investments only need to support one operations scenario. One possible formulation of the static problem using the lossless DC power flow equations is (Garver 1970, Seifu, Salon, and List 1989, Romero and Monticelli 1994):

$$(1.1) \qquad \min \sum_{\{i,j\}\in\Omega} C_{ij}(B_{ij}, F_{ij}^{\max}) + \sum_{i} C_i(P_{Gi})$$

such that:

$$
\begin{aligned}
& F_{ij} = B_{ij}\delta_{ij} \qquad \forall i, j \\
& P_{Gi} - P_{Li} = \sum_{j} F_{ij} \qquad \forall i \\
& \sum_{i} P_{Gi} = \sum_{i} P_{Li} \qquad \forall i \\
& \sum_{\{i,j\}\in(\Omega\cup S\cup P_G)_{-1}} F_{ij} = \sum_{\{i,j\}\in\Omega\cup S\cup P_G} F_{ij} \qquad \forall i, j \\
& \left|F_{ij}^{\max}\right| \geq \left|F_{ij}\right| \qquad \forall i, j \\
& \left|\delta_{ij}^{\max}\right| \geq \left|\delta_{ij}\right| \qquad \forall i, j \\
& P_{Gi}^{\max} \geq P_{Gi} \qquad \forall i .
\end{aligned}
$$

$C_{ij}(B_{ij}, F_{ij}^{\max})$ in equation (1.1) represents the cost of transmission additions between nodes *i* and *j* (whether those additions amount to upgrades of existing paths or the connection of two nodes that were previously unconnected), *S* is the set of existing links in the transmission network, P_G is the set of generators in the network, and Ω is the set of possible additions to the transmission grid. Thus, the set $(S \cup \Omega \cup P_G)$ represents all of the generation and transmission equipment in the upgraded network. The problem formulation in equation (1.1) only considers additions to the transmission infrastructure, and not the generation infrastructure. The notation $(S \cup \Omega \cup P_G)_{-1}$ indicates the set of network equipment (generators and transmission lines) with one piece of equipment removed. Thus, the constraint $\sum_{\{i,j\}\in(\Omega\cup S\cup P_G)_{-1}} F_{ij} = \sum_{\{i,j\}\in\Omega\cup S\cup P_G} F_{ij}$ represents the *N – 1* reliability criterion. Coxe and Ilić (1998) provide a mathematical formulation of other reliability criteria, such as the loss of load probability.

The dynamic transmission-planning problem considers the evolution of transmission investments over time as the network changes in various ways. Focusing on changes in customer demands throughout the network, the expected-cost minimizing dynamic transmission investment problem can be written as (Yu, Leotard and Ilić):

$$\text{(1.2)} \qquad \min E\left(\sum_{\{i,j\}\in\Omega_T} \int_0^T C_{ij}(t, B_{ij}(t), F_{ij}^{\max}(t)) e^{-rt} dt + \sum_i \int_0^T C_i(t, P_{Gi}(t)) e^{-rt} dt \right)$$

such that:

$$F_{ij}(t) = B_{ij}(t)\delta_{ij}(t) \qquad \forall i, j, t$$

$$P_{Gi}(t) - P_{Li}(t) = \sum_j F_{ij}(t) \qquad \forall i, t$$

$$\sum_i P_{Gi}(t) = \sum_i P_{Li}(t) \qquad \forall i, t$$

$$\sum_{\{i,j\}\in(\Omega(t)\cup S(t)\cup P_G(t))_{-1}} F_{ij}(t) = \sum_{\{i,j\}\in\Omega(t)\cup S(t)\cup P_G(t)} F_{ij}(t) \qquad \forall i, j, t$$

$$\left|F_{ij}^{\max}(t)\right| \geq \left|F_{ij}(t)\right| \qquad \forall i, j, t$$

$$\left|\delta_{ij}^{\max}(t)\right| \geq \left|\delta_{ij}(t)\right| \qquad \forall i, j, t$$

$$P_{Gi}^{\max}(t) \geq P_{Gi}(t) \qquad \forall i, t$$

$$\frac{dP_{Li}(t)}{dt} = g(t, P_{Li}(t)) \qquad \forall i, t.$$

In equation (2.2), Ω_T represents the set of possible investments over a *T*-period time horizon (which may differ from the set of possible investments for the static problem), *r* is the discount rate, and $g(t, P_{Li}(t))$ represents the law of motion for electricity demand at the *i*th bus. The remainder of the notation is identical to the static problem, but with the time dependency formulated explicitly.

The formulation in equation (1.2) incorporates uncertainty in demand, but does not fully incorporate uncertainty in the network topology (beyond the $N-1$ constraint), nor does it capture generator reliability criteria such as the reserve margin. Yu, Leotard, and Ilić provide a formulation in which the matrix of network distribution factors is uncertain along with the level of demand at each bus. The use of expected values to capture uncertainty in equation (1.2) assumes that the utility planner is a risk-neutral decision-maker essentially solving a rational expectations problem. In the real world, planners often consider the value-at-risk (variance) in addition to the expected values of uncertain system variables.

A number of numerical methods exist for solving either the static problem (1.1) or the dynamic problem (1.2) to produce a static or dynamic optimal transmission investment plan; Latorre et. al. (2003) provide a review and extensive list of references. The literature on optimal transmission planning has generally divided the universe of solution methods into optimization routines which seek explicit solutions to problem (1.1) or (1.2), and heuristic or scenario-based methods. Since scenario-based modeling involves choosing a number of different (usually peak) demand profiles and finding the corresponding optimal transmission plan, this method can be viewed as a hybrid of the static and dynamic approach.

Optimization models for transmission planning in the literature tend to use small test systems as examples. Real systems have tens of thousands of pieces of equipment. Thus, finding the optimal transmission plan is a computationally intensive problem. In practice,

transmission planners have favored scenario-based methods for deciding among competing investments. As Hirst (2001) points out, the scenarios run by utility transmission planners generally do not themselves suggest the best set of transmission investments. Instead, the scenarios are used to determine which investments improve system reliability (subject to performance constraints) and which do not. The planner, not the model, chooses the transmission investment plan according to implicit or explicit criteria (also chosen by the planner, and not the model).

A notable feature missing from the transmission-planning problem, as formulated in equations (1.1) and (1.2), is an explicit cost-benefit test for individual plans or investments. Historically, utility system planning has been done with reliability in mind, not cost or economics (Coxe and Ilić 1998, Joskow 2005b). Reliability constraints drove the need for upgrades or new hardware. Since prices and profits were set by regulators, the effect of particular investment plans on electricity rates was a by-product of the planning exercise and not an input to the planning problem.

1.4 Integrated Resource Planning and System Planning Under Competition

In practice, monopoly utility transmission planning has historically been one part of an integrated resource planning process (IRP), which seeks to find the lowest-cost set of resources that satisfy a given set of generator and transmission reliability criteria. Conceptually, the IRP sounds very similar to the planning problem formulated in equations (1.1) and (1.2). However, as Coxe and Ilić (1998) note, utilities often broke up the single IRP problem into sequential sub-problems. Given some expectation for load

growth in the system, the first stage of the IRP would involve generator reliability and contingency planning. The utility would plan to have a sufficiently large reserve margin to meet expected peak load, and would also choose the appropriate fuel mix to reduce dependency on any one technology. Once the generation-planning stage of IRP was complete, the utility would run a series of power flow studies to examine the effects of particular transmission enhancements to support the generation investments. Thus, utility transmission planning is inherently suboptimal in the sense that IRP does not solve the transmission-planning problem formulated in Section 1.3. Instead, it solves a sequence of problems and there is no guarantee that the solution to the sequence of problems is identical to the solution of the problem which jointly optimizes generation and transmission.[8]

With respect to the system planning process, the most important feature of introducing competition and markets into the electric power industry is that (at least to some degree) the responsibility for generation and transmission reliability falls on decentralized decision-makers rather than a single centralized utility. In the restructured industry, the transmission planning process must also accommodate the market for electric energy along with investment and operations decisions. Decentralized decision-makers in the restructured energy market take prices as an input to the planning and investment problem. This is in contrast to the utility planning problem, which is primarily concerned with reliability and does not consider any possible tradeoffs between prices and reliability.

[8] Systems dominated by hydroelectric capacity (such as Brazil) represent a possible exception, since the marginal cost of generation is very low in these systems.

Under industry restructuring, the investment problem is turned on its head. Decentralized players in the electricity market make investment decisions based on market prices (and expectations of future market prices. Thus, the planning and operations problems become decoupled in the restructured power industry. If operations decisions are left entirely to the energy market, then the operations problem becomes the market-maker's problem (or a decentralized decision problem, if there is no explicit market-maker). A major policy question and subject of this thesis is the degree to which the market can solve not only the short-term operations problem, but also the longer-term transmission-planning problem.

1.4 Outline and Contributions of the Thesis

This thesis addresses some technical and policy issues related to competition and planning in the transmission network, with special attention to the restructured environment. The prospect for non-utility or "merchant" transmission investment will be of particular interest, especially given the decline in utility transmission investment amid changes in the regulatory structure of the industry. The goal of this thesis is to provide some quantitative analysis aimed at redefining the transmission investment problem in the restructured electric power industry. The architects of restructuring originally hoped to define the transmission infrastructure as an input to competition, much like power generation infrastructure. While it is true that transmission is necessary to facilitate competition among generators, this is not the defining element of the transmission

system. This thesis offers the following four policy lessons for transmission management and investment:

1. *A market-based solution to the transmission problem is neither workable nor economically efficient.* At best, compensating new transmission with contracts based on nodal prices will not encourage investors to relieve congestion fully. At worst, it may encourage investors to build lines that further congest the network.
2. *Eliminating congestion is a more complex problem than simply upgrading the most congested line*. The thesis discusses a network topology, common in actual networks, known as the Wheatstone system. In this system, congestion can only be relieved by upgrading multiple lines, or by removing certain other lines. Neither remediation option is suggested by looking at nodal prices or the shadow prices of transmission. An enlightened knowledge of the topological properties of the network is required to efficiently identify and deal with these constraints.
3. *Reliability and congestion are not independent.* Underlying the premise for non-utility transmission is the notion that transmission investments can be cleanly divided into those that enhance reliability and those that relieve (or create) congestion. In meshed networks, this is simply not the case. Over certain ranges of demand, reliability and congestion reflect tradeoffs faced by network designers.
4. *The transmission problem is a systems problem, not a competition problem*. Transmission must facilitate competition among generators, but attempts to frame transmission investment as a competitive problem will not get beneficial lines built. The correct way to define the transmission problem is as a risk-

management problem. The most efficient institution for transmission investment is thus the one that can bear the risks at the lowest cost.

The quantitative analysis behind these five policy lessons is developed in Chapters 2 through 6.

Chapter 2 provides a brief outline of proposed mechanisms to encourage and compensate transmission investment using market-based signals. The two competing models are the point-to-point financial transmission rights formulation of Hogan (1992) and the path-based flowgate formulation of Chao and Peck (1996). Bushnell and Stoft (1996, 1997) have shown that, given a certain set of economic assumptions, the FTR formulation allows market participants to hedge locational price risk in the energy market and gives investors efficient signals for the construction of new transmission infrastructure.

Chapter 3 provides a steady-state analysis of the Wheatstone network structure. Using the method of Ejebe and Wollenberg (1979), we are able to derive an explicit expression describing how flows in the network change once the Wheatstone bridge is added. Thus we can explicitly calculate the conditions necessary for the bridge to cause congestion in the network.

In Chapter 4, the Wheatstone network is presented as a counterexample to the FTR investment efficiency theorems of Bushnell and Stoft (1996, 1997). Even if all of the restrictive economic assumptions required for the FTR theorems to hold were

realistic, investors can still profit from congesting the network by building Wheatstone bridges.

The properties of the Wheatstone network, and its implications for operations and planning, are easy to decipher in a standalone test network. Real networks are more complicated and interconnected. Thus, there is some value to being able to detect Wheatstone sub-networks within larger systems. Chapter 5 discusses a graph-theoretic method to find embedded Wheatstones and demonstrates the method on a modified version of the IEEE fourteen-bus test case.

Chapter 6 applies the search algorithm developed in Chapter 5 to the IEEE 118-bus test system, and tackles the question of whether congestion and reliability are really independent system attributes. The Wheatstone test network is interesting because while the bridge causes congestion in the network, it may also provide a reliability benefit in the case of a line outage. Chapter 6 analyzes four Wheatstone sub-networks within the IEEE 118-bus network, and finds that the congestion-reliability tradeoff holds for embedded Wheatstones just as it does for standalone Wheatstones.

Chapter 7 concludes by attempting to reformulate the transmission investment problem for the restructured electric power industry. Based on the problems with the merchant model, Chapter 7 suggests several alternative structures. The proposals range from redefining the compensation mechanism for non-utility transmission to

eliminating the merchant transmission sector entirely and having the utility or RTO build transmission infrastructure on a regulated basis. Ultimately, the most efficient institutional structure depends on who can use the transmission network to manage risk at the lowest cost.

Chapter 2: The Economics of Transmission Congestion and Market-Based Transmission Planning

Investment in the North American transmission grid has been declining for decades (Hirst 2004), while demand for the grid as a transportation network to serve long-distance wholesale bulk power contracts is rising. The increase in demand for transmission service is reflected in rising RTO congestion costs and larger numbers of TLR events (Joskow 2005b, Blumsack, Apt, and Lave 2006). Prior to industry restructuring, investment in beneficial transmission projects was a matter of securing rights-of-way and persuading regulators to allow costs to be passed through to consumers. The regulatory process had high costs and served to inefficiently delay beneficial investments (Martzoukos and Teplitz-Sembitzky 1992, Saphores et. al. 2004), but at least the institutional framework was well-defined.

Electricity restructuring sought to interrupt this institutional framework by separating the businesses of formerly integrated utilities, but without sufficient thought given to a replacement framework. FERC assigned responsibility for regional transmission planning to the RTO, but left unclear which entity was supposed to implement the RTO transmission plans and how investors would be compensated.

One option is to keep the old institutional framework in place, with transmission remaining a regulated monopoly enterprise. The RTO would conduct regional

transmission plans, presumably with the cooperation and input of the utilities in its footprint, seeking approval from individual state regulators as was done before restructuring. Regulators would decide whether a given project could be included in the rate base. Joskow (2005b) has noted that nearly all transmission projects built since restructuring have, more or less, followed this model. Keeping transmission a regulated enterprise would work, but the RTO introduces a new layer of regulation, in addition to FERC and the state public utility commission. This comes at a cost of increased complexity in the planning and approval process, as illustrated in Figure 2.1. Vajjhalla and Fischbeck (2006) have noted that costs involved in the siting and approval process are roughly identical to the capital cost required to actually construct a transmission line.

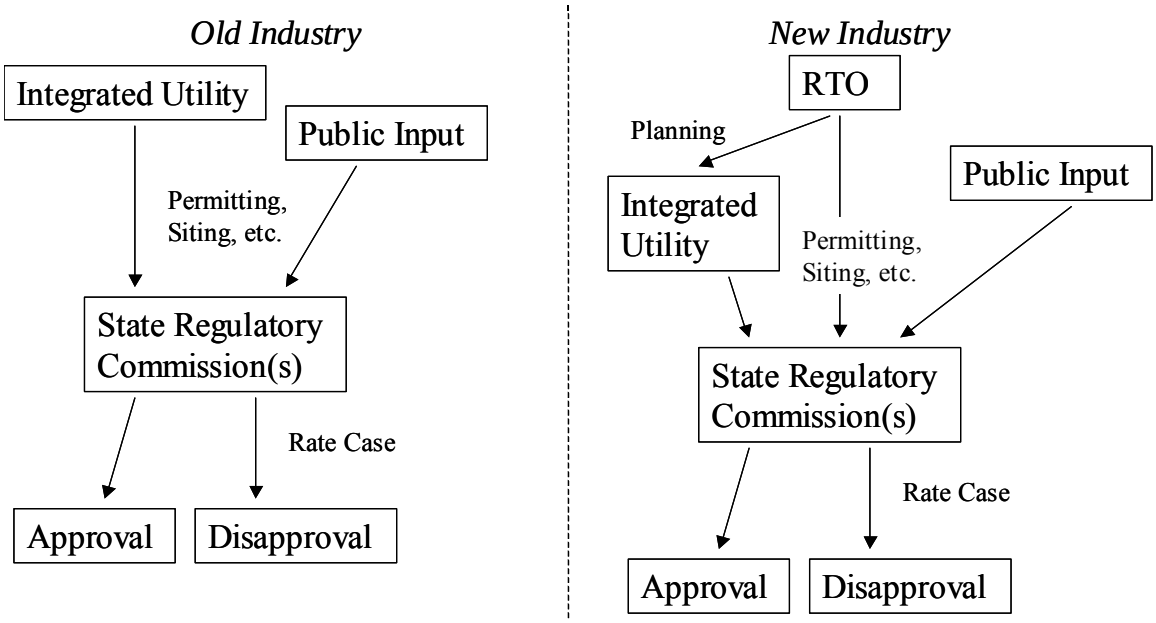

Figure 2.1. Keeping transmission as a regulated utility business is feasible under industry restructuring, but the mix of federal and state jurisdiction would increase the complexity of the process.

Note that the level of complexity in the right-hand panel of Figure 2.1 would remain roughly the same even if the RTO were responsible for transmission planning and construction (leaving the utility completely out of the loop). The reason for this is that the states, and not FERC, currently have jurisdiction over transmission regulation. Transferring regulation of transmission infrastructure to FERC would reduce the level of complexity; the Energy Policy Act of 2005 takes a step in this direction by directing FERC to expedite the siting process for upgrades to designated transmission corridors.[1]

Another option is to rely on market signals to spur investment, particularly among the non-utility or "merchant" sector of the industry. The merchant generation sector invested very actively during the early years of RTO market operations, with nearly 50 gigawatts of new generating capacity connecting to the grid between 1998 and 2002 (Joskow 2005a). The merchant generating sector worked on the simple principle of arbitrage. Generators would sell into regional spot markets whenever they expected to be inframarginal in the dispatch order – that is, when the expected spot price would exceed their generating cost. Merchant transmission was expected to work on much the same principle. Nodal spot prices would form the basis for the investment decisions of transmission-only companies, and would determine the return earned on their investments. This "contract network," originally envisioned by Hogan (1992), has not been successful in encouraging transmission investment. Joskow (2005a) notes that the U.S. has yet to see a transmission line constructed under the merchant-arbitrage transmission model. The remainder of this chapter will explore the economics of

[1] Energy Policy Act of 2005 at ¶1221. Whether the U.S. Congress can constitutionally transfer all transmission regulation to FERC (under the Interstate Commerce Clause) is an interesting and unclear issue, but will not be discussed in this thesis.

transmission congestion, and will offer some explanations as to why the merchant model has not worked in the transmission sector.

2.1. The Economics of Transmission Congestion

Unlike automotive traffic on highways, "congestion" in a transmission line is, at least to a first-order approximation, not a monotonically-increasing function of the amount of flow through the network. Power may be transferred across transmission lines with no penalty until a maximum power flow is reached. Flow across a transmission line is governed by (Wood and Wollenberg 1996):

$$(2.1) \qquad F_{ij} = V_i V_j \sin(\theta_i - \theta_j).$$

Thus, for fixed voltage magnitudes, maximum power transfer between *i* and *j* occurs when $(\theta_i - \theta_j) = \pi / 2$. However, the point of maximum power transfer represents an unstable equilibrium for the system, as small perturbations in either θ_i or θ_j can move the system into a region where the power flow problem has no solution (Ilić and Zaborsky 2000). Power engineers have traditionally set thermal limits on transmission line flows well below the maximum power transfer in order to avoid damage to equipment. During normal operations, a more stringent set of line constraints is in effect. Known as stability limits, these are aimed at maintaining "the ability of an electric system to maintain a state of equilibrium during normal and abnormal conditions or disturbances" (NERC 2005). In practice, the stability limit often pertains to maintaining the synchronous 60-Hertz frequency of rotating generation equipment in the network.

Nodal prices (also called locational marginal prices, or LMP) are calculated as by-products of the optimal power flow (OPF) problem for real power:

$$(2.2) \qquad \min_{P_{Gi},\theta_i,F_{ij}} C_{G1}(P_{G1}) + \ldots + C_{Gn}(P_{Gn})$$

s.t.

$$\sum_i P_{Gi} = \sum_i (P_{Li} + P_{\text{loss},i})$$

$$F_{ij} = V_i V_j \sin(\theta_i - \theta_j) \qquad \forall i, j$$

$$P_i = \sum_j F_{ij} \qquad \forall i$$

$$\left|F_{ij}\right| \le F_{ij}^{\max} \qquad \forall i, j$$

$$0 \le P_{Gi} \le P_{Gi}^{\max} \qquad \forall i$$

$$F_{ij}^{\max} \ge 0. \qquad \forall i, j$$

The LMP at the *i*th bus represents the marginal social cost of providing a unit of power at that bus. It is equal to the marginal cost of generation at the *i*th bus, plus the cost of transporting power to that bus, broken down into the following additive components (Bohn, Caramanis, and Schweppe 1984, Wu et. al., 1996):

1. The marginal social cost of losses;
2. The shadow price associated with the generator capacity constraint, if it is active;
3. The shadow price associated with the active transmission constraints on all lines directly connected to the *i*th bus.

Thus, in a world without transmission constraints, all LMPs are the same and are equal to the marginal cost of the most expensive unit dispatched. This is known as the "system lambda."

The use of nodal pricing is a product of industry restructuring, and serves to signal the market that sending power to a given bus is socially expensive (Wu et. al. 1996). Prior to restructuring, congestion was managed without these price signals, using TLRs or other administrative measures as discussed in Chapter 1. The discussion that follows assumes the existence of a central dispatching entity (such as an RTO) that calculates LMP as in equation (2.2).

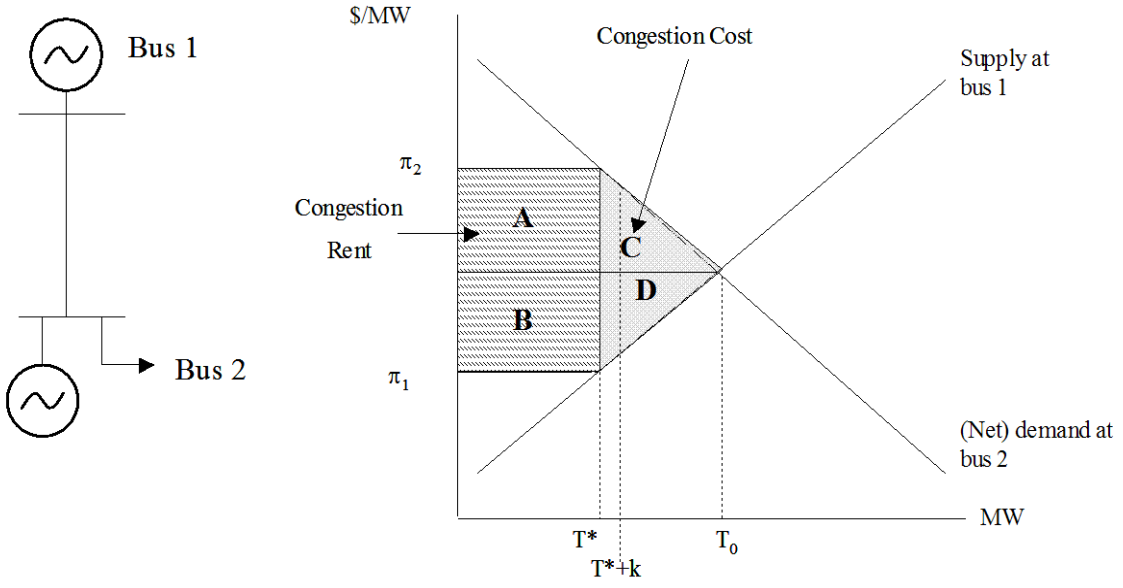

Figure 2.2. A two-node network for illustrating the economic effects of transmission congestion. When the line between buses 1 and 2 is constrained to T megawatts, the generator at bus 2 earns a congestion rent equal to A + B. Social losses are equal to the triangle C + D.*

Transmission congestion is one source of differences in nodal prices, and has distributive effects in the system as well as effects on social welfare. The economic consequences of transmission congestion are most easily demonstrated using a two-bus example, as in Joskow and Tirole (2005a). The example system is shown in Figure 2.2. Assume that an inexpensive generator is located at bus 1, and the load (along with more expensive generation) is located at bus 2. The supply-demand diagram on the right-hand side of Figure 2.2 shows the supply curve at bus 1 and the (net) demand curve at bus 2.

Suppose that T_0 megawatts of real power are demanded at bus 2. If the capacity of the transmission line is large enough to carry T_0 megawatts, then the inexpensive generator at bus 1 will supply the entire demand at load 2. Thus, T_0 represents the socially optimal amount of transmission capacity between buses 1 and 2. If the line between buses 1 and 2 is rated to carry only $T^* < T_0$ megawatts, then some amount of load must be filled using the expensive generator at bus 2. Because there is a shortfall of transmission capacity, the nodal price at bus 2 is higher than the nodal price at bus 1. This creates a congestion rent (area $A + B$ in Figure 2.2); each restructured system has its own method of allocating property rights to this congestion rent.[2] In the absence of contracts for congestion or other allocation schemes, the congestion rent would accrue to the generator at bus 2.

The presence of congestion affects economic welfare. The shaded triangle in Figure 2.2 (area $C + D$) represents the deadweight loss borne by society due to transmission congestion. Increasing capacity on the transmission line to $T^* + k$ decreases the

[2] In centralized spot markets, the RTO is the counterparty to every transaction, and thus it is the RTO who actually collects the congestion rent. For this reason, Wu et. al. (1996) refer to the congestion rent as the merchandizing surplus.

deadweight loss, but this decrease is captured by whomever holds the property rights to the congestion rent. Once capacity on the line is increased to T_0, the congestion disappears, as does the congestion rent. Consumers now enjoy a portion of the social surplus equal to areas $A + C$, while the producer surplus is equal to areas $D + B$. Thus, congestion relief amounts to a social gain of $C + D$, plus a transfer equal to area A from those holding congestion contracts to consumers.

The share of the social surplus transferred from the generator at bus 1 to the holders of congestion contracts is given by:

(2.3) Producer surplus transferred = $(\pi_0 - \pi_1)T^*$,

where π_0 is the marginal cost of serving the load without congestion. Thus, the share of the social surplus transferred from consumers to the holders of congestion contracts is given by the remainder:

(2.4) Consumer surplus transferred to G_2 = $(\pi_2 - \pi_0)T^*$.

Given equations (2.3) and (2.4), we can calculate the total loss in producer surplus (ΔPS) and consumer surplus (ΔCS) as:

$$(2.5) \qquad \Delta PS = (\pi_0 - \pi_1)T^* - \int_{T^*}^{T_0} MC(P_{G1})dP_{G1}$$

$$(2.6) \qquad \Delta CS = \left(\int_0^{T_0 - T^*} MC(P_{G2})dP_{G2} - \int_{T^*}^{T_0} MC(P_{G1})dP_{G1} - \Delta PS \right) + (\pi_2 - \pi_0)T^*.$$

Equation (2.5) represents producer surplus lost by the generator at bus 1. An amount $(\pi_0 - \pi_1)T^*$ is transferred to the holders of congestion contracts (which may include a mix of consumers and producers), while the remainder of equation (2.5) represents the social loss (borne by producers) associated with having to use the generator at bus 2 to serve $T_0 - T^*$ megawatts of demand. The first term in the right-hand side of equation (2.6) represents the consumers' share of total social wealth lost to congestion costs, while the second represents the transfer from consumers to the holders of congestion contracts.

Figure 2.2 can also be used to illustrate the different investment incentives faced by an integrated utility and a merchant transmission company under a system of nodal pricing. An integrated utility upgrading the line from T^* to T_0 would save some amount in dispatch cost equal to area *D*, but would transfer congestion rent equal to area *A* back to consumers. Social welfare increases by *C* + *D*, but *C* is captured by consumers. Thus, the private decision rule for the integrated utility would be to invest only if the amount *D* – *A* was larger than the cost of the transmission upgrade. This is different than the socially optimal investment criteria, which would be to upgrade the line if area *C* + *D* was larger than the upgrade cost.[3] Regulators may be able to force the utility to invest according to the socially optimal criteria, but in a deregulated market the utility generally would not have the incentive to fully upgrade congested lines.

[3] This represents the utility's decision rule in the absence of dynamic effects or uncertainty.

The appeal of non-utility transmission arises from the distribution of the congestion rent. Referencing Figure 2.2, a merchant that invested in a transmission upgrade would capture all of the incremental congestion rent associated with the capacity expansion. The social benefit would be the amount by which the area $C + D$ shrinks following the upgrade. The merchant would not collect this benefit; it would accrue to consumers and the generators (or utility) in the system. Thus, a merchant transmission company would expand the line up to the point where the incremental congestion rent was equal to the cost of the upgrade. Just as in the utility investment case, a merchant upgrading the capacity of the line from T^* to T_0 would transfer a portion of the congestion rent (part of area A) back to consumers. If the merchant were truly a transmission-only company, then it would also transfer another portion of the congestion rent (part of area B) to generators in the system. A merchant transmission company would never, therefore, relieve all congestion along a line, since the congestion rent decreases monotonically with the capacity of the line.

Allowing investors, whether merchants or utilities, to capture congestion rents will not relieve all congestion in the system. An even stronger statement is that neither a merchant nor a utility investor will relieve congestion to the socially efficient point, where the marginal social benefit of transmission upgrades is equal to the marginal construction cost. The reason is that the investors do not fully capture the social surplus associated with the project. Although Hogan (2003) is generally dismissive of this issue, concern over using market prices to compensate investments with high fixed costs and low operation costs can be traced back to Hotelling (1938), who considers the optimal

compensation mechanism for investment in a fixed piece of infrastructure such as a railroad or a bridge. Hotelling's analysis suggests that defining a benefit stream for a fixed-cost investment through market prices will yield an "excessively conservative" decision rule, relative to the social optimum (Hotelling 1938, p. 267).

In the case of merchant investment, the positive externalities accrue to some mix of consumers and other producers in the system. An integrated utility can do somewhat better; it internalizes the portion of the social surplus that would accrue to producers under merchant transmission. Thus, other things being equal, it is possible that utility investment might get the system closer to the social optimum T_0 than would merchant investment.

2.2. Transmission Congestion Contracts

The discussion in Section 2.1 did not mention a specific market mechanism for allocating property rights to the rents generated in the presence of congestion. There is an implicit assumption that they would accrue to the owner of the transmission line. Schweppe's spot prices and Hogan's contract network were originally oriented towards short-term efficient operation of the electric network and did not explicitly consider any long-run implications, although Hogan (1992) discusses long-term transmission rights co-existing with nodal spot prices. Although the spot prices were conceptually simple to compute, interpretation was not necessarily straightforward. Price differences between network nodes represent the marginal social cost of moving power from one node to another. As Wu et. al. (1996) discuss, this correct interpretation was often confused with an incorrect

analogy to other transportation networks, in which nodal price differences signal market participants as to which paths are congested, and also indicate potential profit opportunities.[4]

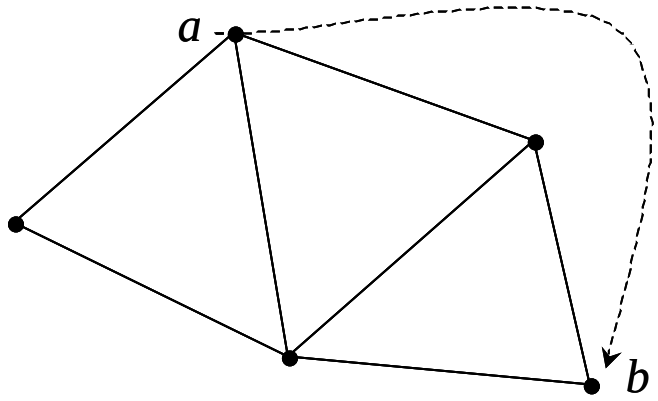

Figure 2.3. A point-to-point financial transmission right can be defined between any two points in the network regardless of the contract path or whether the points are connected neighbors.

Subsequent work has thus focused on the role of the contract market to provide incentives and recover costs, as opposed to relying purely on the spot market. Initially, two flavors of transmission rights emerged. The first, initially suggested by Hogan (1992), and further promoted by Bushnell and Stoft (1996), would allow for contracts based on the difference in nodal prices between any two points in the grid, regardless of the presence of congestion on the link(s) connecting the two points. The two points would not even need to be connected neighbors, as shown in Figure 2.3. Thus, the value of the contract is determined as a by-product of the energy spot market.[5] Such contracts were initially

[4] Wu et. al. (1996) show that nodal price differences in power networks can arise even in the absence of congestion, and thus it is not unusual to see power moving from a high-priced node to a low-priced node. Absent the exercise of market power, in equilibrium these phenomena should not be observed in other transport networks.

[5] For this reason, Oren (1997) refers to these as "passive" transmission rights.

referred to as point-to-point transmission congestion contracts, but are now generally called financial transmission rights (FTRs).

The revenue stream from a financial transmission right is defined over a set of two nodes in the grid *a* and *b*, a specified amount of time *T*, and a specified number of megawatts *Q* as follows:

$$FTR(a,b,T,Q) = Q\sum_{t=1}^{T}\left(\pi_{a,t} - \pi_{b,t}\right). \tag{2.7}$$

It is possible for an FTR to have a negative value as well as a positive value, although FTRs can exist as options instead of obligations. Hogan's (1992) original contract network formulation describes a "feasibility rule" for the allocation of FTRs by the RTO. According to the feasibility rule, FTRs should be allocated in such a way that the total set could be physically dispatched without violating any of the system constraints. The impetus for the feasibility rule is to provide a solvency condition for the RTO; Hogan (1992) and Wu et. al. (1996) prove the "revenue adequacy theorem," which says that if FTRs are allocated according to the feasibility rule, the RTO will at least break even and cannot run an operating deficit. In practice, FTRs have primarily been used for hedging transmission costs on the grid (Patiño-Echeverri 2006), although Bushnell and Stoft (1996, 1997) claim that they have superior efficiency properties for encouraging merchant transmission investment. We will return to this second issue in Chapter 4.

The second type of transmission rights contract, suggested by Chao and Peck (1996) would involve trading transmission rights on a link-by-link basis separately from the energy market. As such, these have become known as "flowgate" rights, as shown in Figure 2.4. Assuming a competitive market for transmission, flowgate rights would have a nonzero price only in the case of congested links. Competition should drive the price of flowgate rights down to the marginal cost of transmitting energy between two points. Thus, the outcome of the competitive market for flowgate rights could be determined through the shadow prices derived from Schweppe's spot price formulation.[6] The appeal of flowgate rights was that the contract value would reflect the value of an underlying physical good (i.e., transmission). In this way, the flowgate model would more closely mirror the pricing model in transportation networks, where nodal price differences signal both the presence of congestion and the cost of transportation between the two nodes. Oren (1997) has also suggested that since the value of a flowgate right only needs to be computed for congested lines, the market for flowgate rights would be more competitive than for FTRs.

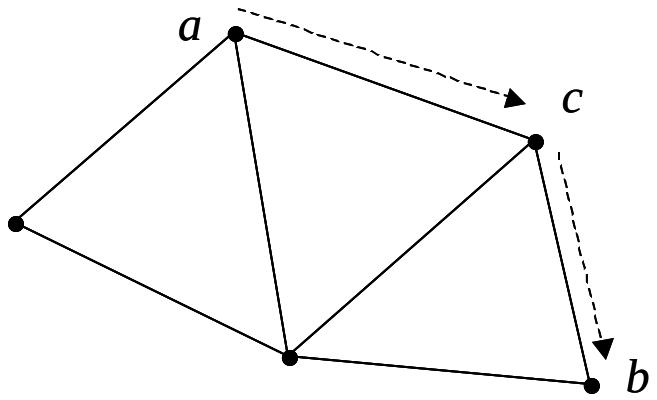

Figure 2.4. Flowgate rights are defined along specific paths in the network.

[6] In one sense, a competitive flowgate market would be just as "passive" as the FTR market, since the equilibrium prices could be determined as a by-product of the nodal price calculations.

Despite its appeal in connecting the financial electricity market with the underlying physical network, the flowgate rights model has not seen much adoption in practice; functioning RTOs and ISOs have largely preferred the point-to-point FTR model. The most serious critique of the flowgate model has come from Hogan (2000). Among the problems with administering a system of flowgate rights is that the set of available rights (i.e., the set of congested lines) must be known prior to the energy auction, the number of flowgate rights necessary to form a contract path between two points *a* and *b* is highly uncertain, and the capacity limits on transmission lines are not as fixed as the flowgate model portrays (they can change due to contingencies or outages, for example). In addition, Bushnell and Stoft (1996) and Joskow and Tirole (2000) point out that under a flowgate rights mechanism, investors can be rewarded for building transmission lines that cause congestion in the grid. The reason, as discussed by Hogan (2000), is that new links automatically create the potential for new flowgate rights; these rights have a positive value when they become congested.

Hogan's critiques of the flowgate model are all valid, particularly with respect to uncertainty regarding the number of congested lines in the system at a given time. To the extent that market participants are unable to learn over time which paths are likely to become congested, and what the equilibrium value of that congestion is (contingent upon demand and the state of the network), similar uncertainties are likely to plague the market for point-to-point financial transmission rights. Siddiqui et. al. (2005) note that participants in the New York FTR auctions have systematically lost money, even after accounting for risk preferences. Patiño-Echeverri (2006) reports a similar pattern in PJM,

but infers from this that FTR market participants are more risk-averse than supposed in Siddiqui et. al. (2005). The claim of Bushnell and Stoft (1996, 1997), that a well-designed FTR market can remove the incentives of merchant transmission companies to modify the grid in detrimental ways, will be the subject of Chapter 4.

The one advantage of flowgate rights over FTRs would seem to be their connection to the underlying physical system. For example, suppose the only line connecting points *a* and *b* in the network became disconnected. In the flowgate model, rights between those two points would cease to be well-defined (and traded) until connection was restored. The implications for an FTR market are less clear. Holders of FTRs could conceivably continue to collect congestion rents on a line that, at least temporarily, does not exist.

The driving force behind the debate between flowgate rights and FTRs is likely rooted in history and geography. Hogan's FTRs are a natural outgrowth of the "tight" power pools of the Northeast, in which multiple utility companies formed agreements to centrally coordinate dispatch and grid management. Flowgate rights, birthed at Berkeley, complement the bilateral market structure common in the Western Systems Power Pool prior to deregulation in California.

As Hogan (2000) points out, the ultimate reason for the adoption of FTRs over flowgates may be simplicity; the value of an FTR at any given time can be trivially computed once the energy market clears, while the flowgate model requires an entirely new set of markets. Centralized electricity markets in the U.S. have historically faced large start-up

costs (Lave, Apt, and Blumsack 2004), so the associated costs of establishing new routines and software to handle the transmission-rights market may have deterred RTOs from embracing the flowgate model.[7]

2.3. Other Approaches

Gribik et. al. (2005) have considered expanding the flowgate concept to include admittance payments in addition to capacity payments. The reasoning of Gribik et. al. is that while flow on networks is largely governed by the line admittances, FTR and flowgate payments are made on the basis of the line's megawatt capacity limit.[8] RTOs auctioning off incremental transmission rights following network expansion would thus expand the number of contracts awarded to include these admittance rights. In the model of Gribik et. al., payments for admittance amount to transfers from holders of incremental capacity flowgate rights. Thus, admittance payments expand the number of contracts awarded, but also amount to a zero-sum game and thus will not violate the revenue adequacy rule. Of course, this also implies that the electrical properties of transmission lines are welfare-neutral; social wealth can neither be created nor destroyed through a change in admittance to a particular line or part of the system (wealth can only be transferred from one party to another). Intuitively, it is difficult to see how this can be the case, and the examples presented in Chapters 3 and 4 will demonstrate that changes in the system admittance matrix can have both positive and deleterious effects on aggregate welfare.

[7] In current RTO markets, FTRs are purchased in a centralized auction but can be traded several times over in the bilateral market.

[8] The capacity and admittance of a transmission line are first-order independent. However, in evaluating the value of a line to the system, they are not necessarily separable. Thus, the notion of separate payments for each has a great deal of appeal.

Apt and Lave (2003) have suggested a two-part tariff to fund transmission upgrades. The tariff would be centrally administered by the RTO and would be similar to the megawatt-mile approach for costing transmission lines proposed by Yu and David (1997). One part of the cost of transmitting electric energy would be the nodal price, calculated from equation (2.2), while the other would be a megawatt-mile charge. Rather than redistributing congestion revenue through FTR or flowgate rights, congestion charges and the megawatt-mile fee would go into a central fund to compensate transmission owners. To the extent that LMP provides incentives to keep lines congested rather than invest in upgrades (as described in Section 2.1), the megawatt-mile charge could offset this incentive problem.

Chapter 3: The Wheatstone Network and the Braess Paradox in Electric Power Systems

Under industry restructuring, the transmission system is asked to fill two roles. The first is to deliver power reliably to customers, and the second is to support a growing number of market transactions. The current transmission grid may find these two obligations conflicting. Many market transactions involve buyers and sellers separated by large geographic or topological distances. The resulting pattern of network loadings is very different from the regulated era, in which vertically-integrated utilities largely relied on self-scheduling to fill demand.[1] An increased incidence of TLR events and rising congestion costs in RTO areas suggest that the stress on certain portions of the transmission system is increasing.

One policy response is to build more transmission lines, in much the same way that transportation officials order new highways built to ease traffic congestion. However, industry restructuring, specifically the separation of ownership from control of the transmission grid, has disrupted the planning process. The issues of where to build transmission lines, who should pay for them, and how investors will be compensated has not been fully resolved in the restructured industry.

[1] "Wheeling" transactions were commonplace prior to industry restructuring, but were not as numerous and sometimes involved long-term bilateral contracts. The overbuilding of transmission capacity by utilities decades prior to restructuring also likely dulled the impact of bilateral market transactions.

Chapter 2 discussed how a market based on nodal prices could take the place of traditional utility planning and investment. If locational marginal prices convey enough information to market participants regarding constraints in the network, then market-based transmission investment is a policy with promise. In simple networks, such as those analyzed by Hogan (1992) and Bushnell and Stoft (1996, 1997), all the information necessary to make wise investment decisions may be embedded in the network LMPs. This is not the case in more highly meshed networks, as this chapter will discuss.

Examining the steady-state properties of a test system known as the Wheatstone network shows that LMP is a good way to measure congestion in the network, but in many cases LMP cannot identify which constraints should be relieved. Thus, LMP may give misleading signals to investors. Choosing among projects based on LMP will, in some cases, result in investment that does not benefit the system or the investor, and in others may yield investments harming the system (these will be discussed in greater detail in Chapter 6).

3.1. Wheatstone Networks and the Braess Paradox

The Wheatstone network describes a graph consisting of four nodes, with four corresponding edges on the boundary creating a diamond or circular shape. A fifth edge connects two of the nodes across the interior of the network, thus splitting the network into two triangular (or semicircular) subsystems. This fifth edge is aptly named the "Wheatstone bridge." Although the network is named for Charles Wheatstone, who was

the first to publish the network topology in 1843, the network design was apparently the work of Samuel Christie some ten years earlier (Ekelöf 2001).

The original motivation for the Wheatstone network was the precise measurement of resistances, as shown in Figure 3.1. In the network, resistances R_1, R_2, and R_3 are known to very high precision, and R_2 is adjustable. The problem is to measure R_x with similar precision. The voltage V across the bridge is equal to:

$$(3.1) \quad V = \frac{R_2}{R_1 + R_2} V_s + \frac{R_x}{R_3 + R_x} V_s ,$$

where V_s is the voltage source. Assuming that $V_s \neq 0$, then the voltage drop across the bridge will be zero at the value of R_x where $R_2 / R_1 = R_x / R_3$. If this condition is satisfied, then the Wheatstone network is said to be *balanced*. If this condition is not satisfied, then there will be a voltage drop across the bridge and the network is said to be *unbalanced*.

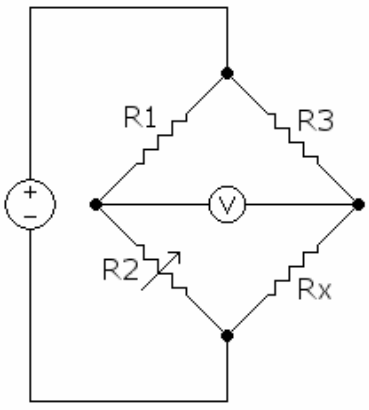

Figure 3.1. Wheatstone circuit example

As a fairly general topology, Wheatstone networks have arisen as structures of interest in other network situations such as traffic, pipes, and computer networks. Much of the attention paid to Wheatstone structures has centered around the network's seemingly paradoxical behavior. Under certain conditions, connecting a Wheatstone bridge to a formerly parallel network (or, in the context of the circuit in Figure 3.1, adjusting the boundary resistances so that the network is unbalanced) can actually increase the total user cost of the network. First studied by Braess (1968) in the context of traffic networks, this behavior has come to be known as Braess's Paradox.

The exact meaning of the "user cost" of the network has various interpretations depending on the network of interest. In Braess's original example, and in Arnott and Small (1994), the user cost of highways is the time it takes motorists to reach their final destination. An increase in the user cost, therefore, corresponds to wasted time and irritation from sitting in larger traffic jams. Costs incurred through internet routing networks, as in Calvert and Keady (1993) and Korilis, Lazar, and Orda (1999), arise through increased latency and possibly lost information (Bean, Kelly, and Taylor 1997). Even in circuits, "user cost" can be interpreted as the voltage drop across the circuit as a whole. Cohen and Horowitz (1991) describe an example in which the addition of a Wheatstone bridge lowers the voltage drop across the network (assuming the network is unbalanced to begin with); thus the "cost" incurred by the Wheatstone bridge is reduced voltage over the circuit as a whole. Braess's Paradox suggests that user costs may increase for reasons independent of the amount of traffic on the network. The network itself, and not its users, may be the ultimate problem, and managing flows or

disconnecting certain network links may actually serve to decrease congestion costs for all users.[2]

Milchtaich (2005) has studied whether Braess's Paradox is unique to the Wheatstone network. Using a result from Duffin (1965) that every network topology can be decomposed into purely series-parallel subnetworks and Wheatstone subnetworks, Milchtaich concludes that (apart from uninteresting situations such as simple bottlenecks) the paradoxical behavior cannot occur outside the Wheatstone structure. Thus, observation of the paradox serves as proof of an embedded Wheatstone subnetwork. Milchtaich (2005), Calvert and Keady (1993), and Korilis, Lazar and Orda (1997, 1999) offer the following technical and policy implications of Braess's Paradox:

1. Braess's Paradox occurs in any network that is not purely series-parallel;
2. Local network upgrades (that is, upgrading only congested links) will not resolve Braess's Paradox. Upgrades must be made throughout the system in order to reduce the user cost of the network;
3. System upgrades should focus on connecting "sources" as close as possible to "sinks."

Underlying the policy recommendations is the assumption that flow networks all behave similarly, at least on the surface. While there are good analogies between the behavior in

[2] Viewing network traffic as a routing game, Braess's Paradox does not seem all that paradoxical. Each user choosing a network path to minimize their private costs easily lends itself to coordination failures such as the Prisoner's Dilemma. All users would benefit through coordination and cooperation, but no individual user has the incentive to initiate (or perhaps even sustain) this coordination.

electric power networks and other networks, the analogies are ultimately flawed. Kirchoff's Laws do not hold in other networks.[3] In traffic and some internet systems, routing is determined by user preference rather than by physical laws (e.g., current flows follow Ohm's Law), although installation of FACTS devices could change this for those paths outfitted with devices. Congestion costs in systems with nodal pricing are discontinuous, while in other networks the cost of additional traffic can be described as a continuous function of current traffic. Despite these differences, power networks do exhibit some of the behavior described in other networks; in particular, Braess's Paradox can hold in simple systems or in subsets of more complex systems.

3.2. A Simple Wheatstone Test System

The four-bus test system used in this discussion is shown in Figure 3.2. There is one generator located at bus 1, an additional generator at bus 4, and one load at bus 4. Buses 2 and 3 are merely tie-points; power is neither injected at nor withdrawn from these two buses. From the analogy to Figure 3.1, the Wheatstone bridge is the link connecting buses 2 and 3. The test system is assumed to be symmetric, in the sense that $B_{12} = B_{34}$ and $B_{13} = B_{24}$. The susceptance of the Wheatstone bridge is given by B_{23} and will be a variable of interest in the discussion that follows. The symmetry assumption implies, among other things, that in the DC load flow, $F_{12} = F_{34}$ and $F_{13} = F_{24}$.[4]

[3] In the case of laminar flow, a version of Kirchoff's Law does hold in piping networks. However, real flows through pipes are almost a combination of turbulent and laminar flow.

[4] In the DC load flow, the current magnitude is identical to the admittance (since the voltage magnitudes are all set to 1 per-unit). The symmetry of the admittance matrix implies that the two cut sets in the system (buses 1, 2, and 3; buses 2, 3, and 4) are also symmetric, and Kirchoff's Current Law must hold for each cut set.

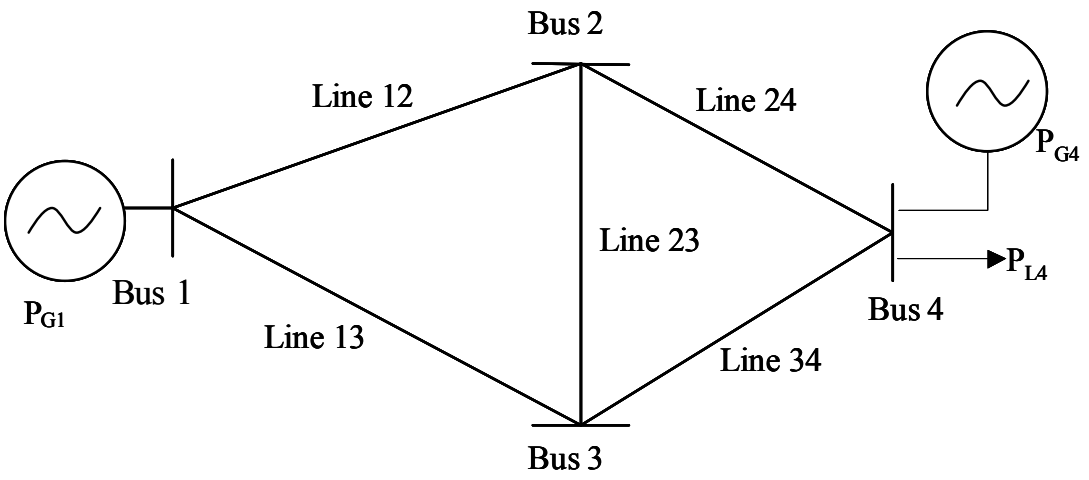

Figure 3.2: The Wheatstone network. The network is defined to be symmetric if the resistances are equal on lines S_{12} and S_{34}, and if the resistances are equal on lines S_{13} and S_{24}.

The following definitions will help solidify concepts:

Definition 3.1: A four-node network is said to be a Wheatstone network if its topology is the same as that in Figure 3.2.

Definition 3.2: A four-node network is said to be a symmetric Wheatstone network if it is a Wheatstone network, and if the susceptance conditions $B_{12} = B_{34}$ and $B_{13} = B_{24}$ hold.

Definition 3.3: A four-node network is said to be a symmetric unbalanced Wheatstone network if it is a symmetric Wheatstone network, and the magnitude of the flow across link S_{23} is nonzero.

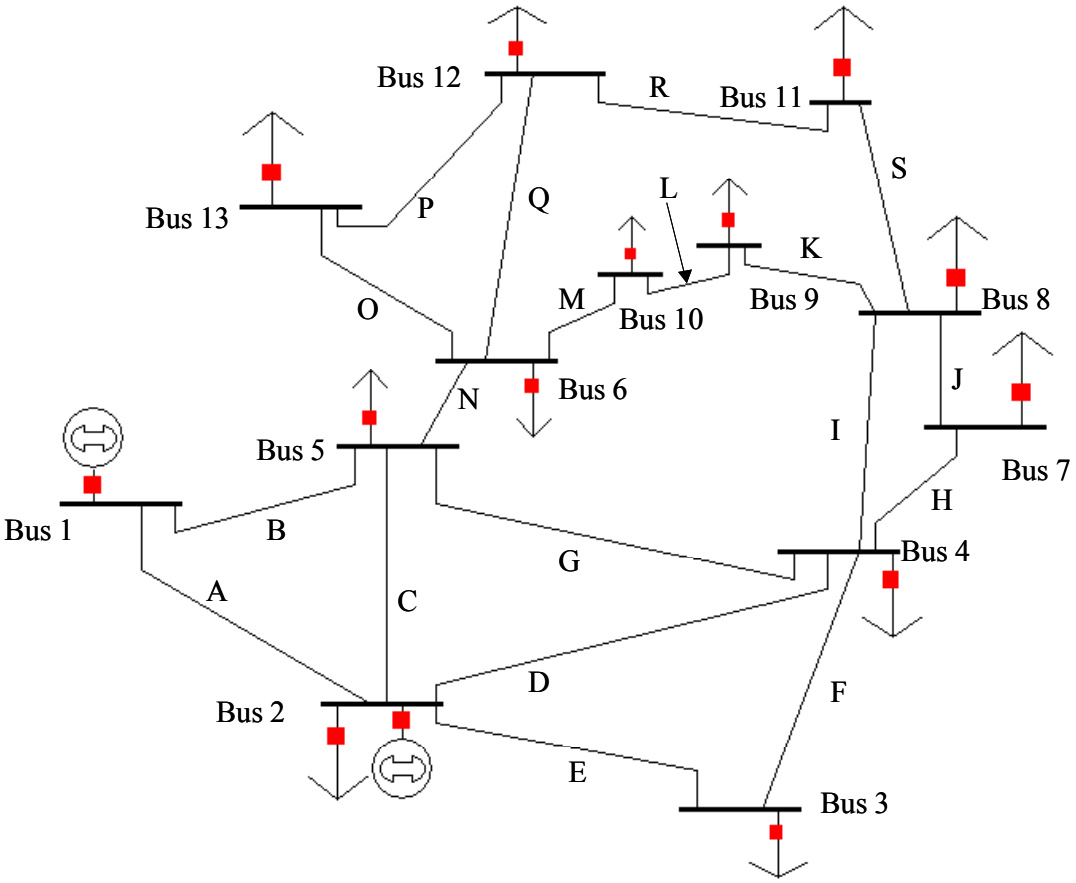

Figure 3.3: Thirteen-bus system based on the IEEE 14-bus system. There are at least six Wheatstone subnetworks in the system. Examples include those formed by lines A, B, C, G, and D; lines C, G, D, E, and F; and lines O, P, Q, (R+S), and (M+L+K).

Although the Wheatstone network shown in Figure 3.2 is simplistic, the Wheatstone structure is actually quite common in actual systems. Figure 3.3 shows a slightly modified version of the IEEE 14-bus test network.[5] There are at least six embedded Wheatstone networks in the 13-bus system of Figure 3.3. An interesting issue is how to decompose a large complex network into its component Wheatstone subnetworks and

[5] It has been modified by removing the synchronous condensers in the system. This reduces the network to 13 buses.

those subnetworks that are purely series-parallel, and how to treat adjacent and overlapping Wheatstone networks.[6]

3.3. Conditions for Braess's Paradox to Hold

Of particular interest here is how the addition of the Wheatstone bridge affects the flows on the boundary lines relative to the "base case" with no Wheatstone bridge. Here we are implicitly assuming that the generator injections, load withdrawals, and line susceptances are such that there is no congestion in the system prior to the addition of the bridge. If we take lines S_{12} and S_{34} and combine them in series to form a line with equivalent susceptance B_a, and we combine lines S_{13} and S_{24} in a similar fashion to construct a line with equivalent susceptance B_b, the network is free of congestion if and only if:

$$(3.2) \quad \frac{B_k}{(B_a + B_b)} P_{G1} < F_k^{\max}, \text{ for } k = \{a, b\}^7$$

To derive an explicit expression for the new network flows following the addition of the Wheatstone bridge, we will use the method derived in Ejebe and Wollenberg (1979) and Irisarri, Levner, and Sasson (1979), which compares steady-state line flows in the network before and after the network modification. Such modifications are represented as changes in the susceptance matrix **B**. Although the Ejebe-Wollenberg method was

[6] A method for network decomposition and Wheatstone detection will be presented in Chapter 5. Duffin (1965) has shown that any non-radial network can be decomposed into series-parallel and embedded-Wheatstone subnetworks; Milchtaich (2005) also proves the same result. In the limit, where the mesh network consists essentially of everything connected to everything else, isolating particular Wheatstone structures may be difficult. Particularly when the network exhibits Braess's Paradox, the hardest question will be to pinpoint which Wheatstone is "causing" the paradoxical behavior.

[7] A similar condition also holds in AC networks, but uses the complex admittance instead of the susceptance.

originally designed to model the effects of contingencies (so that the susceptance change in a given line, ΔB_k, is simply equal to $-B_k$) it is easily adaptable to the construction of a new line.

Since we are using the DC load flow approximation, the admittance matrix consists solely of susceptances:

$$(3.3)\quad B_{ij} = \begin{cases} -\dfrac{1}{X_{ij}} & i \neq j \\ \displaystyle\sum_{i=0, i\neq j} \frac{1}{X_{ij}} & i = j \\ 0 & X_{ij} = 0 \end{cases} .$$

We start with the DC model: [8]

$$(3.4)\quad \mathbf{P} = \mathbf{B}\boldsymbol{\theta}$$

Note that equation (3.4) represents the system prior to the addition of the Wheatstone bridge. After the Wheatstone bridge is connected, the load flow equations become:

$$(3.4')\quad \mathbf{P} = (\mathbf{B} + \mathbf{A}'\boldsymbol{\Delta}\mathbf{B}^{\mathbf{diag}}\mathbf{A})\boldsymbol{\theta}^{new},$$

[8] We could also start with the distribution-factor representation of the DC model, $\mathbf{F} = \mathbf{A'B}^{\mathbf{diag}}\mathbf{A}\boldsymbol{\theta}$, where $\mathbf{B}^{\mathbf{diag}}$ is a ($NL \times NL$) diagonal matrix of line susceptances. However, starting with the injection equations will allow us to write the new flows in the form $\mathbf{F}^{new} = \mathbf{F}^{old}$ + {adjustment factor}.

where $\mathbf{\Delta B^{diag}}$ is a diagonal matrix of changes to the line susceptances. $\mathbf{\Delta B^{diag}}$ has dimensionality ($NL \times NL$). Solving equation (3.4') for the vector of phase angles yields:

$$(3.5) \quad \boldsymbol{\theta}^{new} = (\mathbf{B} + \mathbf{A'\Delta B^{diag} A})^{-1} \mathbf{P}.$$

Using the Sherman-Morrison-Woodbury matrix inversion lemma and substituting equation (3.4), we get:

$$(3.6) \quad \boldsymbol{\theta}^{new} = (\mathbf{B^{-1}} - \mathbf{B^{-1}A}(\mathbf{\Delta B^{diag^{-1}}} + \mathbf{A'B^{-1}A})^{-1} \mathbf{A'B^{-1}}) \mathbf{B}\boldsymbol{\theta}^{old}.$$

Distributing terms,

$$(3.7) \quad \boldsymbol{\theta}^{new} = \boldsymbol{\theta}^{old} - \mathbf{B^{-1}A}(\mathbf{\Delta B^{diag^{-1}}} + \mathbf{A'B^{-1}A})^{-1} \boldsymbol{\delta}^{old},$$

where $\boldsymbol{\delta}$ is the ($NL \times 1$) vector of phase angle differences.

Following the network modification, the DC flow equations can be written

$$(3.8) \quad \mathbf{F}^{new} = (\mathbf{A'}(\mathbf{B^{diag}} + \mathbf{\Delta B^{diag}})\mathbf{A})\boldsymbol{\theta}^{new}.$$

Inserting (3.7) into (3.8) and distributing terms yields:

$$(3.9)\quad \mathbf{F}^{new} = \mathbf{A'}(\mathbf{B}^{\mathbf{diag}})\mathbf{A}\boldsymbol{\theta}^{old} - \mathbf{A'}(\mathbf{B}^{\mathbf{diag}})\mathbf{A}\mathbf{B}^{-1}\mathbf{A}(\Delta\mathbf{B}^{\mathbf{diag}^{-1}} + \mathbf{A'}\mathbf{B}^{-1}\mathbf{A})^{-1}\boldsymbol{\delta}^{old} + \mathbf{A'}(\Delta\mathbf{B}^{\mathbf{diag}})\mathbf{A}\boldsymbol{\theta}^{old}$$
$$- \mathbf{A'}(\Delta\mathbf{B}^{\mathbf{diag}})\mathbf{A}\mathbf{B}^{-1}\mathbf{A}(\Delta\mathbf{B}^{\mathbf{diag}^{-1}} + \mathbf{A'}\mathbf{B}^{-1}\mathbf{A})^{-1}\boldsymbol{\delta}^{old}$$
$$= \mathbf{F}^{old} + \mathbf{A'}(\Delta\mathbf{B}^{\mathbf{diag}})\boldsymbol{\delta}^{old} - (\mathbf{A'}(\mathbf{B}^{\mathbf{diag}} + \Delta\mathbf{B}^{\mathbf{diag}})\mathbf{A})\mathbf{B}^{-1}\mathbf{A}(\Delta\mathbf{B}^{\mathbf{diag}^{-1}} + \mathbf{A'}\mathbf{B}^{-1}\mathbf{A})^{-1}\boldsymbol{\delta}^{old}.$$

The adjustment is $\mathbf{A'}(\Delta\mathbf{B}^{\mathbf{diag}})\boldsymbol{\delta}^{old} - (\mathbf{A'}(\mathbf{B}^{\mathbf{diag}} + \Delta\mathbf{B}^{\mathbf{diag}})\mathbf{A})\mathbf{B}^{-1}\mathbf{A}(\Delta\mathbf{B}^{\mathbf{diag}^{-1}} + \mathbf{A'}\mathbf{B}^{-1}\mathbf{A})^{-1}\boldsymbol{\delta}^{old}$.

In the special case where the susceptance of only one line changes (as is the case with the Wheatstone bridge example), we can replace the $\Delta\mathbf{B}^{\mathbf{diag}}$ matrix with a scalar ΔB_k (where k indicates the line whose susceptance has been altered), and we can replace the incidence matrix with its kth column, denoted $\mathbf{A_k}$. In this case, equation (3.6) is modified to read:

$$(3.6')\quad \boldsymbol{\theta}^{new} = (\mathbf{B} + \Delta B_k \mathbf{A_k}\mathbf{A_k}')^{-1}\mathbf{P},$$

and equation (3.8) becomes:

$$(3.8')\quad \boldsymbol{\theta}^{new} = (\mathbf{I} - (\Delta B_k{}^{-1} + \mathbf{A_k}'\mathbf{B}^{-1}\mathbf{A_k})^{-1}\mathbf{B}^{-1}\mathbf{A_k}'\mathbf{A_k})\boldsymbol{\theta}^{old}.$$

The term $\Delta B^{-1} + \mathbf{A_k}'\mathbf{B}^{-1}\mathbf{A_k}$ can get pulled out because it is a scalar. Recognizing that $\mathbf{A_k}\boldsymbol{\theta} = \delta_k$, the phase angle difference along line k, we get:

(3.10) $\boldsymbol{\theta}^{new} = \boldsymbol{\theta}^{old} - (\Delta B_k^{-1} + \mathbf{A_k}'\mathbf{B^{-1}}\mathbf{A_k})^{-1}\mathbf{B^{-1}}\mathbf{A_k}'\delta_k$.

Returning to the DC load flow equations, the flow across the *l*th line following the network modification is:

(3.11) $F_l^{new} = B_l \delta_l^{new}$.

In the case where $l = k$, equation (3.11) can be modified to read $F_k^{new} = (B_k + \Delta B_k)\delta_k^{new}$, although the emphasis here will be on lines other than *k* (since the object of interest is calculating the effect of the Wheatstone bridge on flows on the other lines). Rewriting equation (3.11) as:

(3.12) $F_l^{new} = B_l \mathbf{A'_l}\,\boldsymbol{\theta}^{new}$

and substituting equation (3.10), we get:

(3.13)
$$\begin{aligned} F_l^{new} &= B_l \mathbf{A'_l}\left[\boldsymbol{\theta}^{old} - (\Delta B_k^{-1} + \mathbf{A_k}'\mathbf{B^{-1}}\mathbf{A_k})^{-1}\mathbf{B^{-1}}\mathbf{A_k}\delta_k^{old}\right] \\ &= F_l^{old} + (\Delta B_k^{-1} + \mathbf{A_k}'\mathbf{B^{-1}}\mathbf{A_k})^{-1}\mathbf{A'_l}\,\mathbf{B^{-1}}\mathbf{A_k}B_l\delta_k^{old} \\ &= F_l^{old} + b_k^{-1}\mathbf{A'_l}\,\mathbf{B^{-1}}\mathbf{A_k}B_l\delta_k^{old}. \end{aligned}$$

In the special case where $l = k$, equation (3.13) becomes:

(3.13') $F_l^{new} = \left(F_l^{old} - \Delta B_l \delta_l^{old}\right)(1 - b_l^{-1}\mathbf{A'_l}\,\mathbf{B^{-1}}\mathbf{A_l})$.

The sensitivity of flows in the Wheatstone network to the bridge susceptance, as described by equations (3.13) and (3.13'), are shown in Figure 3.4, assuming that the boundary links have susceptances $B_{12} = B_{34} = 30$ per-unit (p.u.) and $B_{13} = B_{24} = 15$ p.u.. The flow limit on each line is assumed to be 55 MW; hence the flow on lines S_{12} and S_{34} plateau at this upper limit. Note also that the flow on the Wheatstone bridge and the flow on the remaining two boundary links appear to converge. One implication of this behavior (which will be of importance in the steady-state analysis of congestion in the network) is that if the Wheatstone network is symmetric in the sense of Definition 2, then a maximum of two lines can be congested at a given time.

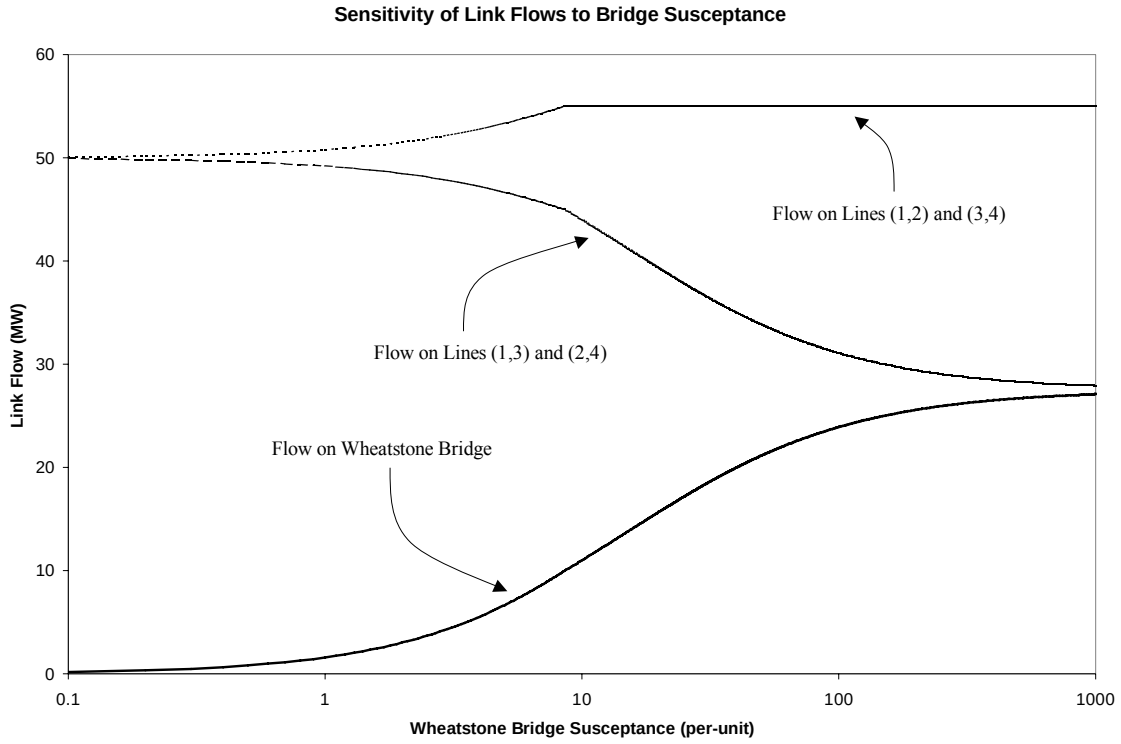

Figure 3.4: Senstivity of flows in the Wheatstone network to changes in the susceptance of the Wheatstone bridge. The x-axis has a logarithmic scale. The flows on lines S_{12} and S_{34} hit the capacity constraint when the susceptance of the bridge reaches 8.6 per-unit.

Of particular interest here are the conditions under which any of the boundary links will become congested with the addition of the Wheatstone bridge (congestion occurs when the generator at bus 4 either does not exist or is not turned on). Without loss of generality, assume that $B_{12} > B_{13}$. Thus, once the bridge is added, more power will flow over link S_{12} than over link S_{23}.[9] We are interested in the conditions under which link S_{12} will become congested. The symmetry assumption implies that a similar condition will hold for link S_{34} to become congested.

Link S_{12} becomes congested if $F_{12}^{new} \geq F_{12}^{\max}$. An equivalent condition is:

$$(3.14) \quad F_{12}^{old} + b_{23}^{-1}\mathbf{A'}_{12}\mathbf{B^{-1}}\mathbf{A}_{23}B_{12}\delta_{23}^{old} \geq F_{12}^{\max}$$
$$\Rightarrow \Delta B_{23}^{-1} \geq \frac{\mathbf{A'}_{12}\mathbf{B^{-1}}\mathbf{A}_{23}B_{12}\delta_{23}^{old}}{F_{12}^{\max} - F_{12}^{old}} - \mathbf{A}_{23}\mathbf{'B^{-1}}\mathbf{A}_{23}.$$

This "feasible region" for the susceptance of the Wheatstone bridge is shown in Figure 3.5 for the configuration where $B_{12} = B_{34} = 30$ p.u., $B_{13} = B_{24} = 15$ p.u., $F_{12}^{\max} = 55$ MW, and $P_{G1} = P_{L4} = 100$ MW. From the DC power flow on this network we get $F_{12}^{old} = 50$ MW and $\delta_{23}^{old} = 1.5$ degrees.

[9] The symmetry assumption implies that equal amounts of power will flow over both paths in the absence of the Wheatstone bridge.

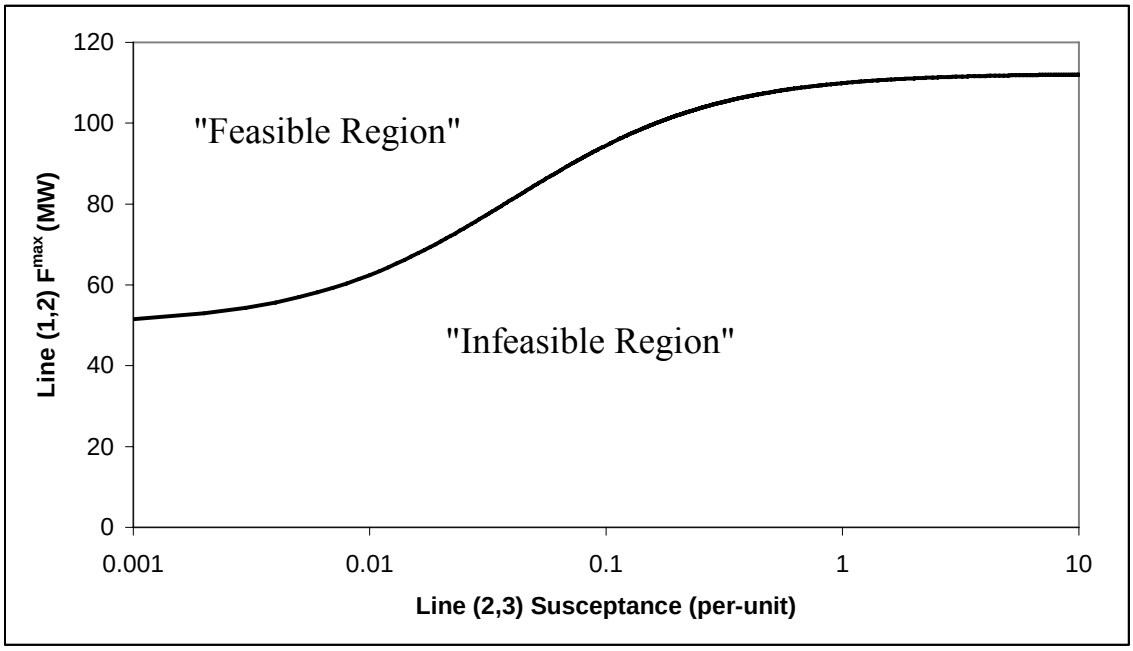

Figure 3.5: Whether the Wheatstone bridge causes congestion on line S_{12} (and also congestion on line S_{34} in the case of a symmetric Wheatstone network) depends on the susceptance of the Wheatstone bridge and the stability limit of line S_{12}. The "feasible region" above the line indicates susceptance-stability limit combinations that will not result in congestion on the network. The "infeasible region" below the line represents susceptance-stability limit combinations for which the network will become congested. Note that the x-axis has a logarithmic scale.

Figure 3.5 shows that unlike other networks such as internet communications (Milchtaich 2005), the existence of a Wheatstone configuration is not in itself sufficient for the network to exhibit Braess's Paradox. Equation (3.14) thus provides two "rules of thumb" for transmission planning. First, it shows conditions under which parallel networks can become more interconnected without causing congestion in the modified system. Second, it provides a condition on the line limit $F_{12}^{\max}$ under which a conversion of a parallel network to a Wheatstone network would be socially beneficial.

Why would the Wheatstone bridge ever be installed in a parallel system? One answer is that in some circumstances the bridge may provide reliability benefits. In the parameterization of the network represented in Figure 3.5, suppose that the load at bus 4 represents a customer with a high demand for reliability, that link S_{24} had an abnormally high outage rate, and that the generator at bus 4 did not exist. In this case, if the remainder of the links had sufficiently small stability limits, the network would not meet $(N-1)$ reliability criteria. With the addition of the Wheatstone bridge, the reliability criteria might be satisfied, but at the cost of a certain amount of congestion during those times in which link S_{24} was operating normally.[10] Thus, in the Wheatstone network, a tradeoff likely exists between the cost of congestion and the benefit of reliability.

3.4. DC Optimal Power Flow on the Wheatstone Network

Assume that the cost curves for the two generators in the symmetric unbalanced Wheatstone network are quadratic with the following parameterization:

(3.15) $C(P_{G1}) = 200 + 10.3P_{G1} + 0.008P_{G1}^2$

(3.16) $C(P_{G4}) = 300 + 50P_{G4} + 0.1P_{G4}^2$.

Also assume that every line in the network has a stability limit of 55 MW. Prior to the addition of the Wheatstone bridge, the DC optimal power flow results show that 50 MW

[10] Ideally, controllers would be installed on the system to prevent power from flowing over the Wheatstone bridge except during contingencies on link S_{24}. The congestion cost thus represents the value of such a controller to the system.

flows on each line towards bus 4; thus there is no congestion in the system. The nodal prices are all equal to \$12.11/MWh, and the total system cost is \$1,620 per hour.

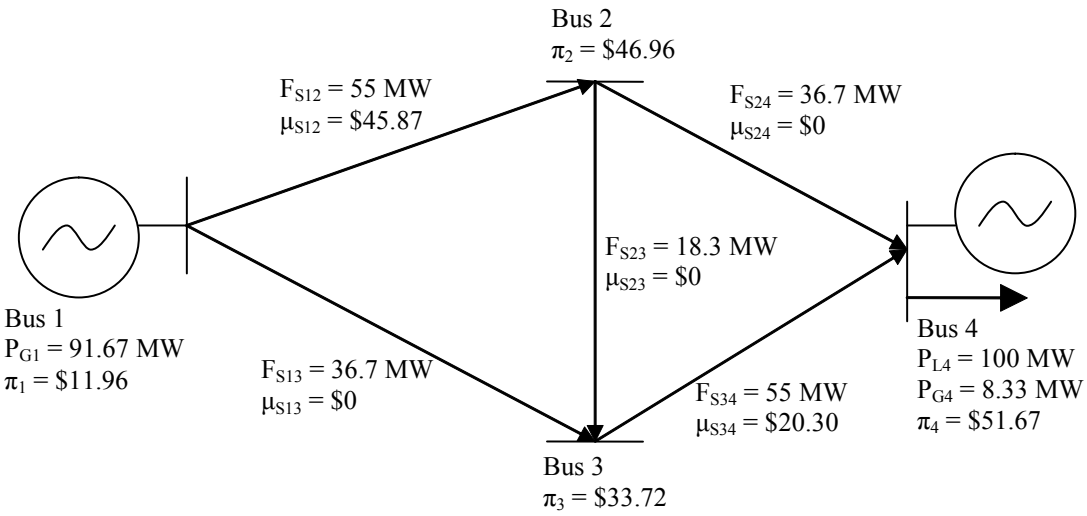

Figure 3.6: The addition of the Wheatstone bridge connecting buses 2 and 3 causes congestion along links S_{12} and S_{34}. The total system cost rises from \$1,620 per hour without the Wheatstone bridge to \$1,945 per hour with the bridge.

Following the addition of the Wheatstone bridge, lines S_{12} and S_{34} become congested, as shown in Figure 3.6. The total system cost rises to \$1,945 per hour as the economic dispatch is forced to run the expensive generator located at bus 4. Among other things, this implies that the value of reliability to the load is at least \$325 per hour that link S_{24} remains functional.

3.5. Implications of Braess's Paradox

Equations (3.13) and (3.14) from Section 3.3 have a number of implications for grid management and investment. Some of these implications mirror results described in

Section 3.1 for other types of networks, while some appear to be unique to electric power networks.

Result 3.1: A symmetric Wheatstone network is balanced (that is, $F_{23} = 0$) if and only if

$$\frac{X_{13}}{X_{12}} = \frac{X_{34}}{X_{24}}.$$

Before proving the result, we note that under the DC power flow approximation, $F_{23} = 0$ is equivalent to $\theta_2 = \theta_3$, so another way of stating the result is that $\theta_2 = \theta_3$ if and only if

$$\frac{X_{13}}{X_{12}} = \frac{X_{34}}{X_{24}}.$$

Proof of Result 3.1: The first part of the proof is to show that $\theta_2 = \theta_3 \Rightarrow \frac{X_{13}}{X_{12}} = \frac{X_{34}}{X_{24}}$.

Suppose that $\theta_2 = \theta_3$, and thus $F_{23} = 0$. Because all the power is flowing towards bus 4, and since there are no losses, this condition is equivalent to stating that $F_{12} = F_{24}$ and $F_{13} = F_{34}$. From the DC load flow equations, we see that

$$\begin{aligned} F_{12} = F_{24} &\Rightarrow \frac{1}{X_{12}}(\theta_1 - \theta_2) = \frac{1}{X_{24}}(\theta_2 - \theta_4) \\ &\Rightarrow \frac{X_{24}}{X_{12}} = \frac{(\theta_2 - \theta_4)}{(\theta_1 - \theta_2)}, \end{aligned}$$

and

$$F_{13} = F_{34} \Rightarrow \frac{1}{X_{13}}(\theta_1 - \theta_3) = \frac{1}{X_{34}}(\theta_3 - \theta_4)$$
$$\Rightarrow \frac{X_{34}}{X_{13}} = \frac{(\theta_3 - \theta_4)}{(\theta_1 - \theta_3)}.$$

Since $\theta_2 = \theta_3$, we see that $\frac{X_{24}}{X_{12}} = \frac{(\theta_2 - \theta_4)}{(\theta_1 - \theta_2)}$ and $\frac{X_{34}}{X_{13}} = \frac{(\theta_2 - \theta_4)}{(\theta_1 - \theta_2)}$; thus, $\frac{X_{13}}{X_{12}} = \frac{X_{34}}{X_{24}}$.

The second part of the proof is to show that $\theta_2 = \theta_3 \Leftarrow \frac{X_{13}}{X_{12}} = \frac{X_{34}}{X_{24}}$.

Suppose that $\frac{X_{13}}{X_{12}} = \frac{X_{34}}{X_{24}}$. From the DC load flow equations, we see that

$$\frac{X_{24}}{X_{12}} = \frac{F_{12}(\theta_2 - \theta_4)}{F_{24}(\theta_1 - \theta_2)}$$

and

$$\frac{X_{34}}{X_{13}} = \frac{F_{13}(\theta_3 - \theta_4)}{F_{34}(\theta_1 - \theta_3)}.$$

Since $\frac{X_{24}}{X_{12}} = \frac{X_{34}}{X_{13}}$, it must be true that $\frac{X_{24}}{X_{12}} \div \frac{X_{34}}{X_{13}} = 1$, and thus it must also be true that:

$$(3.17)\quad \frac{F_{13}(\theta_3-\theta_4)}{F_{34}(\theta_1-\theta_3)} \div \frac{F_{12}(\theta_2-\theta_4)}{F_{24}(\theta_1-\theta_2)} = 1.$$

By the symmetry of the network, we have $F_{12} = F_{34}$ and $F_{13} = F_{24}$. Thus,

$$(3.18)\quad \frac{F_{13}(\theta_3-\theta_4)}{F_{34}(\theta_1-\theta_3)} \div \frac{F_{12}(\theta_2-\theta_4)}{F_{24}(\theta_1-\theta_2)} = \frac{F_{13}^2}{F_{34}^2}\frac{(\theta_3-\theta_4)(\theta_1-\theta_2)}{(\theta_1-\theta_3)(\theta_2-\theta_4)}.$$

For (3.17) and (3.18) to hold, it must be true that $\theta_2 = \theta_3$ and thus, $F_{13} = F_{34}$.

Result 3.2: In a symmetric unbalanced Wheatstone network, suppose that links S_{12} and S_{34} are congested following the construction of the Wheatstone bridge, as in Figure 3.6. The congestion will be relieved, and the total system cost will decline, only to the extent that upgrades are performed on both lines.

Proof of Result 3.2: Using equations (3.12) and (3.14), for the case in which the Wheatstone bridge causes congestion:

$$(3.19)\quad F_{12}^{\max} - F_{12}^{old} \le F_{12}^{new} - F_{12}^{old} = B_{23}^{-1}\mathbf{A'}_{12}\,\mathbf{B^{-1}}\mathbf{A}_{23}B_{12}\delta_{23}^{old}$$

and

$$(3.20)\quad F_{34}^{\max} - F_{34}^{old} \le F_{34}^{new} - F_{34}^{old} = B_{23}^{-1}\mathbf{A'}_{34}\,\mathbf{B^{-1}}\mathbf{A}_{23}B_{34}\delta_{23}^{old}\ .$$

Since $B_{12} = B_{34}$, we get that $F_{34}^{\max} = F_{12}^{\max} \leq F_{12}^{new} = F_{34}^{new}$. Increasing only $F_{12}^{\max}$ will not change this relationship since $F_{34}^{\max} \leq F_{12}^{new} = F_{34}^{new}$ must still hold. A similar argument holds for increasing only $F_{34}^{\max}$.

If we increase the stability limit of both lines by the same amount, to $F^{\max,new}$, then the flows along lines S_{12} and S_{34} can simultaneously increase while maintaining the relationship $F_{34}^{\max,new} = F_{12}^{\max,new} \leq F_{12}^{new} = F_{34}^{new}$. A corollary to this result is that if the total cost (capital cost plus congestion cost) of the Wheatstone bridge exceeds the cost of upgrading the boundary links to the point where a failure on one link would not violate reliability criteria, then the Wheatstone bridge provides no net social benefit and should not be built.

Result 3.3: In the symmetric unbalanced Wheatstone network of Figure 3.6, the Lagrange multipliers on the congested lines are not necessarily unique. However, the sum of the multipliers on the two congested lines is unique. Further, the non-uniqueness is solely a function of the network topology, and is independent of the actual number of binding constraints.

Proof of Result 3.3: Another way of stating Result 3.3 is that in the symmetric unbalanced Wheatstone network of Figure 3.6, the DC line-flow constraints are not linearly independent. Thus, proving the result amounts to demonstrating that the

constraint set violates the constraint qualification condition of the Kuhn-Tucker theorem (Sundaram 1996). We will show this using the linearized DC optimal power flow.

Define $\mathbf{H} = \mathbf{A'B}^{\mathbf{diag}}\mathbf{A}$, and also define $\mathbf{c}$ to be a vector of generator marginal costs. In the linearized DC optimal power flow, $\mathbf{c}$ contains constants (i.e., all generators have constant marginal costs), and the power flow problem can be written as the following linear program:

$$(3.21) \quad \min \mathbf{c}'\mathbf{P}$$

such that:

$$(3.22a) \quad \mathbf{P} = \mathbf{B}\boldsymbol{\theta}$$
$$(3.22b) \quad \mathbf{F} = \mathbf{H}\boldsymbol{\theta}$$
$$(3.22c) \quad \mathbf{F} \leq \mathbf{F}^{\max}.$$

Rewriting to include the equality constraints, the optimal power flow problem is:

$$(3.21') \quad \min \mathbf{c}'\mathbf{B}\boldsymbol{\theta}$$

such that:

$$(3.22') \quad \mathbf{H}\boldsymbol{\theta} \leq \mathbf{F}^{\max}.$$

The constraint qualification condition says that at the optimal solution $\boldsymbol{\theta}^*$, the matrix derivative of the constraint set must have rank equal to the number of binding constraints. That is, if we define $g(\boldsymbol{\theta}) = \mathbf{H}\boldsymbol{\theta} - \mathbf{F}^{\max}$, and define $Dg(\boldsymbol{\theta})$ as the matrix whose (i, j)th entry is $\frac{\partial g_i}{\partial \theta_j}(\theta)$, then the constraint qualification condition is that the rank of $Dg(\boldsymbol{\theta}^*)$ be equal to the number of constraints that hold with equality.

In the case of the DC optimal power flow problem, we see that $Dg(\boldsymbol{\theta}^*)$ is a linear function of $\boldsymbol{\theta}^*$ and is independent of $\boldsymbol{\theta}^*$. Specifically,

$$Dg(\boldsymbol{\theta}^*) = \mathbf{H}'.$$

Thus, the constraint qualification condition for the DC power flow problem is that rank($\mathbf{H}$) be equal to the number of binding constraints.

The matrix $\mathbf{H}$ in the Wheatstone network is given by:

$$\mathbf{H}' = \begin{bmatrix} B_{12} & B_{13} & & & \\ -B_{12} & & B_{24} & & B_{23} \\ & -B_{13} & & B_{34} & -B_{23} \\ & & -B_{24} & -B_{34} & \end{bmatrix}.$$

Since we assume that the Wheatstone network is symmetric, it is easy to see that any column of **H** is a linear combination of the other columns. Thus, rank(**H**) = 3, meaning that only three of the five network constraints are linearly independent.[11]

Due to the symmetry and parameters of the problem, we can see that, at most, two constraints can be binding at the optimal solution. Since the combined capacity of links S_{12} and S_{13} is greater than the production capability of the generator at bus 1, these two lines cannot be simultaneously congested. Thus, the number of active constraints is less than the rank of **H**', and the constraint qualification condition for the Kuhn-Tucker theorem is not satisfied. The dual variables thus may not be unique.

In this special case, it is easy to see that the constraint qualification condition (for the inequality constraints) is violated. In larger and more complex networks, it may be more difficult; verifying the constraint qualification condition would require checking all possible combinations of binding constraints. In real systems, this combinatorial problem could get prohibitively large, particularly for calculations requiring fast solutions (such as calculating nodal prices).

Another way to verify the constraint qualification condition is to consider the dual of the DC optimal power flow problem. If we let μ be the vector of dual variables associated with the network line flow constraints in equation (3.22'), the dual problem can be written:

[11] The result that **H** is not of full rank is independent of the choice of reference bus. In many circumstances, **H** will have full rank, even without a reference bus being explicitly specified. For example, the rank of the complete **H** matrix in the IEEE 118-bus network is 118.

(3.23) $\max -\boldsymbol{\mu}' \mathbf{F}^{\max}$

such that

(3.24) $\mathbf{H}'\boldsymbol{\mu} + \mathbf{Bc} = \mathbf{0}$.

In the dual problem the matrix derivative of the dual constraints, evaluated at the optimal (dual) solution $\boldsymbol{\mu}^*$, is **H**. Since the rank of **H**' is equal to the rank of **H**, we again find that the rank of the derivative of the constraints is 3. In order to satisfy the constraint qualification condition for equality constraints, the rank of the derivative of the constraint matrix must be equal to the number of constraints.[12] In the dual formulation of the DC optimal power flow problem, there are four constraints. Thus, the dual problem does not satisfy the constraint qualification condition.

The rank of **H** provides a simple test for uniqueness of the nodal prices. The nodal prices are unique if the rank of **H** is equal to the number of buses in the network. Any system containing a symmetric Wheatstone sub-network will fail this rank test, since in that sub-network there will be linearly dependent line constraints. The Wheatstone network need not be unbalanced for the network to fail the rank test. Thus, the mere existence of a symmetric Wheatstone network is enough to result in a degenerate solution to the DC optimal power flow problem.

[12] This is really just the same condition as in the primal formulation, except that in the dual problem all constraints are assumed to hold with equality.

Result 3.4: Suppose that $F_l^{\max} = F_l$ for some line *l* in a symmetric unbalanced Wheatstone network in which $\delta_l^{old} > 0$. Increasing B_l for any *l* while simultaneously increasing $F_l^{\max}$ will increase the power flow on that line, even if the Wheatstone network is unbalanced.

Proof of Result 3.4: We are most interested in those situations in which line *l* is not the Wheatstone bridge, but the result will hold either way. The proof is a direct application of the formula of Ejebe and Wollenberg (1979), using equation (3.13'):

$$(3.13') \quad F_l^{new} = \left(F_l^{old} - \Delta B_l \delta_l^{old}\right)\left(1 - b_l^{-1} \mathbf{A'_l B^{-1} A_l}\right).$$

Calculate the sensitivity:

$$\begin{aligned} \frac{\partial F_l^{new}}{\partial \Delta B_l} &= \frac{\partial}{\partial \Delta B_l}\left(\Delta B_l \delta_l^{old} b_l^{-1} \mathbf{A'_l B^{-1} A_l}\right) \\ &= \frac{\partial}{\partial \Delta B_l}\left(\frac{\Delta B_l \delta_l^{old}}{\left(\Delta B_l \mathbf{A'_l B^{-1} A_l}\right)^{-1} + 1}\right) \\ &= \frac{\delta_l^{old}\left(\mathbf{A'_l B^{-1} A_l}\right)^2}{\left(\Delta B_l + \mathbf{A'_l B^{-1} A_l}\right)^2}. \end{aligned} \qquad (3.29)$$

To show that (3.29) is greater than zero, we note that $\delta_l^{old} > 0$ and $\Delta B_l > 0$ by assumption. For the power flow to have a solution, **B** must be positive definite, implying that $\mathbf{B^{-1}}$ is also positive definite and $\mathbf{A'_l B^{-1} A_l} > 0$.

Result 3.5: In a symmetric unbalanced Wheatstone network with fixed susceptances on the boundary links, the stability limits on the boundary links required to avoid congestion are strictly increasing in the susceptance of the Wheatstone bridge. Further, there is an upper bound on the boundary-link flow F_{12}^{crit} once the Wheatstone bridge is added.

Proof of Result 3.5: The first part of the claim, that the $F_{12}^{\max}$ required to keep the Wheatstone network from becoming congested is strictly increasing in ΔB_{23}, follows from equation (3.22). To prove the second part of the claim, we examine F_{12}^{new} in the limit as ΔB_{23} becomes arbitrarily large:

$$(3.30)\quad F_{12}^{crit} = \lim_{\Delta B_{23}\to\infty} F_{12}^{new} = \lim_{\Delta B_{23}\to\infty} F_{12}^{old} + \frac{\mathbf{A'}_{12}\mathbf{B^{-1}A}_{23} B_{12}\delta_{23}^{old}}{\Delta B_{23}^{-1} + \mathbf{A}_{23}\mathbf{'B^{-1}A}_{23}}$$
$$= F_{12}^{old} + \frac{\mathbf{A'}_{12}\mathbf{B^{-1}A}_{23} B_{12}\delta_{23}^{old}}{\mathbf{A}_{23}\mathbf{'B^{-1}A}_{23}}.$$

3.6. Discussion

Results 3.2 through 3.5 have the most interesting implications for pricing, grid management, and investment in the electric transmission network.

Result 3.2 mirrors the results of Milchtaich (2005) and Korilis et. al. (1997, 1999) for internet routing networks. It says that in a symmetric unbalanced Wheatstone network, congestion will occur on two of the four boundary lines (if any congestion occurs at all), and that network upgrades amounting to a capacity expansion on only one of those lines will not alter the dispatch. Both congested lines must be upgraded before the dispatch will be altered and the marginal and total system costs will be lowered. In other words, relieving congestion in Wheatstone configurations requires more than simply upgrading the most congested line. Congestion may occur on two of the boundary links in the Wheatstone network, but the active system constraint is either in those two links together, or in the Wheatstone bridge. Both interpretations are technically correct, but the policy implications are different. If the two boundary links represent the active system constraint, then either reducing demand or expanding capacity on both links would be optimal policies. If the Wheatstone bridge is viewed as the active system constraint, then the optimal policy would be to remove the bridge entirely, or (if the bridge was viewed as beneficial for reliability reasons) equip the bridge with fast relays or phase-angle regulation devices that would permit power to flow over the bridge only during contingencies. The preferable policy is largely a matter of network parameters and the state of technology.

Result 3.3 illustrates how nodal prices in the DC optimal power flow formulation may not always send clear signals to system operators and planners. Note that this phenomenon is general in the sense that it depends only on the network topology and not on the level of demand. The two congested lines in the Wheatstone network will, indeed,

sport non-negative shadow prices (see Figure 3.6, for example). While Wu et. al. (1996) note that nodal price differences do not always have the physical interpretation of being congestion costs, Results 3.2 and 3.3 taken together would seem to say that shadow prices in power networks do not necessarily represent the equilibrium value of capacity expansion in the network. Result 3.3 is particularly important in the context of electric industry restructuring, where nodal prices and shadow prices are supposed to guide operations and investment decisions. In the symmetric unbalanced Wheatstone network, the nodal prices and shadow prices are not representative of investments that would be profitable or socially beneficial. Chapters 4 and 6 will discuss this issue further in the context of transmission investment.

Result 3.3 also suggests that using the DC power flow approximation for the purpose of calculating nodal prices (as well as the value of transmission congestion contracts) may not be appropriate for all systems. One possible remedy is to replace the DC power flow model with a full AC power flow. The nonlinearities in the AC power flow model imply that the flow constraints on the transmission lines are more likely to be independent. As a side benefit, it would also allow for the optimization of real and reactive power dispatch and would account for marginal losses. The tradeoff is that the AC model is computationally more expensive.[13]

Another possible remedy would be a two-stage calculation of the nodal prices. The first stage would run the DC optimal power flow, as in equations (3.23) and (3.24). The second-stage optimization problem would choose from among the set of shadow prices

[13] Marija Ilić has also pointed out that the solution to the AC power flow problem may be non-unique.

satisfying the first-stage problem according to some decision rule. This two-stage method has been proposed in the telecommunications literature, where linear independence of the network flow constraints is rarely satisfied (Larson and Patriksson 1998).

Result 3.4 shows that increasing the susceptance, rather than the stability limit, of congested lines in the unbalanced Wheatstone network will have the desired effect of relieving some congestion. With respect to the current issue of investment in the grid, this suggests that strategically adding susceptance in concert with capacity should be considered as part of an optimal policy. In market settings, where policymakers have emphasized the role of non-utility parties in grid expansion, Result 3.4 also suggests that investors in the grid should be compensated for a portfolio of capacity (megawatts) and susceptance, and not just for capacity as is currently the case.[14]

Result 3.5 shows how congestion in Wheatstone networks can be prevented altogether. It provides an upper bound for the new flows on the boundary links following the construction of the Wheatstone bridge (for a fixed level of demand in the system). In the planning stage, the stability limit should be set above F^{crit} to avoid the problem of congestion in the Wheatstone network. This introduces yet another aspect of the cost-benefit calculus of the Wheatstone bridge. If the cost of attaining F^{crit} on the boundary links exceeds the total social cost of the Wheatstone bridge, then the boundary

[14] Of course, as Wu et. al. (1996) point out, it is possible to cause congestion by raising the susceptance of a line, so any such payments would need to be structured carefully.

links should be strengthened and the bridge should not be built; reliability criteria can be met more cheaply with a smaller number of higher-capacity transmission links.

3.7. Economic Welfare Analysis

Aside from causing congestion in the network, Braess's Paradox has implications for the economic welfare of the system, as well as distributional implications. The power market represented in the Wheatstone network is similar to that in Figure 2.2, shown here as Figure 3.7. Suppose that T_0 is the amount of power transferred across the network (from bus 1 to bus 4) for a given level of demand in the absence of any transmission constraints. Once the Wheatstone bridge is built, the transfer capability decreases to T^* (thus, $T_0 - T^*$ megawatts must be generated at the load bus).

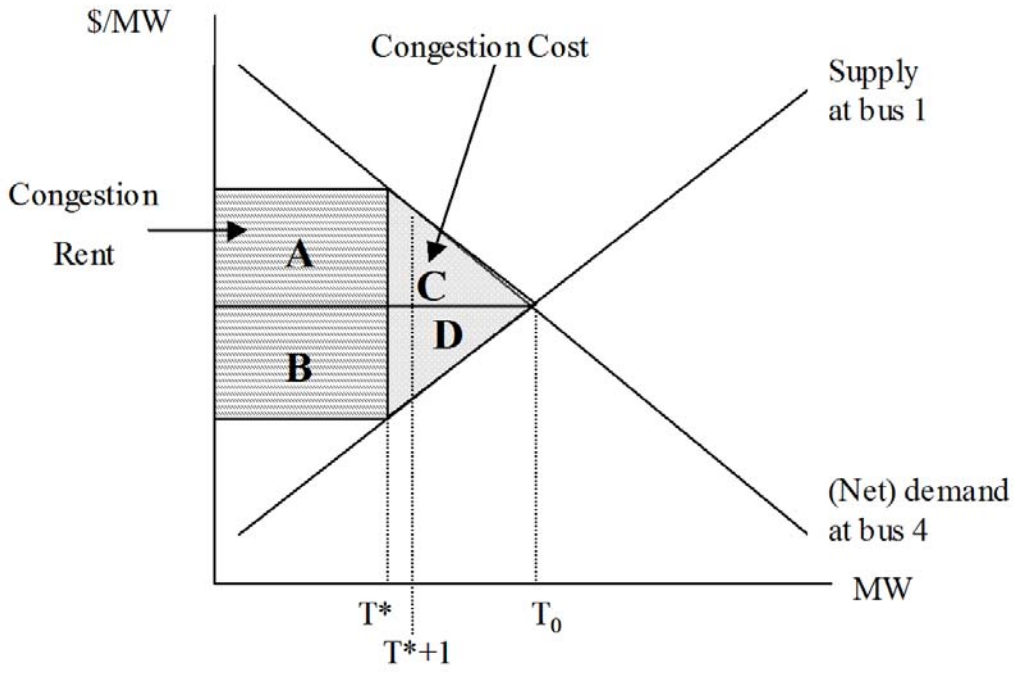

Figure 3.7: Distribution of congestion rent, congestion cost, and social surplus in the four-bus Wheatstone network.

Figure 3.7 illustrates two distinct welfare concepts. First, congestion in the network results in the generator at bus 4 collecting revenue that would not have been generated in the absence of congestion. This amount, equal to area *A* + *B* in Figure 3.7, is known as congestion rent (or merchandizing surplus) and can be calculated as $(\pi_4 - \pi_1)F_{12}^{\max}$. The area *C* + *D* represents extra congestion costs borne by the system, equal to the higher generation cost from having to use the generator at bus 4. Area *C* represents social wealth that is lost by consumers in the form of higher congestion costs, while area *D* represents the loss borne by producers. The general expression for the congestion cost is:

$$\text{(3.31)} \quad \text{CongCost} = \int_0^{T_0 - T^*} MC(P_{G4})dP_{G4} - \int_{T^*}^{T_0} MC(P_{G1})dP_{G1}.$$

Assume that there are no congestion contracts in the system; that is, assume that the merchandizing surplus amounts to a transfer of social wealth to the generator located at bus 4. Some of this wealth is transferred from consumers and some is transferred from the remaining producers in the system (i.e., the generator at bus 1).

The share of the social surplus transferred from the generator at bus 1 to the generator at bus 4 is given by:

$$\text{(3.32)} \quad \text{Producer surplus transferred to } G_4 = (\pi_0 - \pi_1)F_{12}^{\max},$$

where π_0 is the marginal cost of serving the load without congestion (this is also equal to the nodal price prevailing at all four buses in the system). Thus, the share of the social surplus transferred from consumers to the generator at bus 4 is given by the remainder:

(3.33) Consumer surplus transferred to $G_4 = (\pi_4 - \pi_0)F_{12}^{\max}$.

Given equations (3.32) and (3.33), we can calculate the total loss in producer surplus (ΔPS) and consumer surplus (ΔCS) as:

$$(3.34a) \qquad \Delta PS = (F_{12}^{old} - F_{12}^{\max})\pi_0 - \int_{F_{12}^{old}}^{F_{12}^{\max}} MC(P_{G1})dP_{G1}$$

$$(3.34b) \qquad \Delta CS = (\text{CongCost} - \Delta PS) + (\pi_4 - \pi_0)F_{12}^{\max}.$$

Equation (3.34a) represents producer surplus lost by the generator at bus 1. An amount $(\pi_0 - \pi_1)F_{12}^{\max}$ is simply transferred to the generator at bus 4 (and thus is still social wealth captured by producers), while the remainder of equation (3.34a) represents the social loss associated with having to use the generator at bus 4 to serve $F_{12}^{old} - F_{12}^{\max}$ megawatts of demand. The first term in the right-hand side of equation (3.34b) represents the consumers' share of total social wealth lost to congestion costs, while the second represents the transfer from consumers to the generator at bus 4 in the form of congestion rent.

Equations (3.34) can be applied to the system in Figure 3.6 to illustrate the social losses associated with a congested Wheatstone network. First, we note that with the

Wheatstone bridge, the hourly prices for a demand of 100 MW are π_1 = \$11.96/MW and π_4 = \$51.67/MW, per Figure 3.6. In the absence of the Wheatstone bridge, the prevailing price at all four nodes would be π_0 = \$12.11/MW. We note also that T_0 = 100 MW, and T^* = 91.67 MW. As noted in Section 3.2, the hourly congestion cost is equal to \$323.27.

First, we calculate the loss in producer surplus due to the addition of the Wheatstone bridge, using equation (3.34a):

$$\Delta PS = (100 - 91.67) \times 12.11 - (C_{G1}(100) - C_{G1}(91.67)) = \$0.71 \text{ per hour.}$$

From this, we evaluate equation (3.34b) to calculate the loss accrued by consumers:

$$\Delta CS = (323.27 - 0.71) + (51.67 - 12.11) \times 91.67 = \$3{,}949.03 .$$

Thus, we see that nearly all of the social losses are borne by consumers. Note that more than 90% of the loss in consumer surplus is reflected in the congestion rent transferred to the generator at bus 4.

3.8. Examples

To illustrate how the behavior described in Result 3.3 could arise in a more realistic and interconnected system than that shown in Figure 3.6, consider the 13-bus network of Figure 3.3. The network is based on the 14-bus IEEE test system, though the removal of

the network's synchronous condensers reduces the number of buses to 13. The assumed susceptance matrix of the network, in per-unit, is shown in Figure 3.8.

Generators are assumed to be located at buses 1, 2, and 8. For this example, the generator marginal cost curves are held constant at MC_{G1} = \$20/MWh, MC_{G2} = \$20/MWh, and MC_{G8} = \$40/MWh. All transmission lines are given a rated limit of 55 MW. The nodal demands are shown in Table 3.1.

B =

	1	**2**	**3**	**4**	**5**	**6**	**7**	**8**	**9**	**10**	**11**	**12**	**13**
1	-13.1	6.6	0	0	6.6	0	0	0	0	0	0	0	0
2	6.6	-28.0	9.8	6.4	5.3	0	0	0	0	0	0	0	0
3	0	9.8	-17.3	7.5	0	0	0	0	0	0	0	0	0
4	0	6.4	7.5	-27.6	6.6	0	5.1	1.9	0	0	0	0	0
5	6.6	5.3	0	6.6	-23.0	4.3	0	0	0	0	0	0	0
6	0	0	0	0	4.3	-16.2	0	0	0	5.3	3.2	3.7	0
7	0	0	0	5.1	0	0	-10.9	5.9	0	0	0	0	0
8	0	0	0	1.9	0	0	5.9	-20.6	9.1	0	0	0	3.8
9	0	0	0	0	0	0	0	9.1	-15.1	6.0	0	0	0
10	0	0	0	0	0	5.3	0	0	6.0	-11.2	0	0	0
11	0	0	0	0	0	3.2	0	0	0	0	-5.4	2.2	0
12	0	0	0	0	0	3.7	0	0	0	0	2.2	-8.8	2.9
13	0	0	0	0	0	0	0	3.8	0	0	0	2.9	-6.7

Figure 3.8: Susceptance matrix for the modified IEEE network in Figure 3.3.

Node	**Demand (MW)**
2	77.6
3	7.8
4	94.7
5	7.6
6	11.2
8	29.5
9	9
10	3.5
11	6.1
12	13.5
13	14.9

Table 3.1: Nodal demands in the 13-bus test system. All loads are given in MW, and all demand buses are modeled as PQ buses.

	Interior-Point Solution		Simplex Method	
Line	Flow (MW)	μ ($/MW)	Flow (MW)	μ ($/MW)
1,2	49.7	0	49.7	0
1,5	55.0	17.11	55.0	0
2,3	11.0	0	11.0	0
2,4	55.0	49.69	55.0	66.8
2,5	4.3	0	4.3	0
3,4	3.5	0	3.5	0
4,5	-52.4	0	-52.4	0
4,7	10.1	0	10.1	0
4,8	7.0	0	7.0	0
5,6	15.7	0	15.7	0
6,10	-18.5	0	-18.5	0
6,11	4.6	0	4.6	0
6,12	2.7	0	2.7	0
7,8	10.1	0	10.1	0
8,9	31.0	0	31.0	0
8,13	27.2	0	27.2	0
9,10	22.0	0	22.0	0
11,12	-1.5	0	-1.5	0
12,13	-12.3	0	-12.3	0

Table 3.2: In systems containing symmetric unbalanced Wheatstone networks, the shadow prices on congested lines may not be unique.

In this example, we will focus on the symmetric Wheatstone network consisting of buses 1, 2, 4, and 5. The nodal demands have been formulated to force lines S_{15} and S_{24} to become congested. A DC optimal power flow was run on the 13-bus system; the resulting line loadings and shadow prices are shown in Table 3.2.

The optimal power flow algorithm was run using two different methods. The first method is the interior-point default algorithm used in Matlab's `linprog` routine, which is a variation of the predictor-corrector method. The second is the simplex method,

which looks for corner solutions. Comparing the shadow prices in the columns of Table 3.2, the interior-point method computes two distinct positive shadow prices on the two congested transmission lines while the simplex method places a positive shadow price only on line S_{24}. The single nonzero shadow price calculated using the simplex method is assigned to the line which had the higher of the two shadow prices when the optimal power flow was run using Matlab's default interior-point solver. Whether there is any connection (whether line S_{24} being assigned the larger of the two shadow prices indicates that the constraint on line S_{24} is somehow more binding than the constraint on line S_{15}) is not clear.

Relaxing one of the two constraints in this case has no effect on the shadow prices or total dispatch cost computed by the OPF. The pattern of flows does change to accommodate the relaxed capacity constraint.

3.9. Conclusion

Let us briefly return to the three network characteristics arising from the study of Braess' Paradox in networks other than power systems, as mentioned in Section 3.1:

1. Braess's Paradox occurs only in Wheatstone networks, and these networks are guaranteed to exhibit the Paradox over a certain range of flows;
2. When the network is upgraded, such upgrades should be made system-wide and should not focus on correcting local congestion;
3. "Sources" should not be located far from "sinks," at least not topologically.

This chapter has largely addressed the first two points, although easy arguments can be made that the third is applicable to power systems just as it is to other systems. The first point, that the existence of Braess's Paradox and the Wheatstone network structure are equivalent, simply does not hold in power networks. The dependency actually fails to hold both ways. A network exhibiting Braess's Paradox is neither a necessary nor a sufficient condition for that network to have an embedded Wheatstone structure. Nor is the presence of congestion a necessary or sufficient condition for the network to have an embedded Wheatstone sub-network. The most general form of Braess's Paradox, that adding capacity can constrain a network, has been shown to hold for a simple two-bus parallel network. The conditions for a Wheatstone exhibiting Braess's Paradox are much more stringent in power systems than they appear to be in other networks. The line limits and susceptance of the Wheatstone bridge must be within certain limits for the addition of the bridge to constrain the system. Transmission and resource planners might keep this condition in mind to help determine optimal line limits for new and existing lines.

If a Wheatstone network is constrained by the addition of the bridge, increasing the capacity of one congested line will not remove the constraint. All congested lines must receive capacity upgrades, or the bridge must be disconnected. Thus, the second point (that system upgrades should not be made locally) seems to hold true in power systems. Local upgrades will at best do nothing and at worst shift the problem somewhere else. Further, focusing attention to upgrading the megawatt capacity of a line may, in the Wheatstone network, be misguided. Upgrading the line's susceptance can also have a beneficial effect, depending on the relative upgrade cost.

The discussion in this chapter has mentioned several times that the primary motivation for installing the Wheatstone bridge is that it may provide a reliability benefit. This reliability, however, comes at the cost of increased congestion. The amount of congestion actually caused is representative of the system's willingness-to-pay for flow control devices (relays, FACTS, and so on). Based on some simple simulations using the four-bus Wheatstone test network, the amount by which the reliability benefit will exceed the congestion cost over time is increasing in the variability of demand. Even with more variable demand levels, the probability of a line outage must be relatively large for the Wheatstone network to yield any net benefit over time. We will return to the issue of the congestion cost of the Wheatstone network and its reliability benefits in Chapter 6.

Chapter 4: The Efficiency of Point-to-Point Financial Transmission Rights is Limited by the Network Topology

Early visions of the restructured electric power industry envisioned replacing the transmission business of a regulated utility with a "transco," or regulated transmission company. Such entities would be responsible for maintaining and investing in the electric power grid, subject to rate-of-return regulation in much the same way as the regulated vertically-integrated utility (Joskow and Schmalensee 1983). This, however, subjects transmission to the same regulatory challenges that were supposed to be removed with the deregulation of the generation portion of the business. A further problem is that managing a large power grid is difficult. Managing congestion and deciding what upgrades are needed are extremely difficult tasks.

A different vision of electric-sector restructuring would place transmission under a market regime similar to generation. Sometimes called the "merchant transmission" model (Joskow and Tirole 2005a), this institutional arrangement would place the responsibility for transmission-grid investment and enhancement on independent transmission companies, much in the same way that the deregulated generation sector looks to merchant generation to maintain resource adequacy.[1] The merchant transmission model, like the merchant generation model, relies on nodal prices to send signals to investors in a competitive environment. Price signals would provide incentives for

[1] The merchant transmission model has a number of variations other than the direct analogue to merchant generation. One such variation is "participant-funded transmission," in which a group of firms (possibly including merchant parties) makes a joint investment in new transmission infrastructure.

independent transmission companies to invest in the grid so as to alleviate congestion; these companies would then earn a return on their investment based on nodal price differences.

To operate a large grid efficiently, a transco needs to solve the same problems as the merchant model, absent the incentive problem. Managing a network above a small size requires calculating congestion costs and indicators of where investments are needed. Thus, the only major difference between managing a transco and merchant transmission is the incentives that each face.

4.1. The Merchant Transmission Model

The rationale for the merchant transmission model, as discussed by Hogan (1992), Chao and Peck (1996) and Bushnell and Stoft (1996, 1997), and more recently analyzed by Joskow and Tirole (2005a) rests on the analysis of investment incentives shown in Figure 4.1.[2] As in Chapter 2, we assume that the socially optimal amount of transmission between the two buses in the system is T_0 and that the actual amount of transmission is T^*. The total congestion rent is given by $(\pi_2 - \pi_1)T^*$.[3] Assuming that network upgrades are compensated on the basis of this congestion rent, an investor other than the incumbent utility upgrading the transmission line by one megawatt would earn $(\hat{\pi}_2 - \hat{\pi}_1)(T^*+1)$.[4] If the construction cost were less than this amount, then the non-utility investor would proceed with the upgrade. A vertically-integrated utility investor,

[2] Figure 4.1 draws on Figure 2.2 from Chapter 2.
[3] We use "optimal" in the sense of solving the transmission-planning problem in equations (1.1) or (1.2).
[4] This also assumes that the payment is based on the shadow price of transmission congestion.

on the other hand, would have to weigh the construction cost and the loss of congestion rent against the savings in generation costs from being able to dispatch an additional megawatt from bus 1 (and against any congestion rent earned on the first *T** units of transmission capacity). Thus, the argument for merchant transmission rests on the degree to which a utility's investment decisions are distorted by its monopoly status.

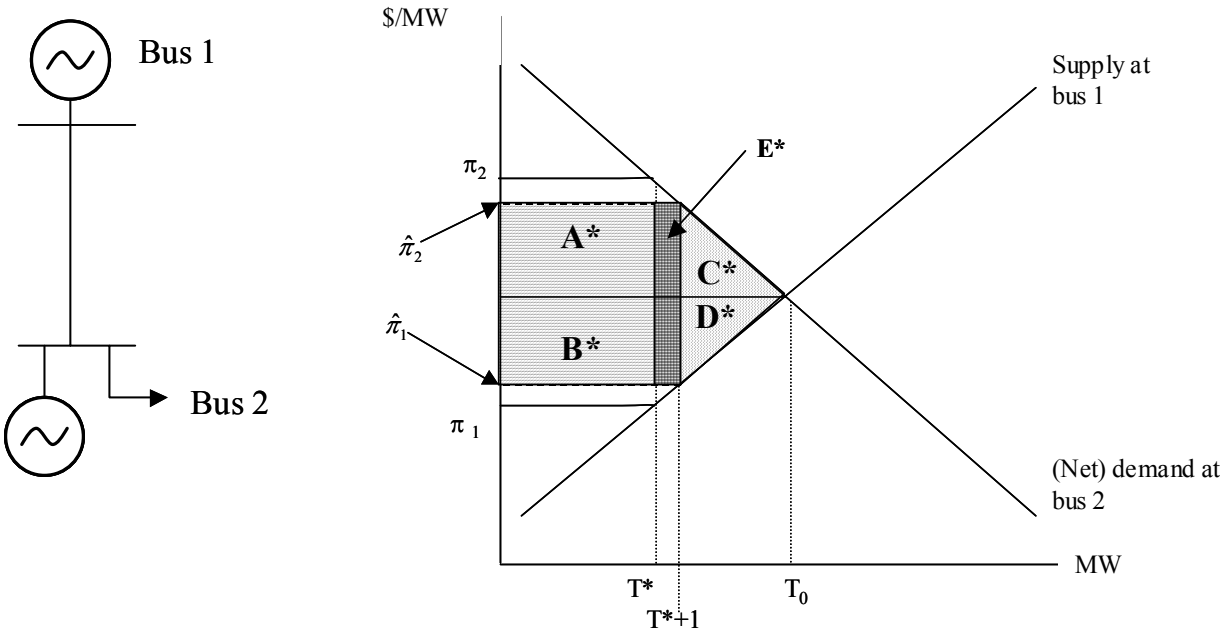

Figure 4.1: A vertically-integrated utility performing an incremental upgrade on the transmission line connecting buses 1 and 2 would have to weigh the benefit of lost congestion rent, equal to $(\pi_2 - \pi_1)T^* - (\hat{\pi}_2 - \hat{\pi}_1)(T^* + 1)$*, against the savings in dispatch cost, equal to* $\hat{\pi}_2 - \hat{\pi}_1$ *(area E*). A merchant transmission company considering an incremental upgrade on the transmission line would earn congestion rent equal to* $(\hat{\pi}_2 - \hat{\pi}_1)(T^* + 1)$*, and would invest if the rents exceeded the construction cost.*

The merchant transmission model has come under attack on a number of fronts. Chapter 2 discussed the free-rider effect associated with merchant transmission investment; since the merchant only captures congestion rent and not any of the added social surplus (the amount by which the triangle *C* +*D* shrinks in Figure 4.1), there may

be some socially beneficial projects that would not pass the merchant's private cost-benefit test. Side payments from consumers or other generators in the system would be required to induce the merchant to invest in the upgrade.

Oren (1997) analyzes the behavior of competitive generators in congested systems and finds that the combination of congestion and FTRs encourages implicit Cournot collusion among the generators.[5] Yu, Leotard, and Ilić (1999) argue that network investments should be viewed as risk-management activities and not through the lens of supporting competition in the generation market.[6] Joskow and Tirole (2005a) examine the implications of relaxing the stringent economic assumptions underlying the Bushnell-Stoft FTR efficiency theorem. Unsurprisingly, they find that relaxing the competitive and static assumptions introduces inefficiencies, and suggest that in the real electric power industry, the merchant transmission model may be untenable.

The final problem with the merchant model rests on a failure in locational marginal pricing. Shadow prices can be good signals as to which lines are congested (and thus act as signals to avoid scheduling on these lines), but in meshed networks they often do not tell planners how the constraints should be relieved. As an example, consider the unbalanced Wheatstone network in Figure 4.2.[7] The existence of the Wheatstone bridge (link S_{23}) causes congestion on lines S_{12} and S_{34}. Running a DC optimal power flow on

[5] Naturally, Oren (1997) suggests that this problem will not occur in systems with tradeable flowgate rights.
[6] Still, if competition among generators is to flourish, then the transmission grid must be robust enough to facilitate such competition (Lave, Apt, and Blumsack 2004). Thus, one important issue is who should bear the risk.
[7] This test network was described in more detail in Chapter 3. These network structures are quite common in realistic systems; for example, the IEEE 14-bus test network has at least six embedded Wheatstone subnetworks.

the network in Figure 4.2 yields Lagrange multipliers of \$45.87 on line S_{12} and \$20.30 on line S_{34}.[8]

In a competitive market for flowgate rights, the value of transmission contracts on these two links would be based on these Lagrange multipliers. The other, uncongested links, would have zero value attached to their associated transmission contracts.

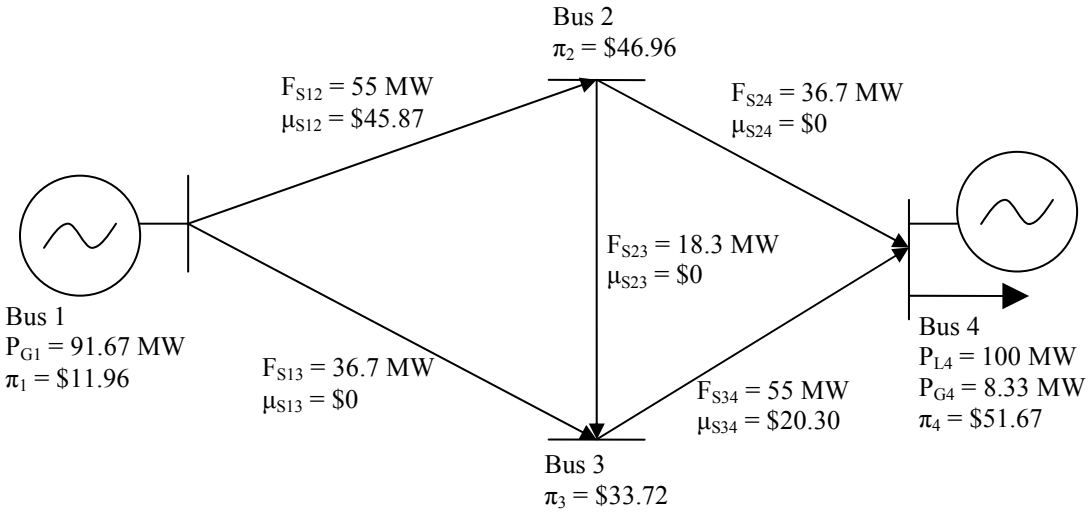

Figure 4.2: A Wheatstone transmission network. The nodal prices and shadow prices for transmission are obtained from a DC optimal power flow simulation. Each line has a stability limit of 55 MW.

Under market-based transmission provision, the positive flowgate value assigned to links S_{12} and S_{34} should signal independent transmission companies to invest in either of those two lines. However, the parameters of the network in Figure 4.2 yield misleading signals in two important respects, as discussed in Chapter 3. First, conservation of energy and the symmetry of the network impliy that increasing the carrying capacity of either of lines

[8] The load at bus 2 has a constant real power demand of 100 MW. The line resistances are all 0.03 per-unit, except for lines S_{13} and S_{24}, which have resistances of 0.06 per-unit. The cost curves for the generators are $C(P_{G1}) = 200 + 10.3P_{G1} + 0.008P_{G1}^2$ and $C(P_{G4}) = 300 + 50P_{G4} + 0.1P_{G4}^2$.

S_{12} or S_{34} without increasing the capacity of the other will not relieve congestion on the system. This phenomenon is a function of the network parameters since the network in Figure 4.2 is symmetric, in the sense that the admittances on lines S_{12} and S_{34} are identical and the admittances on lines S_{13} and S_{24} are identical. Conservation of energy requires that the flow patterns in the cut sets represented by buses {1,2,3} and buses {2,3,4} be identical. Second, the shadow prices obtained through the linearized optimal power flow are not unique. Symmetry in the network implies symmetry in the constraint set; the transmission-line flow constraints are parallel to one another. Thus, the correct signal is actually the sum of the two positive shadow prices, indicating that both transmission constraints would need to be relieved before the system would see any benefit.[9]

It may seem obvious that the price signals in the network of Figure 4.2 are misleading. But in larger networks, it may be more difficult to identify which price signals are misleading, particularly if network participants cannot identify sub-topologies similar to the Wheatstone network. A merchant or other investor, given incentives solely through nodal and/or shadow prices, might make an investment (and earn a return on the investment, paid for by consumers on the grid) without resolving any congestion in the network.

Hogan (1992) and Bushnell and Stoft (1996) have advocated a system of point-to-point transmission rights, combined with a feasibility allocation rule, instead of the flowgate

[9] An alternative would be to disconnect line S_{23} from the system entirely. In this case, the network would reduce to a purely parallel system, with 50 MW flowing along each path. Line S_{23} might, however, be justified on the basis of some system security or reliability criteria. Chapter 6 includes a quantitative analysis of these tradeoffs.

model. The feasibility allocation rule is based on the "revenue adequacy theorem" proven by Hogan (1992) and Wu et. al. (1996), which shows that the total congestion rent earned by a centralized transmission authority defines the revenue possibility frontier for an independent transmission company operating under a system of FTRs.[10] If FTRs are allocated in such a way that the net position of all the players in the system is identical to the actual flow of power through the system, then the holders of FTRs will have maximized revenue. Further, Bushnell and Stoft (1996) show that when the feasibility condition is satsified, under a number of other assumptions (including constant returns to scale and marginal-cost pricing in spot and forward energy markets), then profitable investments are also socially beneficial. Attempts to extort the system by making detrimental investments will yield negative returns for the merchant transmission company. Thus, the feasibility allocation rule for FTRs allows for economically efficient merchant transmission.

History has largely supported the analysis of Joskow and Tirole (2005a). Enthusiasm for the purest form of the merchant transmission model has largely waned, amid the deteriorating financial position of the merchant sector in electricity (Joskow 2005a, Blumsack, Apt, and Lave 2005) and the realization that siting costs, which are not reflected in the short-run locational price calculations may be the dominant factor in determining which projects are built and which are not (Vajjhalla and Fischbeck 2006). RTOs in the northeastern U.S., however, still appear to support the merchant transmission

[10] The original motivation for the revenue adequacy theorem was a solvency condition for the transco. This would ensure that the transco collected enough congestion revenue to fulfill its FTR obligations. More recently, Lesieutre and Hiskens (2005) have shown that the revenue adequacy theorem fails to hold in AC power flows due to nonconvexity. Since most RTOs use the DC load flow approximation to determine the feasible set of FTRs, the issue may be moot.

model, and continue to dangle FTRs as carrots in exchange for investment (see, for example, New York ISO 2005). The contract network is thus not as dead as it might appear.

The analysis of Chapter 3 suggests examples where merchant transmission might lead to economic inefficiencies. We elaborate on that analysis here to show the precise problem with the merchant model, and more importantly to show the difficulties in designing and pricing a transmission grid to serve markets that have undergone restructuring.

Even if all of the assumptions used by Hogan (1992) and Bushnell and Stoft (1996) in formulating the contract network hold, there still may be network-specific adverse incentive problems associated with merchant transmission. Allocation of incremental FTRs to merchant transmission provides an incentive to increase the grid capacity in directions in which market participants expect to be using the grid and in which they have nominated and have been awarded FTRs. At the same time merchant transmission may affect capacity in unexpected directions in which little or no FTRs were nominated. The merchant investment can be detrimental if actual flows on the grid move in these unexpected directions. Thus, under certain network specifications with point-to-point FTRs, independent transmission companies may still be able to profitably add links to a network in ways that cause congestion in other parts of the network.

4.2 FTR Efficiency Theorems and Counterexamples

An FTR is defined as a contract that entitles the holder to the nodal price difference between any two points in the network times the number of megawatts specified in the contract, for the duration specified in the contract. Following Bushnell and Stoft (1996), we will denote an FTR of size *m* between nodes *i* and *j* by an *n*-vector **m** whose only nonzero entries are *–m* in the *i*th row, and *m* in the *j*th row. The revenue stream accruing from an individual FTR in a given hour is therefore $\boldsymbol{\pi}'\mathbf{m}$, where $\boldsymbol{\pi}$ is the *n*-vector of hourly nodal prices. Since FTRs that are equal in magnitude and duration, but in opposing directions cancel each other out, we can write the total (net) amount of FTRs in the entire system as $\mathbf{M} = \sum_k \mathbf{m}_k$ and the total revenue earned by all parties in the system as $\boldsymbol{\pi}'\mathbf{M}$. Further, define a dispatch as a vector of nodal (net) real power injections **p**, where p_i is the real power injection at node *i*. The system dispatch can similarly be defined as a vector $\mathbf{P} = \sum_k \mathbf{p}_k$. Contracts are said to match dispatch at the individual level if **m** = -**p**, and at the systemwide level if $\mathbf{M} = -\mathbf{P}$. The physical interpretation of contracts matching dispatch is that any physical transaction (e.g., on the spot market) is cancelled out by an equal (in MW magnitude) FTR. Thus, the condition that contracts match dispatch is equivalent to individual market participants or the system as a whole being perfectly hedged (Patiño-Echeverri 2006). On a more general level, a set of FTRs is said to be feasible if an equivalent dispatch would not violate any of the system constraints.

In addition, Bushnell and Stoft define the social surplus arising from a system dispatch **P**, denoted $W(\mathbf{P})$, as the difference between the total benefit enjoyed by all loads in the system and the (minimized) total cost of serving that load. Thus, $W(\mathbf{P}) = \sum_k C_k(\mathbf{p}^*_k)$, where **p*** is the cost-minimizing dispatch vector and C(**p**) is the (convex) cost or benefit function at each node in the system. Benefits are assumed to have a positive sign and costs are assumed to have a negative sign.

Bushnell and Stoft offer two key results that imply the economic efficiency of FTRs. The first, which is Lemma 2 in their 1996 paper, says that any player in the system whose individual contracts match their individual dispatch will be at least as well off in the event of a change in (optimal) nodal prices in the system. The second result, which Bushnell and Stoft refer to as Theorem 2, says that when contracts match dispatch at the system level, then any player who causes congestion through their investments in the grid will be compensated by a set of FTRs that have a negative value. The Wheatstone network shown in Figure 4.2 can be used to construct counterexamples to both of these assertions.

Lemma 2 (Bushnell and Stoft): For any player in the system whose contracts match its dispatch (so **m** = **-p** for that player), the net benefit accruing to that player is greater than or equal to zero for any price change.

Counterexample to Lemma 2: Bushnell and Stoft define net benefits for the *k*th player as $NB = \boldsymbol{\pi}'\mathbf{p}_k - \boldsymbol{\pi}'\mathbf{m}_k - C_k(\mathbf{p}_k)$. They show that if contracts match dispatch, $\mathbf{m}_k = -\mathbf{p}_k$, then the change in net benefit accruing to the *k*th player after any price change is:

$$\Delta NB = \boldsymbol{\pi}^{*\prime}(\mathbf{p}^*_k - \mathbf{p}_k) - \left(C_k(\mathbf{p}^*_k) - C_k(\mathbf{p}_k)\right),$$

where variables with asterisks refer to the new set of prices and associated optimal quantities. Lemma 2 states that $\Delta NB \geq 0$; the proof uses the convexity of C_k, as well as the assumption that nodal price differences in the network reflect differences in marginal costs (and congestion costs). As noted in Chapter 3, the symmetry of the Wheatstone network leads to non-convexities in the constraint set of the optimal power flow problem. Lemma 2 of Bushnell and Stoft will not necessarily hold in the face of these non-convexities.

Consider the generator located at node 1 in the network shown in Figure 4.2. The cost function of the generator is assumed to be $C(P_{G1}) = 200 + 10.3P_{G1} + 0.009P_{G1}^2$. Assume that the only spot market position taken by the generator is to inject power into the grid at node 1. In other words, the **p** vectors for generator 1 contains all zeros except for the real power production of the generator, which is in the first entry of the injection vector:

$$p_{G1} = \begin{pmatrix} P_{G1} \\ 0 \\ 0 \\ 0 \end{pmatrix}$$

$$p^*_{G1} = \begin{pmatrix} P^*_{G1} \\ 0 \\ 0 \\ 0 \end{pmatrix}.$$

In addition to injecting P_{G1} MW of real power into the grid, suppose that the generator's contracts match its dispatch; thus, the generator also has an FTR between node 1 and any other node in the network. The size of the FTR is equal to P_{G1} in magnitude.

Suppose that prior to the construction of the link between nodes 2 and 3 of the network in Figure 4.2, the generator at node 1 could supply the entire load at a lower cost than generator 2. Thus, P_{G1} = 100 MW and $\mathbf{p}_{G1}$ = (100, 0, 0, 0). After the construction of the link between nodes 2 and 3, the network becomes congested and generator 1 is only able to supply 91.67 MW (as shown in Figure 4.2). Thus, $\mathbf{p}^*_{G1}$ = (91.67, 0, 0, 0). The vector of nodal prices following the network expansion is $\boldsymbol{\pi}^*$ = (11.96, 46.96, 33.72, 51.67). According to the formula derived by Bushnell and Stoft, the change in net benefit to generator 1 from the construction of line S_{23} is:

$$\Delta NB = \begin{pmatrix} 11.96 \\ 46.96 \\ 33.72 \\ 51.67 \end{pmatrix}' \left(\begin{pmatrix} 91.67 \\ 0 \\ 0 \\ 0 \end{pmatrix} - \begin{pmatrix} 100 \\ 0 \\ 0 \\ 0 \end{pmatrix} \right) - \left[C_{G1}(91.67) - C_{G1}(100) \right] = -1.05 .$$

Thus, generator 1 sees her net benefit decline with the addition of the Wheatstone bridge to the network. This is contrary to the assertion in Lemma 2 of Bushnell and Stoft that fully-hedged market participants cannot be harmed by network additions that cause nodal prices to change.

Theorem 2 (Bushnell and Stoft): Suppose that the total set of FTRs in the system matches the systemwide dispatch (so that **M** = **-P**), and suppose that an investment is made in the grid which lowers the social surplus of the system, so that $\Delta W < 0$. If the new set of FTRs **m*** allocated to the builder of the detrimental investment is feasible, then the revenue stream arising from these new FTRs will be negative and larger in magnitude than the loss in social surplus. Mathematically, $\boldsymbol{\pi}^{*\prime}\mathbf{m}^* < 0$ and $\boldsymbol{\pi}^{*\prime}\mathbf{m}^* < \Delta W$, where $\boldsymbol{\pi}^*$ represents the vector of (optimal) nodal prices after the new investment is made.

Theorem 2 is meant to illustrate that no player or group of players (whether they be merchant transmission owners or not) would ever have an incentive to modify the grid in such a way as to cause additional congestion in the network. (Bushnell and Stoft state this explicitly in their two corollaries to Theorem 2.) The proof of Theorem 2 offered by Bushnell and Stoft makes use of Lemma 2. However, since the result in Lemma 2 does

not necessarily hold in the Wheatstone network of Figure 4.2, it follows that Theorem 2 does not necessarily hold.

Counterexample to Theorem 2: Again, we will use the Wheatstone network of Figure 4.2 as an example. Suppose that a merchant transmission company decided to build a link between nodes 2 and 3 in the network of Figure 4.2. The stability limit of line S_{23} is 55 MW. According to the feasibility allocation rule, the merchant transmission owner would be free to take up to 55 MW worth of FTRs in either direction (from node 2 to node 3 or from node 3 to node 2). In this case, line S_{23} causes congestion along line S_{12}, so the nodal price at node 2 is greater than the nodal price at node 3. The total cost of serving the load without line S_{23} is \$1,622.20, while the total cost of serving the load with line S_{23} is \$1,945.50. The difference in social surplus is therefore \$323.30. The profit-maximizing merchant transmisson owner would clearly take the FTRs from node 2 to node 3, earning a net benefit of $\pi_2 - \pi_3 = \$46.96 - \$33.72 = \$13.24$ per MW.[11]

Another counterexample to Theorem 2: The first counterexample to theorem 2 is somewhat weak in the sense that the positive net benefit earned by the merchant transmission company could be made negative by forcing the merchant transmission owner to accept an allocation of FTRs that matches the dispatch along the new line.[12] In this case, when the merchant transmission company builds a line connecting nodes 2 and

[11] In private communication, Dmitri Perekhodtsev has suggested that in reality, RTOs would insist that the investor has not added capacity between buses 2 and 3, but rather has reduced capacity between buses 1 and 4. In both the flowgate model and in the admittance-payment formulation of Gribik et. al. (2005), this point is moot, since payments are only made in the case of congested lines. Both the feasibility allocation rule discussed by Bushnell and Stoft (1996) and actual RTO protocols are vague on this issue.

[12] This is technically a stronger condition than that suggested by Bushnell and Stoft, but similar rules are used by exisiting RTOs. For examples, see PJM (2006), New York ISO (2006), and ISO New England (2006).

3, they will be forced to take 18.3 MW of FTRs from node 3 to node 2. The net benefit of these FTRs is 18.3 MW × ($33.72 - $46.96) = -$242.29, which is in fact negative, although smaller in magnitude than the -$323.30 loss in social surplus from the construction of line S_{23}.

Note that after construction of the new line, the load carried on lines S_{12} and S_{34} increases to 55 MW. For the feasibility rule to be maintained, the merchant transmission company would then be given FTRs in order to match the dispatch on lines S_{12} and S_{34}. This would involve acquiring 5 MW of FTRs from node 2 to node 1 and 5 MW of FTRs from node 4 to node 3. The net benefit to the merchant transmission company from this transaction would be equal to:

$$5 \times (\pi_2 - \pi_1) + 5 \times (\pi_4 - \pi_3)$$

$$= 5 \times [(\$46.96 - \$11.96) + (\$51.67 - \$33.72) = \$264.75.$$

Combining the net loss from the allocated FTRs on line S_{23} and the net gain from the acquired FTRs on lines S_{12} and S_{34}, the total net benefit to the merchant transmission company is $264.75 - $242.29 = $22.46, so the merchant transmission company would still see a net benefit from adding the constraining line to the system. Recall that the construction of the Wheatstone bridge increases the system cost by $323.30, which is larger in magnitude than the profits (net of side payments) earned by the investor. Thus, the system sees a net loss in social surplus (a deadweight loss) from the construction of link S_{23}.

4.3. Discussion and Conclusions

Although restructuring in the electric power sector has largely been focused on generation, with the liberalization of markets for electric energy, arguments have been made that the transmission segment of the industry could operate efficiently under a competitive model. Central to the success of commoditization of transmission is a competitive market for transmission contracts that will allocate generation resources efficiently and encourage investment in new transmission assets in the right places. Two market-based models have been proposed for such a merchant transmission sector. Both use the difference in locational prices as signals for investment. The flowgate rights model would place a positive value on transmission contracts only for congested lines; the FTR model would use point-to-point nodal price differences for any nodes, regardless of their geographic proximity or the presence of congestion.

Under the contract network regime suggested by Hogan (1992), flowgate rights have been criticized for giving independent players an incentive to modify the grid in detrimental ways. The theorems of Bushnell and Stoft (1996) would support the FTR model. The efficiency of the FTR model has been criticized on economic grounds by Joskow and Tirole (2005a) who argue that the assumptions used by Bushnell and Stoft are unrealistically strict.

Regardless of the economic assumptions made, the efficiency of a contract network with point-to-point financial transmission rights is not independent of the network topology. The counterexamples provided here using the Wheatstone network show that even if

contract markets are complete and competitive, independent players can still invest in the grid in ways that are profitable, but not socially beneficial. The counterexamples also show that grid investments must be evaluated on a case-by-case basis; simply expanding the grid will not benefit all parties, even in the presence of a robust transmission contract market. The results also caution a transco that making investments to upgrade their grid is more difficult than relieving the most congested line.

Chapter 5: Detecting and Analyzing Wheatstone Structures in Larger Networks

Chapter 3 derived several important properties regarding the behavior of Wheatstone subnetworks within larger systems:

1. The network does not display localized response. That is, upgrading the capacity on one of the two congested lines will not relieve the systemwide constraint.
2. The shadow prices on transmission generated by optimal power flow calculations are positive in the case of congested lines and zero in the case of uncongested lines. They may not show the true value of incremental upgrades to congested lines.
3. Unlike in other sorts of networks, the existence of an embedded Wheatstone sub-network is neither a necessary nor a sufficient condition for a power network to exhibit the Braess Paradox.
4. Locational marginal prices are effective tools for identifying congestion, but in many cases are not effective in suggesting how to best go about relieving constraints.

Compensating investors with transmission contracts based on nodal prices or the shadow price of transmission across a given path can provide opportunities for investors to earn profits while simultaneously lowering the capacity of the system. Flowgate rights can

provide poor incentives since each new path creates a potential new physical right to be traded in the transmission market (Chao and Peck 1996, Hogan 2000). Adding lines that constrain the system will necessarily create new flowgates with positive value. Bushnell and Stoft (1996, 1997) illustrate how the use of point-to-point financial transmission rights, allocated according to Hogan's (1992) feasibility rule, can encourage efficient investment in the system by non-utility transmission companies. However, as Chapter 4 illustrated, even if FTRs are handed out in an enlightened way, certain network topologies can still allow investors to profit from modifying the grid in detrimental ways. Either a merchant or a utility investor, therefore, could potentiallybenefit from converting a parallel network into a Wheatstone network.

The point of Apt and Lave (2003) is well-taken here: LMP may be a good operational tool, encouraging market participants not to schedule over congested lines, but in many cases cannot convey enough information about the system for planning and investment purposes. Contrary to the claims of Bushnell and Stoft (1996, 1997) or Oren (1997), the use of nodal prices cannot systematically substitute for the traditional transmission planning method. Nodal prices alone will not yield a globally optimal investment plan, and scenario-based transmission planning can do no better than a local optimum.

Knowledge of the network's topological properties can aid in both system operations and planning. The ability to identify and detect Wheatstone sub-networks can be particularly helpful. This chapter develops a two-part tool to analyze embedded Wheatstone sub-networks within larger systems. The first part of the tool is a heuristic network

search algorithm that uses several unique graph-theoretic properties of Wheatstone networks to identify them within larger systems. Given a known set of Wheatstone sub-networks, the second part of the tool analyzes the impact of each particular Wheatstone on the remainder of the network by constructing an equivalent external network. In effect, the state of the remainder of the network is held constant, and interactions between the embedded Wheatstone and the external network are modeled as bulk injections/withdrawals at each of the four Wheatstone nodes. Embedded Wheatstone networks can thus be analyzed in the same way as the standalone Wheatstone test network developed in Chapter 3.

5.1 A Graph-Theoretic Approach to Network Search

Wheatstone networks are ubiquitous in real electric power systems. The IEEE 14-bus network, a modified version of which is shown in Figure 3.3, has at least six Wheatstone sub-networks. In small networks such as the IEEE 14-bus network, Wheatstone structures can be found easily by visual inspection. In real power networks, which may have tens or hundreds of thousands of buses, a more systematic approach is needed.

A purely combinatorial approach to finding embedded Wheatstone structures is possible on extremely small scales, but quickly becomes infeasible as the number of nodes increases. On a topological basis alone, comparing all four-node substructures of an n-bus network requires checking 4^n different combinations. To find all Wheatstone networks in the IEEE 14-bus network by brute force would therefore require 2.7×10^8 calculations. Checking for Wheatstones in the IEEE 118-bus network would require

approximately 10^{71} calculations. By comparison, the approximate number of seconds since the beginning of the universe is only 3×10^{17}.

Designing a feasible algorithm for detecting Wheatstone sub-networks is essentially a problem of decomposing the network into portions that might represent Wheatstones, and portions that definitely do not. From a graph-theoretic perspective, electric power systems are nice test-beds for decomposition algorithms, since they tend to be very sparsely connected, with a given bus attached to a reasonably small number of other buses.

Gabriel Kron (1953) and Henry Happ (1973, 1974) pioneered the study of diakoptics, or tearing, in electric circuits. Kron, in particular, developed a method of tearing very large physical systems into smaller, tractable sub-systems. Each of these sub-systems could be analyzed separately and then the pieces could be put back together. Kron and Happ focused on applying this method to the analysis of large power systems; a more general mathematical formulation, applicable to general physical systems, is provided by Aitchison (1983).

Inspired by the study of electric circuits, Duffin (1965) shows that, on a purely topological basis, any network can be decomposed into series-parallel sub-networks and Wheatstone sub-networks. Milchtaich (2005) provides a similar proof for more general networks.

The approach taken here to identifying and analyzing Wheatstone sub-networks borrows heavily from the ideas of graph theory and network analysis, and is therefore more in line with the topological decompositions suggested by Duffin and Milchtaich than the explicit physical models underlying the diakoptics of Kron and Happ.

Newman (2003) discusses how network theory has evolved from primarily a study of the social sciences and social networks to include physical networks (such as power grids) and information networks (such as the World Wide Web). The shift away from social networks, which have a relatively small number of nodes and edges, towards much larger physical and information networks has forced graph theorists and network theorists to develop a suite of analytic tools with which to study graphs. Beyond tens of nodes or even a few thousand nodes, the human eye cannot pick out vital associations or patterns in real-life networks. Among the most important of these new network-theoretic tools for studying Wheatstone sub-networks are a number of metrics to capture many of the most important properties of graphs or networks.

Some preliminaries are necessary before defining any specific metrics. A *graph* or a *network* $G(NB,NL)$ is defined as a set of nodes NB and a set of edges NL connecting the nodes. While complex networks often assume the existence of *hyper-edges* connecting more than two nodes (Newman 2003), an edge in this analysis will be assumed to connect only two nodes. A *path* is a sequence of nodes $\{i_1, i_2,\ldots,j\}$, all of which are connected by edges; in many circumstances, paths will be denoted only by their endpoints i and j.

It is often convenient to represent the topology of a network using structures known as the adjacency matrices or incidence matrices (the former term will be used here, although in computer science applications the latter appears to be more common). The first structure is the node-node adjacency matrix. Notational conventions vary, but the node-node adjacency matrix will be referred to here as **N**. The node-node adjacency matrix **N** is an ($NB \times NB$) square matrix with n_{ij} equal to one if nodes (or buses) i and j are connected by a single edge, and equal to zero otherwise. A graph or network is said to be undirected if **N** is symmetric; that is, if $n_{ij} = n_{ji}$. AC power networks are best described as undirected networks, although they could also be described by a set of two undirected node-node adjacency matrices. The first would be a lower-triangular matrix describing allowable flow from node i to node j, and the second would be an upper-triangular matrix describing allowable flow from node j to node i. DC power networks, or networks equipped with flow-control devices such as phase-angle regulators or voltage regulators, could be described as directed networks. The current U.S. high-voltage transmission grid represents a mix of AC and DC interconnections, with very few flow-control devices. Thus, representing the transmission system as an undirected network is a reasonable approximation of the current system.

The second structure, similar to the first, is the node-edge (or node-line, in the context of power systems) adjacency matrix. Denoted as **A**, the node-edge adjacency matrix is an ($NB \times NL$) matrix with $a_{li} = +1$ and $a_{lj} = -1$, signifying that edge l connects nodes i and j. The sign of the entries in the **A** matrix indicates an assumed direction of flow throughout

the network (that is, from node *i* to node *j*). The principle of superposition says that either sign convention is appropriate, as long as it is consistent.

The node-node and node-edge adjacency matrices are identical in structure to the susceptance matrix **B** and the matrix $\mathbf{H} = \mathbf{A'B}^{\mathbf{diag}}\mathbf{A}$ used in the steady-state Wheatstone analysis in Chapter 3. **N** can be obtained from **B** by dividing all nonzero entries of **B** by themselves, and setting all diagonal entries of **N** equal to zero. **N** and **A** are assumed to have the following properties:

1. $\forall j, \quad \sum_i a_{ij} = 0$. This is just an application of Kirchoff's Law; it says that every link in the system connects exactly two nodes.

2. There are no columns of **A** containing all zeros. In other words, there are no loops in the system.

3. There are no rows or columns of **N** containing all zeros. In other words, there are no atomistic nodes or sub-systems in the network; each node is connected to at least one other node.

4. rank(**A**) = *NL* – 1. This is a consequence of Euler's formula, which says that (nodes) – (edges) + (loops) = 1.

5. **N** and **A** are related by the formula $\mathbf{N} = \mathbf{AA'} - 2\mathbf{I}$, where **I** is the ($NB \times NB$) identity matrix.

In addition, Newman (2003) mentions without proof that $\mathbf{N}^k$ contains the number of paths of length k beginning at node i and ending at node j (thus, $\mathbf{N}^k$ is symmetric for $k > 1$). We will refer to $\mathbf{N}^k$ as the k-th order adjacency matrix. Of particular importance will be the matrix $\mathbf{N}^2$, which shows the combinations of nodes that are connected by a path of length 2, and the diagonal entries of $\mathbf{N}^3$, which show the number of triangles in a directed network; multiplying the diagonal entries of $\mathbf{N}^3$ by a factor of 1/2 gives the number of triangles in an undirected network.

Several network metrics will be useful in decomposing systems to find embedded Wheatstone sub-networks.

Definition 5.1: The degree of node i, denoted d_i, is the number of edges connected to node i.

Definition 5.2: The distance of a path between nodes i and j is the number of edges associated with the path.

Note that the definition of distance used here is purely topological. In many situations, such as the small-world networks described by Watts and Strogatz (1998), this definition of distance is difficult to apply to electric power systems (a better definition would be the

electrical distance between two nodes, represented by the equivalent resistance between the two nodes). For the Wheatstone-identification algorithm presented here, the canonical definition of distance will be adequate.

Definition 5.3: The geodesic path between nodes *i* and *j* is the minimum-distance path between nodes *i* and *j*.

The geodesic path need not be unique; in many circumstances there will be multiple geodesic paths connecting any two nodes. Newman (2003) also defines a network-wide geodesic path metric as the harmonic mean of all geodesic path lengths. The network search algorithm will only require knowing whether the geodesic path between any two nodes *i* and *j* is equal to one, two, or three. This is easily verified directly using the node-node adjacency matrix raised to the appropriate power.

Definition 5.4: The local clustering metric for node *i*, denoted K_i, is given by the ratio of the number of triangles connected to vertex *i* to the number of triples centered on vertex *i*.

This definition of clustering is due to Watts and Strogatz (1998). Nodes with only one connecting edge are given a clustering value of zero for K_i. An equivalent definition, given by Newman (2003) is:

$\frac{|\{e_i\}|}{d_i(d_i-1)}$ for directed networks, and

$\frac{2|\{e_i\}|}{d_i(d_i-1)}$ for undirected networks.

In these definitions, $|\{e_i\}|$ is the number of nodes connected to the *i*th node that are also connected to each other. Since $d_i(d_i - 1)$ is the number of possible interconnections between nodes connected to node *i*, the clustering coefficient measures the proportion of possible interconnections among neighbors of node *i* that actually exist.

Definition 5.5: The network clustering metric is given by $K = \frac{1}{\left|\{i \mid K_i \neq 0\}\right|} \sum_{\{i|K_i \neq 0\}} K_i$.

Values of K_i equal to zero are ignored in the computation; thus, the denominator and the limit of summation are both determined by the number of nodes having more than one connecting edge.

This network clustering metric is also due to Watts and Strogatz (1998). An alternative clustering metric has been proposed by Barrat and Weigt (2000), which measures the ratio of triangles in the network to paths of length 3 in the network, multiplied by a factor of three to account for each triangle being represented as a part of three triples (Newman 2003).

Clustering metrics, however they are defined, describe the connectedness of the network relative to a completely connected network, with every node connected to every other node. Therefore, the clustering metric lies between zero and one, with zero representing a collection of atomistic nodes and with one representing a completely connected

network. The clustering metric takes on the same range of values whether the Watts-Strogatz metric or the Barrat-Weigt metric is used.

The clustering metric is not necessarily related to the network geodesic path metric. Real power systems tend to have small clustering metrics but large network geodesic path metrics. This represents the fact that power systems tend to comprise several reasonably small clusters of nodes connected by a small number of edges. Figure 5.1 shows the clustering metrics and geodesic path metrics for several IEEE test networks plus values for the New York Power Pool, as reported by Newman (2003) and Watts and Strogatz (1998). For this data set, the relationship between network size (as defined by the number of nodes) and the clustering metric is described reasonably well by both a cubic equation and a logarithmic equation. The cubic regression line is given by:

$$(\text{Clustering metric}) = 1.25 - 0.35 \times NB + 0.02 \times NB^2 + 2\times10^{-4} \times NB^3,$$

with an R^2 value of 0.87. The logarithmic regression line is given by:

$$(\text{Clustering metric}) = 0.9 - 0.43\times\ln(NB),$$

with an R^2 value of 0.81.

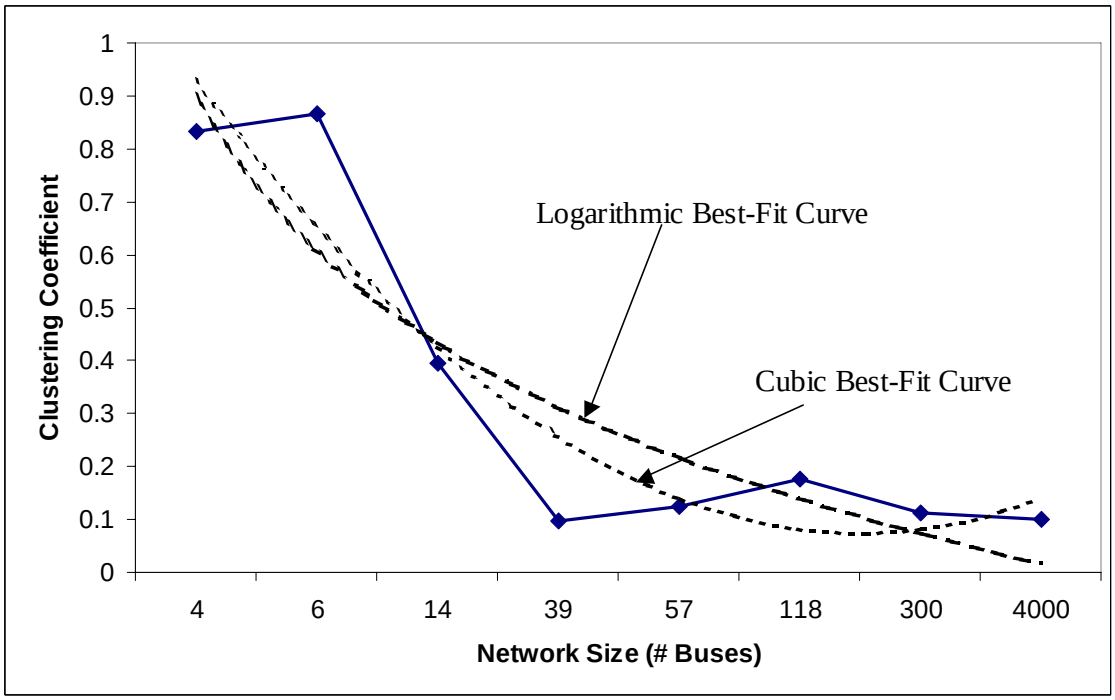

Figure 5.1. Clustering metrics for several IEEE test networks and the New York Power Pool (Newman 2003).

Figure 5.2 shows a purely topological representation of the Wheatstone network. Definitions 5.1 through 5.5 will assist in establishing the following key results concerning the structure of the Wheatstone network.

Result 5.1: The network geodesic path metric for the Wheatstone network is two. The cardinality of this geodesic path metric is also two.

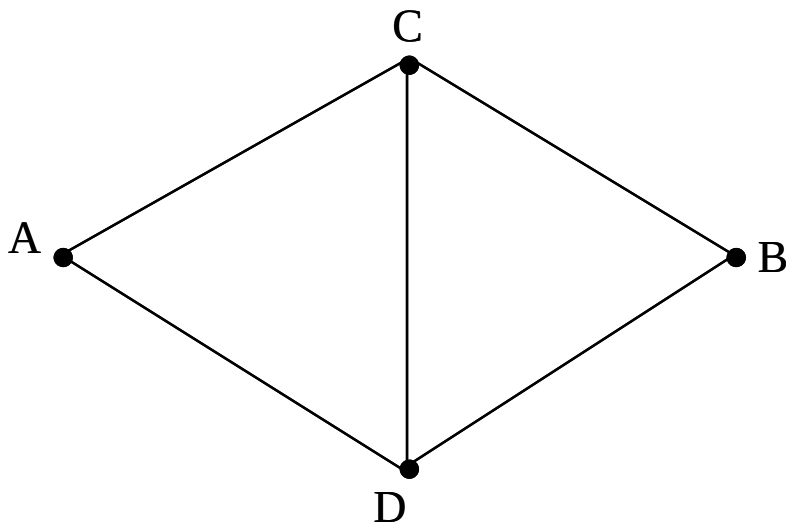

Figure 5.2. Topological representation of the Wheatstone network, which has NB = four nodes and NL = five edges. Nodes A and B are referred to as the endpoints of the network.

Proof of Result 5.1: The result can easily be seen by examining the Wheatstone network in Figure 5.2. The geodesic paths are {A,C,B} and {A,D,B}, which traverse the boundary of the Wheatstone network.

Result 5.2: The Wheatstone network has a clustering metric of $K = 5/6$, where K is defined using the formulae in Definitions 5.4 and 5.5. Further, the clustering metric of the Wheatstone network is unique among four-node networks where the minimum-distance geodesic path (of all pairs of nodes) is two.

Proof of Result 5.2: A network where the minimum-distance geodesic path is greater than one represents a network with no atomistic nodes. Without loss of generality, the family of four-node networks meeting this qualification is shown in Figure 5.3.

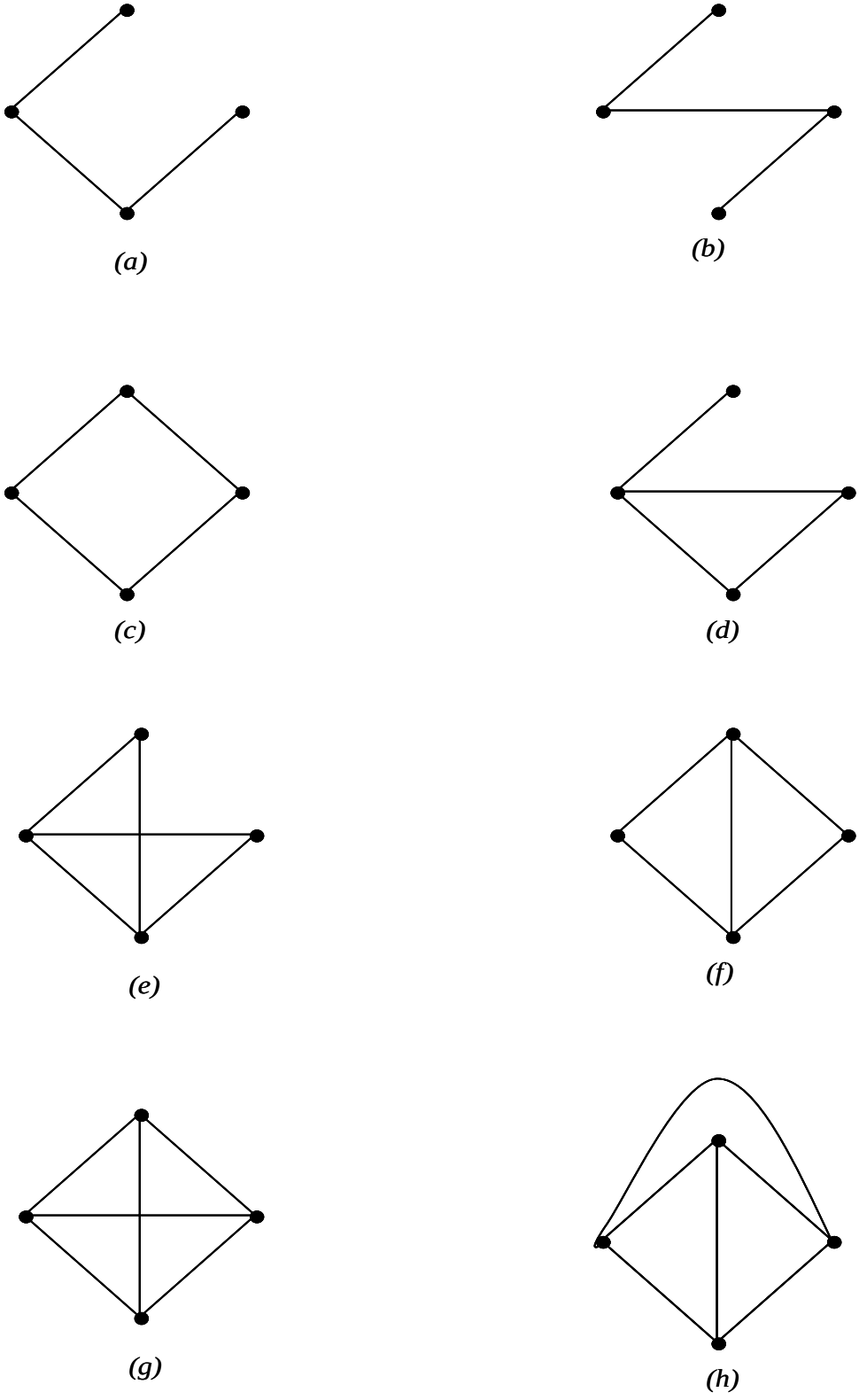

Figure 5.3. A family of four-node networks.

The first part of the proof is established by calculating the clustering metric of the Wheatstone network in Figure 5.3(f), using Definitions 5.4 and 5.5:

$$K_{wheatstone} = \frac{1}{4}\left(1+\frac{2}{3}+\frac{2}{3}+1\right) = \frac{5}{6}.$$

The remainder of the proof calculates the clustering metric for the other networks in Figure 5.3.

First, note that Figures 5.3(a) through 5.3(c) have no triangles, and thus have a clustering metric of zero. Also, the completely connected network in Figure 5.3(g) has a clustering metric of one.

The clustering metric of the network in Figure 5.3(d) is:

$$K_{5.3(d)} = \frac{1}{4}(1+1+1) = \frac{3}{4}.$$

The clustering metric of the network in Figure 5.3(e) is:

$$K_{5.3(e)} = \frac{1}{4}\left(\frac{1}{3}+1+\frac{2}{3}+1\right) = \frac{3}{4}.$$

The clustering metric of the network in Figure 5.3(h) is:

$$K_{5.3(h)} = \frac{1}{4}\left(\frac{2}{3}+\frac{2}{3}+\frac{2}{3}+\frac{2}{3}\right) = \frac{2}{3}.$$

Note that there is a Wheatstone network embedded in Figure 5.3(h). However, the link paralleling the Wheatstone sub-network reduces the minimum-distance geodesic path to one.

5.2 An Algorithm for Detecting Embedded Wheatstone Networks

The graph-theoretic development in Section 5.1 has provided the following characteristics of Wheatstone topologies, which distinguishes Wheatstones from other network sub-structures:

1. For the Wheatstone, $NB = 4$ and $NL = 5$;
2. The Wheatstone network has two distinct triangles;
3. $K_{wheatstone} = \frac{5}{6}$;
4. The network minimum-distance path between "endpoints" of the Wheatstone network (defined as nodes A and B in figure 5.2) is two;
5. The network maximum-distance path between endpoints of the Wheatstone network is three;
6. Each node in the Wheatstone network has degree greater than one.

One goal of the Wheatstone detection algorithm is to disqualify certain nodes, paths, or pairs of nodes from possibly being part of a Wheatstone sub-network. The matrices **A**, $\mathbf{N}^2$ and $\mathbf{N}^3$ will be particularly useful for this purpose. The six Wheatstone properties just listed give us the following exclusion principles:

1. Any node having degree one cannot be part of a Wheatstone sub-network. This can be verified using the node-line adjacency matrix **A**. If the *i*th row of **A** has at most one non-zero entry, then the degree of node *i* is equal to one. This property can also be verified using **N**. If the *i*th row or column of **N** sums to exactly one, then node *i* has degree one.
2. For any pair of nodes *i* and *j*, if there is no path of length two or three connecting *i* and *j*, then that pair of nodes cannot be part of a Wheatstone network. This property can be verified by looking at the *i*, *j*th entry of $\mathbf{N}^2$ and $\mathbf{N}^3$.
3. If there are no triangles attached to the *i*th node, then that node cannot be part of a Wheatstone network. The diagonal entries of $\mathbf{N}^3$ can verify this property.

Nodes that are connected simply in series or parallel within larger Wheatstone networks, as in Figure 5.4, would result in violations of the Wheatstone criteria. The algorithm would thus return a "false negative" for these types of sub-networks, failing to identify an embedded Wheatstone sub-network. Simple series and parallel connections will need to be compressed into single edges or nodes in order to avoid false negatives. Note that the algorithm will create equivalent series-parallel nodes and edges only in a topological sense. Once the Wheatstone networks in the larger system have been identified, the

electrical topology of the entire system will be preserved in order to analyze the Wheatstones.

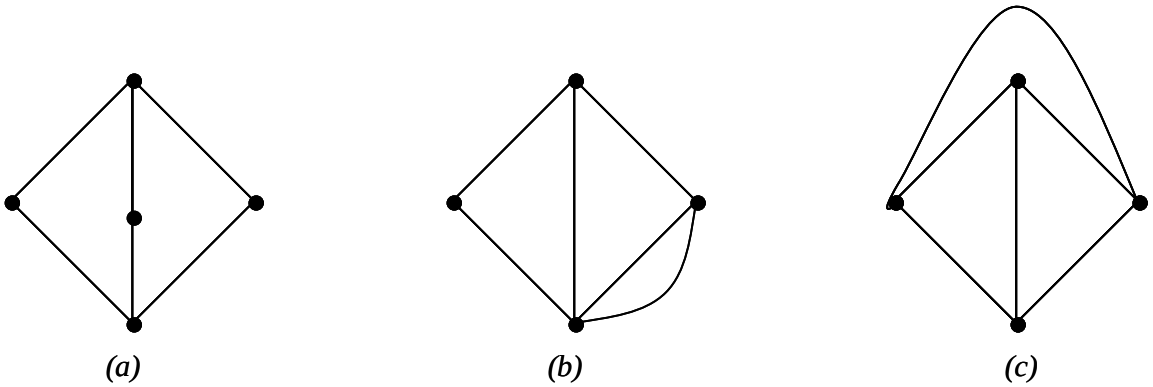

Figure 5.4. Wheatstone networks with embedded series or parallel connections. The Wheatstone detection algorithm needs to suppress these in order to avoid the "false negative" result of failing to identify an embedded Wheatstone.

The Wheatstone detection algorithm proceeds as follows:

Step 1: Calculate the node-node adjacency matrices **N**, $\mathbf{N}^2$ and $\mathbf{N}^3$ for the network, as well as the node-edge adjacency matrix **A**.

Step 2: Compress all simple series and parallel connections into single equivalent nodes or edges. Simple parallel connections can be detected easily using the **A** matrix; two edges are parallel if their corresponding columns in the **A** matrix are equal. Two edges connected in series can be detected by noting that the node connecting them has degree two and is not connected to any triangles (Duffin 1965). The degree of each node can be calculated using the **A** matrix, while the number of triangles connected to each node can

be read from the diagonal entries of $\mathbf{N}^3$. More than one iteration of this step may be required.

Step 3: Define *T* as the set of nodes that are part of at least one triangle.

Step 4: Define *D* as the set of nodes that have degree greater than one.

Step 5: Define R_1 as the set of all pairs of nodes that have geodesic path length equal to two. Define R_2 as the set of all pairs of nodes that have geodesic path length equal to two and also have two geodesic paths. Thus, $R_2 \subset R_1$. Note the strategy behind the definitions of R_1 and R_2; the aim is to determine whether a given pair of nodes might represent the endpoints of an embedded Wheatstone sub-network (as in Figure 5.2). Define R_3 as the set of all pairs of nodes connected by exactly two paths of length three.

Step 6: Define $WS = T \cap D \cap R_2 \cap R_3$. Some care is required in defining the intersection of these sets, since *T* and *D* contain a list of nodes, whereas R_2 and R_3 contain a list of pairs of nodes. If Ω is a set of single elements, and Ψ is a set of pairs of elements, then we will say that $\{\psi_i, \psi_j\} \in \Omega \cap \Psi$ if and only if $\psi_i \in \Omega$ and $\psi_j \in \Omega$, for all $\psi_i, \psi_j \in \Psi$.

WS represents pairs of nodes that meet the necessary conditions for being part of a Wheatstone network; Steps 7 and 8 will determine whether the nodes in *WS* also meet the sufficiency conditions.

Step 7: For all pairs of nodes {(*i*,*j*)} in *WS*, construct the node-node adjacency matrix for the subgraph consisting of *i, j*, and all nodes that are neighbors of both *i* and *j* (that is, those nodes which have a geodesic path distance of one from both *i* and *j*). Ignore any direct links between *i* and *j*.

Step 8: Calculate the clustering coefficient for all the subgraphs generated in Step 7. Those for which $K = 5/6$ represent Wheatstone sub-networks.

The workings of each step in the Wheatstone detection algorithm will be illustrated with a simple example.

5.3 Illustrating the Wheatstone Detection Algorithm

The thirteen-bus network shown in Figure 5.5 is used to illustrate how the algorithm identifies Wheatstone sub-networks. The network is based on the IEEE fourteen-bus test case, but has been altered by removing all of the synchronous condensers and winding transformers from the system, which reduces the size to thirteen buses and alters the network topology.

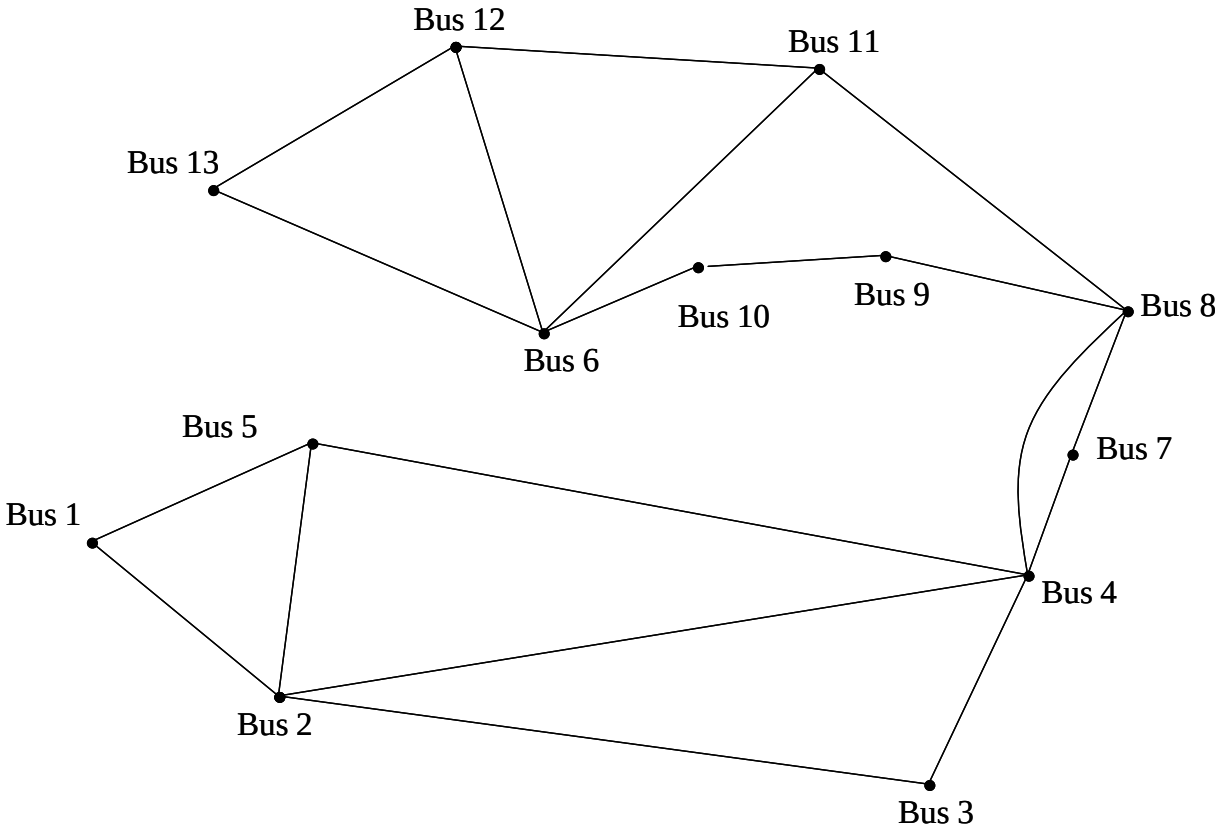

Figure 5.5. Topological representation of the thirteen-bus test network used to illustrate the Wheatstone detection algorithm. The network is based on the IEEE fourteen-bus network, but the synchronous condensers and winding transformers have been removed.

The first step in the algorithm is to calculate the node-line adjacency matrix **A**, as shown in panel (a) of Figure 5.6. Examining Figure 5.6(a), we see that nodes 6, 8, 9, and 10 are all connected in series; thus, for topological purposes, we can compress this group into a single line connecting nodes 6 and 8. Similarly, nodes 4 and 8 have a simple series-parallel connection; thus, we can also eliminate bus 7. This reduces the network down to ten nodes and fifteen lines. The node-line adjacency matrix **A*** for the reduced network is shown in panel (b) of Figure 5.6.

$$\mathbf{A} = \begin{bmatrix}
1 & 1 & 0 & 0 & 0 & 0 & 0 & 0 & 0 & 0 & 0 & 0 & 0 \\
1 & 0 & 0 & 0 & 1 & 0 & 0 & 0 & 0 & 0 & 0 & 0 & 0 \\
0 & 1 & 1 & 0 & 0 & 0 & 0 & 0 & 0 & 0 & 0 & 0 & 0 \\
0 & 1 & 0 & 1 & 0 & 0 & 0 & 0 & 0 & 0 & 0 & 0 & 0 \\
0 & 1 & 0 & 0 & 1 & 0 & 0 & 0 & 0 & 0 & 0 & 0 & 0 \\
0 & 0 & 1 & 1 & 0 & 0 & 0 & 0 & 0 & 0 & 0 & 0 & 0 \\
0 & 0 & 0 & 1 & 1 & 0 & 0 & 0 & 0 & 0 & 0 & 0 & 0 \\
0 & 0 & 0 & 1 & 0 & 0 & 1 & 0 & 0 & 0 & 0 & 0 & 0 \\
0 & 0 & 0 & 1 & 0 & 0 & 0 & 1 & 0 & 0 & 0 & 0 & 0 \\
0 & 0 & 0 & 0 & 0 & 1 & 0 & 0 & 0 & 1 & 0 & 0 & 0 \\
0 & 0 & 0 & 0 & 0 & 1 & 0 & 0 & 0 & 0 & 1 & 0 & 0 \\
0 & 0 & 0 & 0 & 0 & 1 & 0 & 0 & 0 & 0 & 0 & 1 & 0 \\
0 & 0 & 0 & 0 & 0 & 0 & 1 & 1 & 0 & 0 & 0 & 0 & 0 \\
0 & 0 & 0 & 0 & 0 & 0 & 0 & 1 & 1 & 0 & 0 & 0 & 0 \\
0 & 0 & 0 & 0 & 0 & 0 & 0 & 1 & 0 & 0 & 0 & 0 & 1 \\
0 & 0 & 0 & 0 & 0 & 0 & 0 & 0 & 1 & 1 & 0 & 0 & 0 \\
0 & 0 & 0 & 0 & 0 & 0 & 0 & 0 & 0 & 0 & 1 & 1 & 0 \\
0 & 0 & 0 & 0 & 0 & 0 & 0 & 0 & 0 & 0 & 0 & 1 & 1
\end{bmatrix}$$

(a)

$$\mathbf{A^*} = \begin{bmatrix}
1 & 1 & 0 & 0 & 0 & 0 & 0 & 0 & 0 \\
1 & 0 & 0 & 0 & 1 & 0 & 0 & 0 & 0 \\
0 & 1 & 1 & 0 & 0 & 0 & 0 & 0 & 0 \\
0 & 1 & 0 & 1 & 0 & 0 & 0 & 0 & 0 \\
0 & 1 & 0 & 0 & 1 & 0 & 0 & 0 & 0 \\
0 & 0 & 1 & 1 & 0 & 0 & 0 & 0 & 0 \\
0 & 0 & 0 & 1 & 1 & 0 & 0 & 0 & 0 \\
0 & 0 & 0 & 1 & 0 & 0 & 1 & 0 & 0 \\
0 & 0 & 0 & 0 & 0 & 1 & 0 & 1 & 0 \\
0 & 0 & 0 & 0 & 0 & 0 & 1 & 0 & 1 \\
0 & 0 & 0 & 0 & 0 & 0 & 0 & 1 & 1
\end{bmatrix}$$

(b)

Figure 5.6. The node-line adjacency matrix for the 13-bus test network. Panel (a) shows the node-line adjacency matrix of the full 13-bus networks. Panel (b) shows the equivalent node-line adjacency matrix following the series-parallel reduction.

The node-node adjacency matrices **N**, $\mathbf{N}^2$ and $\mathbf{N}^3$ for the reduced network are calculated next; these are shown in Figures 5.7 through 5.9.

$$\mathbf{N} = \begin{bmatrix} 0 & 1 & 0 & 0 & 1 & 0 & 0 & 0 & 0 & 0 \\ 1 & 0 & 1 & 1 & 1 & 0 & 0 & 0 & 0 & 0 \\ 0 & 1 & 0 & 1 & 0 & 0 & 0 & 0 & 0 & 0 \\ 0 & 1 & 1 & 0 & 1 & 0 & 1 & 0 & 0 & 0 \\ 1 & 1 & 0 & 1 & 0 & 0 & 0 & 0 & 0 & 0 \\ 0 & 0 & 0 & 0 & 0 & 0 & 1 & 1 & 1 & 1 \\ 0 & 0 & 0 & 1 & 0 & 1 & 0 & 1 & 0 & 0 \\ 0 & 0 & 0 & 0 & 0 & 1 & 1 & 0 & 1 & 0 \\ 0 & 0 & 0 & 0 & 0 & 1 & 0 & 1 & 0 & 1 \\ 0 & 0 & 0 & 0 & 0 & 1 & 0 & 0 & 1 & 0 \end{bmatrix}$$

Figure 5.7. The node-node adjacency matrix for the reduced-form 13-bus test network.

$$\mathbf{N}^2 = \begin{bmatrix} 2 & 1 & 1 & 2 & 1 & 0 & 0 & 0 & 0 & 0 \\ 1 & 4 & 1 & 2 & 2 & 0 & 1 & 0 & 0 & 0 \\ 1 & 1 & 2 & 1 & 2 & 0 & 1 & 0 & 0 & 0 \\ 2 & 2 & 1 & 4 & 1 & 1 & 0 & 1 & 0 & 0 \\ 1 & 2 & 2 & 1 & 3 & 0 & 1 & 0 & 0 & 0 \\ 0 & 0 & 0 & 1 & 0 & 4 & 1 & 2 & 2 & 1 \\ 0 & 1 & 1 & 0 & 1 & 1 & 3 & 1 & 2 & 1 \\ 0 & 0 & 0 & 1 & 0 & 2 & 1 & 3 & 1 & 2 \\ 0 & 0 & 0 & 0 & 0 & 2 & 2 & 1 & 3 & 1 \\ 0 & 0 & 0 & 0 & 0 & 1 & 1 & 2 & 1 & 2 \end{bmatrix}$$

Figure 5.8. The second-order node-node adjacency matrix for the reduced-form 13-bus test network.

$$\mathbf{N}^3 = \begin{bmatrix} 2 & 6 & 3 & 3 & 5 & 0 & 2 & 0 & 0 & 0 \\ 6 & 6 & 6 & 8 & 7 & 1 & 2 & 1 & 0 & 0 \\ 3 & 6 & 2 & 6 & 3 & 1 & 1 & 1 & 0 & 0 \\ 3 & 8 & 6 & 4 & 8 & 1 & 6 & 1 & 2 & 1 \\ 5 & 7 & 3 & 8 & 4 & 1 & 1 & 1 & 0 & 0 \\ 0 & 1 & 1 & 1 & 1 & 6 & 7 & 7 & 7 & 6 \\ 2 & 2 & 1 & 6 & 1 & 7 & 2 & 6 & 3 & 3 \\ 0 & 1 & 1 & 1 & 1 & 7 & 6 & 4 & 7 & 3 \\ 0 & 0 & 0 & 2 & 0 & 7 & 3 & 7 & 4 & 5 \\ 0 & 0 & 0 & 1 & 0 & 6 & 3 & 3 & 5 & 2 \end{bmatrix}$$

Figure 5.9. The third-order node-node adjacency matrix for the reduced-form 13-bus test network.

The number of triangles associated with each node is given by the diagonals of $\mathbf{N}^3$ multiplied by a factor of 0.5. It will be useful to define a matrix $\mathbf{T} = \frac{1}{2} diag(\mathbf{N})$, whose *i*th diagonal entry shows the number of distinct triangles connected to the *i*th node in the network. All off-diagonal entries of **T** are equal to zero. The **T** matrix for the reduced network is shown in Figure 5.10.

$$\mathbf{T} = \begin{bmatrix} 1 & & & & & & & & & & & \\ & 3 & & & & & & & & & & \\ & & 1 & & & & & & & & & \\ & & & 2 & & & & & & & & \\ & & & & 2 & & & & & & & \\ & & & & & 3 & & & & & & \\ & & & & & & 1 & & & & & \\ & & & & & & & 2 & & & & \\ & & & & & & & & 2 & & & \\ & & & & & & & & & 1 & & \end{bmatrix}$$

Figure 5.10. The diagonal entries of the **T** *matrix show the number of triangles connected to each node.*

Figures 5.6 through 5.10 amount to performing steps 1 and 2 of the Wheatstone detection algorithm. The topology of the reduced-form network at this point is shown in Figure 5.11. Spotting the Wheatstones in the reduced network with the naked eye is easy; visual inspection will provide a check that the algorithm is performing as expected.

Step 3 requires that we define the set *T* of all nodes in the network that are connected to at least one triangle. For the reduced-form network in Figure 5.11, *T* happens to include all the nodes in the network:

T = {1, 2, 3, 4, 5, 6, 8, 11, 12, 13}.

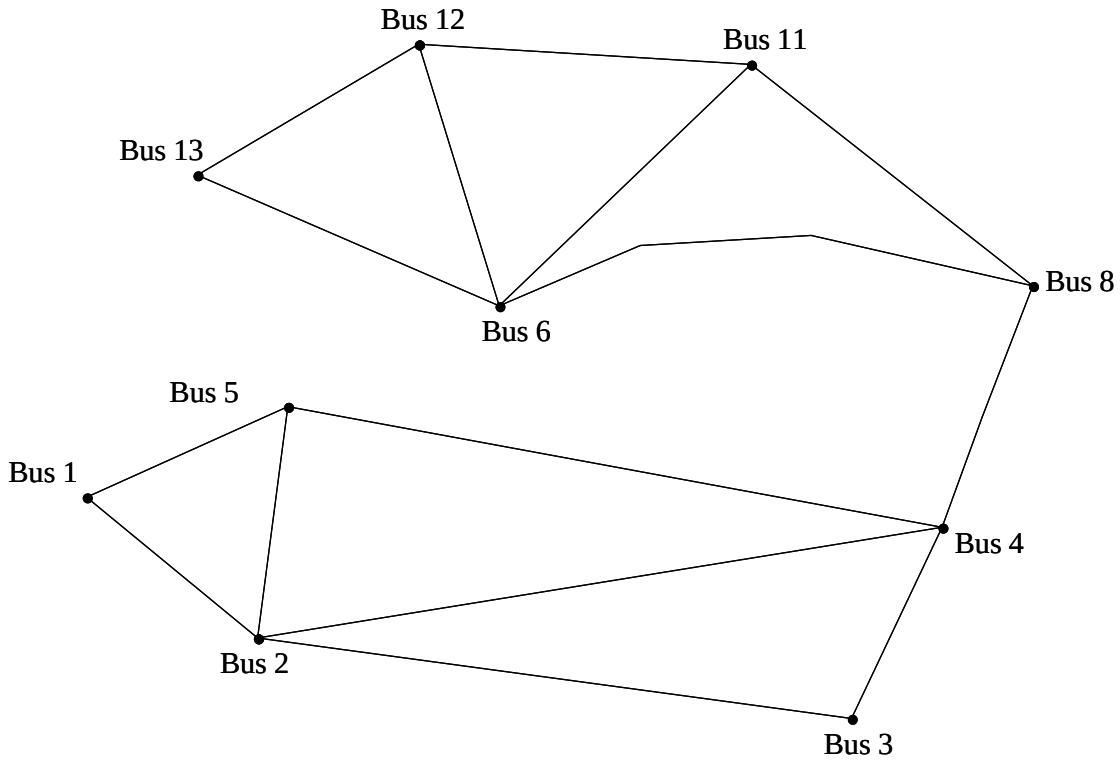

Figure 5.11. The reduced-form thirteen-bus network, after creating equivalent series-parallel connections in the system.

In step 4 we find the set of all nodes with degree greater than one. Recall that the degree of a node is equal to the number of connected neighbors – that is, the number of nodes to which each node is directly connected. The degree of each node can be found in two different ways. The first method uses the node-line adjacency matrix; the degree of each node is equal to the sum of the absolute values of the entries in the corresponding row of the node-line incidence matrix. The second method uses the node-node adjacency matrix. The degree of a given node is equal to the sum of the corresponding row or column in the node-node adjacency matrix. Thus, we have:

Method 1: $d_i = \sum_j | a_{ij} |$, or

Method 2: $d_i = \sum_j N_{ij} = \sum_j N_{ji}$.

Figure 5.12 illustrates the calculation using method 2; the figure shows the reduced network node-node adjacency matrix plus an extra column summing the entries in each row.

$$\mathbf{N} = \begin{bmatrix} 0 & 1 & 0 & 0 & 1 & 0 & 0 & 0 & 0 & 0 \\ 1 & 0 & 1 & 1 & 1 & 0 & 0 & 0 & 0 & 0 \\ 0 & 1 & 0 & 1 & 0 & 0 & 0 & 0 & 0 & 0 \\ 0 & 1 & 1 & 0 & 1 & 0 & 1 & 0 & 0 & 0 \\ 1 & 1 & 0 & 1 & 0 & 0 & 0 & 0 & 0 & 0 \\ 0 & 0 & 0 & 0 & 0 & 0 & 1 & 1 & 1 & 1 \\ 0 & 0 & 0 & 1 & 0 & 1 & 0 & 1 & 0 & 0 \\ 0 & 0 & 0 & 0 & 0 & 1 & 1 & 0 & 1 & 0 \\ 0 & 0 & 0 & 0 & 0 & 1 & 0 & 1 & 0 & 1 \\ 0 & 0 & 0 & 0 & 0 & 1 & 0 & 0 & 1 & 0 \end{bmatrix} \quad \begin{matrix} \textbf{Degree} \\ 2 \\ 4 \\ 2 \\ 4 \\ 3 \\ 4 \\ 3 \\ 3 \\ 3 \\ 2 \end{matrix}$$

Figure 5.12. The degree of all ten nodes in the reduced-form network.

From Figure 5.12, we see that every node in the reduced network has degree greater than one. Thus, the set *D* contains every node in the network (note also that *D* is equal to the set *T* of all nodes connected to at least one distinct triangle):

D = {1, 2, 3, 4, 5, 6, 8, 11, 12, 13}.

Step 5 requires that we determine the membership of three sets, labeled R_1, R_2, and R_3. The set R_1 is made up of all pairs of nodes with geodesic path length equal to two. R_2 is made up of the subset of R_1 consisting of all pairs of nodes whose geodesic path length is

equal to two, and for which the cardinality of the geodesic path is also two (that is, the pairs of nodes for which there are two geodesic paths). R_3 is the set of all pairs of nodes that are separated by two paths of length three. This set is not a subset of either R_1 or R_2, but is grouped with R_1 and R_2 since its members can be determined in parallel with R_1 and R_2.

The set R_1 for the reduced network can be determined using the node-node matrices **N** and $\mathbf{N}^2$. The matrix **N** shows those pairs of nodes that have a geodesic path of one (that is, nodes that are connected neighbors). Thus, if the (i,j)th entry of **N** is equal to one, nodes i and j have a geodesic path of one. If the (i,j)th entry of **N** is equal to zero, nodes i and j have geodesic path of length greater than one.

For those pairs of nodes with geodesic path length greater than one, corresponding to entries in **N** that are equal to zero, we can use $\mathbf{N}^2$ to check for a geodesic path equal to two. Since $\mathbf{N}^2$ shows the number of paths of length two in the network, if the (i,j)th entry of $\mathbf{N}^2$ is non-zero, and the corresponding entry of **N** is zero, then nodes i and j have geodesic path length of two.

In fact, we can construct an indicator matrix from **N** and $\mathbf{N}^2$, whose entries will tell us which pairs of nodes have geodesic path length equal to two. To construct this matrix, which we will call $\mathbf{N}_{g2}$, we first construct a matrix $\tilde{\mathbf{N}} = \mathbf{1} - \mathbf{N}$, where **1** is an ($NB$ by NB) matrix of ones. Thus, if the (i,j)th entry of **N** is equal to one (corresponding to a geodesic path of length one between nodes i and j), then the corresponding entry of $\tilde{\mathbf{N}}$ is zero.

Similarly, if the (*i*,*j*)th entry of **N** is equal to zero, the corresponding entry of $\tilde{\mathbf{N}}$ is equal to one. To calculate $\mathbf{N}_{g2}$, we simply multiply the (*i*,*j*)th entry of $\tilde{\mathbf{N}}$ by the corresponding entry of $\mathbf{N}^2$. Entries of $\mathbf{N}_{g2}$ can be equal to zero if the corresponding entry of $\tilde{\mathbf{N}}$ is equal to zero or if the corresponding entry of $\mathbf{N}^2$ is equal to zero (or both). Nonzero off-diagonal entries of $\mathbf{N}_{g2}$ correspond to pairs of nodes whose geodesic path is equal to two. Thus, we have proven the following result necessary in constructing the set R_1.

Result 5.3: Let **N** and $\mathbf{N}^2$ be the first-order and second-order node-node adjacency matrices of a network, and let $\tilde{\mathbf{N}} = \mathbf{1} - \mathbf{N}$. The pairs of nodes in the network with a geodesic path of length two correspond to the off-diagonal nonzero entries of $\mathbf{N}_{g2}$, where the (*i*,*j*)th entry of $\mathbf{N}_{g2}$ is given by $N_{g2,ij} = \tilde{N}_{ij} N_{ij}$.

$$\mathbf{N_{g2}} = \begin{bmatrix} 2 & 0 & 1 & 2 & 0 & 0 & 0 & 0 & 0 & 0 \\ 0 & 4 & 0 & 0 & 0 & 0 & 1 & 0 & 0 & 0 \\ 1 & 0 & 2 & 0 & 2 & 0 & 1 & 0 & 0 & 0 \\ 2 & 0 & 0 & 4 & 0 & 1 & 0 & 1 & 0 & 0 \\ 0 & 0 & 2 & 0 & 3 & 0 & 1 & 0 & 0 & 0 \\ 0 & 0 & 0 & 1 & 0 & 4 & 0 & 0 & 0 & 0 \\ 0 & 1 & 1 & 0 & 1 & 0 & 3 & 0 & 2 & 1 \\ 0 & 0 & 0 & 1 & 0 & 0 & 0 & 3 & 0 & 2 \\ 0 & 0 & 0 & 0 & 0 & 0 & 2 & 0 & 3 & 0 \\ 0 & 0 & 0 & 0 & 0 & 0 & 1 & 2 & 0 & 2 \end{bmatrix}$$

Figure 5.13. The off-diagonal entries of the matrix $\mathbf{N}_{g2}$ show the pairs of nodes with geodesic path length equal to two.

Figure 5.13 shows the matrix $\mathbf{N}_{g2}$ for the reduced network. Reading off the nonzero off-diagonal entries yields the set R_1:

R_1 = {{1,3}, {1,4}, {2,8}, {3,5}, {3,8}, {4,6}, {4,11}, {5,8}, {8,12}, {8,13}, {11,13}}.

Since $\mathbf{N}^2$ contains all paths of length two between pairs of nodes in the network, and since $\mathbf{N}_{g2}$ indicates which pairs of nodes have a geodesic path length equal to two, those entries of $\mathbf{N}_{g2}$ equal to two indicate which pairs of nodes have exactly two geodesic paths. These pairs of nodes form the set R_2. Figure 5.13 allows us to identify the set R_2:

R_2 = {{1,4}, {3,5}, {8,12}, {11,13}}.

To complete step 5 of the Wheatstone detection algorithm, we must find the set R_3. Since we are looking for pairs of nodes that are separated by at least two paths of length three, we need only look at the entries of $\mathbf{N}^3$. For a reasonably meshed network, R_3 will be quite large; for the reduced network shown in Figure 5.11, we get:

R_3 = {{1,2}, {1,3}, {1,4}, {1,5}, {1,8}, {2,3}, {2,4}, {2,5}, {2,8}, {3,4}, {3,5}, {4,5}, {4,8}, {4,12}, {6,8}, {6,11}, {6,12}, {6,13}, {8,11}, {8,12}, {8,13}, {11,12}, {11,13}, {12,13}}.

The set $R_2 \cap R_3$ consists of pairs of nodes that might represent the endpoints of a Wheatstone sub-network (these correspond to nodes A and B in Figure 5.2), and in this case, $R_2 \cap R_3 = R_2$ since $R_2 \subset R_3$. Thus, from Figure 5.13, we see that there are at most four Wheatstone sub-networks in the reduced network shown in Figure 5.11.

Step 6 of the Wheatstone detection algorithm requires that we calculate the set *WS*, defined as the intersection of *T, D,* R_2, and R_3. To handle calculating the intersection of

two sets, the first of which contains a list of nodes, and the second of which contains a set of pairs of nodes, we will require that both members of each pair of nodes in the second set also individually be members of the first set. Since both *T* and *D* contain all the nodes in the reduced network, and $R_2 \cap R_3 = R_2$, we see that $WS = R_2$.

In step 7 of the Wheatstone detection algorithm, we construct the sub-graphs consisting of pairs of nodes $\{i,j\}$ in the set *WS* and all nodes connected to both *i* and *j* with degree one. Step 8 verifies that these are indeed Wheatstone sub-networks by calculating the clustering coefficient of each sub-graph. Since there are four pairs of nodes in the set *WS*, we must construct four distinct sub-graphs.

The set of nodes connected to both *i* and *j* with degree one can be found by scanning the *i*th and *j*th column (or row) of the node-node adjacency matrix **N**, looking for common elements whose entry is equal to one:

$$\{\text{nodes connected to } i \text{ and } j \text{ with degree one}\} = \{k \mid N_{ik} = 1\} \cap \{k \mid N_{jk} = 1\}, k = 1,..., NB .$$

The node-node adjacency matrices for the four candidate Wheatstone sub-networks of the reduced network shown in Figure 5.11 are shown in Figure 5.14. Using the clustering metric given in Definition 5.5, we see that $K = 5/6$ for all four candidate Wheatstone sub-networks in Figure 5.14. Thus, all four are actual Wheatstone sub-networks.

$$\mathbf{WS_1} = \begin{array}{c} \\ \mathbf{1} \\ \mathbf{2} \\ \mathbf{4} \\ \mathbf{5} \end{array} \begin{array}{c} \begin{array}{cccc} \mathbf{1} & \mathbf{2} & \mathbf{4} & \mathbf{5} \end{array} \\ \begin{bmatrix} 0 & 1 & 0 & 1 \\ 1 & 0 & 1 & 1 \\ 0 & 1 & 0 & 1 \\ 1 & 1 & 1 & 0 \end{bmatrix} \end{array}$$

$$\mathbf{WS_2} = \begin{array}{c} \\ \mathbf{2} \\ \mathbf{3} \\ \mathbf{4} \\ \mathbf{5} \end{array} \begin{array}{c} \begin{array}{cccc} \mathbf{2} & \mathbf{3} & \mathbf{4} & \mathbf{5} \end{array} \\ \begin{bmatrix} 0 & 1 & 1 & 1 \\ 1 & 0 & 1 & 0 \\ 1 & 1 & 0 & 1 \\ 1 & 0 & 1 & 0 \end{bmatrix} \end{array}$$

$$\mathbf{WS_3} = \begin{array}{c} \\ \mathbf{6} \\ \mathbf{8} \\ \mathbf{11} \\ \mathbf{12} \end{array} \begin{array}{c} \begin{array}{cccc} \mathbf{6} & \mathbf{8} & \mathbf{11} & \mathbf{12} \end{array} \\ \begin{bmatrix} 0 & 1 & 1 & 1 \\ 1 & 0 & 1 & 0 \\ 1 & 1 & 0 & 1 \\ 1 & 0 & 1 & 0 \end{bmatrix} \end{array}$$

$$\mathbf{WS_4} = \begin{array}{c} \\ \mathbf{6} \\ \mathbf{11} \\ \mathbf{12} \\ \mathbf{13} \end{array} \begin{array}{c} \begin{array}{cccc} \mathbf{6} & \mathbf{11} & \mathbf{12} & \mathbf{13} \end{array} \\ \begin{bmatrix} 0 & 1 & 1 & 1 \\ 1 & 0 & 1 & 0 \\ 1 & 1 & 0 & 1 \\ 1 & 0 & 1 & 0 \end{bmatrix} \end{array}$$

Figure 5.14. The node-node adjacency matrices for the four candidate Wheatstone sub-networks of the ten-bus reduced network.

The algorithm presented here for finding embedded Wheatstone sub-networks has a lot of steps. However, exploiting the graph-theoretic properties of the macro-level network and the Wheatstone network reduces the combinatorial nature of the search problem. For those steps that require a global network search (such as step 5, where finding the set R_2 requires searching through the entire $\mathbf{N}_{g2}$ matrix), the number of operations required is the same order of magnitude as the dimensionality of the network.[1]

[1] Actually, the number of operations required is only half of the dimensionality, since **N** is symmetric about the principal diagonal.

5.4 An Equivalencing Method for Steady-State Analysis of Embedded Wheatstone Sub-Networks

Chapter 3 derived the most relevant steady-state properties of the standalone Wheatstone test network. Wheatstones embedded in larger networks can be analyzed much the same way, but the effects of the external network must also be taken into account. Further, the series-parallel reductions that are made in the Wheatstone search algorithm are perfectly acceptable from a graph-theoretic standpoint, in which the electrical network is reduced to a set of nodes and edges. In real electric power systems, calculating series-parallel equivalent buses and branches must be done carefully.

This section outlines two common equivalencing tools for the steady-state analysis of power networks. The first tool can be used to create equivalent single nodes and lines from series-parallel network structures. The second tool, known as the Ward equivalent, is useful for creating a reduced-form model of the network external to the Wheatstone network. This equivalent is modeled as a constant real power injection or withdrawal at the boundary of the Wheatstone sub-network.

These equivalencing methods are often useful for near-real-time system monitoring of certain portions of the network, since they do not require running power flows on the full system model. The methods are not perfect. The Ward equivalent in particular has two well-known drawbacks. The first is that while it replicates real power flows reasonably well (Lo et. al. 1993), it is less accurate in reproducing the full-network reactive flows.

The second is that it assumes that the external network is in a static steady state. Thus, injections, withdrawals, line impedances, and so forth do not deviate from their constant steady-state values. Thus, the equivalencing methods are most useful for examining the effects of small changes in the network.

The series-parallel equivalencing method will be discussed first, followed by the Ward equivalent. An example using the 13-bus network in Figure 5.5 appears as Section 5.5.

Ohm's Law states that for resistors R_a and R_b in parallel, an equivalent resistance can be calculated using the formula $\frac{1}{R_{ab_{eq}}} = \frac{1}{R_a} + \frac{1}{R_b}$. Thus, the reciprocals of resistances are additive in parallel.

Resistances in series are simply additive: $R_{ab} = R_a + R_b$. In power systems applications, on the other hand, nodes are often buses, whose structures are more complex than simple resistors in a circuit. Imagine two transmission lines connected in series by a bus containing only a load, as shown in the left-hand panel of Figure 5.15. In this case we are only concerned with the point where the transmission lines meet, and not with the other ends of the two lines. In calculating the equivalent series resistance for these two lines, we cannot simply add the resistances of the individual lines, as that would neglect the bus resistance in line C.

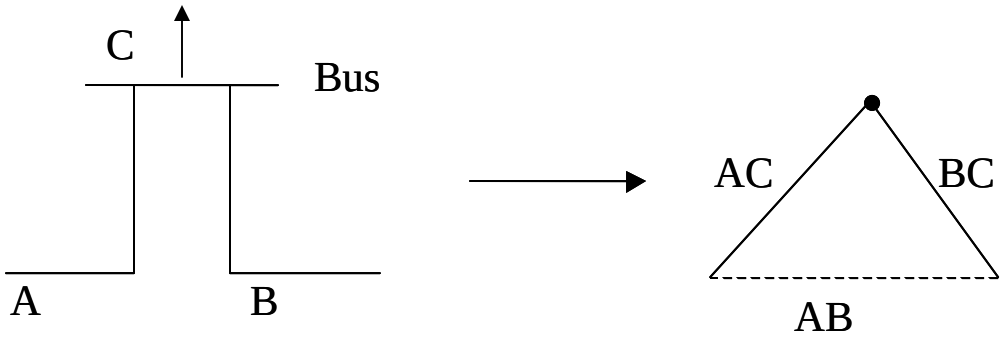

Figure 5.15. Delta-star equivalencies must be used to calculate series-parallel equivalencies in power networks.

Series connections in buses are actually so-called Wye connections, as shown in the left-hand side of Figure 5.15 and the right-hand panels of Figure 5.16. An equivalence relation exists between the Wye connection and the triangular Delta connection (see the right-hand side of Figure 5.15 and the left-hand panels of Figure 5.16). For any given Delta network, it is always possible to construct terminal connections in the Wye configuration such that the two networks are electrically equivalent (and vice versa). In other words, if we have a set of three resistors arranged in a Delta configuration, through examining the terminals alone (voltages and currents) we can figure out the resistances necessary to construct an equivalent Wye network.

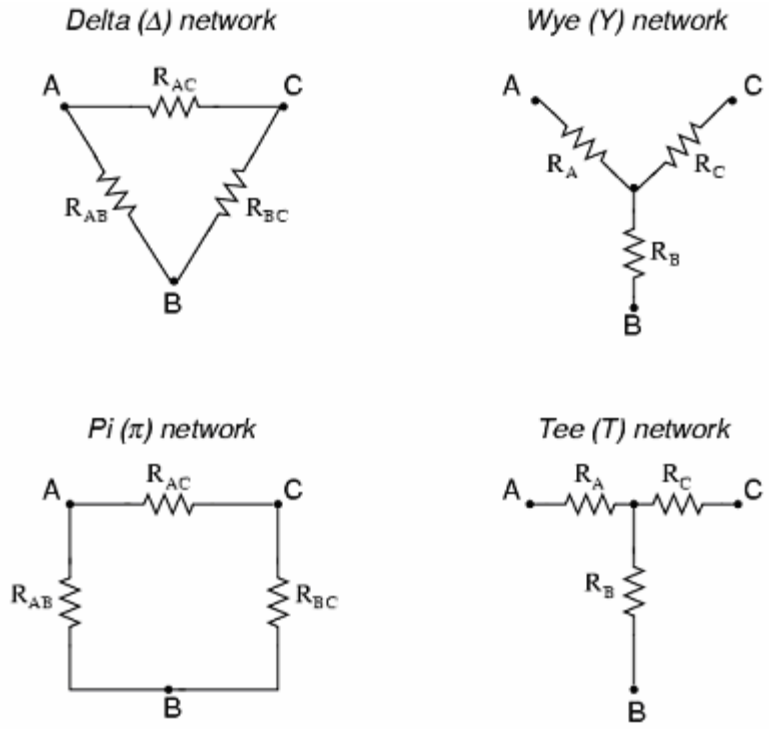

Figure 5.16. Various representations of Delta and Wye networks.

The equations to convert a Delta network into its equivalent Wye network are:

$$(5.1a) \quad X_A = \frac{X_{AB} X_{AC}}{X_{AB} + X_{AC} + X_{BC}}$$

$$(5.1b) \quad X_B = \frac{X_{AB} X_{BC}}{X_{AB} + X_{AC} + X_{BC}}$$

$$(5.1c) \quad X_C = \frac{X_{BC} X_{AC}}{X_{AB} + X_{AC} + X_{BC}}.$$

The equations to convert a Wye network into its equivalent Delta network are:

$$(5.2a) \quad X_{AB} = \frac{X_A X_C + X_A X_B + X_B X_C}{X_C}$$

$$(5.2b) \quad X_{AC} = \frac{X_A X_C + X_A X_B + X_B X_C}{X_B}$$

$$(5.2c) \quad X_{BC} = \frac{X_A X_C + X_A X_B + X_B X_C}{X_A}.$$

The following algorithm will create equivalent parallel and series connections. Consider a network with *NB* nodes and *NL* edges. Suppose that we wanted to consider a reduced network with lines connected in series such that *k* of the *NB* nodes would be removed from the system. The following algorithm will take the original ($NB \times NB$) admittance matrix **Y** and will yield an equivalent reduced-form ($NB - k \times NB - k$) admittance matrix $\mathbf{Y_{red}}$.[2]

To modify the admittance matrix, we begin with the current-voltage relation **I = YV**. We partition **I** into an ($NB - k$)-dimensional vector $\mathbf{I_{-k}}$ (containing the $NB - k$ nodes not being eliminated from the network) and a *k*-dimensional vector of zeroes:

$$(5.3) \quad \mathbf{I} = \begin{bmatrix} i_1 \\ \vdots \\ i_n \end{bmatrix} \rightarrow \begin{bmatrix} \mathbf{I}_k \\ \mathbf{0} \end{bmatrix}.$$

[2] The applications here will focus on the DC power flow model, which uses only the reactive portion **B** of the admittance matrix. However, the series-parallel reduction equations presented here will work whether the full admittance matrix is used, or just the susceptance matrix.

We similarly partition the voltage vector into an ($NB - k$)-dimensional vector $\mathbf{V_{-k}}$ (containing the $NB - k$ nodes not being eliminated from the network) and a k-dimensional vector of zeroes. This implies the following partitioning of the admittance matrix:

$$(5.4) \qquad \begin{bmatrix} \mathbf{I}_{-k} \\ \mathbf{0} \end{bmatrix} = \begin{bmatrix} \mathbf{Y}_{11} & \mathbf{Y}_{12} \\ \mathbf{Y}_{21} & \mathbf{Y}_{22} \end{bmatrix} \begin{bmatrix} \mathbf{V}_{-k} \\ \mathbf{V}_{k} \end{bmatrix}.$$

The dimensionality of the partitioned admittance matrix is that $\mathbf{Y_{11}}$ is ($NB - k \times NB - k$), $\mathbf{Y_{12}}$ is ($NB - k \times k$), $\mathbf{Y_{21}}$ is ($k \times NB - k$), and $\mathbf{Y_{22}}$ is ($k \times k$).

After the partitioning, we have the following system of equations:

(5.5a) $\mathbf{I_{-k}} = \mathbf{Y_{11}V_{-k}} + \mathbf{Y_{12}V_{k}}$ ($NB - k$ equations)

(5.5b) $\mathbf{0} = \mathbf{Y_{21}V_{-k}} + \mathbf{Y_{22}V_{k}}$ (k equations)

From equation (5.5b), we get $\mathbf{V_k} = -\mathbf{Y_{22}}^{-1}\mathbf{Y_{21}V_{-k}}$. Plugging this into equation (5.5a) yields

$$(5.6) \qquad \mathbf{I_{-k}} = \mathbf{Y_{11}V_{-k}} - \mathbf{Y_{12}}(\mathbf{Y_{22}}^{-1}\mathbf{Y_{21}V_{-k}})$$
$$= (\mathbf{Y_{11}} - \mathbf{Y_{12}Y_{22}}^{-1}\mathbf{Y_{21}})\mathbf{V_{-k}}$$
$$= \mathbf{Y_{red}V_{-k}}$$

where $\mathbf{Y_{red}} = (\mathbf{Y_{11}} - \mathbf{Y_{12}Y_{22}}^{-1}\mathbf{Y_{21}})$.

The final output of the system decomposition algorithm is essentially a list of all of the subnetworks that have the Wheatstone structure, and those that have a series-parallel structure. Sub-networks of interest can then be analyzed in turn to determine either if the existing configuration amounts to a constraint on the network (the congestion management function) or whether proposed transmission additions are likely to be beneficial or detrimental to the network (the planning function). Since the planning time scale is often months or years in advance, fast calculations are probably not valued as highly as during real-time operations. Planners have enough time to run full power flows to support their system studies.

System operators, on the other hand, are not normally afforded the luxury of time. One fast technique which has been shown to work well for calculating equivalent real power flows is the Ward equivalent. The principal advantage of the Ward equivalent over other methods is that it is largely a function of the topology of the network and does not require a base-case analysis of the power system (Lo et. al. 1993). The idea behind the Ward equivalent is that it divides the power system into three parts. The internal system represents the portion of the network to be studied in detail (for our purposes, such an internal system might be a Wheatstone network detected by the decomposition algorithm). The equivalent external system represents everything outside of the internal system. Finally, the Ward equivalencing method also considers the boundary nodes where the internal system meets the external system.

The primary tool in the Ward equivalent method is the system admittance matrix **Y** (or, in the case of the DC power flow, the system susceptance matrix **B**), which is partitioned according to the number of nodes in each of the internal, external, and boundary subsystems. If there are *e* nodes in the external system, *i* nodes in the internal system, and *b* nodes on the boundary, then we define the following partitions of the **Y** matrix:[3]

$\mathbf{Y_{EE}}$ = the ($e \times e$) sub-matrix of admittances in the external system;

$\mathbf{Y_{BE}}$ = the ($b \times e$) sub-matrix of admittances between the boundary nodes and the external system;

$\mathbf{Y_{BI}}$ = the ($b \times i$) sub-matrix of admittances between the boundary nodes and the internal nodes;

$\mathbf{Y_{II}}$ = the ($i \times i$) sub-matrix of admittances in the internal system.

The full system admittance matrix is thus partitioned as follows:

$$\text{(5.7)} \quad \mathbf{Y_{system}} = \begin{bmatrix} \mathbf{Y_{EE}} & \mathbf{Y_{EB}} & \mathbf{0} \\ \mathbf{Y_{BE}} & \mathbf{Y_{BB}^{E}} + \mathbf{Y_{BB}^{I}} & \mathbf{Y_{BI}} \\ \mathbf{0} & \mathbf{Y_{IB}} & \mathbf{Y_{II}} \end{bmatrix}.$$

Note that $\mathbf{Y}_{\mathrm{BE}} = \mathbf{Y}_{\mathrm{EB}}^{\mathrm{T}}$ and $\mathbf{Y}_{\mathrm{BI}} = \mathbf{Y}_{\mathrm{IB}}^{\mathrm{T}}$. The submatrices $\mathbf{Y_{BB}^{E}}$ and $\mathbf{Y_{BB}^{I}}$ contain the sum of admittances between the boundary buses and the external and internal buses, respectively. The part of the $\mathbf{Y_{system}}$ matrix describing the external system can be divorced from the part representing the internal system, as:

[3] Note that $e + i + b = NB$.

$$(5.8) \quad \mathbf{Y_E} = \begin{bmatrix} \mathbf{Y_{EE}} & \mathbf{Y_{EB}} \\ \mathbf{Y_{BE}} & \mathbf{Y_{BB}^E} \end{bmatrix}.$$

Through repeated application of Ohm's Law for the external, internal, and boundary systems, the external equivalent admittance matrix is (Monticelli et. al. 1979):

$$(5.9) \quad \mathbf{Y_{eq}} = \mathbf{Y_{BB}^E} - \mathbf{Y_{BE}}\mathbf{Y_{EE}}^{-1}\mathbf{Y_{EB}}.$$

Particularly in the cases considered here, the number of external buses will far exceed the number of boundary buses, so the dimensionality of $\mathbf{Y_{eq}}$ should be quite small. The equivalent admittance matrix can then be used to calculate equivalent real and reactive power injections on the boundary of the internal system using the normal load flow equations.

5.5 An Example Using the Thirteen-Bus Network

This section demonstrates the equivalencing method developed in Section 5.4 using the 13-bus network shown in Figure 5.5. From Section 5.3, we know that the equivalent reduced network has ten buses; buses 7, 9, and 10 are eliminated in series. Thus, the reduced susceptance matrix $\mathbf{B_{red}}$ is a (10×10) matrix of equivalent susceptances. The example presented here will focus on the four-bus Wheatstone network consisting of buses 6, 11, 12, and 13.

The partitioned system susceptance matrix (denoted $\mathbf{B_{part}}$) is shown in Figure 5.17. The system submatrices $\mathbf{B_{11}}$, $\mathbf{B_{12}}$, and $\mathbf{B_{22}}$ can be easily seen in Figure 5.17.

$\mathbf{B_{11}}$

$$\mathbf{B_{part}} = \left[\begin{array}{cccccccccc|ccc}
-1.76 & 0.07 & -3.76 & -0.09 & 4.53 & 0.22 & 0.10 & -0.83 & -0.14 & 0.50 & 1.85 & -0.55 & -0.14 \\
0.07 & -3.27 & 4.81 & 0.15 & 0.04 & -0.39 & -0.18 & 1.48 & 0.26 & -0.89 & -3.31 & 0.99 & 0.25 \\
-3.76 & 4.81 & 2.66 & 0.23 & -1.31 & -0.58 & -0.26 & 2.16 & 0.37 & -1.30 & -4.82 & 1.44 & 0.36 \\
-0.09 & 0.15 & 0.23 & -2.37 & -0.04 & 0.46 & 0.21 & -1.74 & -0.30 & 1.05 & 3.89 & -1.16 & -0.29 \\
4.53 & 0.04 & -1.31 & -0.04 & -3.70 & 0.11 & 0.05 & -0.40 & -0.07 & 0.24 & 0.90 & -0.27 & -0.07 \\
0.22 & -0.39 & -0.58 & 0.46 & 0.11 & -7.34 & -0.54 & -3.65 & 0.77 & 5.01 & 2.23 & 2.96 & 0.74 \\
0.10 & -0.18 & -0.26 & 0.21 & 0.05 & -0.54 & -3.25 & 2.03 & 0.35 & -1.23 & 1.02 & 1.35 & 0.34 \\
-0.83 & 1.48 & 2.16 & -1.74 & -0.40 & -3.65 & 2.03 & 1.05 & 2.37 & -0.45 & -8.36 & 9.13 & -2.80 \\
-0.14 & 0.26 & 0.37 & -0.30 & -0.07 & 0.77 & 0.35 & 2.37 & -1.50 & 1.74 & -1.45 & -1.92 & -0.48 \\
0.50 & -0.89 & -1.30 & 1.05 & 0.24 & 5.01 & -1.23 & -0.45 & 1.74 & 1.11 & 5.05 & -12.52 & 1.69 \\
\hline
1.85 & -3.31 & -4.82 & 3.89 & 0.90 & 2.23 & 1.02 & -8.36 & -1.45 & 5.05 & 9.97 & -5.57 & -1.40 \\
-0.55 & 0.99 & 1.44 & -1.16 & -0.27 & 2.96 & 1.35 & 9.13 & -1.92 & -12.52 & -5.57 & -4.51 & 10.64 \\
-0.14 & 0.25 & 0.36 & -0.29 & -0.07 & 0.74 & 0.34 & -2.80 & -0.48 & 1.69 & -1.40 & 10.64 & -8.84
\end{array}\right]$$

$\mathbf{B_{12}}$ $\mathbf{B_{22}}$

Figure 5.17. The partitioned susceptance matrix for the thirteen-bus network.

The inverse of $\mathbf{B_{22}}$ is given by:

$$\mathbf{B}_{22}^{-1} = \begin{bmatrix} 0.26 & 0.23 & 0.23 \\ 0.23 & 0.32 & 0.35 \\ 0.23 & 0.35 & 0.27 \end{bmatrix},$$

and thus the reduced-form system susceptance matrix is given by:

$$\mathbf{B_{red}} = \begin{bmatrix}
0.46 & -0.82 & -1.20 & 0.97 & 0.22 & 1.45 & 0.66 & -1.47 & -0.94 & -0.49 \\
-0.82 & 1.47 & 2.15 & -1.73 & -0.40 & -2.59 & -1.18 & 2.63 & 1.68 & 0.87 \\
-1.20 & 2.15 & 3.14 & -2.53 & -0.59 & -3.78 & -1.73 & 3.84 & 2.46 & 1.27 \\
0.97 & -1.73 & -2.53 & 2.04 & 0.47 & 3.05 & 1.39 & -3.09 & -1.98 & -1.02 \\
0.22 & -0.40 & -0.59 & 0.47 & 0.11 & 0.71 & 0.32 & -0.72 & -0.46 & -0.24 \\
1.45 & -2.59 & -3.78 & 3.05 & 0.71 & 9.55 & 4.37 & -1.17 & -6.21 & -11.30 \\
0.66 & -1.18 & -1.73 & 1.39 & 0.32 & 4.37 & 2.00 & -0.54 & -2.84 & -5.17 \\
-1.47 & 2.63 & 3.84 & -3.09 & -0.72 & -1.17 & -0.54 & 5.28 & 0.76 & -3.49 \\
-0.94 & 1.68 & 2.46 & -1.98 & -0.46 & -6.21 & -2.84 & 0.76 & 4.04 & 7.35 \\
-0.49 & 0.87 & 1.27 & -1.02 & -0.24 & -11.30 & -5.17 & -3.49 & 7.35 & 18.00
\end{bmatrix}.$$

We are now ready to move on to calculating the Ward equivalent for the Wheatstone network at buses 6, 11, 12, and 13. The internal buses for the Ward calculation are buses 12 and 13 (not all four buses of the Wheatstone network, since the Ward equivalent technique makes a distinction between the internal and boundary buses). Referencing Figure 5.5, the boundary buses are buses 6 and 11. The external buses consist of the remainder of the network. Thus, the Ward matrices are:

$$\mathbf{B}_{\mathbf{II}} = \begin{bmatrix} 4.04 & 7.35 \\ 7.35 & 18 \end{bmatrix}$$

$$\mathbf{B}_{\mathbf{BI}} = \begin{bmatrix} -6.21 & -11.3 \\ 0.76 & -3.49 \end{bmatrix}$$

$$\mathbf{B}_{\mathbf{BE}} = \begin{bmatrix} 1.45 & -2.59 & -3.78 & 3.05 & 0.71 & 4.37 \\ -1.47 & 2.63 & 3.84 & -3.09 & -0.72 & -0.54 \end{bmatrix}$$

$$\mathbf{B}_{\mathbf{EE}} = \begin{bmatrix} 0.46 & -0.82 & -1.2 & 0.97 & 0.22 & 0.66 \\ -0.82 & 1.47 & 2.15 & -1.73 & -0.4 & -1.18 \\ -1.2 & 2.15 & 3.14 & -2.53 & -0.59 & -1.73 \\ 0.97 & -1.73 & -2.53 & 2.04 & 0.47 & 1.39 \\ 0.22 & -0.4 & -0.59 & 0.47 & 0.11 & 0.32 \\ 0.66 & -1.18 & -1.73 & 1.39 & 0.32 & 2 \end{bmatrix}.$$

The Ward equivalent external susceptance matrix is given by:

$$\mathbf{B}_{\mathbf{E,eq}} = \begin{bmatrix} -13.61 & 2.04 \\ -0.53 & -5.98 \end{bmatrix}.$$

Lo et. al. (1993) acknowledge that the elements of $\mathbf{B_{eq}}$ may be large in magnitude; they suggest that industry practice is to ignore any equivalent susceptances larger than, say, three per-unit. For the purposes of this example, we will take the equivalent susceptances as given and proceed to calculate equivalent injections/withdrawals at the boundary nodes.

Thus, the Ward equivalent susceptance matrix for the Wheatstone subnetwork is

$$B_{I,eq} = \begin{bmatrix} -13.61 & 2.04 & -6.21 & 0.76 \\ -0.53 & -5.98 & -11.3 & -3.49 \\ -6.21 & -11.3 & 4.04 & 7.35 \\ 0.76 & -3.49 & 7.35 & 48 \end{bmatrix}.$$

The information in the equivalent susceptance matrix can be combined with the topological information from the Wheatstone network in order to characterize the injections or withdrawals at the boundary buses, as well as the flows through the network. Figure 5.18 shows the Wheatstone sub-network without the additional information from the equivalent external system and Figure 5.19 shows the Wheatstone following the equivalencing procedure.

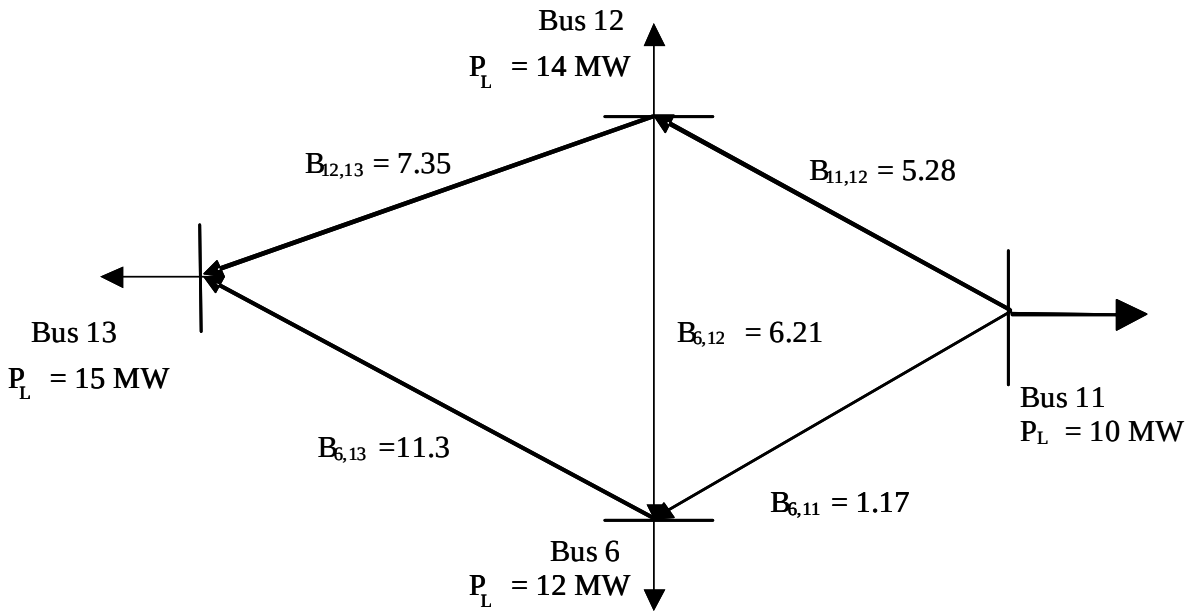

Figure 5.18. The original form of a Wheatstone sub-network embedded in the thirteen-bus network.

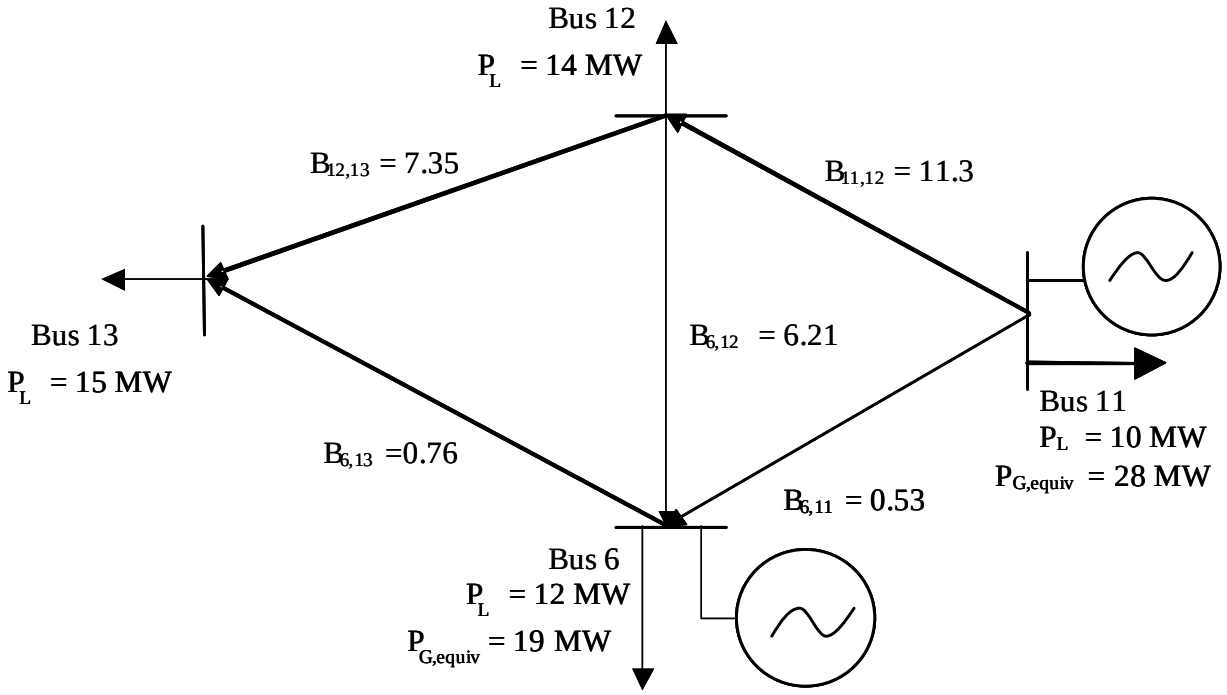

Figure 5.19. The equivalent Wheatstone sub-network.

In Figure 5.18, we see that every node of the Wheatstone network represents a load bus; there is no generation native to this Wheatstone sub-network. In the IEEE fourteen-bus network on which the thirteen-bus network is based, all generation is located at buses 1, 2 and 8. Power flows through the network from other parts of the network into the Wheatstone. Unsurprisingly, the direction of flow is towards bus 13.

Figure 5.19 shows the effect of creating an equivalent external network with boundary buses 6 and 11. The equivalent network behaves as if buses 6 and 11 were generators, producing 28 MW and 19 MW of real power, respectively. Note that the direction of flows has not changed with the creation of the equivalent network.

5.6 Summary

Chapter 3 demonstrated that the presence of a Wheatstone sub-network in a larger power system may cause some unexpected effects, such as congestion that is not relieved with incremental upgrades. The pricing signals in Wheatstone sub-networks may also be misleading. While this behavior is easy to analyze in the context of a standalone Wheatstone test system, it may be harder to pin down in a large meshed network. Being able to find embedded Wheatstone structures is valuable in both the operations and planning functions of grid management.

This chapter developed a graph-theoretic network search tool to find Wheatstone sub-networks in larger systems. The search tool is heuristic in the sense that it does not perform a complete combinatorial scan of all possible four-node sub-networks. For even

modestly-sized systems, the combinatorial problem is too large. Instead the search algorithm exploits the unique graph-theoretic structure of the Wheatstone network. The tool was illustrated on a modified version of the IEEE fourteen-bus network; this network was chosen in order to provide a sufficiently interesting example where the outcome could also be seen though a simple visual scan of the network. In Chapter 6, we will apply the tool to the IEEE 118-bus network.

Chapter 6: The Tradeoff Between Congestion Cost and Reliability in Meshed Networks

When a Wheatstone bridge is built, bisecting a parallel network, the immediate effect is to congest the network unless the rated capacities of the transmission lines in the Wheatstone are very large relative to the expected flow across the network. From a congestion-management perspective, Wheatstone networks seem to be a losing proposition. However, as discussed in Chapter 3, under some circumstances the Wheatstone bridge may provide a reliability benefit. Consider the Wheatstone network shown in Figure 6.1, which is similar to the networks described in Chapters 3 and 4, except that lines S_{24} and S_{34} have a capacity limit of 100 MW as opposed to 55 MW. Without the Wheatstone bridge, an outage on either line S_{24} or S_{34} will restrict the power transfer to 55 MW between buses 1 and 4. Thus, for a load of 100 MW at bus 4, the expensive generator at bus 4 must generate 45 MW in order to avoid shedding any load. This increases the cost of operating the network according to the differences in marginal costs of the two generators. If the Wheatstone bridge is installed in the network, the power transfer between buses 1 and 4 in event of an outage across line S_{24} or S_{34}, is 100 MW, and the load can continue to be served with the inexpensive generator at bus 1.

During normal system operations, the Wheatstone bridge imposes a cost on the system in the form of congestion. In the case of a contingency on line S_{24} or S_{34} the Wheatstone bridge offers a reliability benefit to the system. Specifically, the Wheatstone bridge serves to satisfy the $N - 1$ reliability criterion with respect to transmission lines. The

loss-of-load probability also falls accordingly. Increased reliability is earned at the cost of increased congestion. The only exception to this tradeoff occurs at very low levels of demand – less than 55 MW in the case of the Wheatstone network in Figure 6.1. Thus, the value of the Wheatstone bridge is the difference between the reliability benefit that it offers to the system over some period of time and the congestion costs it imposes on the system.

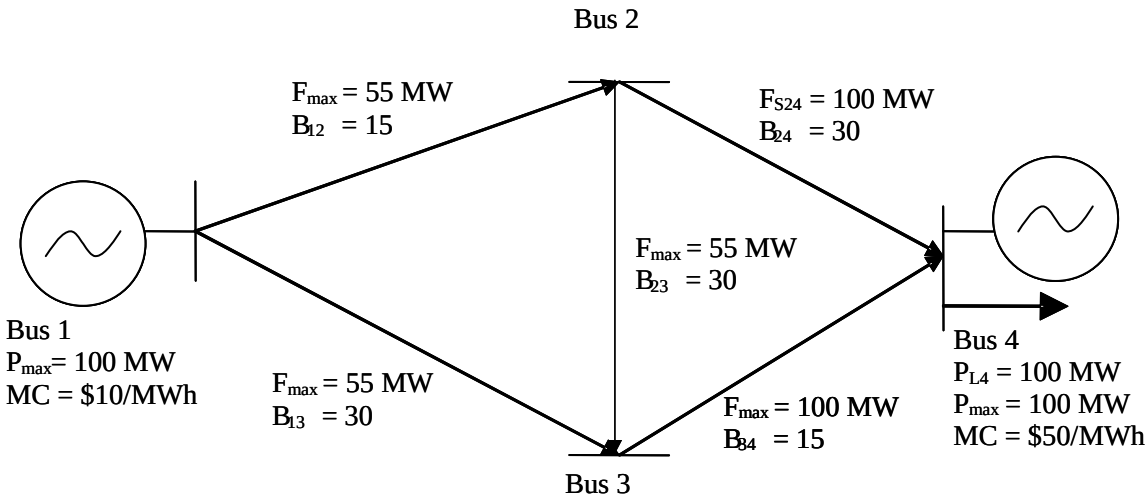

Figure 6.1. The four-bus Wheatstone test network with the stability limits of lines S_{34} and S_{24} increased to 100 MW.

In the restructured electric power industry, various non-utility transmission investment proposals have shared the common theme of identifying economic transmission corridors as a distinct concept from reliability transmission corridors. Perhaps as a signal of the failure of the merchant transmission model, the Energy Policy Act of 2005 has taken the opposite approach, allowing for certain transmission corridors to attain special "national

interest" status.[1] The Energy Policy Act gives FERC the authority to intervene and speed up the siting process for these projects. Transmission investments conferring primarily economic benefits (that is, those not designated as being in the national interest) are, under restructuring, expected to go forward on their own merits. Funding for economic transmission projects is expected to come from either merchant transmission companies operating within larger systems (Hogan 1992, Bushnell and Stoft 1996) or from a group of interested beneficiaries (the participant funding approach favored by Hébert 2004).

Joskow (2005b) has suggested that the separation of economic-based transmission investments from reliability-based investments amounts to a meaningless dichotomy. The failure of the merchant model to gain popularity implies that transmission assets will be constructed primarily by vertically-integrated utilities recovering costs in a regulated framework. This has certainly been the experience in the United States (Hirst 2004).

The dichotomy discussed by Joskow is more than meaningless; as Figure 6.1 shows, in many cases it is incorrect. Reliability often comes at the expense of additional congestion in the network. In meshed networks such as power networks, economics and reliability are not unrelated; they actually represent a natural tradeoff faced by system operators and planners in systems with loop flows. Sparser networks are less congestible (in the sense that the Wheatstone network is congestible) but may not meet reliability criteria. Increased interconnection can offer redundancy in the network, but the network will also likely be subject to Braess's Paradox.

[1] Energy Policy Act of 2005 at ¶1221.

6.1 A Framework for Cost-Benefit Analysis of Wheatstone Networks

Setting aside the issue of generator contingencies, the extent of the tradeoff is a function of the level of demand and the probability of an outage on the lines downstream of the Wheatstone bridge. Conditional on an outage on either line S_{24} or S_{34}, let T_W be the feasible transfer capacity between buses 1 and 4 and let T_0 be the feasible transfer capacity between buses 1 and 4 without the Wheatstone bridge.[2] Define U to be the event of an outage on line S_{24} or S_{34}. U is assumed to be a Bernoulli random variable that is equal to one (the case of an outage) with probability u, and equal to zero (no outage) with probability $1 - u$. The level of demand at bus 4, P_{L4}, is assumed to be constant or perfectly predictable. The analysis will be extended to include stochastic demand in Section 6.5.

The congestion cost imposed on the system during normal operations is measured by the difference in total cost of serving a given demand profile P_L^* with the Wheatstone bridge in the network, and the total cost of serving an identical demand profile without the Wheatstone bridge. With the Wheatstone bridge, suppose that the generation profile of the network is $\{P_{G1}^*,...,P_{Gn}^*\}$ and that the generation profile without the Wheatstone network is $\{P_{G1}^{'},...,P_{Gn}^{'}\}$. The congestion cost associated with the Wheatstone can be written as:

$$(6.1) \quad CC = \sum_{i=1}^{NB}\left(\int_0^{P_{Gi}^*} MC_i(P_{Gi})dP_{Gi} - \int_0^{P_{Gi}^{'}} MC_i(P_{Gi})dP_{Gi}\right).$$

[2] "Feasible transfer capacity" means the total amount of power that can be transferred from bus 1 to bus 4 while respecting all network constraints.

In the case of the Wheatstone network in Figure 6.1, we have $CC \geq 0$, but in theory this need not necessarily hold in more general networks.

Quantifying the reliability benefit of the Wheatstone network involves comparing the amount of unserved energy in a network equipped with a Wheatstone bridge to the amount of unserved energy in a network without the Wheatstone bridge:

$$UE = \begin{cases} T_W - T_0, & U = 1 \\ 0, & U = 0 \end{cases}. \quad (6.2)$$

Note that *UE* measures only the decrease in unserved energy associated with the Wheatstone bridge. In the case of the Wheatstone network shown in Figure 6.1, we have $UE \geq 0$, but this need not necessarily be the case. Assuming that the customer value of electricity is described by a continuous, differentiable, and non-negative marginal value function *v*, the cost of an amount of unserved energy $T_W - T_0$ is:

$$CUE = U \times \left(\int_0^{T_W} v(T)dT - \int_0^{T_0} v(T)dT \right). \quad (6.3)$$

If there is no outage on the line, then *UE* = 0 and thus *CUE* = 0. Also, if $T_W = T_0$ (that is, the possible transfer across the network is not affected by line outages or the presence of the Wheatstone bridge), then the cost of unserved energy is also zero. Assuming that the outage probability is independent of the level of demand, system reliability can be measured using the expected cost of unserved energy:

$$(6.4) \qquad ECUE = u \times \left(\int_0^{T_W} v(T)dT - \int_0^{T_0} v(T)dT \right).$$

The (expected) net benefit of the Wheatstone bridge in the presence of nonstochastic demand is thus $NB = ECUE - CC$.

6.2 Application to the Four-Bus Wheatstone Test Network

Applying the cost-benefit calculus of equations (6.1) through (6.4) to the four-bus Wheatstone network in Figure 6.1 is straightforward. Assuming that the generator at bus 4 has sufficient capacity, the cost difference between the two generators in the network can be used as a measure of the cost of unserved energy.[3] The congestion cost at time t, CC_t, and the reliability benefit at time t, RB_t, are given by:

$$(6.5) \qquad CC_t = \max\left\{0, \int_0^{P_{L,t}-T_W} MC_4(P_{G4,t})dP_{G4} - \int_{T_W}^{P_{L,t}} MC_1(P_{G1,t})dP_{G1}\right\}$$

$$(6.6) \qquad RB_t = U_t \times \left(\int_0^{P_{L,t}-T_0} MC_4(P_{G4,t})dP_{G4} - \int_{T_0}^{P_{L,t}} MC_1(P_{G1,t})dP_{G1} \right).$$

Since the reliability benefit is equal to zero unless an outage occurs, and since the congestion cost is nonstochastic, the expected net benefit of the Wheatstone bridge at time t is given by $uRB_t - (1-u)CC_t$.

[3] The implicit assumption is that the value of reliability to the load at bus 4 can be given by the negative of the generation cost at bus 4.

Equations (6.5) and (6.6) provide some insight as to how the net benefit function is expected to behave. For sufficiently low levels of demand, the congestion cost will be zero since the rated megawatt limit of the lines in the network is large relative to demand. Similarly, the reliability benefit of the Wheatstone will also be zero if demand is low relative to the amount of capacity in the network. In this case, even if a line goes out and the network does not have a Wheatstone bridge to redirect flows, outages will not occur in the downstream portion of the Wheatstone (bus 4 in the case of Figure 6.1).

As loading across the Wheatstone network increases, the meshed nature of the network implies that some lines will become congested. For these higher levels of demand, the Wheatstone will also provide a reliability benefit, acting to re-route flows throughout the network in the case of an outage on one of the boundary links. Thus, for a given outage probability, the net benefit of the Wheatstone should either monotonically increase or decrease (depending on which of the congestion cost or reliability benefit is greater in magnitude), or it might decrease over a range of demand and increase over a different range of demand.

The independence of congestion and reliability can be examined by looking at the congestion cost and the reliability benefit functions over different ranges of demand. If one function is constant while the other is not, then the two can be viewed as independent over that range of demand.

Under the DC power flow assumptions, flows on the lines in the Wheatstone network can be written as:

(6.7) $\mathbf{F} = \mathbf{H}\boldsymbol{\theta}$,

where $\mathbf{H} = \mathbf{A'B}^{diag}\mathbf{A}$. Net bus injections in the DC power flow model are given by:

(6.8) $\mathbf{P} = \mathbf{B}\boldsymbol{\theta}$.

Thus, $\boldsymbol{\theta} = \mathbf{B}^{-1}\mathbf{P}$. Combining (6.7) and (6.8) yields:

(6.9) $\mathbf{F} = \mathbf{H}\mathbf{B}^{-1}\mathbf{P}$.

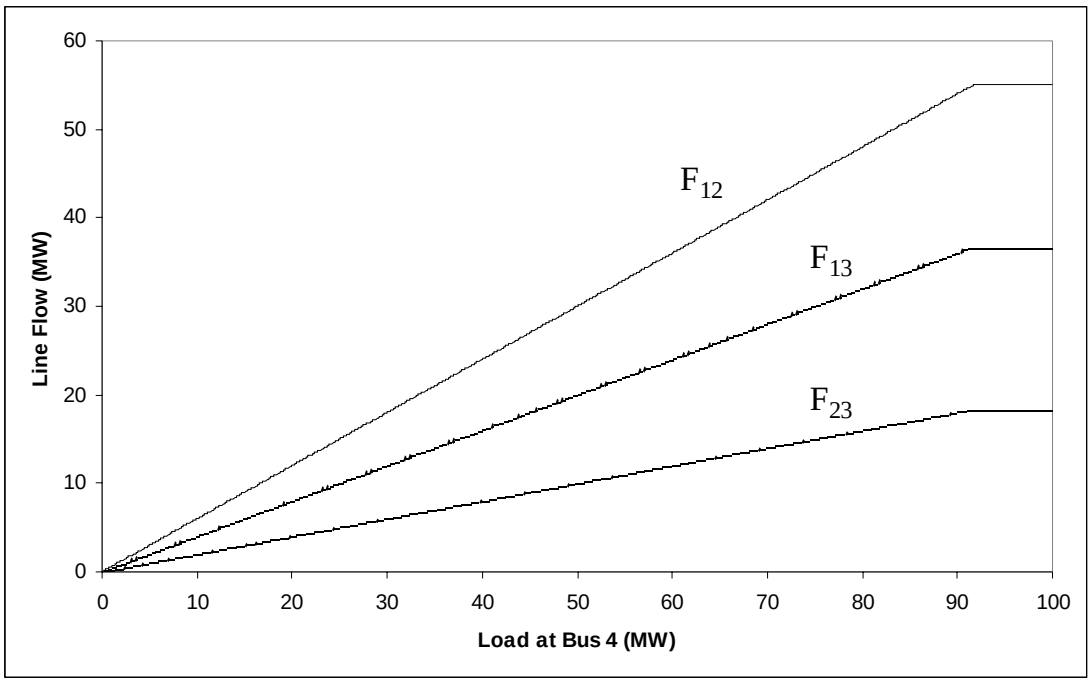

Figure 6.2. Flows in the four-bus Wheatstone test network as a function of the demand at bus 4.

In equation 6.9, the sensitivity $\partial\mathbf{F}/\partial\mathbf{P}$ (the network distribution matrix) is a constant function of the network parameters. Thus, a unit increase in net injections at any bus will change the flows through the network by an amount independent of the level of the bus injections. This linear relationship between the load at bus 4 and the line flows in the Wheatstone network is shown in Figure 6.2. As demand increases, the flows increase linearly until line S_{12} hits its limit of 55 MW. The network constraint on line S_{12} effectively constrains the remaining lines in the system.

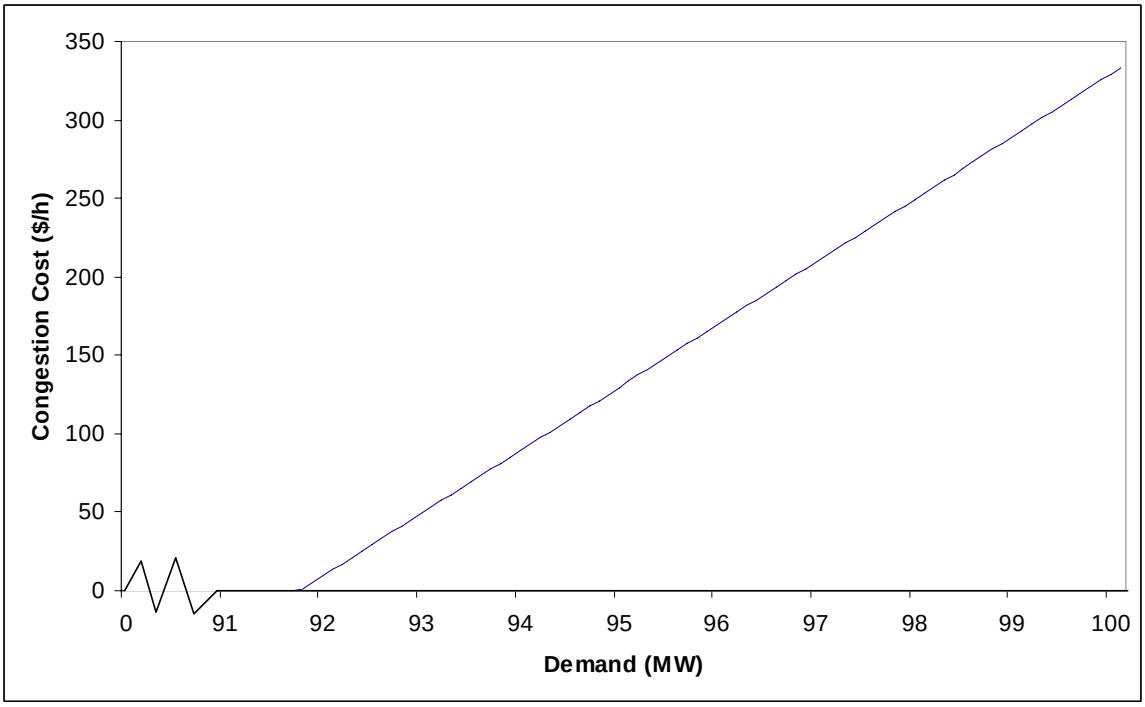

Figure 6.3. The cost of congestion in the four-bus Wheatstone test network. The generator at bus 4 is assumed to have a constant marginal cost of $50.

The maximum transfer across the Wheatstone network, T_W, can be calculated using Figure 6.2. T_W is equal to the sum of the maximum power that can be transferred across each of the lines S_{12} and S_{13} (power transfer across the bridge is simply equal to the difference $F_{12} - F_{23}$). For the network in Figure 6.1, we get T_W = 91.67 MW (see the

discussion in Chapter 3). The congestion cost associated with the Wheatstone bridge will be zero at all levels of demand below T_W. For levels of demand larger than T_W, the congestion cost will rise according to equation (6.5). Figure 6.3 shows the congestion cost in the Wheatstone network, assuming that the generator at bus 4 has a constant marginal cost of $50/MWh.

Without the Wheatstone bridge, an outage on line S_{24} or S_{34} limits the transfer capability across the network to 55 MW; this is the network's value for T_0. With the Wheatstone bridge, 100 MW could be transferred across the network in the event of an outage. If the generator at bus 1 is assumed to have a constant marginal cost, the expected reliability benefit of the Wheatstone bridge (equation 6.6) is equal to:

$$E(RB) = u \times \left[\left(MC_4 - MC_1 \right) \times \max\{0, P_L - T_0\} \right]. \tag{6.10}$$

Thus, the expected net benefit of the Wheatstone bridge in Figure 6.1 is given by:

$$\begin{aligned} E(NB) &= E(RB) - CC \\ &= u \times \left[\left(MC_4 - MC_1 \right) \times \max\{0, P_L - T_0\} \right] - \left(MC_4 \times \max\{0, P_L - T_W\} \right). \end{aligned} \tag{6.11}$$

Equation (6.11) is displayed graphically in Figure 6.4 for the network shown in Figure 6.1. Demand is assumed to be between 0.1 MW and 100 MW, and the outage probability is assumed to be between 1×10^{-6} and 1×10^{-3}. The marginal costs of the

generators are assumed to be constant and are set at MC_1 = \$10/MWh and MC_4 = \$50/MWh.

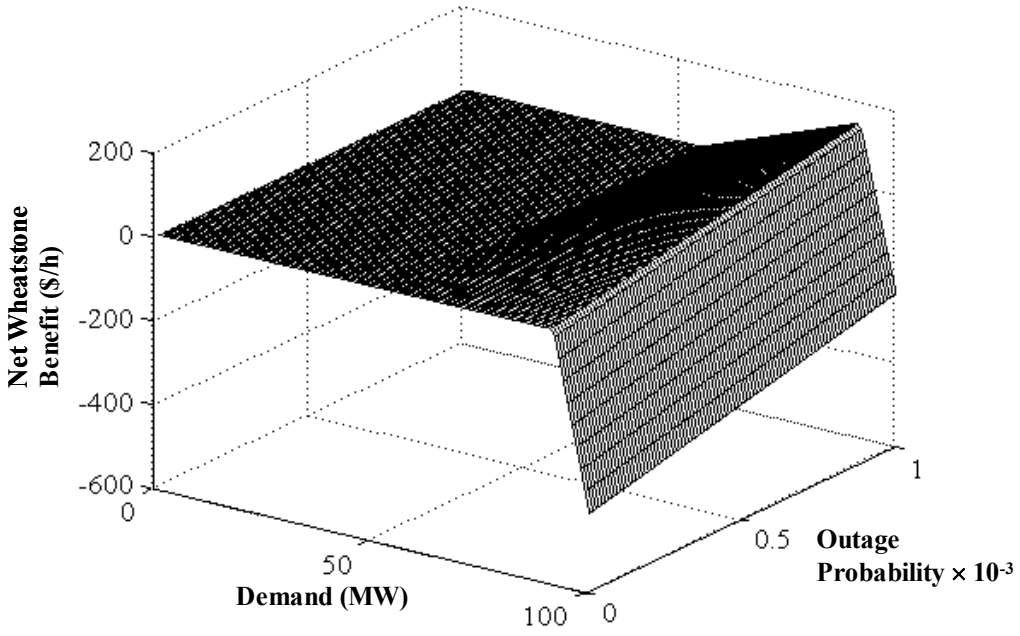

Figure 6.4. Expected net benefit of the Wheatstone bridge in the four-bus test network.

6.3 Application to the IEEE 118-Bus Test Network

The four-bus test network of Figure 6.1 is useful for illustrating the concepts behind equations (6.1) through (6.4), but is not a very descriptive model of an actual system. A Wheatstone network embedded in a larger system might have net generation or load at all four buses; generation or load at one end of the Wheatstone bridge could sufficiently alter the pattern of flows such that congestion is avoided. The reliability benefit of the Wheatstone bridge also depends on how it interacts with the rest of the network; the loss of one of the boundary links might simply be made up by increased flows from other portions of the network, with the Wheatstone bridge not adding any benefit to the system at all.

A useful behavioral distinction in this regard can be made between Wheatstone sub-networks on the boundary of larger networks and Wheatstone sub-networks in the interior of a larger network. Boundary Wheatstones have fewer connections with the external network and should behave more like the standalone Wheatstone network shown in Figure 6.1. It may even be possible to determine the behavior of a boundary Wheatstone through visual examination alone. The behavior of interior Wheatstones, on the other hand, may be less clear, particularly if there is net generation or load at all four buses.

A conceptual illustration of the difference between boundary and interior Wheatstone networks is provided in Figure 6.5. Panel (a) shows a Wheatstone network on the boundary of some (unspecified) larger network, with only buses 1 and 2 connected to the larger network, while panel (b) shows a Wheatstone in the middle of a larger network.

In the Wheatstone test network of Figure 6.1, congestion in the network is a function of the load at bus 4 and the network susceptance matrix, as shown in Chapter 3. The effect of an outage on line S_{34} can be dampened or eliminated by the Wheatstone bridge; the bridge allows an extra 45 MW of power to be delivered to the load at bus 4 (relative to the amount of power that could be delivered without the bridge). The reliability benefit is easily bounded by the capacity of the bridge, the capacity of lines S_{12} and S_{24}, and the capacity of the generators.

Now consider the Wheatstone sub-network shown in Figure 6.5(a). Whether congestion exists in the network cannot be determined simply by comparing the demand at bus 4 to the network topology and the generation at bus 1. Since bus 3 is also connected to the remainder of the network, the external behavior influences the condition of the

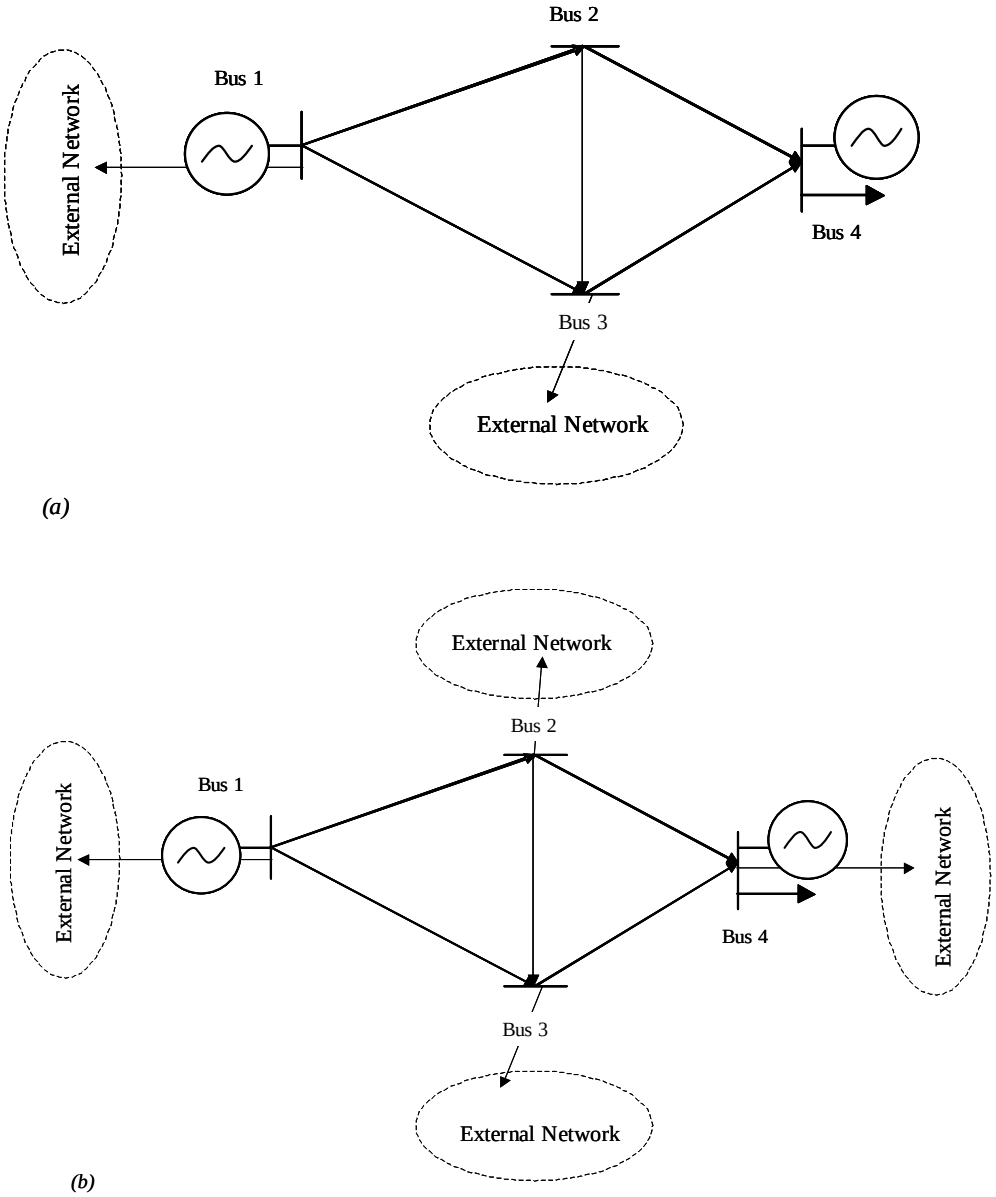

Figure 6.5. Boundary versus Internal Wheatstone sub-networks. Panel (a) shows a boundary Wheatstone, and panel (b) shows an interior Wheatstone.

Wheatstone. If the interchange between the Wheatstone and the rest of the network at bus 3 is minimal, then the Wheatstone will likely be congested if demand at bus 4 is high enough. If the external network draws a large amount of power out of the Wheatstone through bus 3, or injects a large amount of power through bus 3, congestion in the Wheatstone sub-network will fall or rise accordingly. The reliability benefit of the Wheatstone bridge also depends on the amount of interchange between the Wheatstone and the remainder of the network. If a bottleneck exists coming into the Wheatstone sub-network at bus 3, then very little power is likely to be transferred through the Wheatstone from the rest of the network in case of a line outage. On the other hand, to the extent that the path connecting to the Wheatstone sub-network via bus 3 is unconstrained, this will reduce the reliability benefit attributable to the Wheatstone bridge.

If the Wheatstone is connected to the larger network at all four points, as in Figure 6.5(b), the analysis is similar to Figure 6.5(a) but there are more factors to consider. Assuming that the direction of flow through the Wheatstone is towards bus 4, the congestion cost associated with the Wheatstone is highly dependent on the behavior of the external network near bus 4. Particularly if generation is plentiful and inexpensive downstream of bus 4, then the Wheatstone bridge may not have any associated congestion cost at all. Similarly, the Wheatstone bridge may not contribute any real reliability benefit if other network resources exist to serve the load in the event of a transmission-line contingency within the Wheatstone sub-network. Whether embedded Wheatstone sub-networks behave similarly to the four-bus test network is thus an empirical question.

Even for Wheatstone networks embedded in larger systems, the congestion effect of the Wheatstone bridge is not independent from its reliability effect. That is, contrary to implicit and explicit assumptions underlying the market-based transmission investment model, embedded Wheatstone bridges cannot be considered solely economic or reliability investments. Four Wheatstone sub-networks from the IEEE 118-bus networks are used to illustrate that the basic behavior seen in the test network of Figure 6.1 applies more generally to embedded Wheatstone structures.

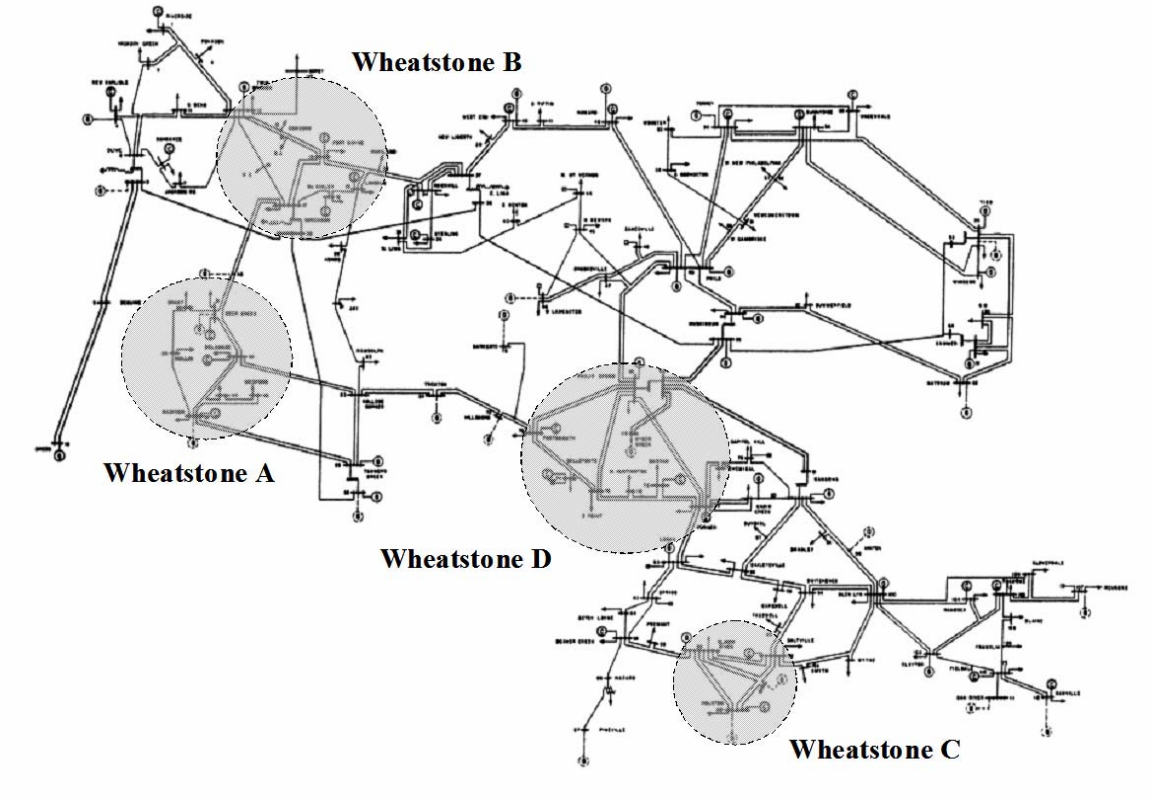

Figure 6.6. Four Wheatstone sub-networks of the IEEE 118-bus test network.

The four Wheatstone sub-networks to be considered are indicated in Figure 6.6, which also shows the topology of the IEEE 118-bus test network.[4] The networks are labeled A, B, C, and D. The system topologies for the four networks and illustrative base case power flows are shown in the one-line diagrams of Figures 6.7 through 6.10. Arrows on the branches of Figures 6.7 through 6.10 indicate the direction of power flow; arrows at the buses in Figures 6.7 through 6.10 indicate loads, not necessarily connections with the larger network. Network A is located in the western portion of the 118-bus network and is based on a modified version of the four-node sub-network consisting of buses 27, 28, 31, and 32. It has been modified by connecting buses 31 and 32. Network B is located in the far northwestern corner of the 118-bus network. Although network B is topologically more of a boundary Wheatstone sub-network than an interior Wheatstone sub-network, the flow of power through the network is towards the center (away from the northwest corner), as can be seen in Figure 6.8. Network C is located on the southeastern boundary of the 118-bus network; although it has two connections to the rest of the network, one of them is simply a tie-point with no generation or load.[5] Thus, this network should behave more like to a boundary Wheatstone sub-network, as described above. Network D is located in the middle of the 118-bus network, just northeast of network B. Three of the four nodes of the Wheatstone sub-network interchange with the remainder of the system, so this network will most likely behave as an interior Wheatstone.

[4] Data for the test network were downloaded from the IEEE Power Systems Test Case Archive at http://www.ee.washington.edu/research/pstca/. The network parameters are shown in Appendix A.
[5] The network specifications indicate that synchronous condensers are located at more than one of these nodes. The synchronous condensers were removed from the system prior to analysis. Since this analysis uses only the DC power flow model, the synchronous condensers do not have any effect on the network behavior.

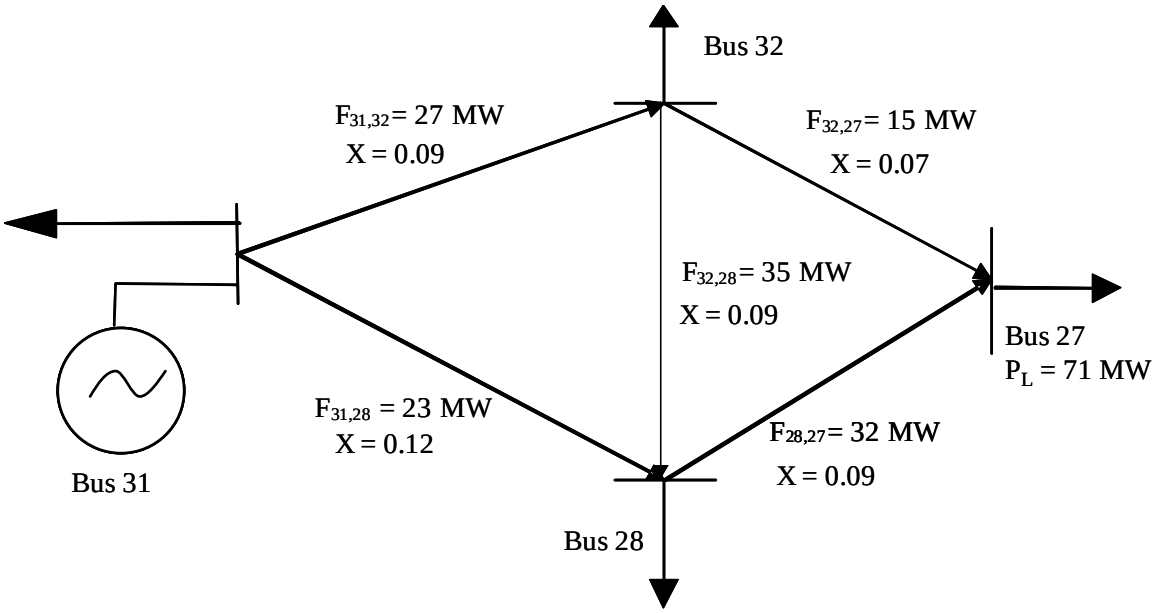

Figure 6.7. One-line diagram of Wheatstone A.

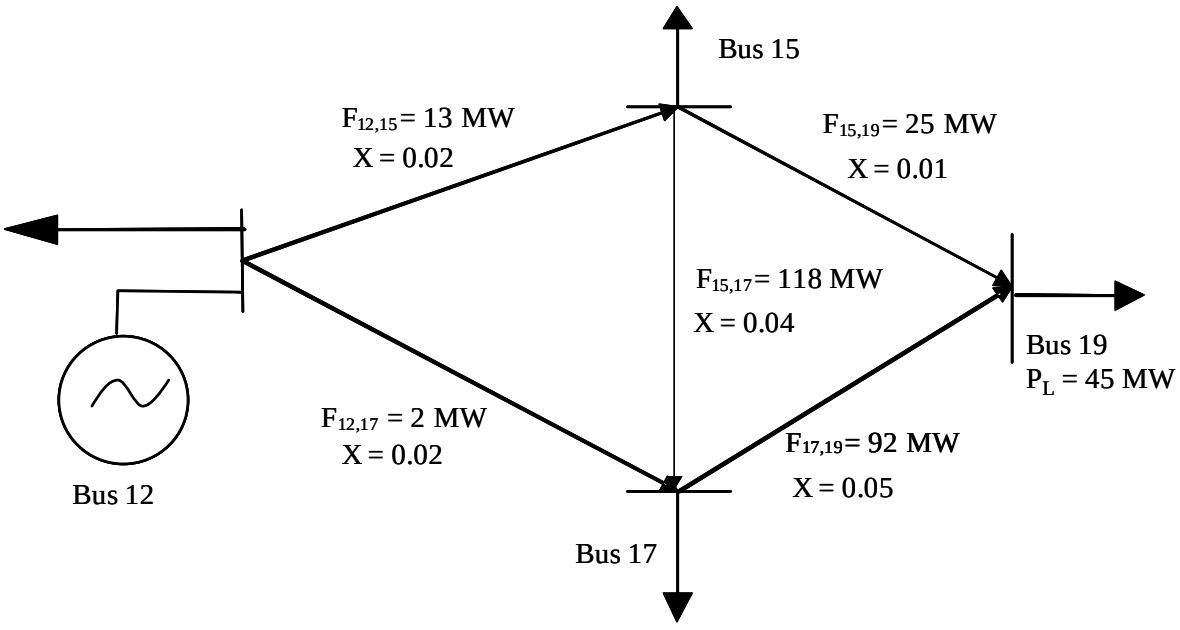

Figure 6.8. One-line diagram of Wheatstone B.

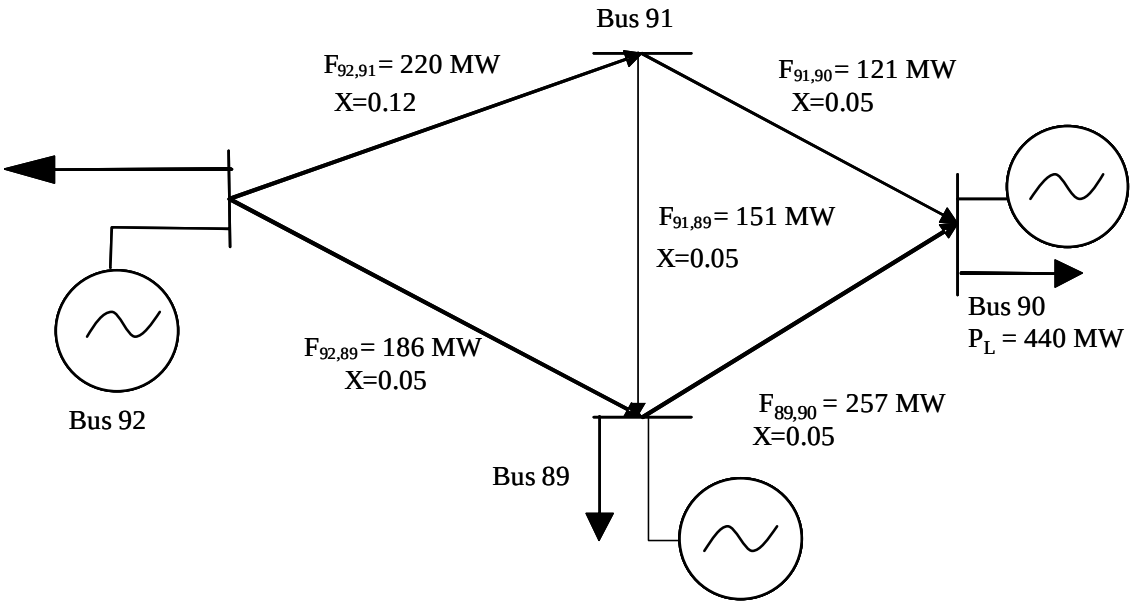

Figure 6.9. One-line diagram of Wheatstone C.

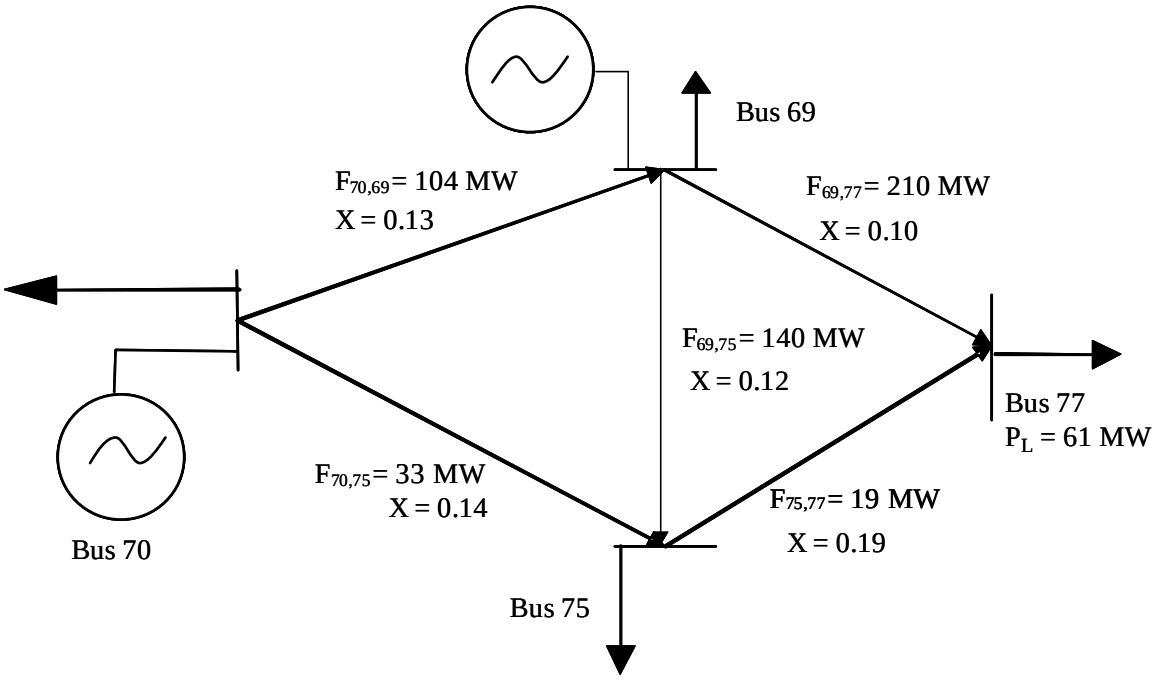

Figure 6.10. One-line diagram of Wheatstone D.

For each of the four Wheatstone sub-networks, four sets of DC optimal power flows were run on the IEEE 118-bus network for a level of demand at the "downstream" node of the Wheatstone varying between 0 and 500 MW. The first two DC power flows were run on the network including the Wheatstone bridge, with and without a contingency on one of the Wheatstone boundary links. The remaining two DC power flows were run on the network without the Wheatstone bridge, with and without a contingency on one of the Wheatstone boundary links. The downstream node for each network was chosen based on the results of the base-case power flows, as shown in Figures 6.7 through 6.10. For network A, bus 27 was defined as the downstream bus (see Figure 6.7). For network B, bus 19 was defined as the downstream bus (see Figure 6.8). For network C, bus 90 was defined as the downstream bus (see Figure 6.9). For network D, bus 77 was defined as the downstream bus (see Figure 6.10).

In each of the four Wheatstone sub-networks within the IEEE 118-bus system, an outage was simulated on the line analogous to link S_{24} in the Wheatstone test network of Figure 6.1. In network A, an outage was simulated on link $S_{32,27}$. In network B, an outage was simulated on link $S_{15,19}$. In network C, an outage was simulated on link $S_{91,90}$. In network D, an outage was simulated on link $S_{69,77}$.

For each level of demand in each Wheatstone sub-network, the associated congestion cost is measured using equation (6.1). Thus, the congestion cost is defined to be the difference in total system cost to serve identical demand profiles in a system with the Wheatstone bridge and without the Wheatstone bridge.

The reliability benefit of the Wheatstone bridge is measured using equations (6.2) through (6.4). The marginal value of consuming power is assumed to be constant and identical for all three networks. This constant marginal value is called the value of lost load (*VOLL*), and is set at $1,000/MWh. Using a constant *VOLL* yields a particularly simple form for the cost of unserved energy:

$$(6.3') \qquad CUE = U \times \left(VOLL \times T_W - VOLL \times T_0\right),$$

where, from Section 6.1, T_W represents the transfer capability across the Wheatstone network with the bridge, and T_0 represents the transfer capability without the Wheatstone bridge, conditional on an outage in one of the boundary links.

Combining equations (6.1) and (6.3'), the expected net benefit of the Wheatstone bridge is given by:

$$(6.12) \qquad E(NB) = \underbrace{u \times \left(VOLL \times T_W - VOLL \times T_0\right)}_{\text{reliability}} - \underbrace{(1-u)\sum_{i=1}^{n}\left(\int_0^{P_{Gi}^*} MC_i(P_{Gi})dP_{Gi} - \int_0^{P_{Gi}'} MC_i(P_{Gi})dP_{Gi}\right)}_{\text{congestion}}.$$

The analysis considers a range of outage probabilities between 10^{-7} and 10^{-1}, so the $(1-u)$ term in equation (6.12) is never large.[6]

Calculating the net benefit function in equation (6.12) requires running four sets of optimal power flows on the IEEE 118-bus network for each of the four Wheatstone sub-networks under consideration (amounting to a total of sixteen power flows). The DC optimal power flow model is used throughout this analysis. The four power-flow cases are:

Case I: The "base case" set of DC optimal power flows, where the sub-network has the Wheatstone bridge, and there is no assumed contingency on any of the transmission lines.

Case II: Same as Case I, but the DC optimal power flows are run on the sub-network without the Wheatstone bridge.

Case III: This case assumes an outage on one of the boundary links in the Wheatstone sub-network, but assumes the sub-network has a Wheatstone bridge.

Case IV: An outage is assumed on one of the links, and there is no Wheatstone bridge in the sub-network.

[6] Larger outage probabilities were examined but are not included here. Once the outage probability becomes much larger than 10% (u = 0.1), at larger levels of demand, both the congestion cost and reliability benefit explode. This is an interesting result in and of itself, but it obscures the interesting behavior of the net benefit function at lower levels of demand.

Thus, the results from Case I and Case II will figure most heavily in the calculation of the congestion cost associated with the Wheatstone bridge, while the results from Case III and Case IV will be most influential in calculating the reliability benefit flowing from the Wheatstone bridge.

Analysis of Wheatstone A

The first Wheatstone sub-network to be discussed here is located in the far western portion of the IEEE 118-bus network, south of Wheatstone sub-network B. Although three of the four buses are connected to the external network, the connections are largely in series with other nodes, which then connect to the meshed portions of the larger network (see Figure 6.6). The base-case optimal power flow on the sub-network, shown in Figure 6.7, indicates that the direction of flow through the Wheatstone is towards bus 27, which is designated as the downstream bus for the purposes of this analysis.

The first step in the analysis is to examine flows throughout the sub-network for each of the four power-flow cases. These flows are shown in Figures 6.11 through 6.15; demand at bus 27 is assumed to range between 0 and 500 MW. Each of Figures 6.11 through 6.15 shows the flows on one line in the Wheatstone sub-network for each of the four power flow cases. Thus, Figure 6.11 shows the flow on line $S_{31,32}$, Figure 6.12 shows the flow on line $S_{21,28}$, Figure 6.13 shows the flow on line $S_{32,27}$, Figure 6.14 shows the flow on line $S_{28,27}$, and Figure 6.15 shows the flow on the Wheatstone bridge. Note that the Wheatstone bridge is included in the network only for power-flow cases I and III. This analysis examines an outage on line $S_{32,27}$; this line is only included in the network for

power flow cases I and II. This explains why Figures 6.13 and 6.15 contain data from only two power-flow cases, while the remainder of the figures contain data from all four.

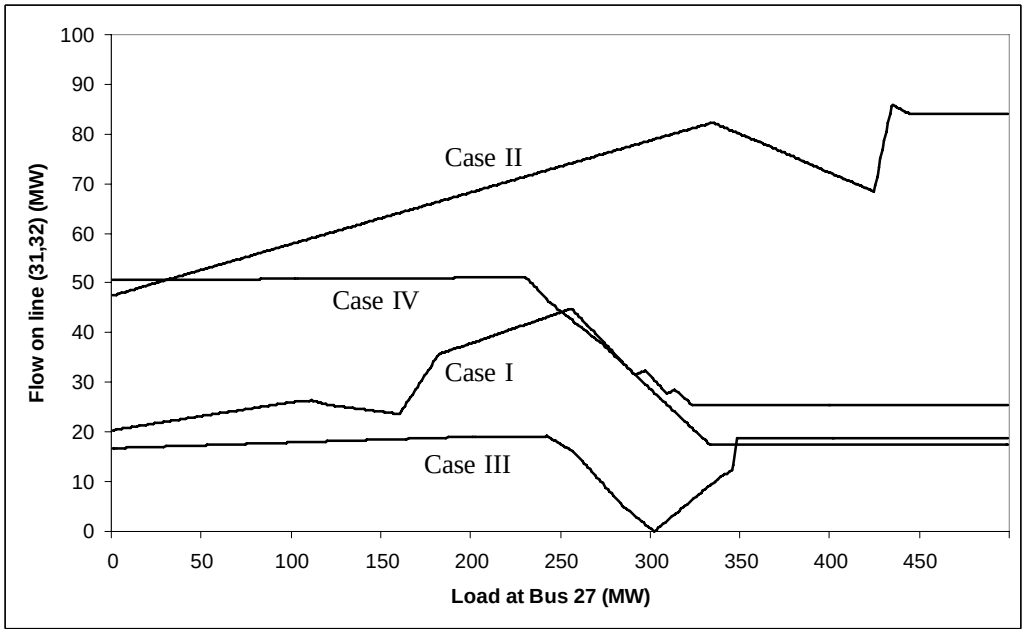

Figure 6.11. Flows on line $S_{31,32}$ of Wheatstone A, as a function of the load at bus 27.

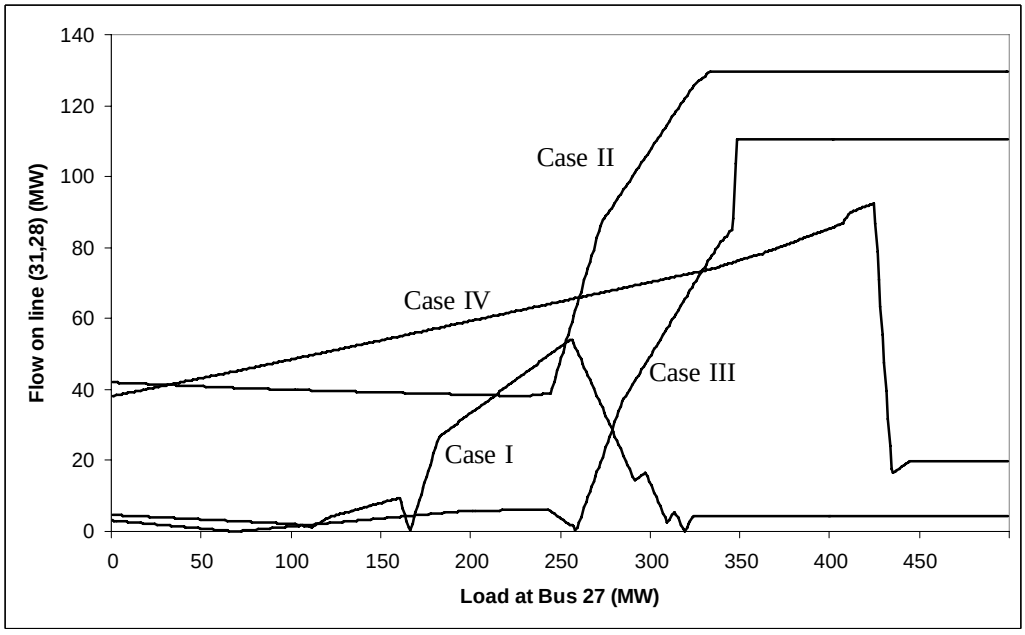

Figure 6.12. Flows on line $S_{31,28}$ of Wheatstone A, as a function of the load at bus 27.

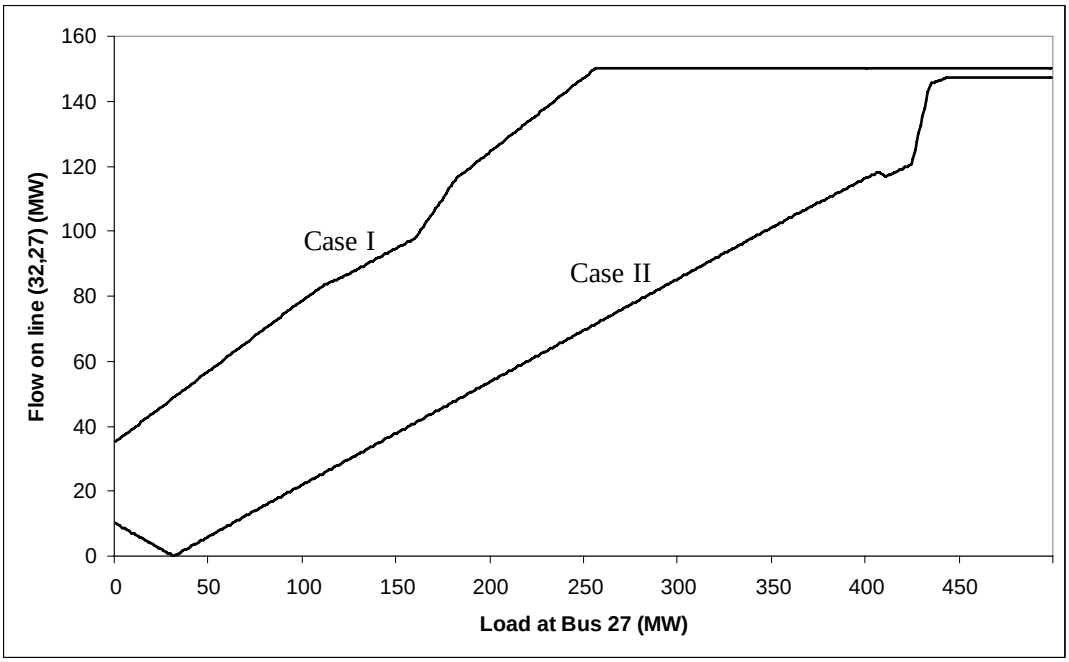

Figure 6.13. Flows on line $S_{32,27}$ of Wheatstone A, as a function of the load at bus 27.

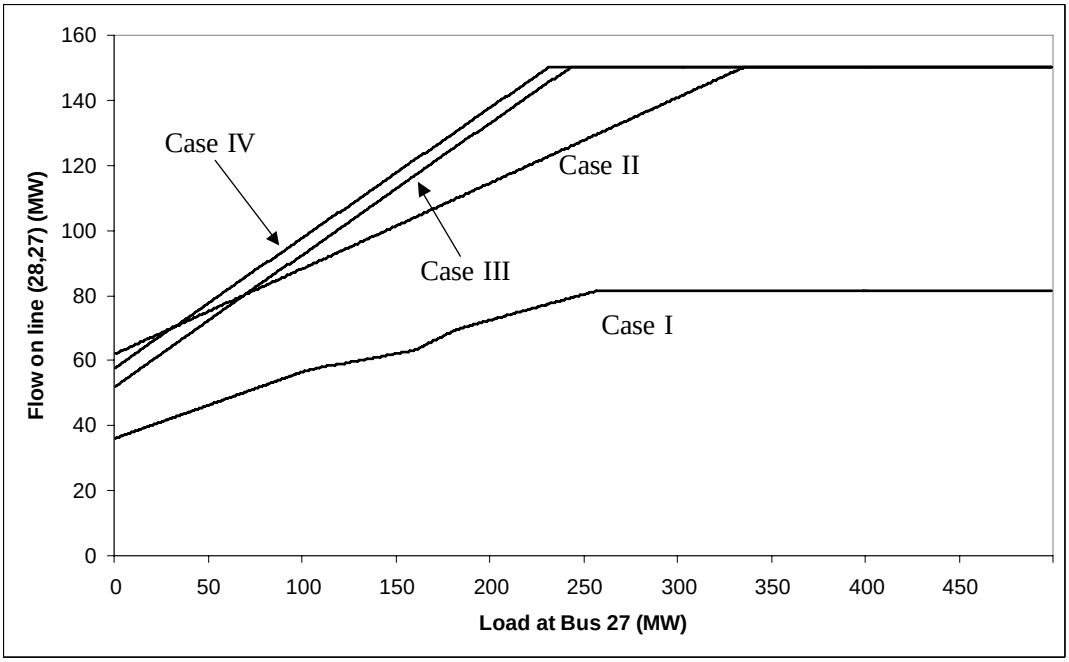

Figure 6.14. Flows on line $S_{28,27}$ of Wheatstone A, as a function of load at bus 27.

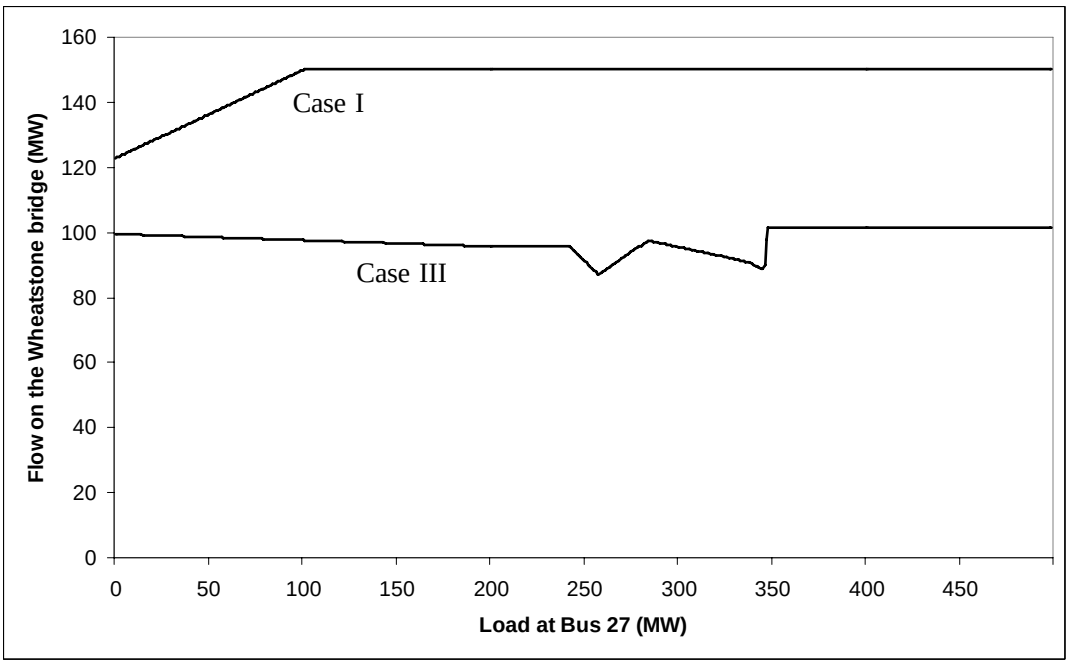

Figure 6.15. Flows on the bridge of Wheatstone A, as a function of load at bus 27.

In the standalone Wheatstone network of Figure 6.1, flows on each line in the network increase with demand until the network hit its capacity constraints or became congested by the Wheatstone bridge. Figures 6.13 through 6.15 show that Wheatstone A exhibits similar behavior on lines $S_{32,27}$, $S_{28,27}$, and on the Wheatstone bridge (although flows over the bridge in the event of an outage on line $S_{32,27}$ are fairly invariant to demand). Line $S_{21,28}$ exhibits the same behavior when either the bridge is removed from the sub-network (Case II) or an outage occurs on line $S_{32,27}$ (Case III). When there are no outages in the network and the Wheatstone bridge is in place (Case I), loadings on line $S_{21,28}$ increase with demand up until around 250 MW, when flows fall to near zero. A similar loading pattern occurs on line $S_{31,32}$ for Case I. Based on the data in Figures 6.11 through 6.15, it appears that the decrease in loadings on lines $S_{31,32}$ and $S_{31,28}$ are matched by an increase

in flows across the Wheatstone bridge; the bridge is likely being fed by a generator from the external network.

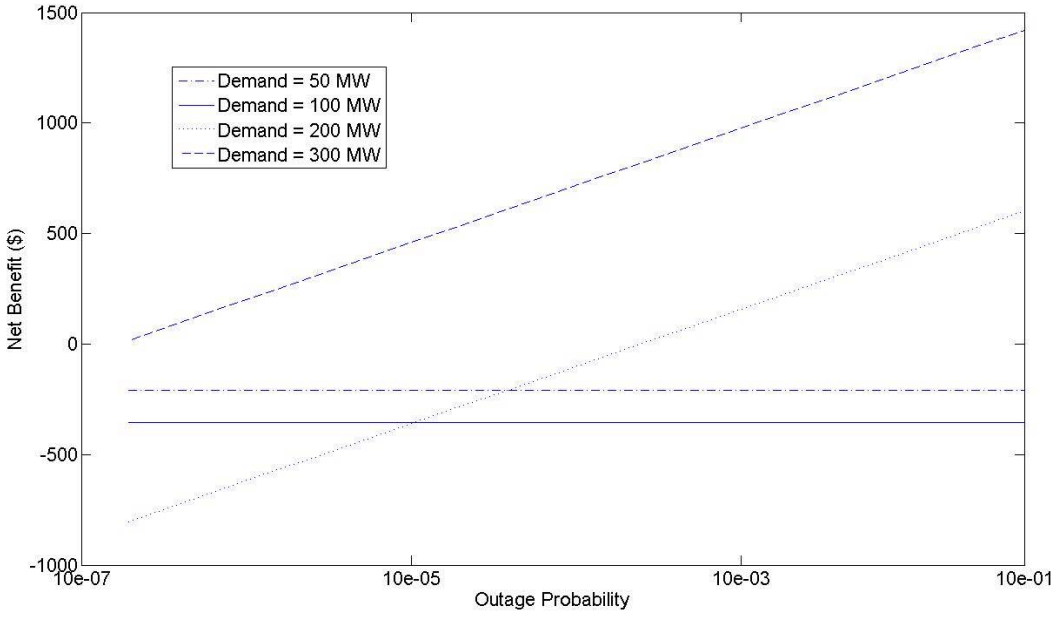

Figure 6.16. Expected net benefit of the bridge in Wheatstone A as a function of the outage probability on line $S_{32,27}$.

Figures 6.16 and 6.17 show two different cross-sectional views of the net benefit accruing to the network from the Wheatstone bridge. In Figure 6.16, the probability of an outage on line $S_{32,27}$ is allowed to vary, while the load at bus 27 is held constant. Figure 6.16 shows this relationship for several different values of the load at bus 27; these represent contour lines (in the demand dimension) of the three-dimensional net benefit function in Figure 6.20. For Wheatstone A, Figures 6.16 and 6.17 only show the net benefit function for levels of demand up to 300 MW. For this particular Wheatstone, demand levels above 300 MW resulted in load shedding, whether the sub-network had a Wheatstone bridge or not.

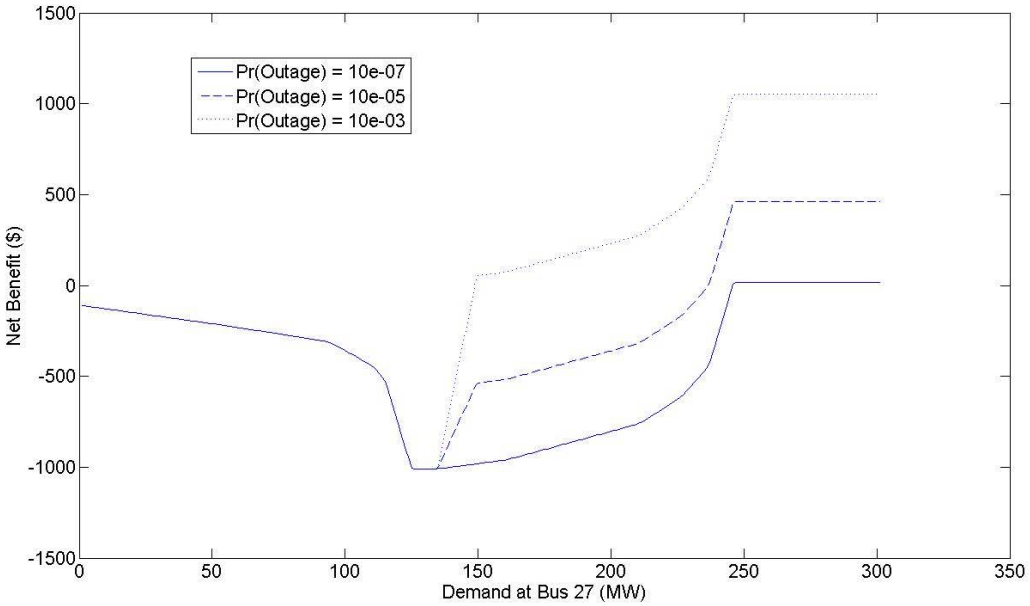

Figure 6.17. Expected net benefit of the bridge in Wheatstone A as a function of the level of demand at bus 27.

In Figure 6.17, the level of demand at bus 27 is allowed to vary, while the probability of an outage on line $S_{32,27}$ is held constant. Each of the lines in Figure 6.17 represents a different outage-probability contour of the net benefit function in Figure 6.20.

To the extent that the behavior in the standalone Wheatstone network of Figure 6.1 exists in Wheatstone sub-networks of larger systems, the net benefit of the Wheatstone bridge should be an increasing function of the outage probability, holding demand constant. Figure 6.16 shows that Wheatstone A does indeed exhibit this behavior. At lower levels of demand, the net benefit is negative and invariant to the probability of an outage, indicating that the congestion cost is the dominant factor in the net benefit calculation. At higher levels of demand (200 MW and higher), the possibility of blackouts exists, and

the Wheatstone bridge can mitigate this risk. Based on Figure 6.16, the level of demand must be very high (around 300 MW), and the outage probability must also be reasonably high in order for the Wheatstone bridge to have a positive net benefit to the system.

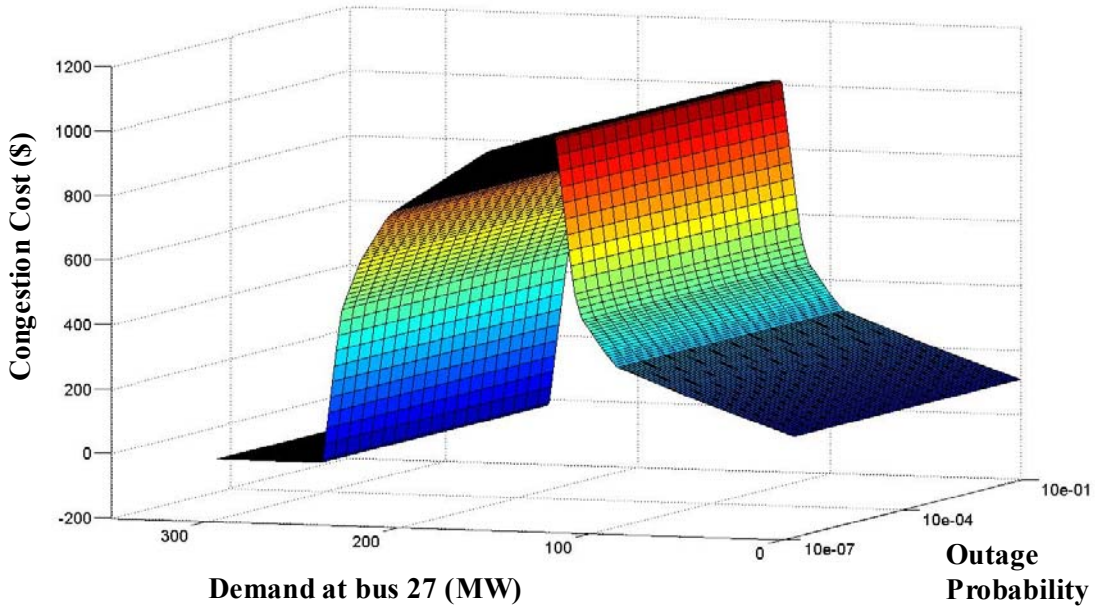

Figure 6.18. Expected congestion cost associated with the bridge in Wheatstone A.

Holding the outage probability constant, the net benefit of the Wheatstone bridge should be approximately parabolic, falling as congestion builds up in the network, and then rising once demand gets high enough that the Wheatstone bridge can support a significant reliability benefit. The parabola should not necessarily be symmetric about the extreme point, as shown in Figure 6.17. Once the reliability benefit kicks in, the net benefit function will rise more sharply if the probability of an outage is larger. The apparent upper bound on the net benefit function indicates that at a certain level of demand, not even a Wheatstone bridge is sufficient to prevent blackouts.

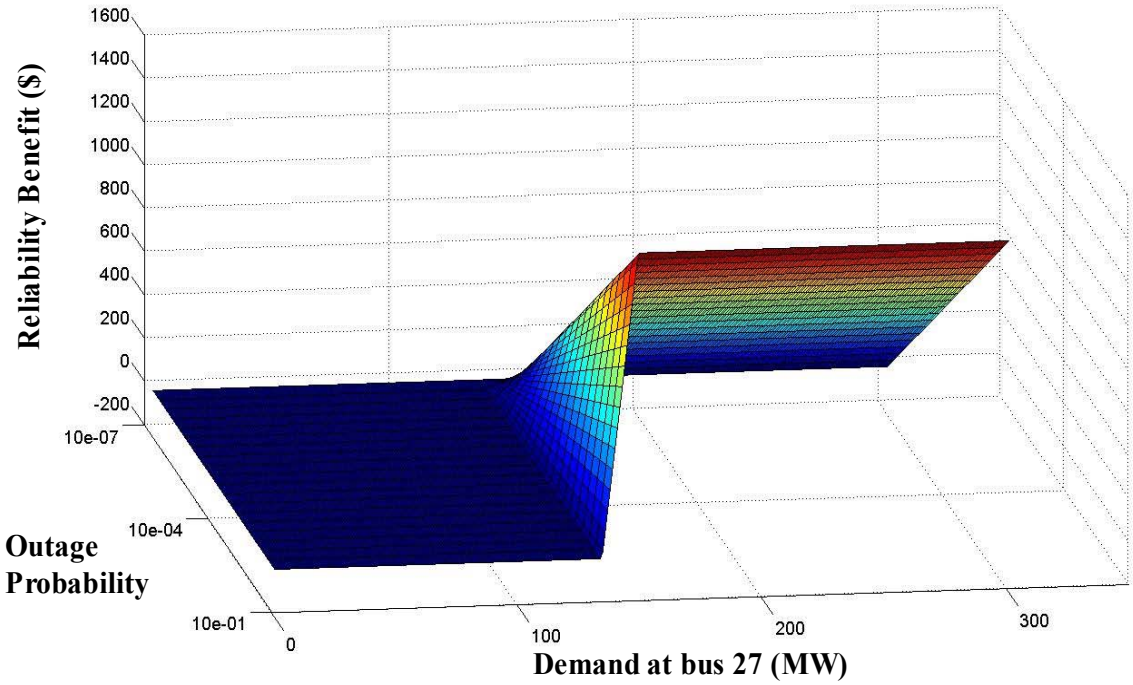

Figure 6.19. Expected reliability benefit associated with the bridge in Wheaststone A.

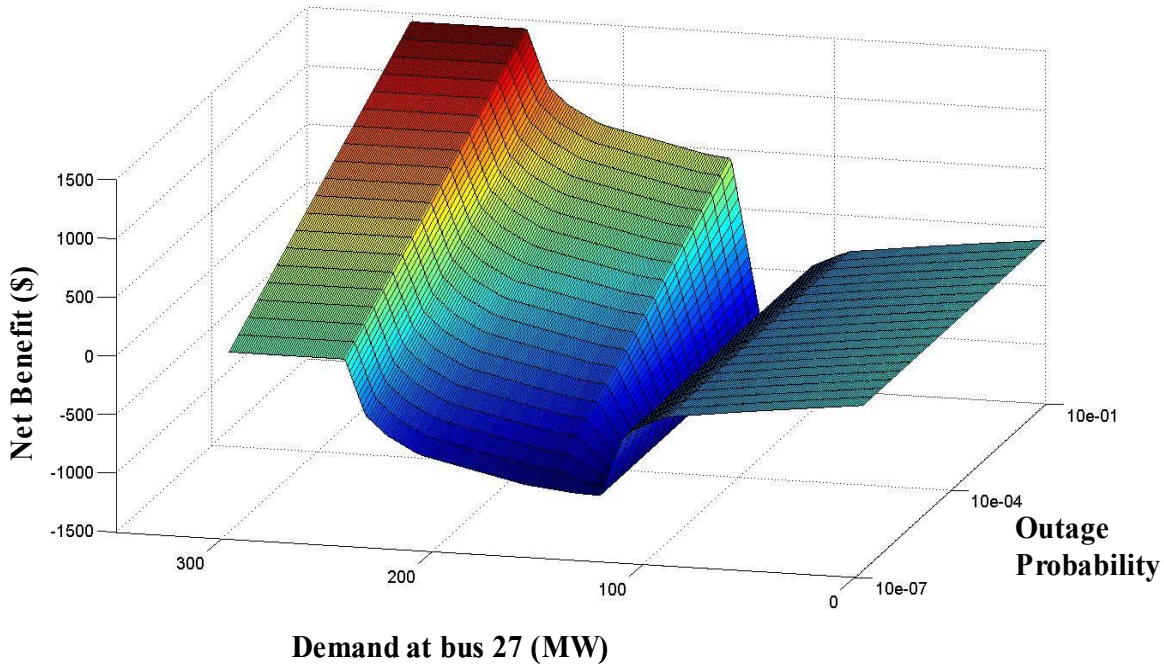

Figure 6.20. Expected net benefit associated with the bridge in Wheatstone A.

The congestion cost and reliability benefit functions (allowing both the demand at bus 27 and the probability of an outage on line $S_{32,27}$ to vary) are shown in Figures 6.18 and 6.19. The total net benefit function is shown in Figure 6.20. In Wheatstone A, congestion and reliability are only independent for low levels of demand (less than 100 MW). For this range of demand, the Wheatstone imposes a congestion cost (as shown in Figure 6.18) while the reliability benefit is zero (as shown in Figure 6.19). Only at higher levels of demand does the net benefit function (Figure 6.20) indicate the tradeoff between the congestion cost imposed by the Wheatstone bridge and its reliability benefit.

Analysis of Wheatstone B

Wheatstone B is located in the northwest corner of the IEEE 118-bus network, as shown in Figure 6.6. Although it is near the edge of the network, three of the four buses that comprise the Wheatstone are connected to the larger network. Based on the power flow shown in Figure 6.8, the direction of flow is out of the Wheatstone towards the center of the network. This reflects the presence of a large generating unit located just outside the Wheatstone, closer to the "upstream" end of the network (bus 12).

Figures 6.21 through 6.25 plot flows on each of the lines in Wheatstone B for each of the four power-flow cases. Demand at bus 19 is assumed to run between 0 and 500 MW. Figure 6.21 shows the flow on line $S_{12,15}$, Figure 6.22 shows the flow on line $S_{12,17}$, Figure 6.23 shows the flow on line $S_{15,19}$, Figure 6.24 shows the flow on line $S_{17,19}$, and Figure 6.25 shows the flow on the Wheatstone bridge. Note that the Wheatstone bridge is

included in the network only for power-flow cases I and III, while line $S_{15,19}$ is included in the network only for power-flow cases I and II.

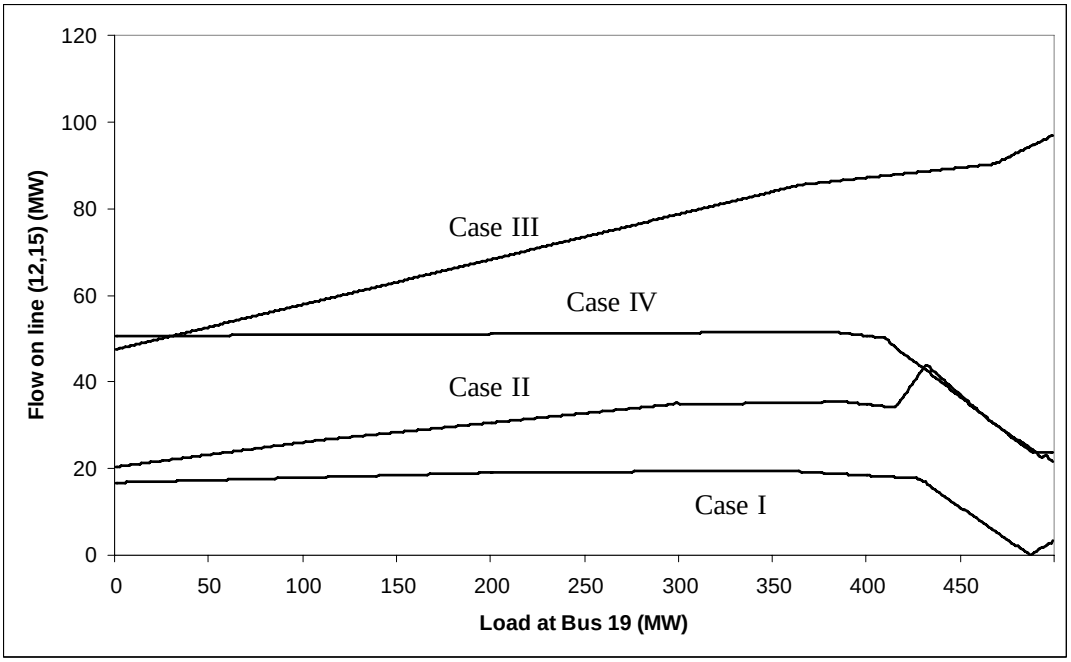

Figure 6.21. Flows on line $S_{12,15}$ of Wheatstone B as a function of load at bus 19.

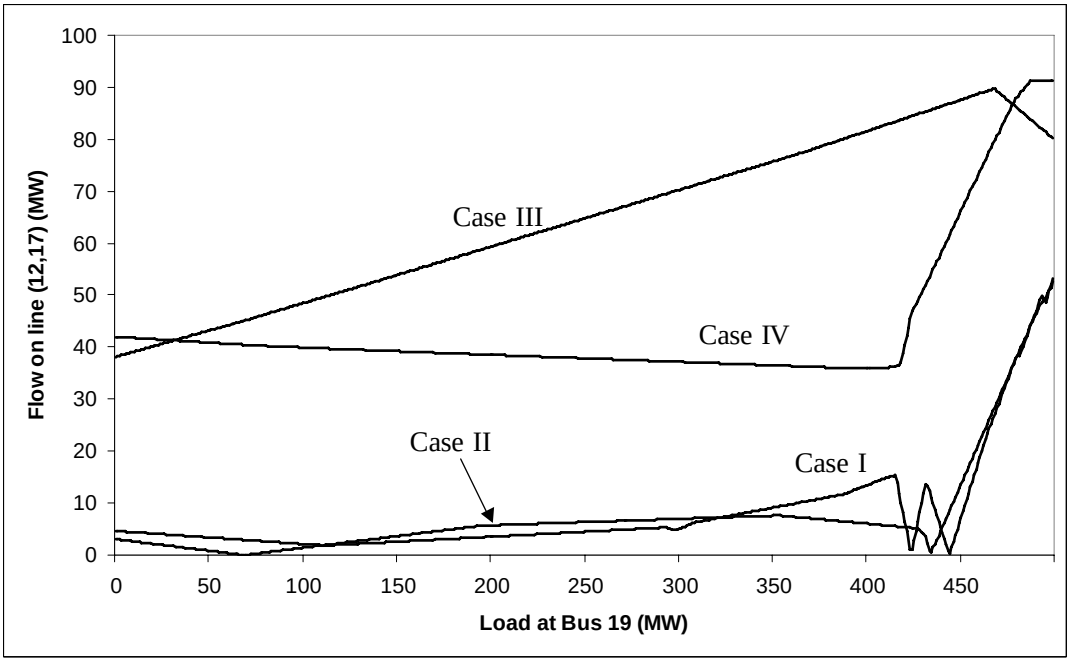

Figure 6.22. Flows on line $S_{12,17}$ of Wheatstone B, as a function of load at bus 19.

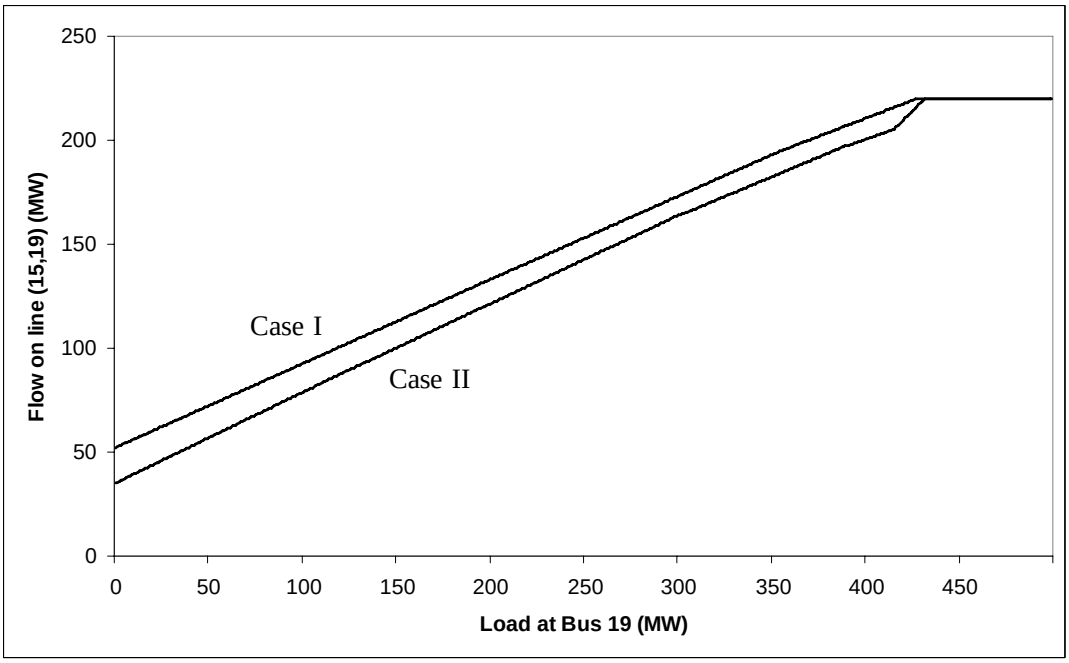

Figure 6.23. Flows on line $S_{15,19}$ of Wheatstone B, as a function of load at bus 19.

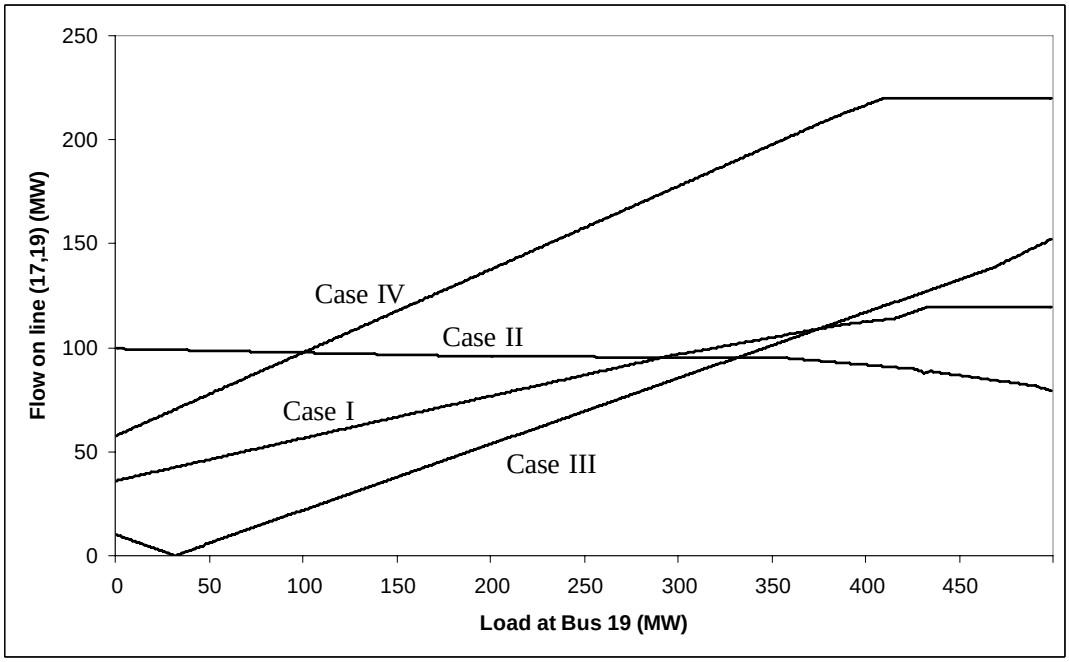

Figure 6.24. Flows on line $S_{17,19}$ of Wheatstone B, as a function of load at bus 19.

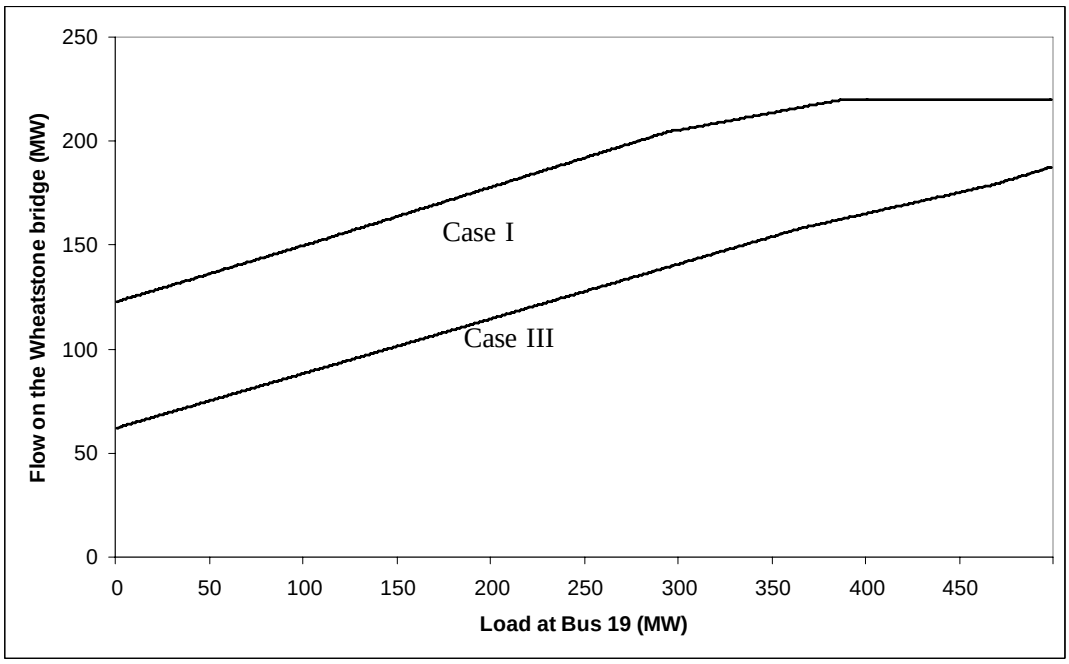

Figure 6.25. Flows on the bridge of Wheatstone B, as a function of load at bus 19.

Figures 6.23 and 6.25 show that only for the Wheatstone bridge and line $S_{15,19}$ is the line loading behavior in Wheatstone B similar to the standalone four-bus Wheatstone test network, in the sense that loadings rise monotonically with demand until the capacity constraint is hit. Figures 6.24 and 6.25 show the reliability value of the Wheatstone bridge. For Case III, in which line $S_{15,19}$ becomes disconnected from the network, loadings increase linearly with demand on both the Wheatstone bridge and line $S_{17,19}$ until the capacity constraints are hit. Figure 6.24 also indicates that congestion in this particular Wheatstone sub-network is likely to be problematic only at the highest levels of demand. Line $S_{17,19}$, downstream from the Wheatstone bridge, does not hit its capacity constraint until demand at bus 19 is around 425 MW.

Figure 6.26 plots the net benefit of the bridge in Wheatstone B against various values of the outage probability. This cross-section shows how the net benefit of the Wheatstone is influenced by the expected reliability benefit. The amount of capacity in the Wheatstone implies that there is virtually no reliability benefit until demand at bus 19 is close to 500 MW. At a demand of 400 MW, the net benefit function is nearly flat and independent of the outage level, reflecting small amounts of congestion in the network (likely influenced by supply and demand conditions in the external network). At demand levels of 490 and 500 MW, outages in the boundary links will result in blackouts at bus 19 (and possibly other portions of the network), and the expected reliability benefit increases accordingly.

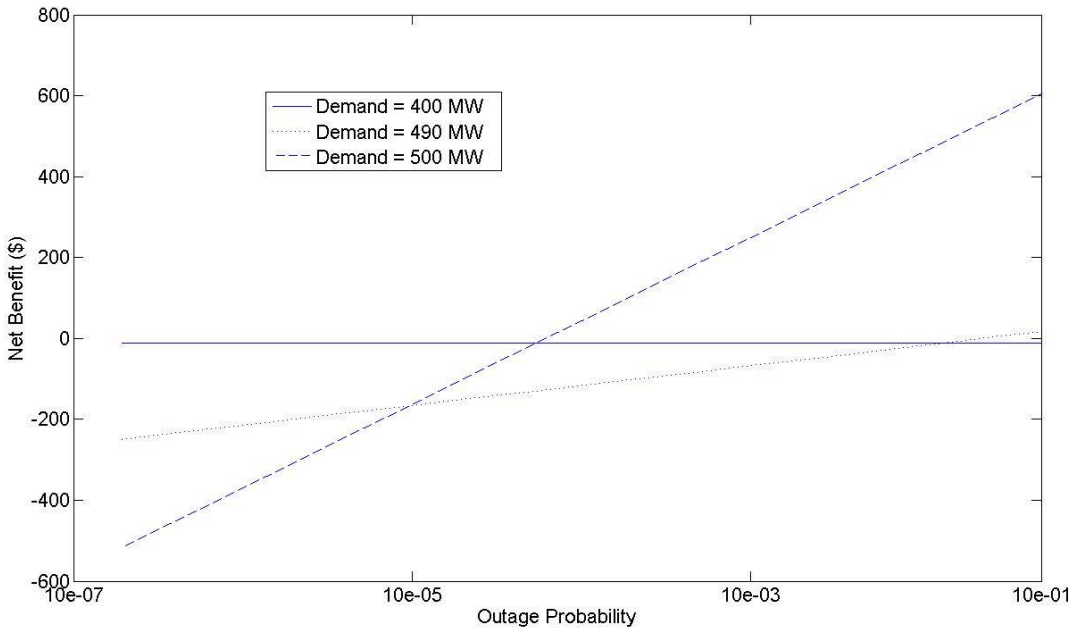

Figure 6.26. Expected net benefit of the bridge in Wheatstone B, as a function of the outage probability on line $S_{15,19}$.

The other cross-section of the net benefit function, which shows the net benefit as a function of the level of demand, is displayed in Figure 6.27. Up until a demand level of nearly 490 MW, the net benefit is influenced entirely by the monotonically-increasing congestion cost. With smaller outage probabilities, such as 10^{-7} and 10^{-5}, the reliability benefit does not outweigh the congestion cost for large levels of demand, and the net benefit of the Wheatstone is negative. Only at higher outage probabilities, such as 10^{-3} and 10^{-1}, does the reliability benefit increase enough in expectation to counter the congestion cost and yield a positive net benefit of the Wheatstone.

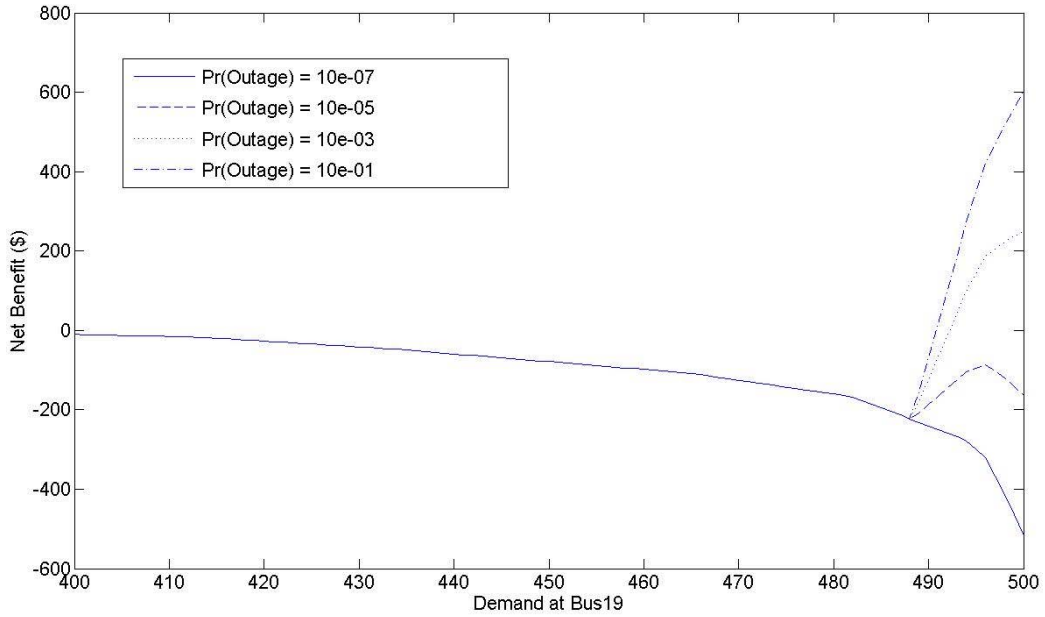

Figure 6.27. Expected net benefit of the bridge in Wheatstone B, as a function of the level of demand at bus 19.

Figures 6.28 through 6.30 show the congestion cost, reliability benefit, and net benefit functions for Wheatstone B, allowing both the outage probability and the level of demand at the downstream node (bus 19) to vary. Note that the demand scales in Figures 6.28 through 6.30 are more expansive than in Figures 6.27 (in Figure 6.27 demand runs from

400 MW to 500 MW, and in Figures 6.28 through 6.30 demand runs from 0 MW to 500 MW). Figure 6.27 has a different scale so that the contribution of the congestion cost to total system benefit can be seen more clearly. Figure 6.30 provides a higher-level view of the net benefit. Throughout much of the demand profile, the net benefit of the Wheatstone bridge is essentially zero, since (as shown in Figures 6.26 and 6.27) no significant congestion cost or reliability exists in the network over this range of demand. For levels of demand where congestion and the risk of blackouts become significant (higher than around 475 MW in this example), Figure 6.30 clearly shows that a tradeoff between congestion cost and reliability benefit exists in Wheatstone B. For a given (high) level of demand, the net benefit function is negative and large in magnitude for a small outage probability, and positive and large in magnitude for a larger outage probability.

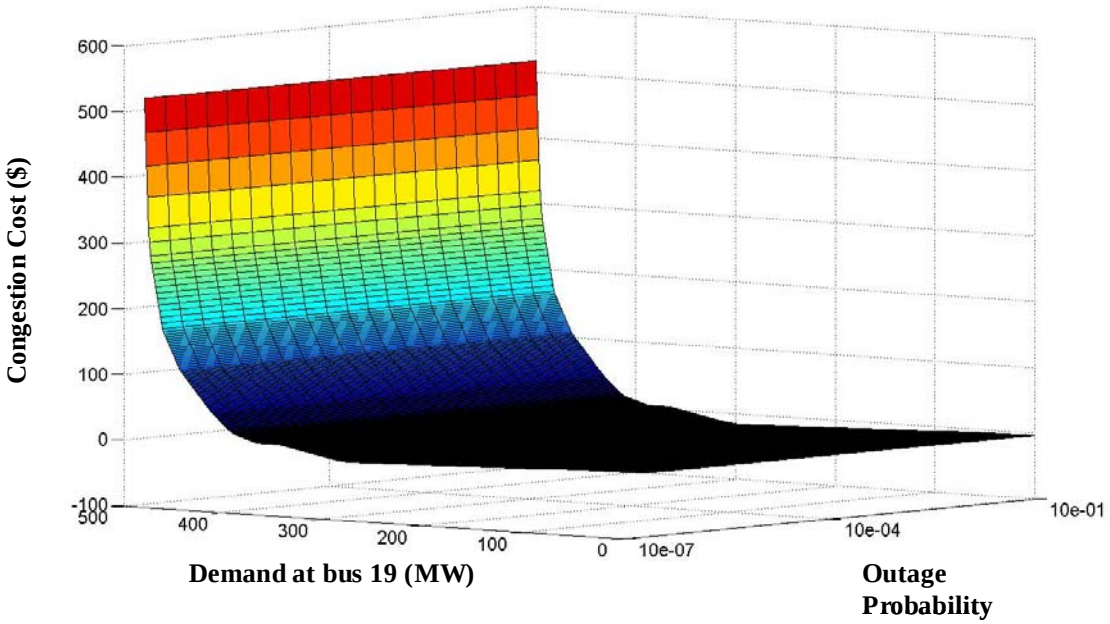

Figure 6.28. Expected congestion cost associated with the bridge in Wheatstone B.

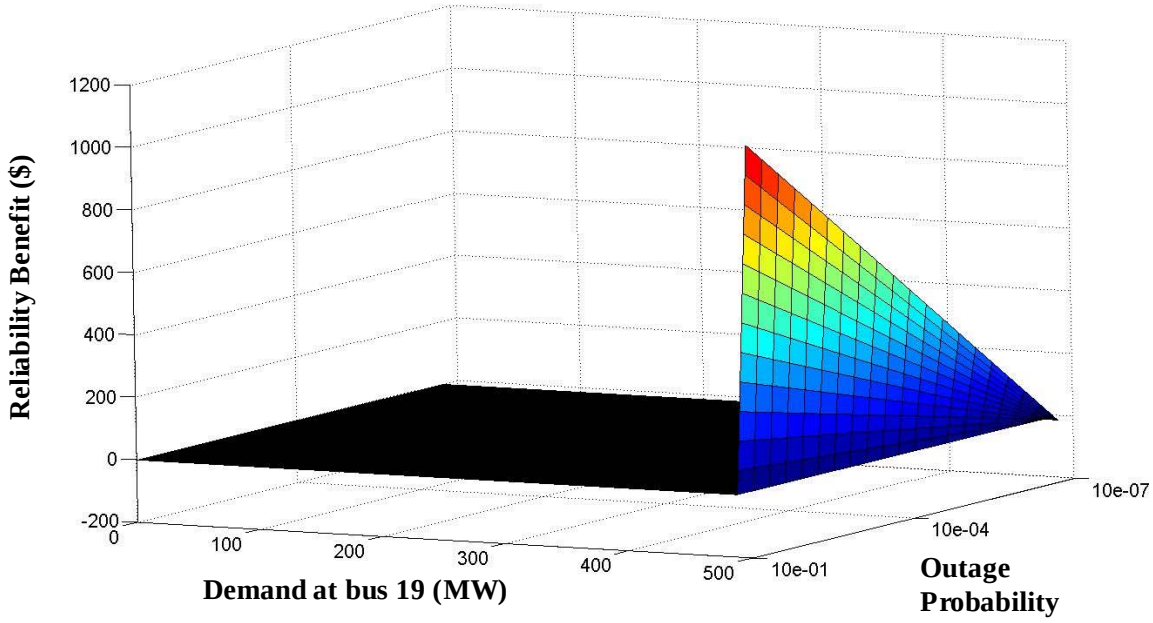

Figure 6.29. Expected reliability benefit associated with the bridge in Wheatstone B.

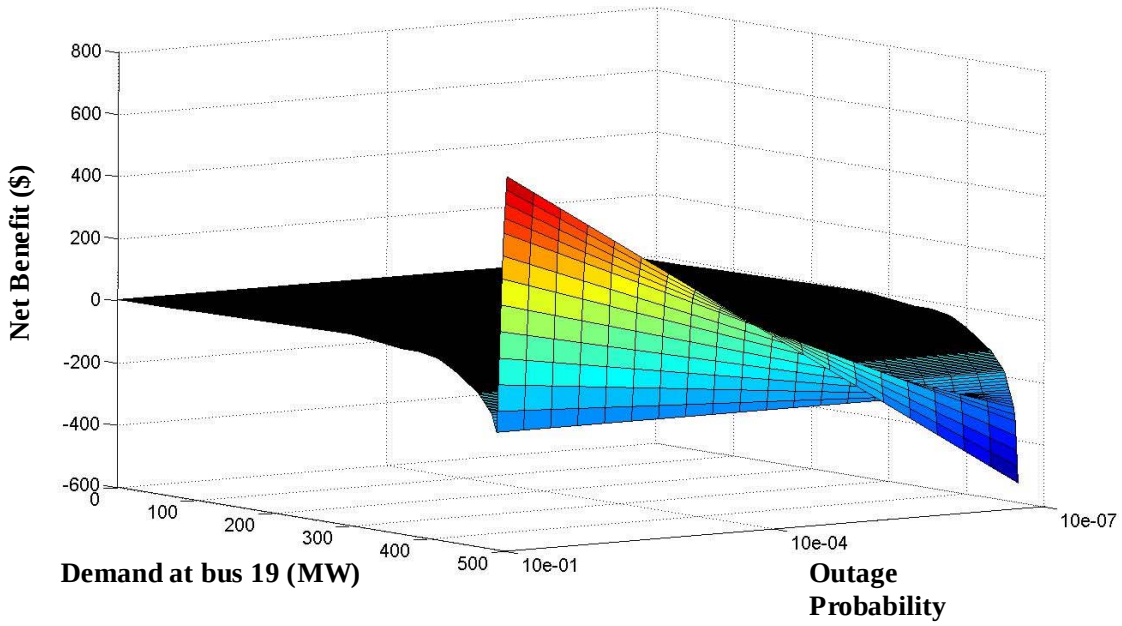

Figure 6.30. Expected net benefit associated with the bridge in Wheatstone B.

Analysis of Wheatstone C

The third Wheatstone sub-network considered here is located in the southeastern portion of the IEEE 118-bus network, as shown in Figure 6.6. This Wheatstone has two of its four component buses connected to the external network. From the base-case power flow (shown in Figure 6.9), power flows from the external network through the Wheatstone network towards bus 90. Thus, bus 90 is designated as the downstream node for this sub-network.

Figures 6.31 through 6.35 show the sensitivity in the flows on each of the lines in Wheatstone C to the level of demand at the downstream bus, for each of the four power-flow cases. Demand at bus 90 is assumed to run between 0 and 500 MW. Figure 6.31 shows the flow on line $S_{92,91}$, Figure 6.32 shows the flow on line $S_{92,89}$, Figure 6.33 shows the flow on line $S_{91,90}$, Figure 6.34 shows the flow on line $S_{89,90}$, and Figure 6.35 shows the flow on the Wheatstone bridge. The Wheatstone bridge is included in the network only for cases I and III, while line $S_{91,90}$ is included in the network only for cases I and II.

Analysis of the network flows shows that Wheatstone C behaves very closely to the four-bus test network described in Section 6.3. For all lines in the network, flows rise monotonically with the level of demand at the downstream node. Flows on lines $S_{92,89}$ and lines $S_{89,90}$ are highest for Case IV, in which an outage occurs on line $S_{91,90}$ and there is no Wheatstone bridge in the network (Figures 6.32 and 6.34). Note that flows along line $S_{92,89}$ level off at a lower level of demand in Case IV than in Case III, where a

Wheatstone bridge exists to redirect flows after an outage on line $S_{91,90}$. Furthermore, line $S_{89,90}$ never hits its loading limit in Case III. This suggests that the Wheatstone sub-network will provide a reliability benefit in this network. After an outage on line $S_{91,90}$, the network can transfer more power to bus 90 with the Wheatstone bridge than without the Wheatstone bridge.

Figure 6.32 also indicates that during normal operations, Wheatstone C will become congested for sufficiently high levels of demand. Figures 6.32 and 6.33 show that flows on lines $S_{92,89}$ and $S_{91,90}$ level off at a lower level of demand with the Wheatstone bridge in place during normal operations than without the Wheatstone bridge.

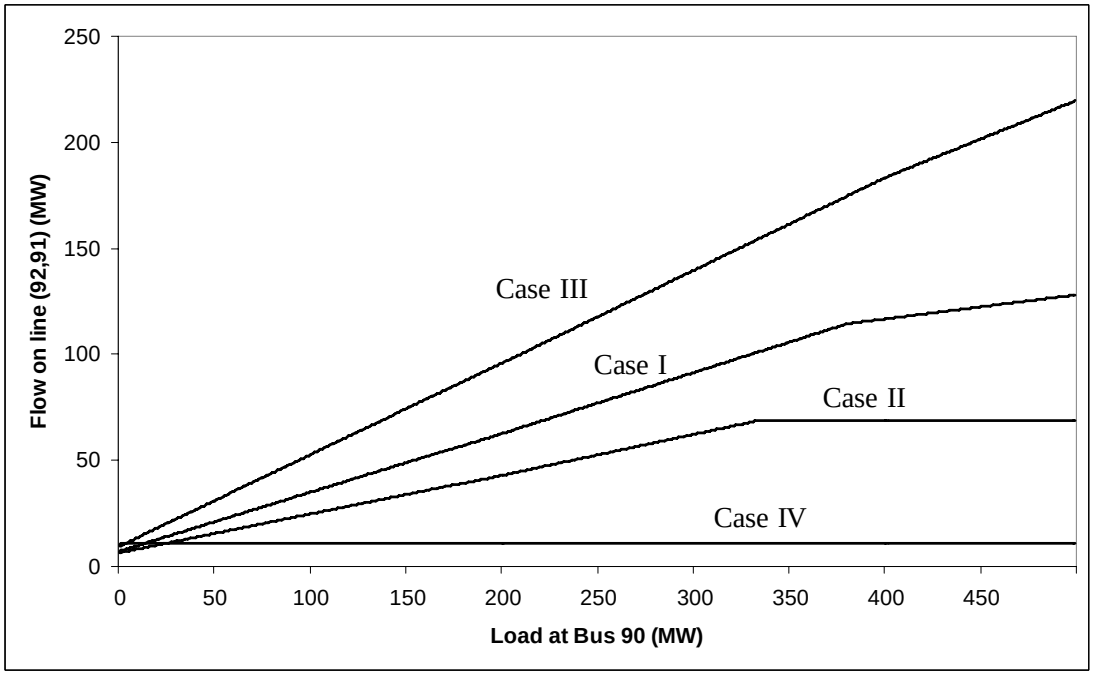

Figure 6.31. Flows on line $S_{92,91}$ of Wheatstone C, as a function of load at bus 90.

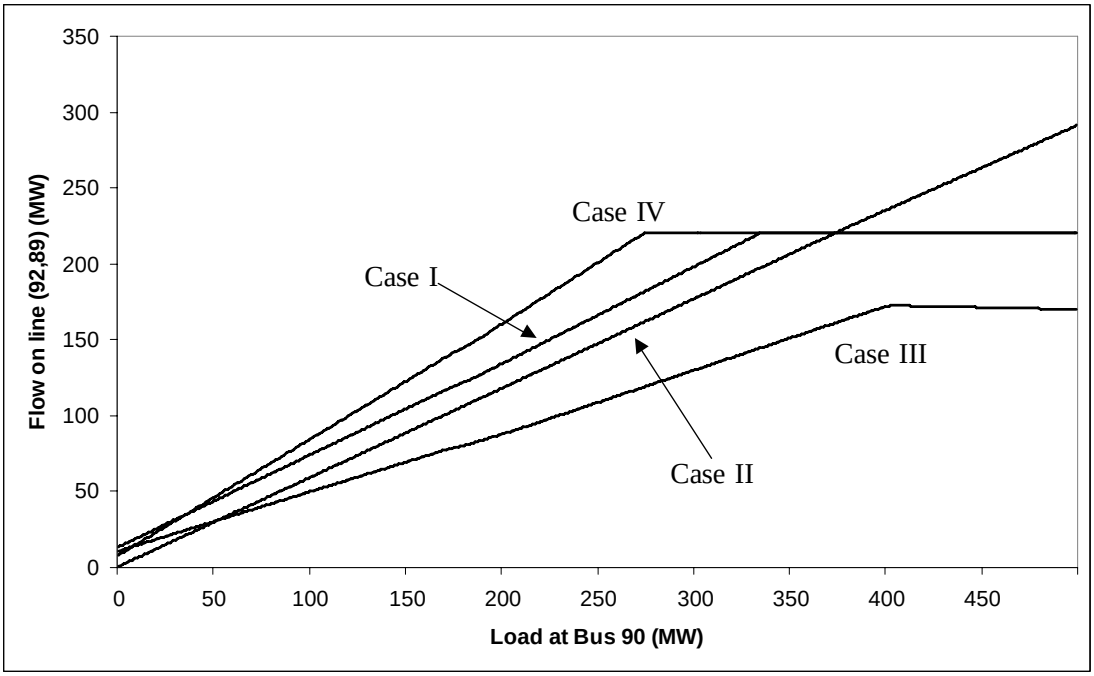

Figure 6.32. Flows on line $S_{92,89}$ of Wheatstone C, as a function of load at bus 90.

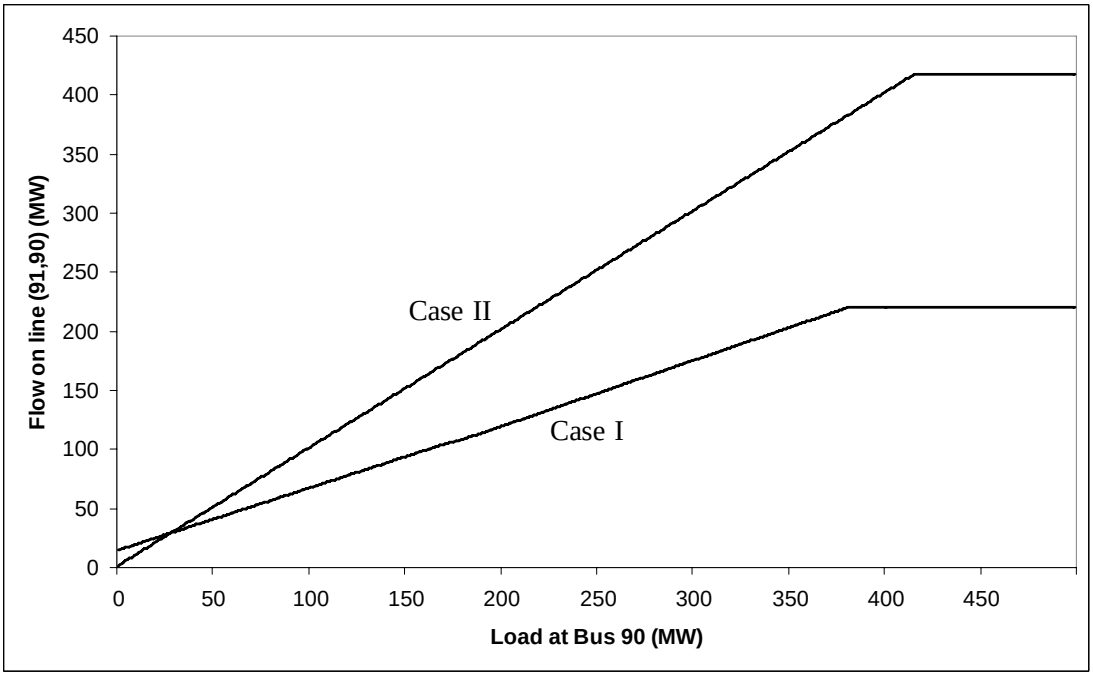

Figure 6.33. Flows on line $S_{91,90}$ of Wheatstone C, as a function of load at bus 90.

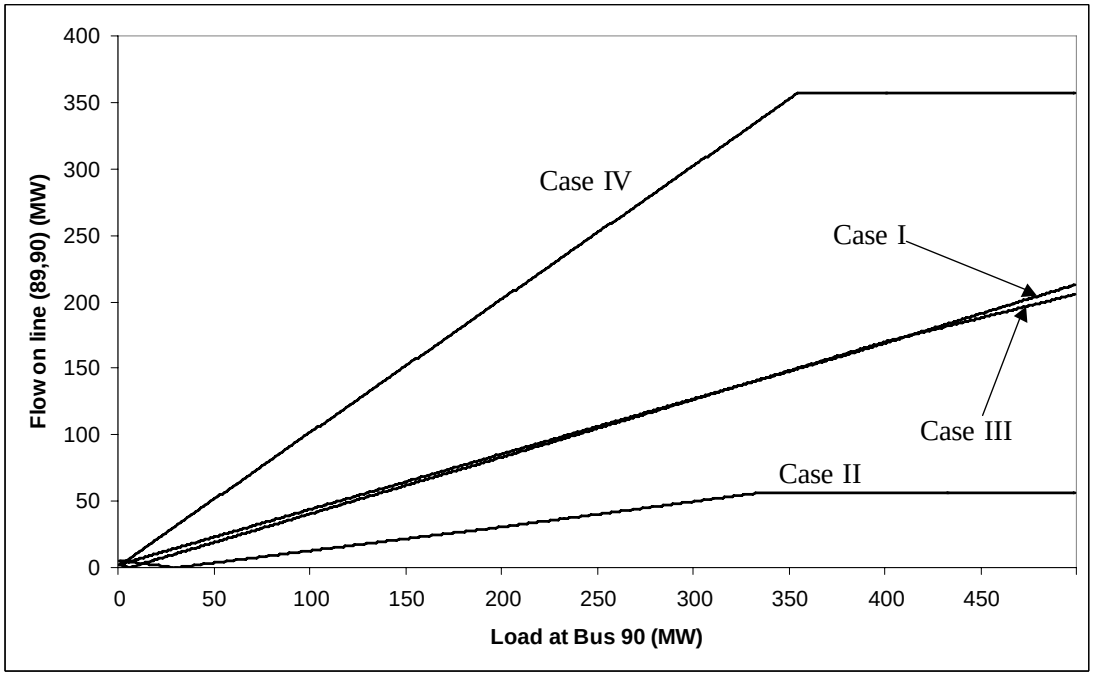

Figure 6.34. Flows on line $S_{89,90}$ of Wheatstone C, as a function of load at bus 90.

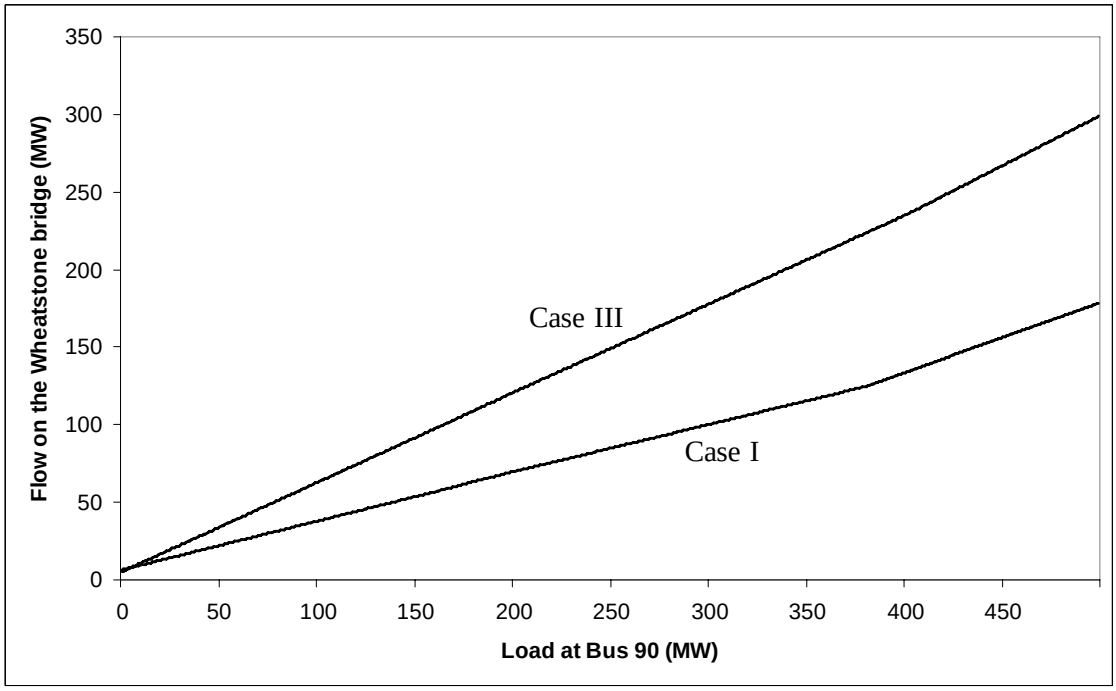

Figure 6.35. Flows on the bridge of Wheatstone C, as a function of load at bus 90.

Figure 6.36 plots the net benefit of the Wheatstone bridge as a function of the outage probability for various levels of demand. There are many similarities to the behavior of Wheatstone B, in that the net benefit is essentially zero for lower levels of demand, and is insensitive to the outage probability (this can be seen in Figure 6.37 as well). At higher levels of demand, the net benefit is strictly increasing in the outage probability. The contour lines for demand equal to 300 MW and demand equal to 500 MW reflect some redispatch that occurs in the vicinity of Wheatstone C, as a response to changes in the level of demand and topology of Wheatstone C.

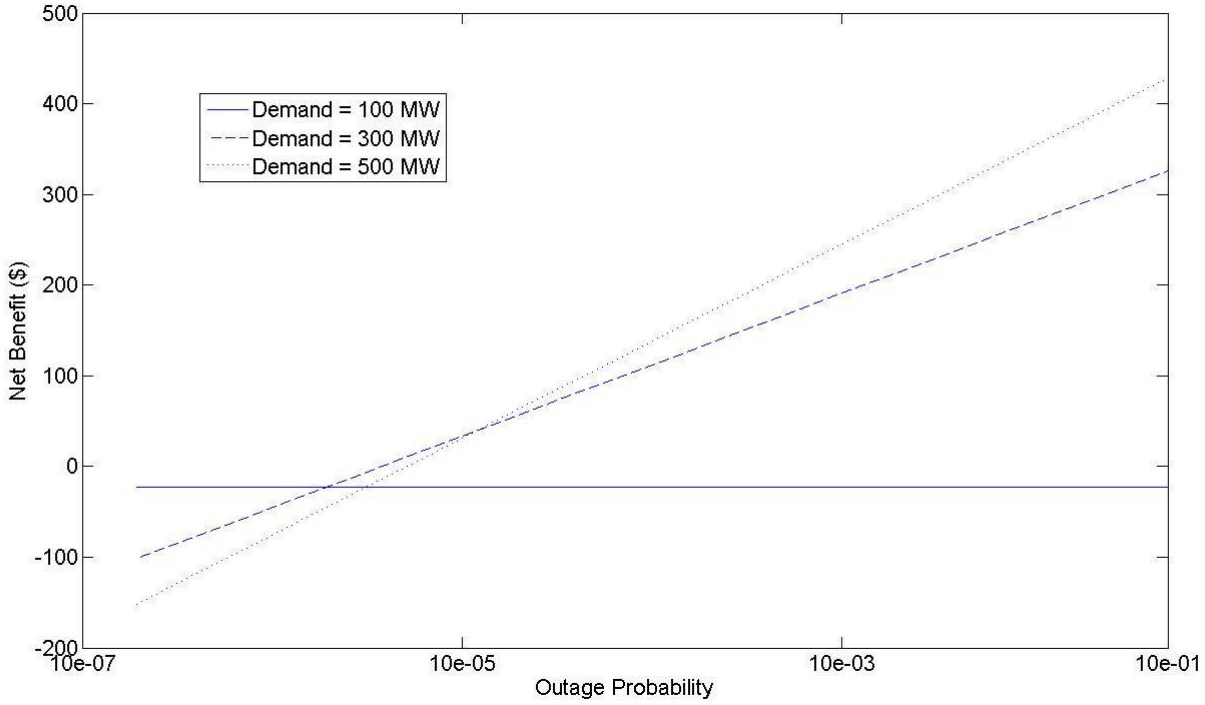

Figure 6.36. Expected net benefit of the bridge in Wheatstone C, as a function of the outage probability on line $S_{91,90}$.

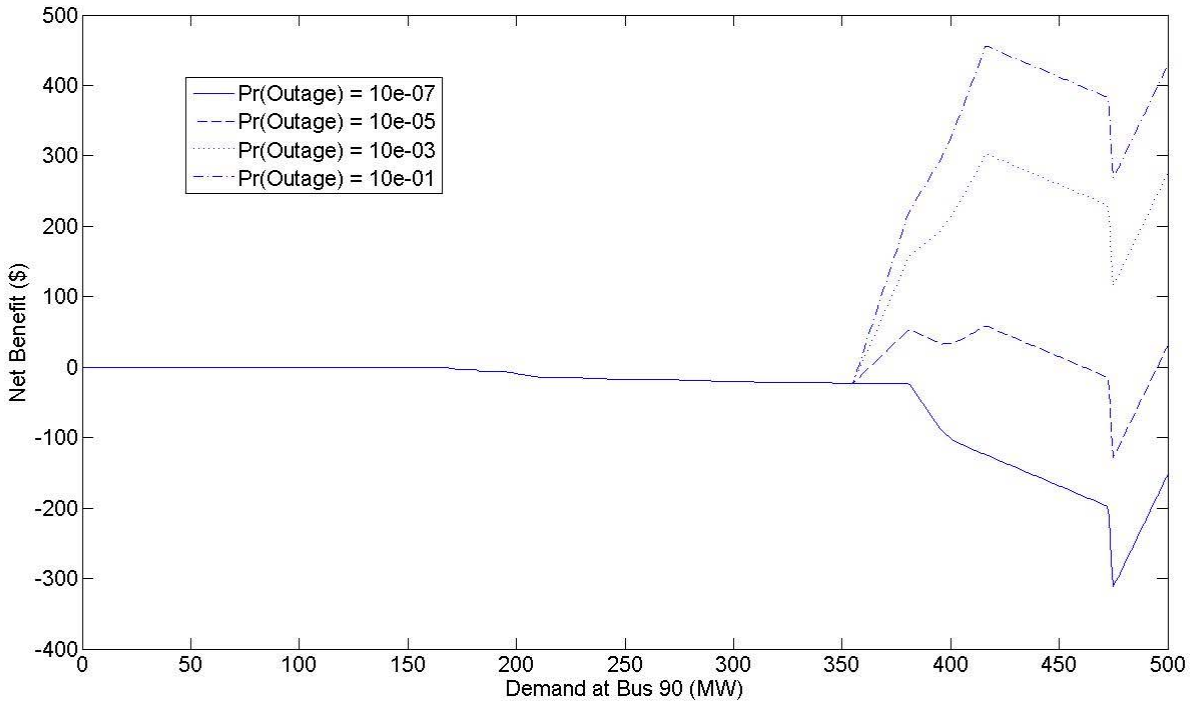

Figure 6.37. Expected net benefit of the bridge in Wheatstone C, as a function of the level of demand at bus 90.

Figure 6.37 plots the net benefit of the Wheatstone bridge as a function of the level of demand at bus 90, for several different values of the outage probability. This highlights the congestion-cost component of the net benefit calculation. As with Wheatstone B, for lower levels of demand (up until about 150 MW of demand at bus 90) there is no congestion in the network. A small amount of congestion exists from 150 MW of demand up to around 350 MW of demand. At levels of demand higher than 350 MW, an outage on line $S_{91,90}$ will cause blackouts and the net benefit becomes sensitive to the outage probability. The net benefit of the Wheatstone bridge is not consistently positive until the outage probability exceeds 10^{-5}. The behavior of the net benefit function over this higher demand range reflects the influence of other generators in the network being

redispatched as conditions change at bus 90 (and in the event of outages). This behavior, also common to Wheatstone D, is discussed below.

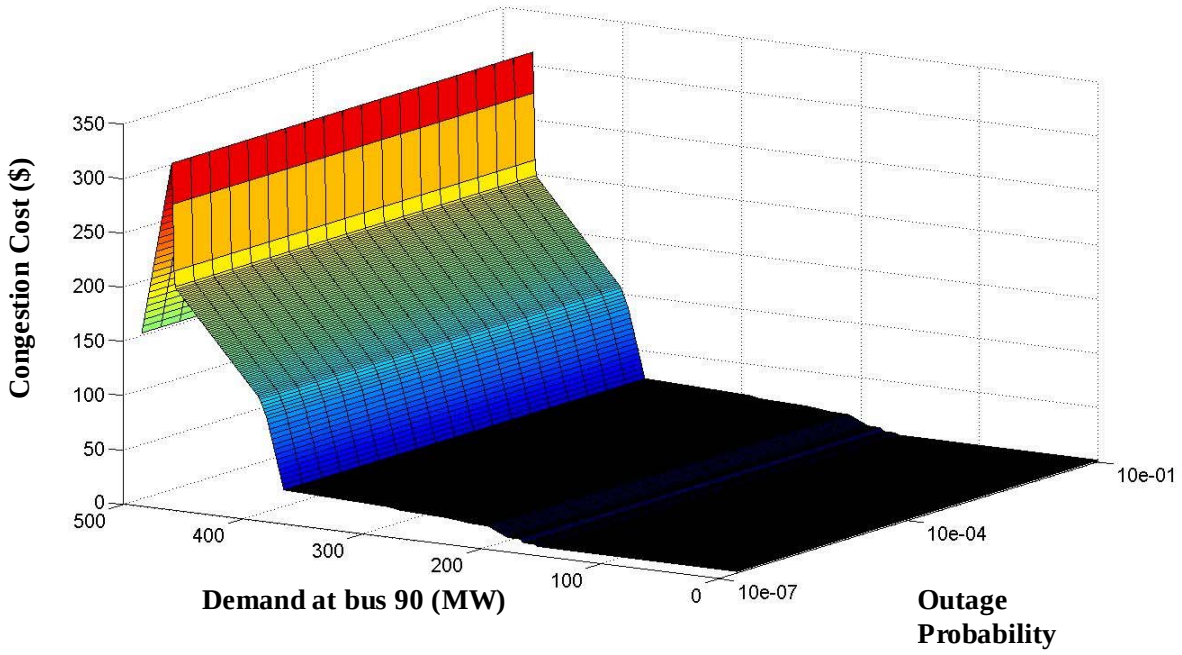

Figure 6.38. Expected congestion cost associated with the bridge in Wheatstone C.

The congestion cost and reliability benefit associated with Wheatstone C is shown in Figures 6.38 and 6.39. The relationship between the net benefit of the Wheatstone bridge, the level of demand through the network, and the outage probability is shown in Figure 6.40. As with Wheatstone B, enough network capacity exists so that both the congestion cost and reliability benefit are zero for lower levels of demand. Thus, up until demand reaches 400 MW, the net benefit of the Wheatstone bridge is essentially zero. For higher levels of demand, Wheatstone C exhibits the same tradeoff between congestion cost and reliability benefit as Wheastones A and B. For a given level of demand, the net benefit is negative at lower outage probabilities (the congestion cost

dominates the reliability benefit) and positive at higher outage probabilities (the reliability benefit overshadows the congestion cost).

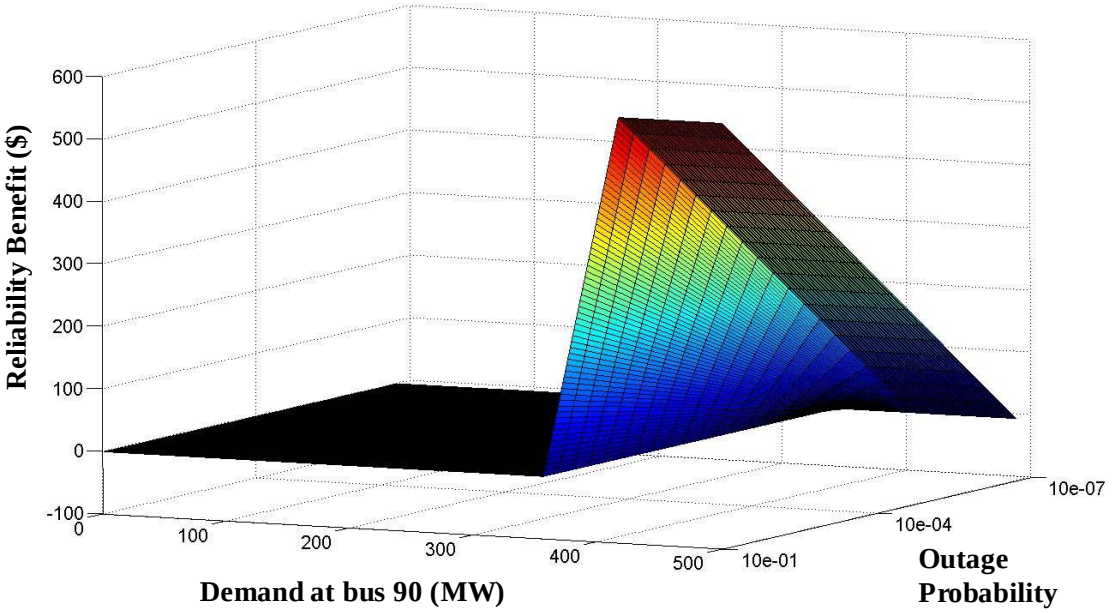

Figure 6.39. Expected reliability benefit associated with the bridge in Wheatstone C.

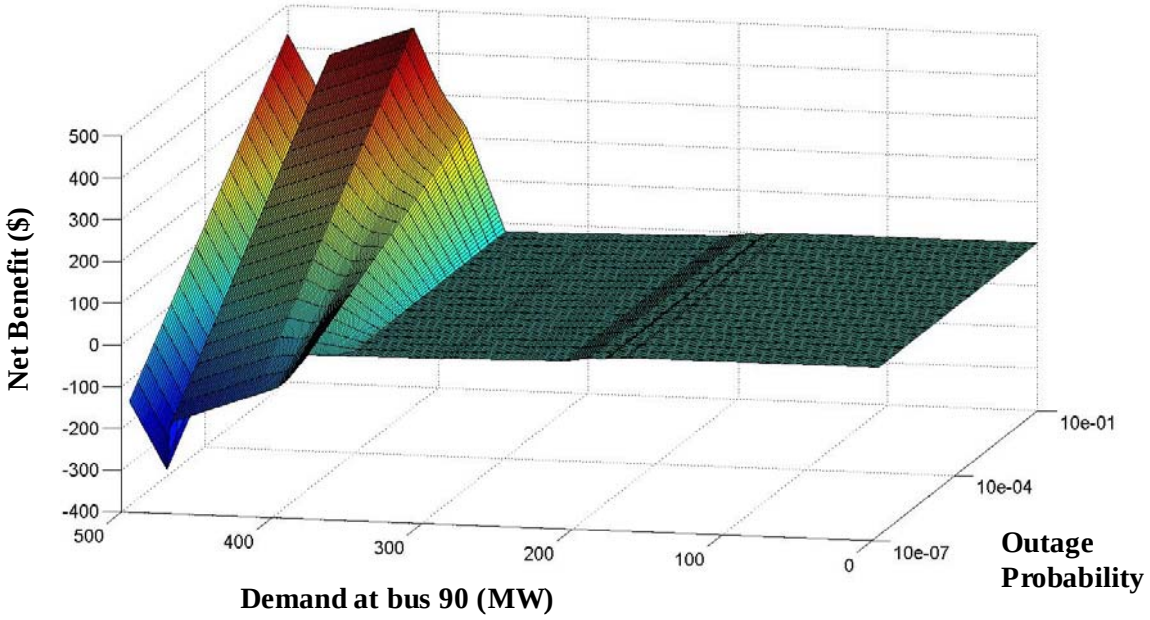

Figure 6.40. Expected net benefit associated with the bridge in Wheatstone C.

Analysis of Wheatstone D

The final Wheatstone sub-network discussed here is located in the middle of the IEEE 118-bus network, just northwest of Wheatstone C. Topologically, Wheatstone D appears to be more of an interior Wheatstone than the other three sub-networks, as it is located near some of the system's larger and less expensive generating units located at buses 80 and 65. The congestion and reliability properties of this sub-network should be different than the other three Wheatstone sub-networks. The base-case power flow run on this Wheatstone sub-network (shown in Figure 6.10) indicates that bus 77 should be considered the downstream bus; power flows from the external network through the Wheatstone towards bus 77.

Figures 6.41 through 6.45 show the sensitivity in the flows on each of the lines in Wheatstone C to the level of demand at the downstream bus, for each of the four power-flow cases. Demand at bus 77 is assumed to run between 0 and 500 MW. Figure 6.41 shows the flow on line $S_{70,69}$, Figure 6.42 shows the flow on line $S_{70,75}$, Figure 6.43 shows the flow on line $S_{69,77}$, Figure 6.44 shows the flow on line $S_{75,77}$, and Figure 6.45 shows the flow on the Wheatstone bridge. The Wheatstone bridge is included in the network only for cases I and III, while line $S_{69,77}$ is included in the network only for cases I and II.

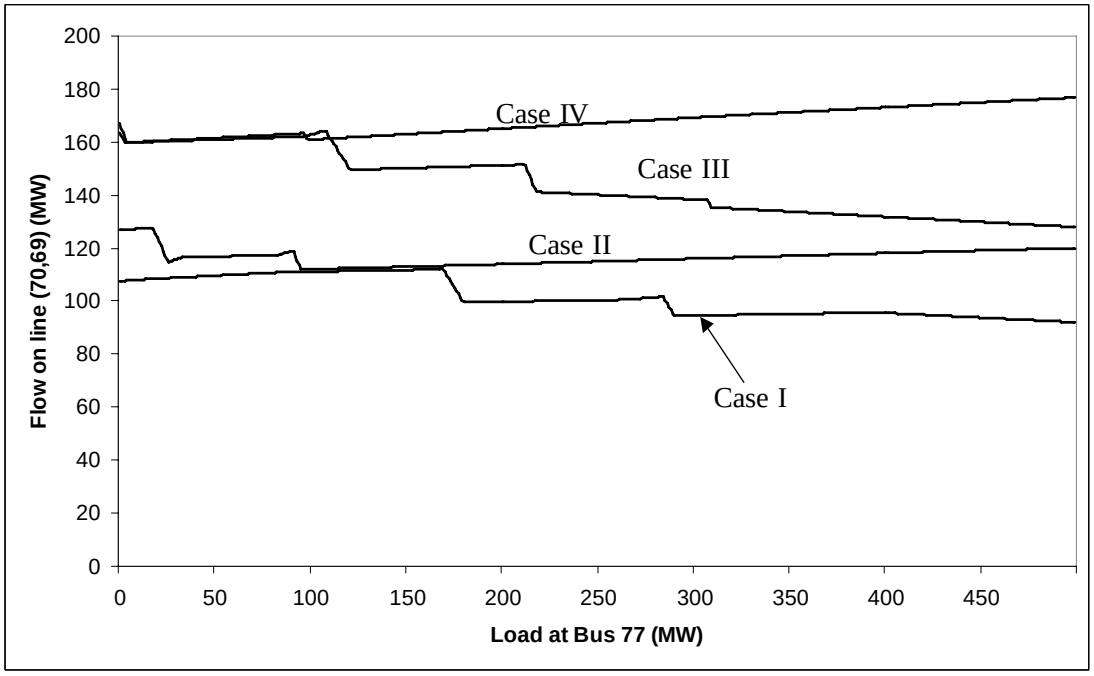

Figure 6.41. Flows on line $S_{70,69}$ of Wheatstone D, as a function of load at bus 77.

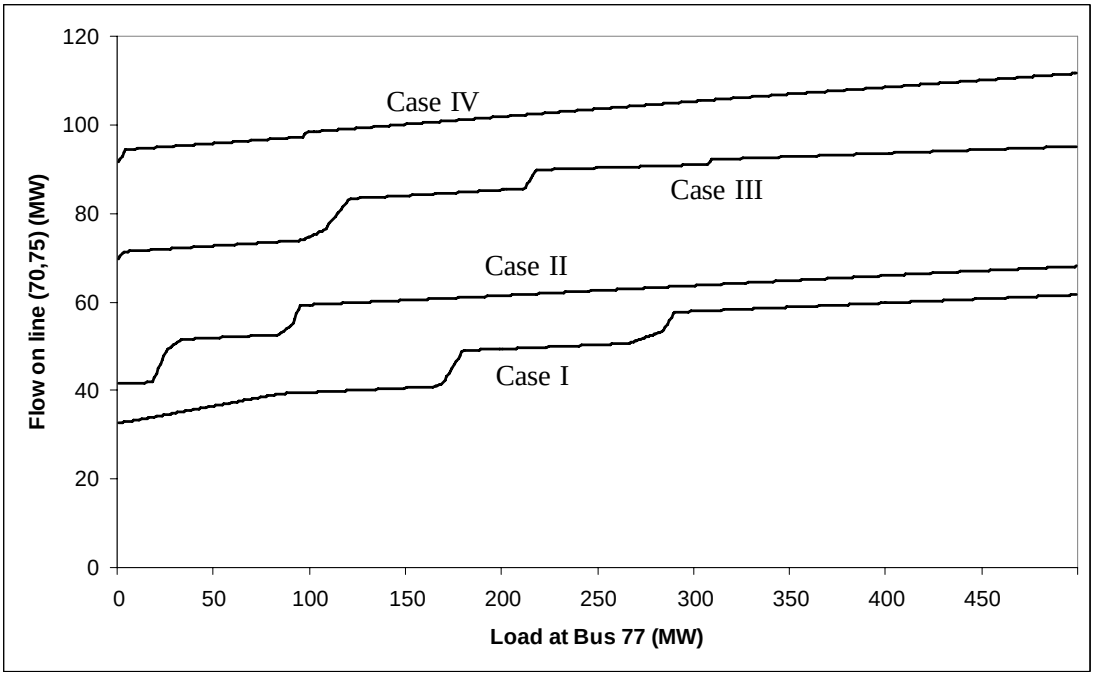

Figure 6.42. Flows on line $S_{70,75}$ of Wheatstone D, as a function of load at bus 77.

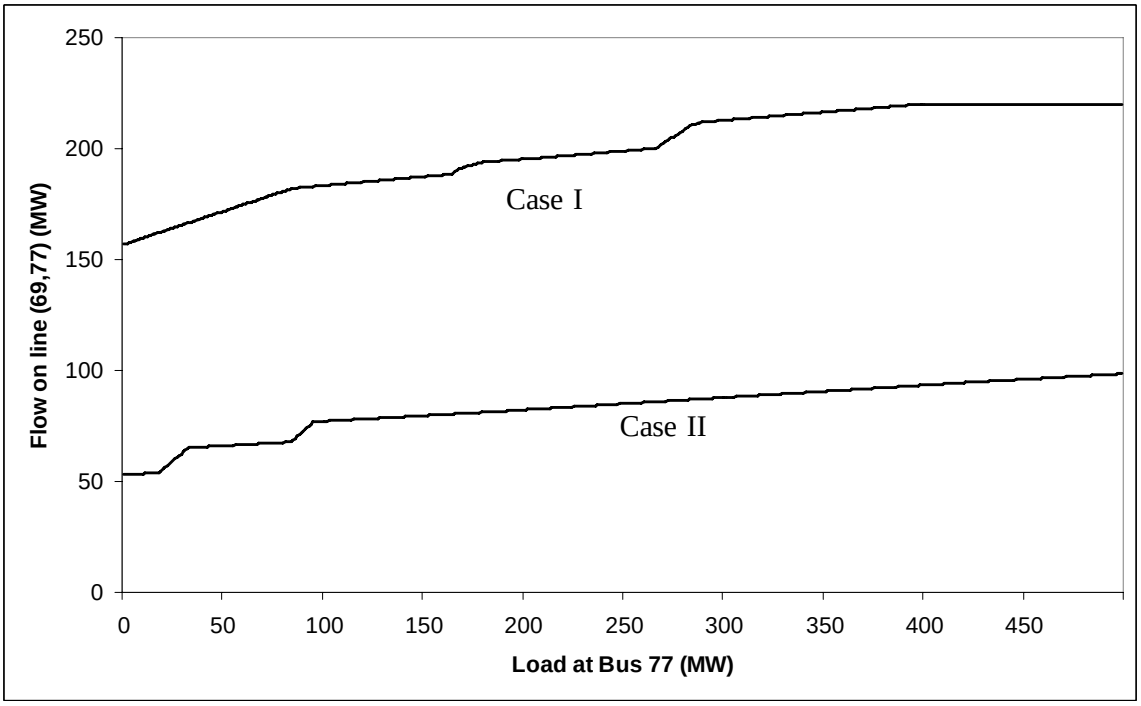

Figure 6.43. Flows on line $S_{69,77}$ of Wheatstone D, as a function of load at bus 77.

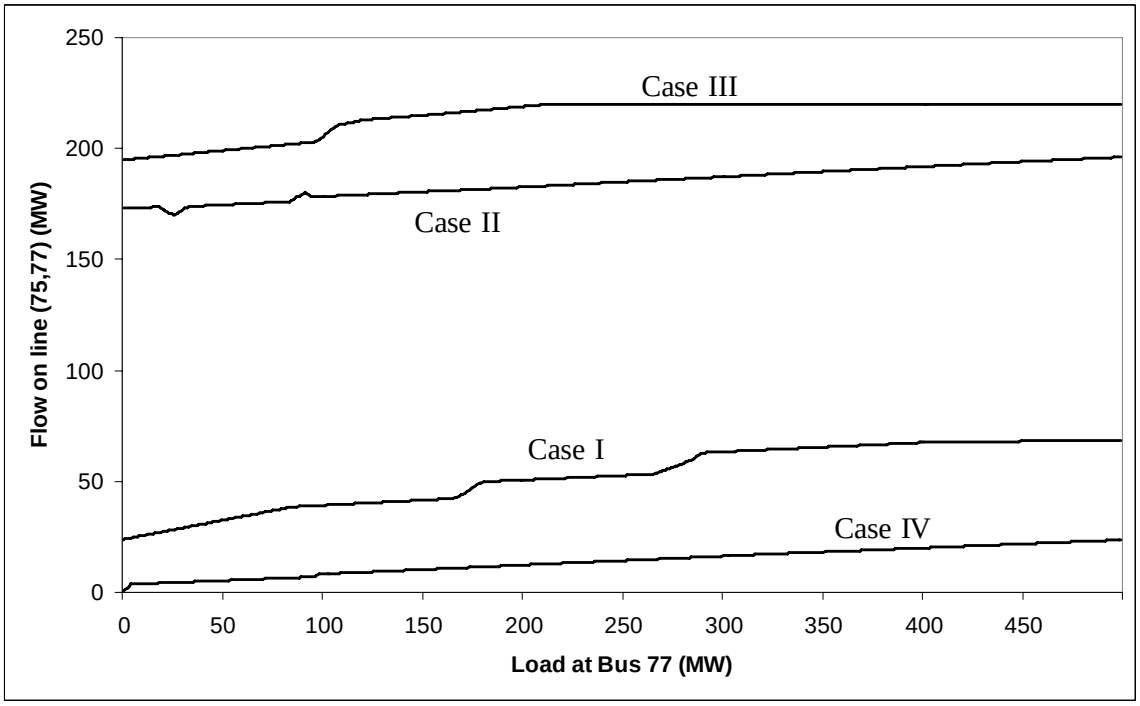

Figure 6.44. Flows on line $S_{75,77}$ of Wheatstone D, as a function of load at bus 77.

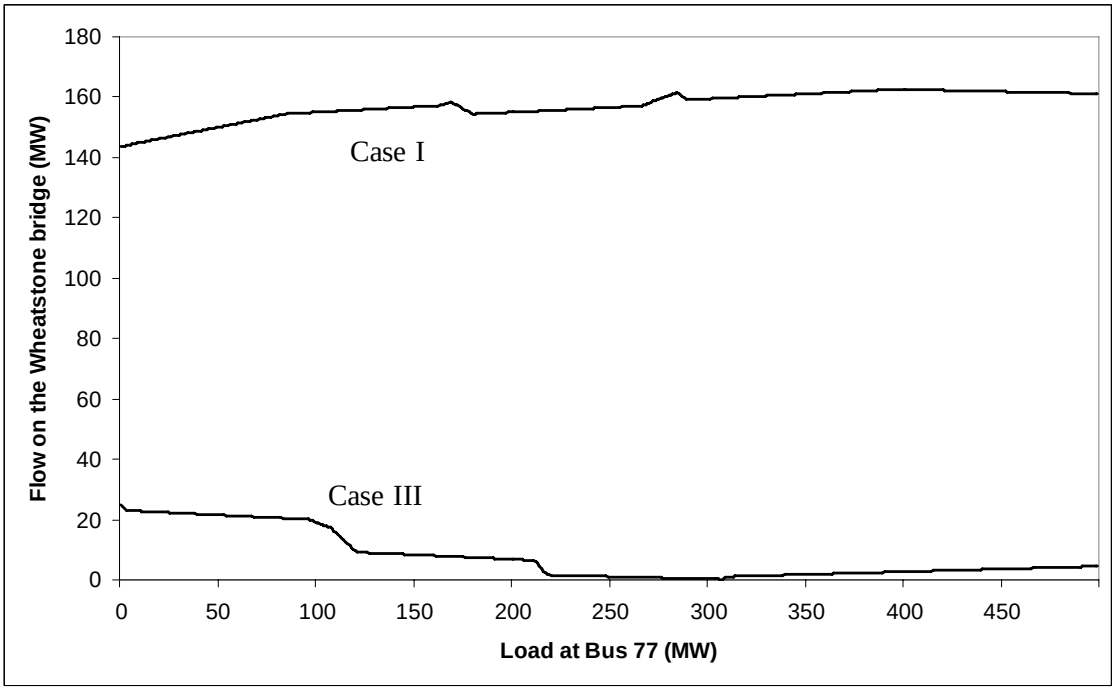

Figure 6.45. Flows on the bridge of Wheatstone D, as a function of load at bus 77.

The pattern of flows in Wheatstone D is similar to the other Wheatstone sub-networks; as demand at the downstream node (bus 77 in this case) rises, the flows rise on nearly all links in the Wheatstone sub-network. However, the flows do not increase as fast as in the other Wheatstones discussed previously. In Cases I and III, flows on line $S_{70,69}$ actually decrease as the demand at bus 77 increases.

Figure 6.46 shows the net benefit of the bridge in Wheatstone sub-network D as a function of the outage probability, with several different demand contours. This view of the total net benefit function emphasizes the reliability benefit from the Wheatstone bridge. For a given level of demand, the net benefit does increase with the outage probability, as expected. However, the net benefit contour for 100 MW of demand at bus 77 crosses the contours for 300 MW of demand and 500 MW of demand (the

contours for 300 MW of demand and 500 MW of demand do not cross). This unexpected behavior turns out to largely be a function of Wheatstone D's proximity to several large and inexpensive generating stations with direct connections to bus 77.

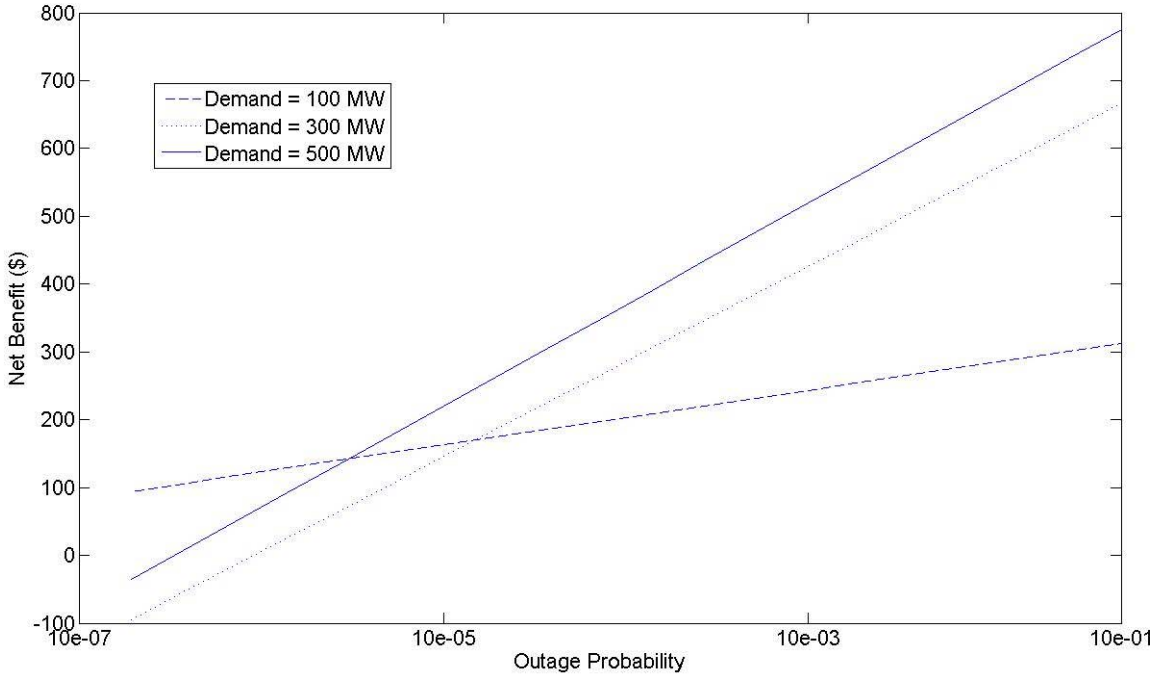

Figure 6.46. Expected net benefit of the bridge in Wheatstone D, as a function of the outage probability on line $S_{69,77}$.

The other cross-section of the net benefit of the Wheatstone configuration in sub-network D, which shows how the congestion cost affects the net benefit calculation, is shown in Figure 6.47 for several levels of the outage probability on line $S_{69,77}$. For a given level of demand, the net benefit of the Wheatstone bridge rises with the outage probability, just as in Figure 6.46. The influence of the external network on the cost of congestion in the Wheatstone sub-network can be plainly seen in Figure 6.47. *A priori*, the congestion cost should rise monotonically with demand, for a given outage probability, as shown in

Figure 6.1. Figure 6.47, however, shows the congestion cost rising and falling in a roller-coaster pattern.

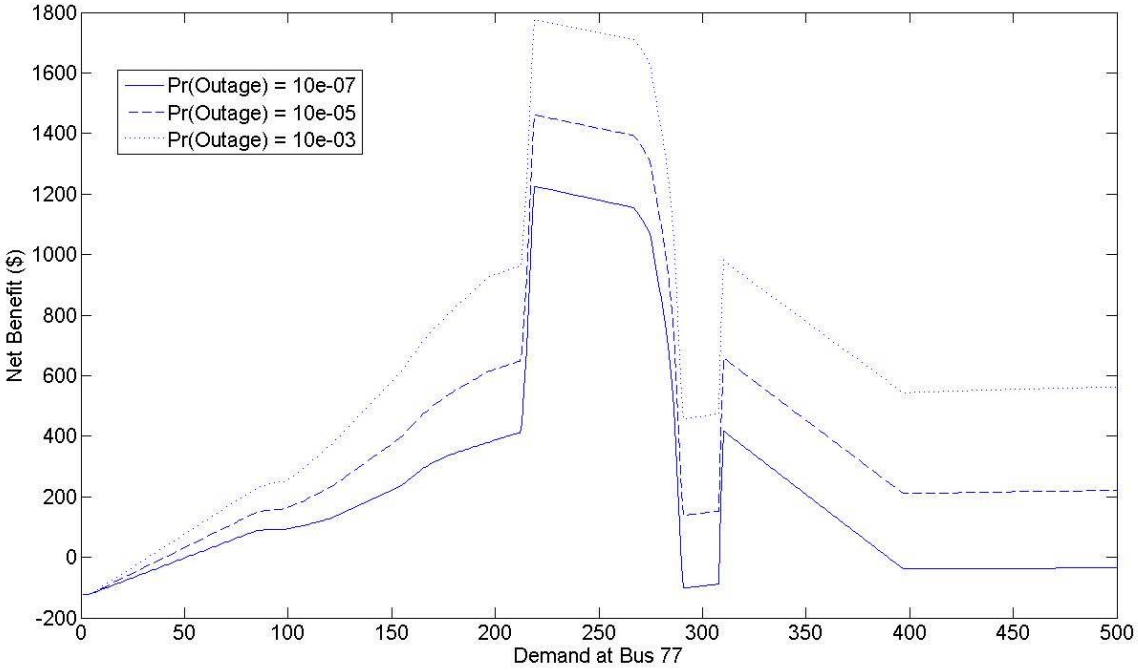

Figure 6.47. Expected net benefit of the bridge in Wheatstone D, as a function of the level of demand at bus 77.

The same roller-coaster pattern of the net benefit function can be seen in Figure 6.50, which shows the total net benefit function as both demand at bus 77 and the outage probability vary. The congestion cost and reliability benefit functions are shown in Figures 6.48 and 6.49. Note that the congestion cost is negative over large ranges of demand (as shown in Figure 6.48), meaning that the bridge in Wheatstone D actually reduces congestion rather than causing congestion as in the first three Wheatstone sub-networks and the four-bus Wheatstone test system. The reliability benefit curve in Figure 6.49 is similar to the other three Wheatstone sub-networks, rising in both the demand dimension and the outage probability dimension. The shape of the total net

benefit function is nearly identical to the shape of the congestion cost curve in Figure 6.48. We conclude from Figures 6.48 through 6.50 that congestion and reliability are not independent in Wheatstone D, but neither do they represent tradeoffs. In this case, congestion and reliability are complementary. The Wheatstone bridge could be justified for reliability reasons, but (over a large range of demand) congestion would decrease as well.

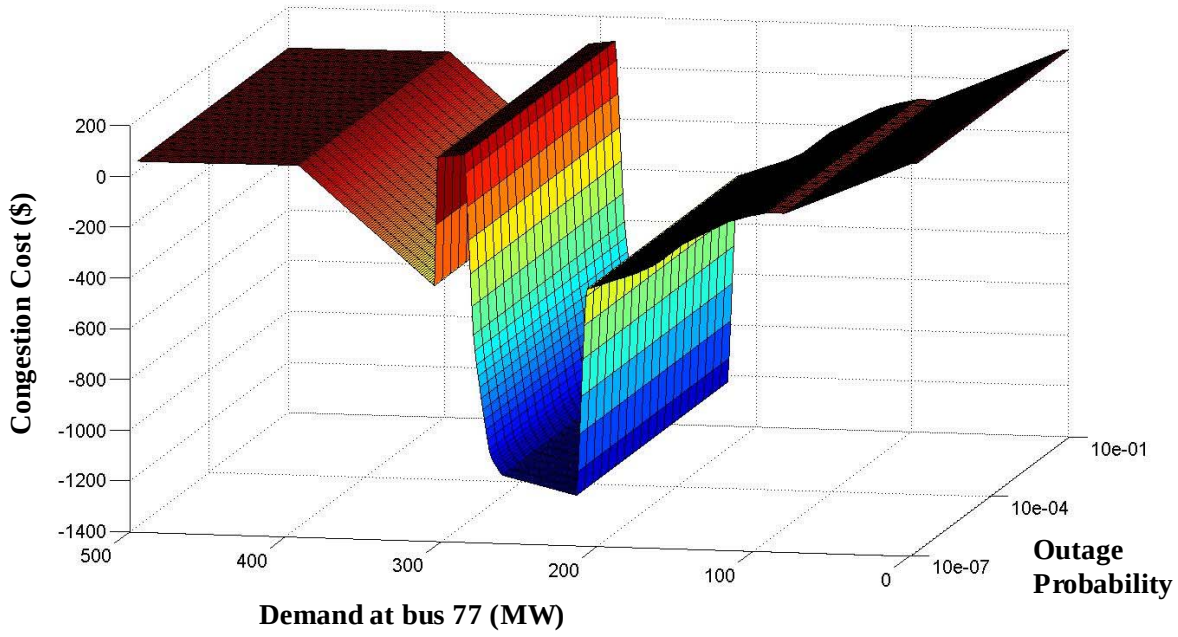

Figure 6.48. Expected congestion cost associated with the bridge in Wheatstone D.

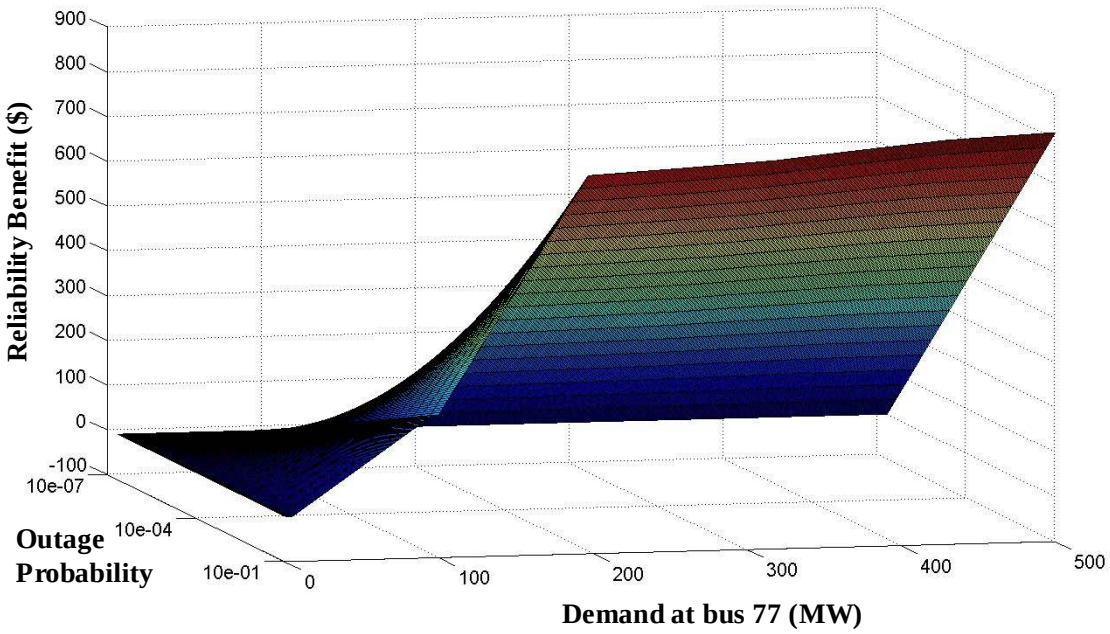

Figure 6.49. Expected reliability benefit associated with the bridge in Wheatstone D.

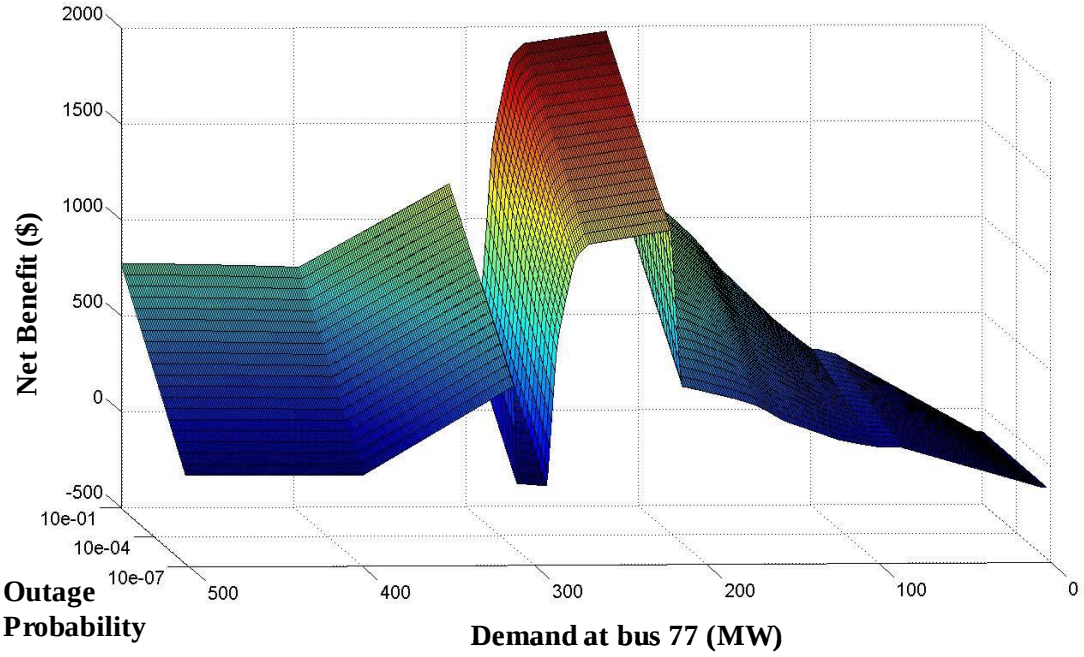

Figure 6.50. Expected net benefit associated with the bridge in Wheatstone D.

For a given level of the outage probability, the net benefit of the Wheatstone bridge should be an increasing function of the level of demand. Wheatstones A and C both behave this way, but the relationship is somewhat less clear for Wheatstone B and is virtually nonexistent for Wheatstone D. In one sense, this cleanly separates boundary Wheatstones from interior Wheatstones. Wheatstone sub-networks A and C are located topologically further away from the center of the 118-bus network. More importantly, Wheatstones A and C have fewer connections to the external network. Thus, the external network has less influence over the behavior of Wheatstones A and C than over the behavior of Wheatstones B and D.

The most significant portion of the external network in explaining the behavior of Wheatstones D is the location of large and inexpensive generation in close proximity. Generators at buses 80 and 65 are directly connected to Wheatstone sub-network D; the generator at bus 80 is directly connected to the downstream load bus of Wheatstone D. These generators thus have a high amount of influence over the congestion cost and expected reliability benefit associated with the Wheatstone network.

The generator located at bus 69 is assumed (in the IEEE network specifications) to have a capacity limit of 805 MW and a marginal cost of $0.20/MWh. The generator at bus 65 has a capacity limit of 491 MW and a marginal cost of $0.25/MWh. The behavior of Wheatstone D is also influenced by an expensive generator at bus 87, which has a marginal cost of $7.14/MWh. This generator is located to the south of Wheatstone D, but is directly connected to the downstream load at bus 77.

Figure 6.51 illustrates how these generators impact the congestion cost associated with Wheatstone D. The figure shows the change in output of the generators at buses 69, 65, and 87 after the Wheatstone bridge is removed, but with no line outages. Thus, Figure 6.51 shows the difference between case II generation (no Wheatstone bridge) and case I generation (including the Wheatstone bridge). Once the Wheatstone bridge is removed, the increased flow of inexpensive power through the network allows some power from the generator at bus 87 to be displaced until demand at bus 77 reaches about 225 MW. At the same level of demand, the generator at bus 69 increases production to accommodate increased demand at bus 77. The generator at bus 80 is not shown in Figure 6.51 since its output level does not change when the Wheatstone bridge is removed.

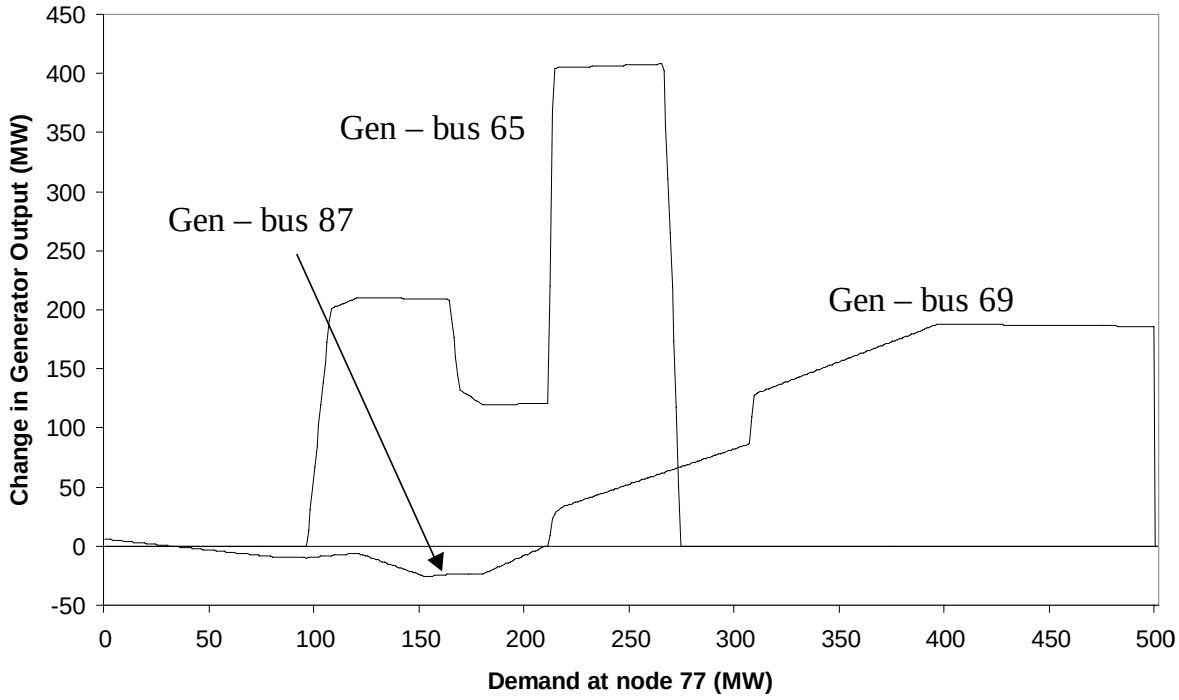

Figure 6.51. Change in output of the generators at buses 65, 69, and 87 as a result of the bridge being removed from Wheatstone D.

Figure 6.51 suggests that the change in output of the generator at bus 65 is the primary factor in the odd shape of the Wheatstone net benefit function for sub-network D, shown in Figure 6.50. The influence of this particular generator can be illustrated by artificially inflating its marginal cost to $2/MWh. All four power-flow cases were then re-run on this modified version of the 118-bus network. The total net benefit function is shown in Figure 6.52. After increasing the marginal cost of the generator at bus 65 to the point where it no longer changes dispatch in response to changes in demand at bus 77, the Wheatstone net benefit function looks much like the net benefit functions from Wheatstones A or C.

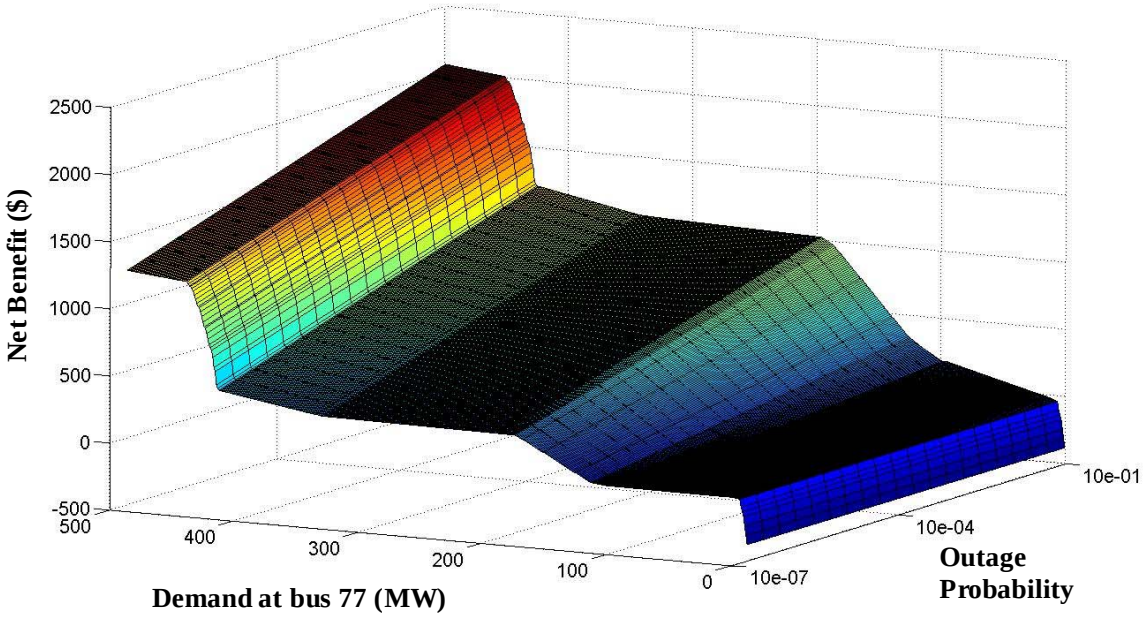

Figure 6.52. Expected net benefit associated with the bridge in Wheatstone D, after the marginal cost of generation has been increased at bus 65.

6.5. The Net Benefit of Wheatstone Sub-Networks When Demand Throughout the Network is Stochastic

The analysis in Section 6.4 showed that embedded Wheatstone sub-networks display many of the same behaviors as the standalone Wheatstone test network shown in Figure 6.1, despite the influence of the rest of the network. Over some range of demand, there is enough transmission capacity in the Wheatstone sub-network that flows through the network are not affected by either the presence of the Wheatstone bridge or by an outage in one of the boundary links. Over other ranges of demand, the Wheatstone bridge may cause congestion in the network, but it also tends to provide a reliability benefit.

In Section 6.4, the only variation in network demand was represented by the desired power transfer across each Wheatstone sub-network to the downstream demand node. Generators responded to the change in desired transfer level, sometimes by redispatching so as to compensate for additional congestion in the network (as in Wheatstone D, discussed in Section 6.4). In real networks, loads are continuously changing at all locations. In systems with a large amount of demand response, congestion in Wheatstone networks, or the possibility of transmission-line outages, could be offset by the willing curtailment of consumption in certain locations. In this sense, demand response can be viewed as a substitute for investment in new transmission lines or even in flow-control devices. The value of this demand response to the network can be bounded by the net benefit calculations in Section 6.4.

Another possibility is that loads at different locations may simply vary independently of one another. This introduces another possible system effect that could either mitigate or exacerbate the congestion costs imposed on the network by the Wheatstone bridge. For example, consider Wheatstone C, shown in Figure 6.9. Bus 90 is the downstream node, in that variation in demand at bus 90 represents variation in demand to move power in a given direction through the Wheatstone sub-network. As shown in Figure 6.38, for a certain range of demand at bus 90, an increase in demand at bus 90 is associated with an increase in network congestion costs. Figure 6.38 holds demand at buses 89 and 92 constant. If demand at those buses is variable, then for some levels of demand, buses 89 and 92 may cause counterflows in the network that balance out the congestion. For some other range of demand, buses 89 and 92 may increase congestion in the network. Whether the variability of demand at buses 89 and 92 acts to increase or decrease congestion is a function of the level of demand at these buses and the generation dispatch; it is not necessarily a function of the level of correlation between buses 89, 92, and 90.[1]

Variation in demand at buses outside the Wheatstone sub-network may also affect flows through the Wheatstone sub-network and thus the net benefit of the Wheatstone bridge. The basic analysis is the same as in Section 6.1, but demand at each node is assumed to follow some stochastic process, and thus the total demand in the network is also stochastic. (Note the difference between this framework and the analysis in Section 6.4,

[1] Ultimately, variation in demand at buses 89 and 92 amounts to a change in the desired level of electric power to be transferred through the Wheatstone sub-network. Thus, there is little difference between considering demand variation at all four Wheatstone buses and considering demand variation solely at the downstream bus, as in Section 6.4.

which calculated the Wheatstone net benefit for a deterministic level of demand, which was systematically allowed to vary.) Thus, the analysis of Section 6.4 amounts to a sensitivity analysis on the level of demand in the Wheatstone network and the probability of an outage on one of the Wheatstone boundary links.

Demand at each node in the network is assumed to follow the diffusion process:

$$(6.13) \qquad dP_{Li} = \sigma_i P_{Li} dz, \qquad i = 1,..., NB,$$

where dz is the increment of a Wiener process:

$$(6.14) \qquad dz = \varepsilon_t \sqrt{dt},$$

and thus $E(dz) = 0$ and $\text{Var}(dz) = dt$. Equations (6.13) and (6.14) amount to assuming that demand follows a geometric Brownian motion with no drift (Dixit and Pindyck 1994). Thus, changes in demand are lognormally distributed. We will also assume that the standard deviation of demand is equal at all nodes, so we can rewrite equation (6.13) as:

$$(6.13') \qquad dP_{Li} = \sigma P_{Li} dz, \qquad i = 1,..., NB.$$

The formulation in Section 6.4 featured only one stochastic element: the outage probability. In this formulation, there are two stochastic elements: the outage probability

and the level of demand at each node (and thus, the total level of demand in the network). Stochastic demand also implies stochastic generator outputs and total system costs. Equations (6.1) through (6.4) must be modified accordingly.

If any component of the nodal demand vector $\mathbf{P_L}$ is random, then the vector itself is random, as is the total demand in the network $P_L = \sum_{i=1}^{NB} P_{Li}$. Assume that $\mathbf{P_L}$ is a random variable with distribution function $f(\mathbf{P_L})$. Let $K(\mathbf{P_L})$ be the system marginal cost function to serve the last P_{Li}-th megawatt of demand at each node *i*. Then the system total cost function can be written as:

$$(6.15) \qquad TC(f(\mathbf{P}_L)) = \int_0^{f(\mathbf{P}_L)} K(f(\mathbf{P}_L))df(\mathbf{P}_L).$$

Using (6.15) and assuming that outages are independent of the level of demand, the expected net benefit of a Wheatstone bridge to the network, with stochastic demand and stochastic outages, can be written as:

$$(6.16) \qquad \begin{aligned} E(NB(U,\mathbf{P_L})) = {} & u(VOLL \times T_W - VOLL \times T_0) \\ & -(1-u)\left[E(TC^*(\mathbf{P_L})) - E(TC'(\mathbf{P_L}))\right], \end{aligned}$$

where *TC** represents the total cost with the Wheatstone bridge in the system, and *TC'* represents the total cost without the Wheatstone bridge in the system. For a given level

of demand in the system, the conditional expectation is identical to the expression given by equation (6.4).

With a closed-form expression for $TC(f(\mathbf{P}_L))$, we could also generate a closed-form expression for the expected Wheatstone net benefit in equation (6.16). However, particularly when the number of binding constraints in the system changes with the level of demand and the network topology, there is no clean way to translate between the level of demand in the network and the (state-contingent) total network cost to serve that demand. The total cost function must be determined empirically through simulations.

As an example, we will look at the congestion cost and net benefit associated with Wheatstone C (Figure 6.9) in the IEEE 118-bus network when demand throughout the network is allowed to vary according to the process in equation (6.13'). The simulations proceed as follows:

1. For all nodes in the network, initialize demand at the level specified in the IEEE 118-bus test case.
2. Specify a standard deviation σ for the demand evolution process and a probability u of an outage on line $S_{91,90}$.
3. Generate 10,000 realizations of demand at each bus according to the process in equation (6.13'). Also generate a 10,000 by 1 vector whose entries are equal to 1 (with probability u) if there is an outage, and equal to zero (with probability $1 - u$) if there is no outage. Thus, outages are generated as a series along with demand.

4. For each realization of demand and line outage, run two sets of DC power flows on the 118-bus system. The first set of power flows corresponds to the network with the Wheatstone bridge in sub-network C. The second set corresponds to the network without the Wheatstone bridge in sub-network C. Note that if there are line outages, the optimal level of demand served may not be the same as the specified level of demand at a given node (that is, there may be load-shedding).
5. For each realization of demand, Step 4 yields values for the congestion cost (the difference in total cost with the Wheatstone bridge and without the Wheatstone bridge) and the amount of load shed (the difference between the amount of load actually served and the amount of load specified at each bus). The expected net benefit, conditional on $\mathbf{P_L}$, can be calculated, as well as the expectation value in equation (6.16).
6. Repeat Steps 1 through 5 for various values of σ and u. The simulations performed here considered values of σ in the interval [0.1, 2] and considered values of u in the interval $[10^{-7}, 10^{-1}]$.

The data output from Steps 1 through 5 can be used to construct a cumulative distribution function for the net benefit of the Wheatstone bridge. These are shown in Figures 6.53 and 6.54. Figure 6.53 shows the CDF of the net benefit function for various levels of σ, assuming that $u = 10^{-3}$ and *VOLL* = \$1,000/MWh. Figure 6.54 shows the CDF of the net benefit function for various levels of u, assuming $\sigma = 1$ and *VOLL* = \$1,000/MWh.

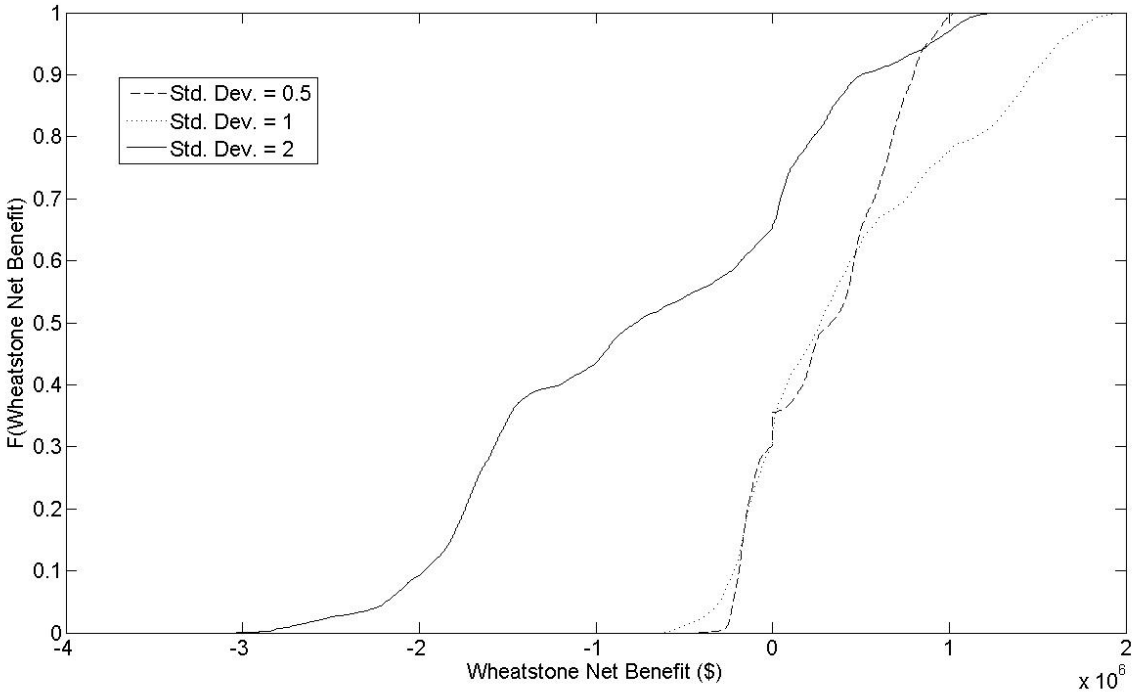

Figure 6.53. CDF of the Wheatstone net benefit function for various values of σ. The figure assumes that $u = 10^{-3}$ and VOLL = $1,000/MWh.

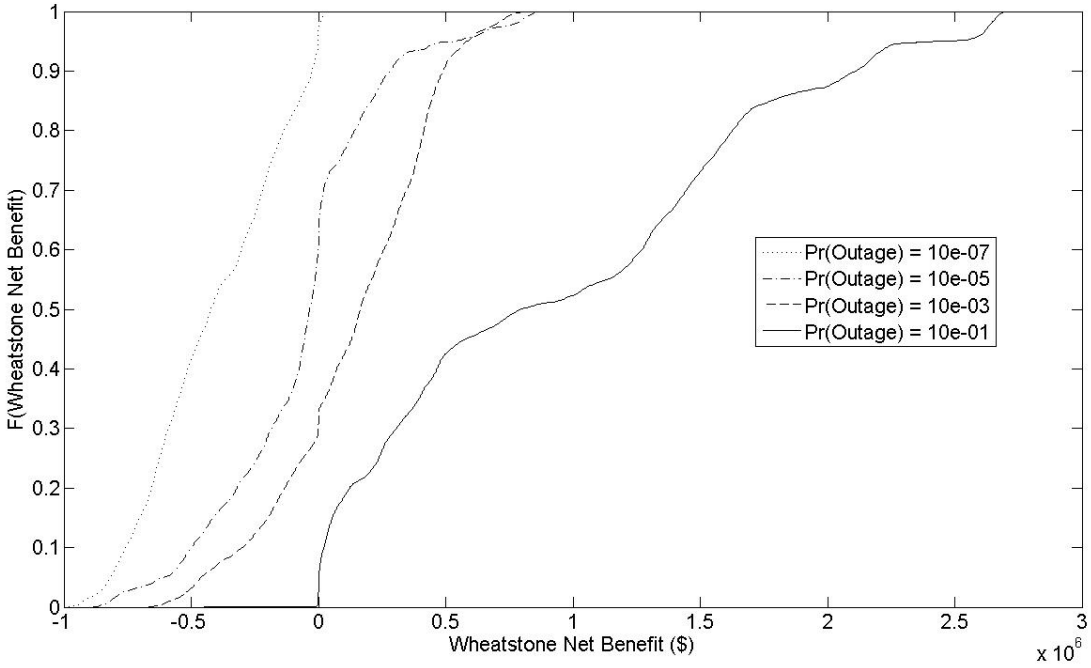

Figure 6.54. CDF of the Wheatstone net benefit function for various values of u. The figure assumes that $\sigma = 1$ and VOLL = $1,000/MWh.

The spreads in Figure 6.53 behave exactly as expected. When the standard deviation is smaller (meaning that period-to-period changes in the load are smaller), the net benefit CDF clusters more tightly around the mean. For larger values of the standard deviation, corresponding to larger swings in total system demand, the CDF of the Wheatstone net benefit will have longer tails. This means that a demand profile with a higher standard deviation is more likely to see larger (in magnitude) values of the net benefit function relative to the mean. It does not necessarily imply a correspondence between the variability in demand and the net benefit function. Figure 6.53 is a good example of this; for $\sigma = 0.5$ and $\sigma = 1$, the expected net benefit is positive ($60,000 and $250,000, respectively).

There should, however, be a reasonably good correspondence between the outage probability and the net benefit of the Wheatstone bridge. Higher outage probabilities should be associated with larger net benefits. Figure 6.54 demonstrates that this relationship holds for Wheatstone C in the 118-bus network. Only when the outage probability exceeds 10^{-3} does the expected net benefit of the Wheatstone bridge become positive. In Figure 6.54, the expected net benefit for $u = 10^{-5}$ is approximately -$195,000, the expected net benefit for $u = 10^{-3}$ is approximately -$66,000, and the net benefit for $u = 10^{-1}$ is approximately $138,000.

6.6. Summary and Conclusions

Chapter 3 introduced the Wheatstone network and noted that while the presence of the Wheatstone bridge will cause congestion for a certain range of demands, the network

may also provide a reliability benefit in the event of an outage along one of the boundary links. The analysis in Chapter 3 was limited to a standalone Wheatstone test network; the analysis in this chapter suggests that Wheatstone sub-networks embedded in larger networks will exhibit many of the same behaviors.

This chapter has presented a framework for decomposing the congestion costs imposed on the system by the Wheatstone bridge and the reliability benefit conveyed on the system. Using this framework to analyze four Wheatstone sub-networks embedded in the IEEE 118-bus network, we found that congestion and reliability represent tradeoffs for three of the four sub-networks. In the remaining Wheatstone sub-network, congestion and reliability are complementary – increasing one leads to an increase in the other. In no case could we say definitively that congestion and reliability were independent, except (for some sub-networks) at very low levels of demand.

We conclude that the behavioral attributes of the four-bus standalone Wheatstone network are not universally generalizable to Wheatstone structures within larger systems, although the similarities to the standalone test network are sharpest for those Wheatstones located at or near the boundary of the larger network. Wheatstone sub-networks located in the interior of larger networks are more likely to be influenced by variations in adjacent load and generation. One implication for the planning process is that locating a Wheatstone in the middle of a meshed network and near large sources of inexpensive generation is unlikely to cause major congestion problems that would exist if the same Wheatstone were placed at the boundary of the network.

The key to analyzing embedded Wheatstone networks is recognizing the nature of the relationship between congestion and reliability. As with any economic externality, the tradeoff needs to be defined over the relevant range of demand. It is especially important to realize that the framework developed here has decomposed the congestion cost from the reliability benefit, but the two are not uniformly independent, as claimed by Hogan (2003) and Shanker (2003). Current transmission policy endorsed by RTOs, FERC, and even the U.S. Congress errs in failing to realize these distinctions. Current policy treats the transmission system as if individual lines could be divided into those that benefit the system through added redundancy, and those that harm the system by causing congestion. Transmission lines are also treated as if their contribution to the system is independent of the state of the system. The RTO and FERC rationale for market-based merchant transmission is largely based on this false congestion-reliability dichotomy.

Chapter 7: Reformulating the Transmission Investment Problem Under Electric Industry Restructuring

Competitive markets for electric power generation began in earnest in 1992, following the Energy Policy Act of 1992, when Merrill Lynch became the first non-utility entity to be licensed by FERC to trade wholesale electric power at market-based rates (Lehr and van Vactor 1997). Prior to the 1992 Energy Policy Act, markets for bulk power existed throughout the North American electric grid, but trading volumes were low, the number of participants was limited, and reliable information on prices and other market activity was scarce (van Vactor 2004). Industry restructuring brought with it the rise of the centralized power exchange, first in the form of California's Power Exchange and the PJM centralized spot market. Whether these new trading institutions are good or bad has been the subject of extensive debate (Lave, Apt, and Blumsack 2004), but their rise was associated with a surge in generation investment (Joskow 2005a).

Practically all of this investment was in natural-gas generation, sized to be either base-load or mid-merit plants. Recent supply/demand imbalance in the natural gas market has pushed up the price of fuel for these plants, rendering them uncompetitive with coal and nuclear power. The new gas plants have moved near the top of the dispatch stack, where they are used as peakers, if at all. Many of the original builders of these merchant plants have since gone bankrupt, with the generation capacity sold at fire-sale

prices to vertically-integrated utilities or larger and more diversified merchant generating firms.

Transmission should not be subject to the same sorts of issues as generation. Wires are more homogenous than power plants, and investments in transmission infrastructure consist almost entirely of capital costs, with low variable operations cost. However, the merchant generation sector that (albeit briefly) flourished with the onset of electric-industry restructuring has not been duplicated in the transmission sector, contrary to the hopes and policy goals of FERC and the RTOs. Not a single merchant transmission line has been built in North America.[1]

With respect to transmission, the industry is stuck. Following the August 2003 blackout, bolstering the North American transmission infrastructure has become a major policy goal. Some significant projects are in the works, such as American Electric Power's proposed 765-kV Interstate line (AEP 2006), but they are relatively few in number and still face major hurdles, including funding, siting, and permitting. The siting problem will continue to be a major challenge, as discussed by Vajjhalla and Fischbeck (2006); our focus here is on the funding issue. The primary analytic and policy failure in the transmission arena has been a failure to properly define the transmission investment problem under restructuring. Restructuring has treated the transmission infrastructure as

[1] By merchant transmission, we mean a transmission-only company building transmission infrastructure in exchange for some market-based compensation. Joskow (2005b) notes that a transmission-only company was hired to build new infrastructure in Long Island, but the Long Island Power Authority paid the company through what amounted to a fixed-price contract, with the costs passed on to ratepayers. At the same time, Krellenstein (2004) discusses how a merchant transmission project from upstate New York to New York City, which likely would have been profitable even with market-based compensation, collapsed due to the unwillingness of investors to lend money for the project.

if it were, for all practical purposes, identical to the generation infrastructure, able to respond to the same sets of locational market signals.

This approach to the transmission system is very intuitive, given the role that transmission plays in facilitating competition among generators (Lave, Apt, and Blumsack 2004). This thesis has demonstrated some of the pitfalls of this approach, and has shown that many of its underlying assumptions do not hold. In this concluding chapter, we will summarize the major policy issues raised by this thesis, and will discuss several alternative frameworks for transmission investment in the restructured era.

7.1. Four Lessons for Transmission Policy in the Restructured North American Electric Power Industry

Chapters 2 through 6 have offered a number of insights on transmission planning, policy, and pricing. Chapter 2 largely summarized the existing literature on market-based transmission investment, Chapters 3 through 6 represent the contributions of this thesis. This section will outline some lessons for transmission policy suggested by this thesis.

Lesson 1: The compensation mechanism in the market-based merchant-transmission model is neither workable nor economically efficient.

Bushnell and Stoft, in their 1996 and 1997 papers, demonstrate that under a certain set of economic assumptions, point-to-point financial transmission rights will yield patterns of investment that are both profitable and socially beneficial. While acknowledging that the

economic assumptions may be restrictive, Hogan (2003) defends the contract-network approach to encouraging investment as workable, if not optimal.[2]

The discussion in Chapters 2 and 4, as well as in Joskow and Tirole (2005a) suggests that neither of these claims is correct. Chapter 4 demonstrated that even if all of the economic assumptions underlying the arguments of Bushnell and Stoft were true, the investment efficiency of FTRs still depends on the network topology. By constructing a line that forms a Wheatstone network topology, an investor may be able to constrain flows through the grid, and profit from doing so. Profits from the line and an associated set of feasible FTRs would be positive, whether the investor was a merchant or a utility. The difference is that utility decision problem would need to incorporate the effects on the other generators and loads in the system, whereas the merchant decision problem would not.

The fault in Hogan's workability claim for transmission investment compensated with contracts based on nodal prices (whether FTRs or flowgate rights) lies in the difference between congestion rent and congestion cost, as discussed in Chapter 2. Compensation mechanisms based on nodal prices or the shadow price of transmission congestion amount to transferring congestion rent to the investor from the rest of the consumers and generators in the network. Transmission upgrades also result in a decrease in congestion cost (which otherwise represent a deadweight loss to the system). This benefit accrues

[2] Hogan does not precisely define "workable," but he conveys the sentiment that the contract network is a (knowingly) sub-optimal, but has better welfare properties than regulated cost-plus transmission planning. Even if all of the Bushnell-Stoft economic assumptions hold, there is no guarantee that the resulting transmission investment will be optimal in the sense of solving the problem in equations (1.1) or (1.2).

not to the investor, but to other generators and consumers in the system. Depending on the magnitude of the decrease in congestion cost (i.e., the magnitude of the free-rider problem), some socially beneficial transmission investments may not get built under this market system. Hogan (2003) claims that this should not be a problem, but concerns over compensating fixed-cost infrastructure investments with market-based prices date back to Hotelling (1938).

Lesson 2: Eliminating congestion is more complex than simply upgrading the most congested line.

Current models for pricing and investing in transmission capacity labor under an implicit assumption that eliminating congestion along a transmission line through upgrades or the construction of new capacity will have the effect of improving the flow of electricity through the network. In small series-parallel or even triangular networks, this may be true. However, the assumption does not necessarily hold in meshed power networks.

Analysis of the Wheatstone network in Chapter 3 suggests that increasing the capacity of a congested transmission line may have no effect, or at least a non-beneficial effect, on network flows. Sometimes multiple lines may need to be upgraded in order for the system to see any benefit. A related problem is that while congestion on transmission lines is largely a function of stability limits, loop flows in the system are a function of the system's electrical topology (the resistance or the susceptance). While the stability limit may be (first-order) independent of the resistance, congestion in the network is a function of both.

The nodal pricing system currently used in restructured electric power markets encourages incorrect analogies with other transportation networks, and perpetuates the notion that energy flows can always be improved by increasing the installed capacity of a given line. Nodal prices are stated in units of currency per MWh, because megawatt-hours represent the usable energy valued and purchased by consumers. Thus, the determining factor in the nodal price calculation is the cost of getting megawatt-hours to a given location in the system. Market-based transmission investment mechanisms reward investors for creating megawatts of transmission capacity, which should (but may not, as we have seen) mean more megawatt-hours able to be delivered to end-use customers. Just as important, but not currently compensated in any way, are the electrical properties of transmission lines. Gribik et. al. (2005) have suggested augmenting the flowgate-rights model to include admittance-based payments for new transmission lines, but their formulation is problematic since they suggest that admittance payments would merely amount to transfers from holders of megawatt-based flowgate rights. Thus, in the Gribik et. al. formulation, the electrical properties of transmission lines neither create nor destroy wealth in the network. The analysis of Wheatstone networks in Chapters 3 and 4 show that the electrical topology of the network can directly affect aggregate welfare.

Lesson 2 also speaks to the transmission planning process. Utility transmission planners recognize that this process amounts to a very difficult combinatorial optimization problem, one that (for a system of any appreciable size) is prohibitively costly to solve completely. Increasing reliability or decreasing congestion in the system is therefore a

matter of strategically choosing where to upgrade the system, and what types of upgrades to pursue.

Markets, on the other hand, respond to price signals. The straw-man argument against market-based transmission planning and investment says that investors will receive congestion prices as signals, and will act on those. The line with the highest congestion price will get upgraded first, then the line with the second-highest congestion price, and so forth. The analysis of Wheatstone snetworks in Chapters 3, 4, and 6 shows that following such an investment strategy will lead to a waste of resources. If the "congestion" prices actually reflected all of the relevant externalities associated with AC power flow and reliability constraints, then market-based transmission planning would deserve further consideration.

A more sophisticated critique of transmission planning under restructuring is based on the Wheatstone analyses in Chapters 3 and 6. The critique offered here says that congestion signals have failed in that they do not identify the relevant states of nature (specifically, the level of demand and the probability of contingencies) for optimal decision-making. Looking to the cost-benefit analysis of Wheatstone sub-networks in Chapter 6, in many cases the optimal investment strategy is state-contingent; it depends on the demand to transfer power across the Wheatstone sub-network and on the stochastic electrical topology in several portions of the network.[3] Over one range of possible levels of demand, construction of a Wheatstone bridge (for example) would seem to be a poor

[3] Joskow and Tirole (2005b) offer a similar criticism of FTRs as a mechanism to compensate transmission investment.

investment, since it will congest the network. Over another range of possible levels of demand, the Wheatstone bridge may provide a reliability benefit (despite causing additional congestion) and thus would make a wise investment. For a given level of demand, over one range of contingency probabilities, the Wheatstone bridge may have a positive net benefit (the reliability benefit outweighs the congestion cost), and over a different range of contingency probabilities the Wheatstone bridge may have a negative net benefit (the opposite result – that the congestion cost swamps the reliability benefit).

Because congestion prices are inherently state-contingent, they tell planners little more than which lines are congested for a given state of the system. They do not give planners any guidance regarding how the congestion should be handled. Flows through the network might improve if some transmission lines were removed or had flow-control devices (FACTS or relays) placed at various strategic positions throughout the network. For example, Chapter 3 suggests that flows through the Wheatstone network might improve if the bridge were removed from the system. Doing so, however, would rob the system of the reliability benefit arising from the bridge. An optimal transmission plan for the Wheatstone network would look at the net benefit (expected congestion cost versus reliability benefit, as discussed in Chapter 6) of the Wheatstone bridge versus the cost and performance of relays or FACTS devices placed at the end-nodes of the bridge.

Congestion prices are useful in certain circumstances; in particular, they can be effective tools for deciding whether transmission or generation investments should be undertaken to relieve a given system constraint. The insight from Chapters 3 and 6 is that the use of

congestion prices should be supplemented by a healthy dose of system awareness. Since the congestion prices in Wheatstone sub-networks must be interpreted with care, planners must know where in the larger network these structures exist. The value of the Wheatstone detection algorithm presented in Chapter 5 is to give planners in market-based systems awareness of places in the network congestion where prices can give good planning recommendations and of places where the network topology might yield more useful information than prices.

Lesson 3: Reliability and congestion are not independent.

Underlying any institutional structure for market-based transmission pricing and planning is the assumption that a clear distinction exists between lines (existing or proposed) that convey primarily economic benefits to the system in the form of congestion relief, and lines that benefit the system primarily through increased redundancy and reliability. The actual degree to which reliability and congestion are separable has been the topic of much debate but little serious analysis (Hogan 2003, Shanker 2003). The contribution of Chapter 6 is to provide a quantitative analysis of the relationship between congestion and reliability using a reasonably-sized test network.

The debate over the reliability versus congestion aspect of individual transmission lines has sometimes been clouded by imprecise language. Shanker (2003) and Roark (2006), both proponents of market-based transmission investment solutions, insist that the reliability property of a transmission line is separable from the economic property. The two attributes are separable, in the sense that we can write down equations for each that

do not depend on the other. Equations (6.1) and (6.4) from Chapter 6 do just that. But the two quantities are seldom independent. For a subset of a meshed transmission network it is rarely the case that the congestion cost varies with the level of demand or with outages in the network, while the reliability benefit is constant at zero. The reverse also holds; the reliability benefit rarely varies with the state of the network while the congestion cost is constant at zero.

An additional problem in the debate is the failure to identify the relevant state of the network. The analysis in Chapter 6 on Wheatstone sub-networks of the IEEE 118-bus system suggest that for some combinations of demand and outage probabilities (such as when both are very low), there may be congestion in the network without an associated reliability benefit. Over this range of system states, reliability and congestion are independent. For a different range of demand and outage probabilities, sharp tradeoffs exist between congestion cost and reliability benefits.

Lesson 4: Needed transmission infrastructure will not be built (without the aid of political will) unless the transmission planning, investment, and compensation problem is viewed as a systems problem.

Prior to restructuring, utility transmission planners built their systems with reliability criteria in mind. Economics or congestion played a minor role (if any) in determining which investments were made and which were not (Joskow 2005b). The transmission-planning problems in equations (1.1) and (1.2) have explicit reliability and

other system constraints, but the objective is to find the minimum transmission investment cost which supports the reliability constraints.

Under restructuring, planners are asked to consider both economic and reliability criteria in choosing among transmission investments (although as Joskow 2005b points out, RTO transmission planners have given substantially more weight to reliability criteria than economic criteria). If a sharp distinction cannot be made between the congestion and reliability attributes of the transmission network on a line-by-line basis, then the entire basis for market-based transmission planning and investment falls apart. Thus, Lesson 4 is in some sense the culmination of Lessons 1 through 3. The purest form of market-based transmission investment, in which merchant transmission companies respond to nodal price signals, and investments are rewarded with FTRs, will not yield optimal transmission plans because nodal prices do not incorporate all relevant externalities, including system reliability. In some circumstances, it may not even yield feasible transmission plans since the total effect of a new line on the network (positive or negative) is more than simply the sum of the congestion rents throughout the network.

Diluted forms of market-based transmission, such as participant funding, are meaningless unless the line between congestion and reliability can be clearly drawn. Merchant transmission contracts signed on the basis of reduced congestion costs for infrastructure that also has significant reliability benefits will result in free-riding and transfers of wealth from investors to those who benefit most from the added system reliability.

Transmission planning, investment, and compensation must consider the systems effects of changes in the grid infrastructure. This means that investors must be compensated on the basis of new transmission lines to the entire system, not just the change in the total congestion charges levied on market participants or the archaic reliability criteria used by utility and RTO planners.

7.2. Reformulating the Transmission Investment Problem

Both Hirst (2004) and the ISO/RTO Council (2005) report that despite a sometimes-ambiguous regulatory responsibility for transmission planning, RTO areas have been more active and more efficient at getting projects built than areas still under the traditional regulated-utility regime. However, Joskow (2005b) notes that many new investments have been socialized into the rate base, thus placing the risk on ratepayers rather than investors. One of the primary motivations for the merchant model has thus been undermined.

The real advantage of an RTO (or a similar institution with a wide geographic footprint, such as a power pool) in encouraging investment may be its ability to form coalitions of stakeholders while incurring reasonably small transactions costs. In particular, RTOs may be effective in facilitating a flavor of merchant transmission known as "participant funding" (Hébert 2004), in which multiple investor-stakeholders share the cost of new upgrades according to the degree to which they would benefit from the new infrastructure.

In regions managed by RTOs, participant funding (should it take hold) will still suffer from the problem of possible free-riding identified by Bushnell and Stoft (1996, 1997), as investors will likely earn returns either through congestion contracts or other appropriation of congestion rents. This does not necessarily have to be the case; instead of relying on price differences along network paths (which can provide incentives for harmful modifications to the grid, as illustrated in Chapter 3), compensation for merchant investments could be made on a marginal-value basis. Projects providing net benefits to the system as a whole would earn positive returns, while those detrimental to the system would not. Such a value-based compensation scheme would require performing some systems analysis of the type suggested in Chapter 6.

A variant of this method is currently used to assess transmission upgrades in the California ISO territory (Awad et. al. 2004). Line upgrades can be proposed by the California Energy Commission or the California ISO itself; those that appear to have the primary benefit of relieving congestion (rather than, for example, increasing system reliability) are subject to a social cost-benefit analysis before being put out to bid and allowed in the rate base. Participant funding was also used with some success in Argentina in the 1990s (Littlechild and Skerk 2004a, 2004b). The Argentinian transmission built under this compensation regime was in the form of high-voltage lines connecting portions of the system with little existing interconnection capacity. The discussion in Chapters 3 and 6 of this thesis suggests that these types of interconnections represent the limit of what market-based transmission can accomplish. Even so, similar

merchant transmission projects in the North American grid have been cancelled due to unwillingness of the investment community to offer funding.

The original merchant transmission model has failed miserably. RTOs currently operating under FERC-approved tariffs should amend those tariffs to reflect the unfortunate fact that the transmission problem is not one of market design or competitiveness. They should stop trying to offer investors FTRs in exchange for merchant AC transmission investment.[4] RTOs starting up or with tariffs pending before FERC should think of new mechanisms to ensure that desired transmission investments are actually built.

In the context of the restructured electric power industry, the transmission problem is one of risk management rather than markets or competition. The transmission infrastructure acts as a vehicle to manage uncertainty in peak demand, as well as in network topology. In this way, the transmission problem under restructuring should not be all that different from transmission planning in regions that still have traditionally-organized regulated utilities. Institutional differences between restructured and non-restructured regions suggest four alternatives to a system of market-based signals to encourage investment, compensate investment, or both.

[4] Joskow (2004b) has described the merchant transmission model as "dead," and as one that is not taken seriously by any industry players. However, at least one RTO continues to believe (at least on paper) that merchant transmission investment can be attracted by offering FTRs or other forms of congestion rent in exchange (New York ISO 2005).

The first alternative, as discussed in Chapter 2, is to simply treat transmission as a regulated business (in much the same way that utility distribution remains a regulated business) and to socialize the cost of all transmission lines through either direct ratepayer charges or market-participant transmission access charges. This would ultimately place all the risk associated with new transmission investment on the ratepayer. Even with transmission access charges, load-serving entities would likely pass these on to ratepayers, especially in the absence of thriving retail electricity markets.

This alternative represents the mechanism under which all transmission investment in restructured areas has taken place. Pending investments also appear likely to be funded this way. Section 1221 of the Energy Policy Act of 2005 allows the U.S. Department of Energy and FERC to designate "national interest transmission corridors," for which the permitting and siting process may be expedited by FERC.

A second alternative would be to have the RTO own, as well as operate, the transmission system. Planning and investment would then proceed as with a vertically-integrated utility, but on a regional scale. RTOs are already supposed to perform regional transmission planning, but who has the responsibility to build new transmission is still shrouded in ambiguity, as is the method of payment. Ownership of the transmission lines would remove some of this ambiguity. Placing responsibility for investment in the hands of the RTO would require the RTO to collect money for some sort of transmission fund. Congestion payments could be used for this purpose, but this would require disrupting the current system of using congestion payments to reimburse holders of FTRs. To the

extent that FTRs represent property rights, holders of long-term FTRs would need to be appropriately compensated.

Eliminating FTRs (as they currently exist) is also problematic in that it would remove one mechanism by which spot-market participants could hedge locational price risk. Prior to the establishment of organized spot markets, locational risk in electricity markets was referred to as "basis risk" (van Vactor 2004) because it was perceived as unhedgeable. The right combination of FTRs and contracts for differences, however, can create a perfect hedge in electricity markets with nodal pricing (Bushnell and Stoft 1996).

The third alternative is essentially the two-part tariff proposed by Apt and Lave (2003), which consists of LMP plus a megawatt-mile charge. In this scenario, the RTO does not necessarily own the lines, but performs regional transmission planning and collects money for transmission upgrades. The appeal of the megawatt-mile approach is the incentives that it provides to the RTO. Since the RTO must immediately redistribute congestion revenue in the form of FTR payments, they are revenue-neutral with respect to congestion. With the megawatt-mile approach, the RTO could still disburse FTR payments based on congestion revenue, but the megawatt-mile charge would encourage the RTO to be more aggressive about regional transmission planning. Upgrades or infrastructure that improve the flow of energy through the network would increase revenue for the RTO. If revenue-neutrality for the RTO with respect to megawatt-mile payments was an important policy goal, then the RTO could transfer these payments to

transmission owners (and the incentive to upgrade the transmission system in beneficial ways would thus also transfer to the transmission owners).

The primary criticism of the megawatt-mile approach is that it relies too much on the "contract path" fallacy that was pervasive prior to restructuring (Hogan 1992, 2003). Scheduling based on contract paths requires that the counterparties to bilateral energy trades name a specific set of links (forming a path from source to sink) over which they believe that the power will travel.[5] Very often, these bear little resemblance to the actual physical flow of power; the megawatt-mile charge would need to be structured to remove the incentive of grid participants to pay based on the shortest physical distance between source and sink (which may be different than the shortest electrical distance, which is a better basis of payment).

The first three reformulations of the transmission investment problem succumb to the criticism that they still leave essentially one entity (the utility or RTO) in charge of transmission planning. One of the appealing features of the merchant model is that it engages multiple entities in the planning process. A merchant may discover a beneficial line that the utility or RTO did not. But, as the thesis has discussed in Chapters 2 and 6, the current merchant model is faulty in its LMP-based compensation structure. It also provides incentives to modify the grid in harmful ways (see Chapter 4).

A fourth alternative would thus simply reformulate the merchant transmission problem, fixing the compensation mechanism. The current mechanism is faulty because it

[5] This is essentially the same criticism that Hogan (2000) levels against the flowgate model.

encourages free-riding in the system (see Figure 2.2 in Chapter 2), which may prevent some socially-beneficial transmission from being built.

Hotelling (1938) considered the case of optimal compensation for a large piece of infrastructure whose costs consist primarily of fixed costs, such as a bridge. He concluded that marginal-use pricing, such as tolls, represents an inefficient compensation mechanism because it imposes a deadweight loss on society, as fewer drivers will choose to use the bridge in the presence of a toll. Since these assets are lumpy in the sense that the marginal cost depends on the amount of spare capacity, Hotelling argues that an average cost mechanism is superior in the presence of high fixed costs.

The argument is nearly identical for investment in transmission lines, as shown in Figure 2.2. A better compensation mechanism for non-utility transmission would be to calculate the value of the line to the system, as demonstrated in Chapter 6, and to use that to define the revenue stream to the investor. During periods in which the line relieves congestion in the system or provided a reliability benefit, the investor would receive a positive payment from the grid.[6] During periods in which the line caused congestion, the investor would receive a negative payment; that is, the investor would be forced to pay the grid operator based on the cost imposed by the line.[7] These costs and benefits can easily be calculated ex-post using the framework presented in Chapter 6.

[6] The grid is assumed to encompass the generators and load-serving entities operating within a pre-defined control area.

[7] The grid operator, in turn, could transfer the money to individual grid participants, or keep the money for an infrastructure upgrade fund.

To the extent that the RTO was risk-averse, it might prefer to sign a fixed-price contract for non-utility transmission based on the expected net benefit of the line to the system, rather than compensating the investor using what amounts to a series of spot contracts. The RTO might also be willing to pay a premium for this contract, which would amount to the average-cost pricing methodology suggested by Hotelling (1938). A risk-neutral RTO would be indifferent between a series of spot contracts and a long-term contract with a fixed price equal to the expected net benefit of the new line.

7.3. Who Can Bear the Risk at the Lowest Cost?

Once the transmission investment problem is correctly formulated as a problem in risk-management, the optimal policy is the one that places the burden of the risk on the entity (or entities) who can manage the risk at the lowest cost. This insight is due to Coase (1960), and was originally developed in the study of transactions costs and externalities. Coase argued that if transaction costs were not minimized while internalizing externalities, deadweight losses would result. The argument is similar for the case of bearing risk. If two parties can mange risk equally effectively, but one can do it at half the cost of the other, choosing the higher-cost risk manager is a waste of society's resources (that is, it does not simply transfer money from the rest of society to the expensive risk manager). This is essentially the same reason that transmission congestion imposes a social cost and does not just transfer money to the holders of congestion rights.

In restructured electric power systems, the transmission risk-management problem boils down to placing three entities in charge of investment: the utility, the RTO, and the merchant sector. If the merchant sector can bear the risk at a lower cost than the utility or RTO sector, then policy efforts should focus on redefining the institutions and market mechanisms to support non-utility transmission, such as the value-based merchant transmission proposal discussed at the end of Section 7.2. If the RTO can bear the risk at a lower cost, then policymakers should think more seriously about transferring ownership of transmission lines to the RTO and giving FERC more regulatory authority over transmission.

	May 2001 Peak	**April 15, 2005**	
Company	**Share Price**	**Share Price**	**Credit Rating**
AES	48.50	16.50	B+
AEP	50.40	34.19	BBB
Calpine	54.70	2.39	B-
Duke	46.10	27.89	BBB
El Paso	64.90	18.91	B-
Mirant	45.40	0.31	N/A
Reliant	33.80	10.91	B+
Southern Cos.	23.54	31.95	A-
Williams	41.00	16.55	B+

Table 7.1. Share prices and bond ratings for various firms in the electric power industry. Sources: Joskow (2005a) and Standard and Poor's.

Joskow (2005a) has emphasized the terrible financial shape of the merchant generation sector of the industry, and Krellenstein (2004) has argued that there have been spillovers to the transmission sector. Table 7.1 shows the stock performance and bond ratings for integrated utility firms and merchants in 2001 and 2005. Merchant electricity investment is viewed as inherently more risky than integrated utility investment (public or private)

due to perceived uncertainty over how merchant investment will be compensated. The uncertainty stems from two sources, but both are a construct of the RTO's institutional structure. The first is simple variability in the RTO spot market and the lack of transparent forward-market substitutes. The second is uncertainty over future RTO rules and regulations, and the intolerant attitude that RTOs have taken towards high spot energy prices.[8]

The uncertainty surrounding the revenue stream for a merchant player in the electricity industry would not pose such a problem if the merchant player had diversified or guaranteed sources of revenue to act as an insurance policy. But the nature of the merchant sector is that it does not have this type of collateral; its projects should succeed or fail on their own merits, and investors (not ratepayers or taxpayers) will reap the reward or pay the cost. Krellenstein's (2004) view is that merchant investments thus amount to "project financing," meaning that investors are essentially taking a bet on a specific project (a generating unit or transmission line). This is distinguished from "system financing," where borrowers can use existing assets or revenue (such as ratepayers) as security. Investments that fall under project financing normally face higher interest rates and the associated debt is classified as sub-investment grade.

Thus, the merchant sector as currently structured is not the lowest-cost solution to the transmission problem. The merchant sector has two strikes against it: the incentive structure in rewarding merchant transmission with contracts based on nodal prices does

[8] Joskow and Tirole (2005b) have also criticized the RTOs for not allowing prices to spike during periods of peak demand.

not promote the socially optimal level of transmission investment, and to the extent that it does promote investment, society will pay more for a merchant line than a utility line.

Blumsack, Apt, and Lave (2006) have noted that the merchant sector is not alone; the vertically-integrated utility sector has not fared uniformly well under restructuring. Prior to restructuring, most debt from investor-owned utilities was seen as reasonably risk-free and was thus given a median rating of "A" by the major credit agencies. Since restructuring, this median rating has dropped to "BBB" amid uncertainties over the future path and scope of restructuring. Public power, much of which is not bound by FERC's restructuring efforts, maintains its "A" debt rating.

The relevant question for designing a new transmission policy is whether a reformulation of non-utility transmission can handle both the incentive problem and the risk problem. Compensation of merchant transmission assets on a value-added basis (this is the fourth alternative discussed in Section 7.2) would certainly take care of the incentive problem. The transmission investor would collect not only the congestion rent along the new or upgraded line, but would also have a right to the reduced congestion cost. Thus, the investment decision would be subject to the right set of incentives.

Value-added transmission payments can reduce the risk associated with the merchant sector only to the extent that the variation in the net benefit of a line to the system is smaller than the congestion rent. Thus, non-utility transmission compensation will have to be structured as long-term contracts. Krellenstein (2004) has noted that potential

investors in merchant transmission projects prefer deals to be structured as long-term contracts and not as a sequence of spot contracts with an expected value equivalent to the average value in the long-term contract. Price certainty is valued at a premium; that is, an investor in a merchant project will need to be paid to enter into a contract that does not have (for example) take-or-pay provisions. This indicates that investors are risk-averse with respect to merchant investment, and perhaps even risk-neutral with respect to investments that qualify as system financing.

If investors are risk-averse towards merchant investments, but less risk-averse or risk-neutral towards an equivalent investment by a non-merchant party, then even if the compensation mechanism reflects the value of the line to the system (and not just the change in congestion prices), merchant transmission cannot represent the least-cost solution to the transmission problem. Whether the utility or RTO is the lowest-cost institution is still an open question. RTOs have established themselves as not-for-profit entities that do not take a physical position in the markets they run. It is not clear how the investment community would view a shift in RTO structure.

In any case, this does not mean the total death of the merchant sector. As mentioned above, merchants may be able to identify beneficial projects that RTOs or utilities cannot. Even if most projects are undertaken by utilities or even RTOs, there is no good reason to exclude merchant investment from RTO tariffs. The analysis in this thesis has suggested ways in which merchant transmission might effectively be integrated into the RTO planning and investment process. First, new lines should be subjected to the type of

cost-benefit test detailed in Chapter 6 and the topological awareness of the grid discussed in Chapters 3 and 5. RTOs and regulators alike should realize that transmission lines may impose congestion costs on the system and convey reliability benefits. This cost-benefit test needs to be defined over the relevant range of demand, since the net benefit of a given line is not independent of the state of the system. Second, compensation for merchant projects needs to reflect these net benefits.

References

Aitchison, P., 1983. "Diakoptics or Tearing: A Mathematical Approach," *Quarterly of Applied Mathematics* 41:3, pp. 265 – 272.

American Electric Power Company, 2006. "The AEP Interstate Project Proposal: A 765 kV Line from West Virginia to New Jersey," available at http://www.aep.com/newsroom/resources/docs/AEP_InterstateProjectProposal.pdf.

Apt, J. and L. Lave, 2003. "Electric Gridlock: A National Solution," *Public Utilities Fortnightly* 141:18, pp. 14 – 17.

Arnott, R. and K. Small, 1994. "The Economics of Traffic Congestion," *American Scientist* 82, pp. 446 – 455.

Awad, M., S. Broad, K. Casey, J. Chen, A. Geevarghese, J. Miller, A. Sheffrin, M. Zhang, E. Toolson, G. Drayton, A. Rahimi, and B. Hobbs, 2004. "The California ISO Transmission Economic Assessment Methodology," paper presented at the first Carnegie-Mellon Conference on Electricity, Pittsburgh PA. Available at http://www.ece.cmu.edu/~electriconf/old2004/.

Baldick, R., 2003. "Variation of Distribution Factors with Loading," *IEEE Transactions on Power Systems* 18:4, pp. 1316 – 1323.

Barrat, A. and M. Weigt, 2000. "On the Properties of Small-World Networks," *European Journal of Physics B* 13, pp. 547 – 560.

Bean, N., F. Kelly, and P. Taylor, 1997. "Braess' Paradox in a Loss Network," *Journal of Applied Probability* 4, pp. 155 – 159.

Blumsack, S., J. Apt, and L. Lave, 2005. "A Cautionary Tale: U.S. Electric Sector Reform," *Economic and Political Weekly* 40:50, pp. 5279 – 5301.

Blumsack, S., J. Apt and L. Lave, 2006. "Lessons From the Failure of U.S. Electricity Restructuring," *Electricity Journal*, forthcoming.

Bohn, R., M. Caramanis and F. Schweppe, 1984. "Optimal Pricing in Electrical Networks Over Space and Time," *Rand Journal of Economics* 15:3, pp. 360 – 376.

Braess, D., 1968. "Über ein Paradoxon aus der Verkehrsplanung," *Unternehmensforschung* 12, pp. 258 – 268.

Bushnell, J. and S. Stoft, 1996. "Electric Grid Investment Under a Contract Network Regime," *Journal of Regulatory Economics* 10, pp. 61 – 79.

Bushnell, J. and S. Stoft, 1997. "Improving Private Incentives for Electric Grid Investment," *Resource and Energy Economics* 19, pp. 85 – 108.

Calvert, B. and G. Keady, 1993. "Braess' Paradox and Power Law Nonlinearities in Networks," *Journal of the Australian Mathematical Society B* 35, pp. 1 – 22.

Chao, H. and S. Peck, 1996. "A Market Mechanism for Electric Power Transmission," *Journal of Regulatory Economics* 10, pp. 25 – 59.

Coase, R., 1960. "The Problem of Social Cost," *Journal of Law and Economics* 3, pp. 1 – 44.

Cohen, J. and P. Horowitz, ,1991. "Paradoxical Behavior of Mechanical and Electrical Networks," *Nature* 352, pp. 699 – 701.

Coxe, R. and M. Ilić, 1998. "System Planning Under Competition," in *Power Systems Restructuring: Engineering and Economics,* M. Ilić, F. Galiana, L. Fink, eds., Kluwer Academic Publishing, Boston MA.

de Vany, Arthur and W. David Walls, 1993. "Pipeline Access and Market Integration in the Natural Gas Industry: Evidence from Cointegration Tests," *The Energy Journal* 14:4, pp. 1 – 19.

Dixit, A. and R. Pindyck, 1994. *Investment Under Uncertainty*, Princeton University Press, Princeton NJ.

Duffin, R., 1965. "Topology of Series-Parallel Networks," *Journal of Mathematical Analysis and Applications* 10, pp. 303 – 318.

Ejebe, G. and B. Wollenberg, 1979. "Automatic Contingency Selection," *IEEE Transactions on Power Apparatus and Systems* PAS-98, pp. 97 – 109.

Ekelöf, S., 2001. "The Genesis of the Wheatstone Bridge," *Engineering Science and Education Journal* 10:1, pp. 37 – 40.

Garver, L., 1970. "Transmission Network Estimation Using Linear Programming," *IEEE Transactions on Power Apparatus and Systems* PAS-89:7, pp. 1688 – 1697.

Gribik, P., D. Shirmohammadi, J. Graves, and J. Kritikson, 2005. "Transmission Rights and Transmission Expansions," *IEEE Transactions on Power Systems* 20:4, pp. 1728 – 1737.

Happ, H., 1973. "The Operation and Control of Large Interconnected Power Systems," *IEEE Transactions on Circuit Theory* CT-20:3, pp. 212 – 222.

Happ, H., 1974. "Diakoptics: The Solution of System Problems by Tearing," *Proceedings of the IEEE* 62:7, pp. 930 – 940.

Hebert, C., 2004. "Profit Without Costs," *Public Utilities Fortnightly*, 142:8, pp. 40 – 48.

Hines, P., J. Apt, H. Liao, and S. Talukdar, 2006. "The Frequency of Large Blackouts in the United States Electrical Transmission System: An Empirical Study," presented at the 2nd Carnegie Mellon Conference on Electric Power, January 2006, available at http://www.ece.cmu.edu/~electriconf/ hines_blackout_frequencies_final.pdf.

Hirst, E., 2004. "U.S. Transmission Capacity: Present Status and Future Prospects," Edison Electric Institute and U.S. Department of Energy working paper.

Hirst, E. and B. Kirby, 2001. "Transmission Investment for a Restructuring U.S. Electricity Industry," Edison Electric Institute working paper.

Hogan, W., 1992. "Contract Networks for Electric Power Transmission," *Journal of Regulatory Economics* 4: pp. 211 – 242.

Hogan, W., 1993. "Markets in Real Electric networks Require Reactive Prices," *Energy Journal* 14:3, pp. 171 – 200.

Hogan, W., 2000. "Flowgate Rights and Wrongs," working paper, available at http://www.whogan.com.

Hogan, W., 2002. "Financial Transmission Right Formulations," working paper, available at http://www.whogan.com.

Hogan, W., 2003. "Transmission Market Design," working paper, available at http://www.whogan.com.

Hotelling, H., 1938. "The General Welfare in Relation to Problems of Taxation and of Railway and Utility Rates," *Econometrica* 6:3, pp. 242 – 269.

Ilić, M., 2003. "Technologies and Management Structures to Support Reliable and Efficient Operation over a Broad Range of Generation and Demand," working paper, Carnegie Mellon University.

Ilić, M. and J. Zaborsky, 2000. *Dynamics and Control of Large Electric Power Systems,* John Wiley & Sons, New York.

Irisarri, G., D. Levner, and A. Sasson, 1979. "Automatic Contingency Selection for On-Line Security Analysis – Real-Time Tests," *IEEE Transactions on Power Apparatus and Systems* PAS-98, pp. 1552 – 1559.

Irisarri, G. and A. Sasson, 1981. "An Automatic Contingency Selection Method for On-Line Security Analysis," *IEEE Transactions on Power Apparatus and Systems* PAS-100:4, pp. 1838 – 1843.

ISO New England, 2006. Financial Transmission Rights Manual, available at http://www.iso-ne.com/rules_proceds/isone_mnls/index.html.

ISO/RTO Council, 2005. "The Value of Regional Grid Operators," report available at http://www.nyiso.com.

Joskow, P., 2003. "The Blackout," working paper, available at http://econ-www.mit.edu/faculty/index.htm?prof_id=pjoskow&type=paper.

Joskow, P., 2004a. "Transmission Policy in the United States," working paper, available at http://econ-www.mit.edu/faculty/index.htm?prof_id=pjoskow&type=paper.

Joskow, P., 2004b. "Competitive Electricity Markets: Challenges for T&D," presented at the 1st Carnegie Mellon Conference on Electric Power, December 2004, available at http://www.ece.cmu.edu/%7Eelectriconf/old2004/JOSKOW-CMU-REVISED.pdf.

Joskow, P., 2005a. "The Difficult Transition to Competitive Electricity Markets in the U.S.," in *Electricity Deregulation: Choices and Challenges*, J. Griffin and S. Puller, eds., University of Chicago Press, Chicago.

Joskow, P., 2005b. "Patterns of Transmission Investment," working paper, available at http://econ-www.mit.edu/faculty/index.htm?prof_id=pjoskow&type=paper.

Joskow, P. and J. Tirole, 2000. "Transmission Rights and Market Power on Electric Power Networks," *RAND Journal of Economics* 31:3, pp. 450 – 487.

Joskow, P. and J. Tirole, 2005a. "Merchant Transmission Investment," *Journal of Industrial Economics* 53:2, pp. 233 – 264.

Joskow, P. and J. Tirole, 2005b. "Reliability and Competitive Electricity Markets," working paper, available at http://econ-www.mit.edu/faculty/index.htm?prof_id=pjoskow&type=paper.

Joskow, P. and R. Schmalensee, 1983. *Markets for Power: An Analysis of Electric Utility Deregulation*, MIT Press, Cambridge MA.

Korilis, Y., Lazar, A., and A. Orda, 1997. "Capacity Allocation Under Non-Cooperative Routing," *IEEE Transactions on Automatic Control* 42, pp. 309 – 325.

Korilis, Y., Lazar, A., and A. Orda, 1999. "Avoiding the Braess Paradox in Non-Cooperative Networks," *Journal of Applied Probability* 36, pp. 211 – 222.

Krellenstein, G., 2004. "Transmission Financing," paper presented at the first Carnegie Mellon Conference on Electricity, Pittsburgh PA. Available at http://www.ece.cmu.edu/~electriconf/old2004/.

Kron, G., 1953. "A Set of Principles to Interconnect the Solutions of Physical Systems," *Journal of Applied Physics* 24:8, pp. 965 – 980.

Lave, L., J. Apt, and S. Blumsack, 2004. "Rethinking Electricity Deregulation," *Electricity Journal* 17:8, pp. 11 – 26.

Lehr, D. and S. van Vactor, "Evolution of Power Price Structures in the Western Power Market," in *The Evolving U.S. Power Market*, Risk Publications, June 1997.

Lesieutre, B. and I. Hiskens, 2005. "Convexity of the Set of Feasible Injections and Revenue Adequacy in FTR Markets," *IEEE Transactions on Power Systems* 20, pp. 1790 – 1798.

Littlechild, S. and C. Skerk, 2004a. "Regulation of Transmission Expansion in Argentina, Part II: Developments Since the Fourth Line," Cambridge Working Papers in Economics CWPE 0465.

Littlechild, S. and C. Skerk, 2004b. "Regulation of Transmission Expansion in Argentina, Part I: State Ownership, Reform, and the Fourth Line," Cambridge Working Papers in Economics CWPE 0464.

Lo, K., L. Peng, J. Macqueen, A. Ekwue, and N. Dandachi, 1993. "Extended Ward Equivalent of External System for On-Line Security Analysis," *Proceedings of the IEEE 2nd International Conference on Advances in Power System Control*, Hong Kong.

Martzoukos, S. and W. Teplitz-Sembitzky, 1992. "Optimal Timing of Transmission Line Investments," *Energy Economics* 14:1, pp. 3 – 10.

Milchtaich, I., 2005. "Network Topology and Efficiency of Equilibrium," Bar-Ilan University Department of Economics Working Paper

Monticelli, A., S. Deckmann, A. Garcia, and B. Stott, 1979. "Real-time External Equivalents for Static Security Analysis," *IEEE Transactions on Power Apparatus and Systems* PAS-98, pp. 498 – 508.

Morgan, G., J.Apt., and L. Lave, with J. Bergerson, S. Blumsack, J. DeCarolis, P. Hines, D. King, D. Patiño-Echeverri, and H. Zerriffi, 2005. "The U.S. Electric Power Sector and Climate Change Mitigation," Pew Center on Global Climate Change, available at http://www.pewclimate.org.

New York ISO, 2006. Transmission Congestion Contracts Manual, available at http://www.nyiso.com/public/documents/manuals/operations.jsp?maxDisplay=20.

New York ISO, 2005. "Opportunities for New Transmission Investment in NYISO's Markets," Presentation of J. Buechler at the December Transmission Workshop, available at http://www.nyiso.com/public/webdocs/services/planning/transmission_investments_workshop/Buechler_presentation_12052005.pdf

Newman, M. E. J., 2003. "The Structure and Function of Complex Networks," *SIAM Review* 45:2, pp. 167 – 256.

North American Electric Reliability Council, 2005. "Approved Reliability Standards," available at http://www.nerc.com/~filez/standards/Reliability_Standards.html.

Oren, S., 1997. "Economic Inefficiency of Passive Transmission Rights in Congested Electricity Systems with Competitive Generation," *Energy Journal* 18, pp. 63 – 83.

Oren, S. and A. Ross, 2002. "Economic Congestion Relief Across Multiple Regions Requires Tradable Physical Flow-Gate Rights," *IEEE Transactions on Power Systems* 17:1, pp. 159 – 165.

Patiño-Echeverri, D., 2006. *Valuing Risk-Reduction: Three Applications in the Electricity Industry*, unpublished Ph.D. dissertation, Carnegie-Mellon University, Pittsburgh PA.

PJM, 2006. Financial Transmission Rights Manual, available at http://www.pjm.com/contributions/pjm-manuals/manuals.html.

Roark, J., 2006. "Redefining Merchant Transmission and Making it Happen," presented at the 2nd Carnegie Mellon Conference on Electric Power, January 2006, available at http://www.ece.cmu.edu/~electriconf/Roark_ReDefining%20Merchant%20Transmission.pdf.

Romero, R. and A. Monticelli, 1994. "A Hierarchical Decomposition Approach for Transmission Network Expansion Planning," *IEEE Transactions on Power Systems* 9:1, pp. 373 – 380.

Saphores, J., E. Gravel, and J. Bernard, 2004. "Regulation and Investment Under Uncertainty: An Application to Power Grid Interconnection," *Journal of Regulatory Economics* 25:2, pp. 169 – 186.

Sauer, P., 1981. "On the Formulation of Power distribution Factors for Linear Load Flow Methods," *IEEE Transactions on Power Apparatus and Systems* PAS-100:2, pp. 764 – 769.

Seifu, A., S. Salon, and G. List, 1989. "Optimization of Transmision Line Planning Including Security Constraints," *IEEE Transactions on Power Systems* 4:4, pp. 1507 – 1513.

Shanker, R., 2003. “Drawing the Line for Transmission Investment,” presentation to the Harvard Energy Policy Group, available at http://www.ksg.harvard.edu/hepg/Papers/Shanker_Line.transm.investment_4-03.pdf.

Siddiqui, A., E. Bartholomew, C. Marnay and S. Oren, 2005. “On the Efficiency of the New York Independent System Operator Market for Transmission Congestion Contracts,” *Journal of Managerial Finance*, 31:1, pp. 1-45.

Sundaram, R., 1996. *A First Course in Optimization*, Cambridge University Press, Cambridge UK.

U.S.-Canada Power System Outage Task Force, 2004. “Final Report on the August 14, 2003 Blackout in the United States and Canada,” available at https://reports.energy.gov.

van Vactor, S., 2004. “Flipping the Switch: The Transformation of Energy Markets,” Ph.D. dissertation, University of Cambridge.

Vajjhalla, S. and P. Fischbeck, 2006. “Quantifying Siting Difficulty: A Case Study of U.S. Transmission Line Siting,” *Energy Policy*, forthcoming.

Watts, D. and H. Strogatz, 1998. “Collective Dynamics of ‘Small-World’ Networks, *Nature* 393, pp. 440 – 442.

Wood, A, and B. Wollenberg, 1996. *Power Generation, Operation and Control*, John Wiley & Sons, New York.

Wu, F., P. Varaiya, P. Spiller, and S. Oren, 1996. “Folk Theorems on Transmission Access: Proofs and Counterexamples,” *Journal of Regulatory Economics* 10, pp. 5 – 23.

Yu, C., J. Leotard and M. Ilić, 1999. "Dynamic Transmission Provision in Competitive Electric Power Industry," *Discrete Event Dynamic Systems: Theory and Applications*, 9, pp. 351-388, Kluwer Academic Publishers, Boston, MA.

Appendix A: Network Data for the IEEE 118-bus System

This appendix contains the network data for the IEEE 118-bus test network used in the Wheatstone analysis of Chapter 6. The data was downloaded from the IEEE power systems test case archive at www.ee.washington.edu/research/pstca/. The data is given in a format consistent with Matpower, a free set of Matlab files for power system simulation and analysis, available at http://www.pserc.cornell.edu/matpower/.

A1. Bus and Demand Data

Bus and demand data for the 118-bus test network is given in Table A1. The variables and units used in the column headings of Table A1 are:

P_L: Real power demand, in [MW]

Q_L: Reactive power demand, in [MVar]

V: Bus voltage magnitude, in per-unit for a voltage base of 100 kV

θ: Bus voltage angle, in degrees

Vmax: Maximum bus voltage magnitude, in per-unit for a voltage base of 100 kV

Vmin: Maximum bus voltage magnitude, in per-unit for a voltage base of 100 kV

Bus	P_L	Q_L	V	θ	Vmax	Vmin
1	51	27	0.955	10.983	1.06	0.94
2	20	9	0.97139	11.523	1.06	0.94
3	39	10	0.96769	11.866	1.06	0.94
4	39	12	0.998	15.583	1.06	0.94
5	0	0	1.00198	16.028	1.06	0.94
6	52	22	0.99	13.302	1.06	0.94
7	19	2	0.98933	12.857	1.06	0.94
8	28	0	1.015	21.049	1.06	0.94
9	0	0	1.04292	28.303	1.06	0.94
10	0	0	1.05	35.884	1.06	0.94
11	70	23	0.98509	13.016	1.06	0.94
12	47	10	0.99	12.499	1.06	0.94
13	34	16	0.9683	11.641	1.06	0.94
14	14	1	0.98359	11.783	1.06	0.94
15	90	30	0.97	11.489	1.06	0.94
16	25	10	0.98391	12.198	1.06	0.94
17	11	3	0.99513	14.006	1.06	0.94
18	60	34	0.973	11.793	1.06	0.94
19	45	25	0.963	11.314	1.06	0.94
20	18	3	0.95776	12.192	1.06	0.94
21	14	8	0.95841	13.779	1.06	0.94
22	10	5	0.96954	16.332	1.06	0.94
23	7	3	0.99972	21.249	1.06	0.94
24	13	0	0.992	21.118	1.06	0.94
25	0	0	1.05	28.184	1.06	0.94
26	0	0	1.015	29.965	1.06	0.94
27	71	13	0.968	15.613	1.06	0.94
28	17	7	0.96157	13.889	1.06	0.94
29	24	4	0.96322	12.897	1.06	0.94
30	0	0	0.98553	19.04	1.06	0.94
31	43	27	0.967	13.014	1.06	0.94
32	59	23	0.964	15.054	1.06	0.94
33	23	9	0.97161	10.864	1.06	0.94
34	59	26	0.986	11.505	1.06	0.94
35	33	9	0.9807	11.08	1.06	0.94
36	31	17	0.98	11.085	1.06	0.94
37	0	0	0.99208	11.969	1.06	0.94
38	0	0	0.96204	17.106	1.06	0.94

Table A1: Bus data for the IEEE 118-bus network

Bus	P_L	Q_L	V	θ	Vmax	Vmin
39	27	11	0.97049	8.598	1.06	0.94
40	66	23	0.97	7.525	1.06	0.94
41	37	10	0.96683	7.079	1.06	0.94
42	96	23	0.985	8.674	1.06	0.94
43	18	7	0.97858	11.459	1.06	0.94
44	16	8	0.98505	13.945	1.06	0.94
45	53	22	0.98667	15.776	1.06	0.94
46	28	10	1.005	18.582	1.06	0.94
47	34	0	1.01705	20.805	1.06	0.94
48	20	11	1.02063	20.025	1.06	0.94
49	87	30	1.025	21.028	1.06	0.94
50	17	4	1.00108	18.989	1.06	0.94
51	17	8	0.96688	16.37	1.06	0.94
52	18	5	0.95682	15.417	1.06	0.94
53	23	11	0.94598	14.442	1.06	0.94
54	113	32	0.955	15.353	1.06	0.94
55	63	22	0.952	15.063	1.06	0.94
56	84	18	0.954	15.25	1.06	0.94
57	12	3	0.97058	16.455	1.06	0.94
58	12	3	0.95904	15.598	1.06	0.94
59	277	113	0.985	19.452	1.06	0.94
60	78	3	0.99316	23.234	1.06	0.94
61	0	0	0.995	24.125	1.06	0.94
62	77	14	0.998	23.509	1.06	0.94
63	0	0	0.96874	22.831	1.06	0.94
64	0	0	0.98374	24.597	1.06	0.94
65	0	0	1.005	27.722	1.06	0.94
66	39	18	1.05	27.563	1.06	0.94
67	28	7	1.01968	24.923	1.06	0.94
68	0	0	1.00325	27.601	1.06	0.94
69	0	0	1.035	30	1.06	0.94
70	66	20	0.984	22.62	1.06	0.94
71	0	0	0.98684	22.209	1.06	0.94
72	12	0	0.98	21.112	1.06	0.94
73	6	0	0.991	21.998	1.06	0.94
74	68	27	0.958	21.671	1.06	0.94
75	47	11	0.96733	22.933	1.06	0.94
76	68	36	0.943	21.803	1.06	0.94
77	61	28	1.006	26.757	1.06	0.94
78	71	26	1.00342	26.453	1.06	0.94

Table A1 (continued)

Bus	P_L	Q_L	V	θ	Vmax	Vmin
79	39	32	1.00922	26.752	1.06	0.94
80	130	26	1.04	28.998	1.06	0.94
81	0	0	0.99681	28.149	1.06	0.94
82	54	27	0.98881	27.276	1.06	0.94
83	20	10	0.98457	28.465	1.06	0.94
84	11	7	0.97977	30.997	1.06	0.94
85	24	15	0.985	32.55	1.06	0.94
86	21	10	0.98669	31.181	1.06	0.94
87	0	0	1.015	31.44	1.06	0.94
88	48	10	0.98746	35.68	1.06	0.94
89	0	0	1.005	39.734	1.06	0.94
90	440	42	0.985	33.331	1.06	0.94
91	10	0	0.98	33.352	1.06	0.94
92	65	10	0.993	33.841	1.06	0.94
93	12	7	0.98737	30.837	1.06	0.94
94	30	16	0.99081	28.687	1.06	0.94
95	42	31	0.98111	27.716	1.06	0.94
96	38	15	0.9928	27.549	1.06	0.94
97	15	9	1.01143	27.923	1.06	0.94
98	34	8	1.02351	27.446	1.06	0.94
99	42	0	1.01	27.085	1.06	0.94
100	37	18	1.017	28.081	1.06	0.94
101	22	15	0.99276	29.649	1.06	0.94
102	5	3	0.99159	32.341	1.06	0.94
103	23	16	1.001	24.48	1.06	0.94
104	38	25	0.971	21.742	1.06	0.94
105	31	26	0.965	20.634	1.06	0.94
106	43	16	0.96114	20.379	1.06	0.94
107	50	12	0.952	17.576	1.06	0.94
108	2	1	0.96621	19.434	1.06	0.94
109	8	3	0.96703	18.982	1.06	0.94
110	39	30	0.973	18.135	1.06	0.94
111	0	0	0.98	19.78	1.06	0.94
112	68	13	0.975	15.036	1.06	0.94
113	6	0	0.993	14.004	1.06	0.94
114	8	3	0.96068	14.727	1.06	0.94
115	22	7	0.96053	14.72	1.06	0.94
116	184	0	1.005	27.166	1.06	0.94
117	20	8	0.97382	10.958	1.06	0.94
118	33	15	0.94944	21.945	1.06	0.94

Table A1 (continued)

A2. Generator Data

Generator data for the IEEE 118-bus test network is shown in Table A2. The variables and units used in the column headings of Table A2 are:

P_G: Real power output, in [MW]

Q_G: Reactive power output, in [MVar]

$Q_{G,max}$: Maximum reactive power output, in [MVar]

$Q_{G,min}$: Minimum reactive power output, in [MVar]

V: Voltage magnitude setpoint, in per-unit for a base voltage of 100 kV.

$P_{G,max}$: Maximum real power output, in [MW]

$P_{G,min}$: Minimum real power output, in [MW]

Bus	P_G	Q_G	$Q_{G,max}$	$Q_{G,min}$	V	$P_{G,max}$	$P_{G,min}$
10	450	-51.04	200	-147	1.05	550	0
12	85	91.27	120	-35	0.99	185	0
25	220	49.72	140	-47	1.05	320	0
26	314	9.89	1000	-1000	1.015	414	0
31	7	31.57	300	-300	0.967	107	0
46	19	-5.25	100	-100	1.005	119	0
49	204	115.63	210	-85	1.025	304	0
54	48	3.9	300	-300	0.955	148	0
59	155	76.83	180	-60	0.985	255	0
61	160	-40.39	300	-100	0.995	260	0
65	391	80.76	200	-67	1.005	491	0
66	392	-1.95	200	-67	1.05	492	0
69	513.48	-82.39	300	-300	1.035	805.2	0
80	477	104.9	280	-165	1.04	577	0
87	4	11.02	1000	-100	1.015	104	0
92	607	0.49	9	-3	0.99	100	0
100	252	108.87	155	-50	1.017	352	0
103	40	41.69	40	-15	1.01	140	0
111	36	-1.84	1000	-100	0.98	136	0

Table A2: Generator data for the IEEE 118-bus network

A3. Branch Data

Branch data for the IEEE 118-bus test network are shown in Table A3. The variables and units used in the column headings of Table A3 are:

From: Identifies the bus number of one end of the branch

To: Identifies the bus number of the other end of the branch

R: Resistance, in per-unit for a base voltage of 100 kV

X: Reactance, in per-unit for a base voltage of 100 kV

B: Line charging susceptance, in per-unit for a base voltage of 100 kV

RateA: Long-term or stability limit of the line, in [MVA]

RateB: Short-term limit of the line, in [MVA]

RateC: Emergency limit of the line, in [MVA]

Users of this data should note that the susceptances used in the DC power flows in this thesis were calculated directly from the line reactances *X*, according to the formula:

$$(A1) \quad B_{ij} = \begin{cases} -\dfrac{1}{X_{ij}} & i \neq j \\ \displaystyle\sum_{i=0, i \neq j} \dfrac{1}{X_{ij}} & i = j \\ 0 & X_{ij} = 0. \end{cases}$$

From	To	R	X	B	RateA	RateB	RateC
1	2	0.0303	0.0999	0.0254	220	230	250
1	3	0.0129	0.0424	0.01082	220	230	250
2	12	0.0187	0.0616	0.01572	220	230	250
3	5	0.0241	0.108	0.0284	220	230	250
3	12	0.0484	0.16	0.0406	220	230	250
4	5	0.00176	0.00798	0.0021	440	460	500
4	11	0.0209	0.0688	0.01748	220	230	250
5	6	0.0119	0.054	0.01426	220	230	250
5	11	0.0203	0.0682	0.01738	220	230	250
6	7	0.00459	0.0208	0.0055	220	230	250
7	12	0.00862	0.034	0.00874	220	230	250
8	9	0.00244	0.0305	1.162	1100	1150	1250
8	5	0	0.0267	0	880	920	1000
8	30	0.00431	0.0504	0.514	220	230	250
9	10	0.00258	0.0322	1.23	1100	1150	1250
11	12	0.00595	0.0196	0.00502	220	230	250
11	13	0.02225	0.0731	0.01876	220	230	250
12	15	0.0215	0.0707	0.01816	220	230	250
12	17	0.0212	0.0834	0.0214	220	230	250
12	117	0.0329	0.14	0.0358	220	230	250
13	15	0.0744	0.2444	0.06268	220	230	250
14	15	0.0595	0.195	0.0502	220	230	250
15	17	0.0132	0.0437	0.0444	440	460	500
15	19	0.012	0.0394	0.0101	220	230	250
15	33	0.038	0.1244	0.03194	220	230	250
16	17	0.0454	0.1801	0.0466	220	230	250
17	19	0.0123	0.0505	0.01298	220	230	250
17	31	0.0474	0.1563	0.0399	220	230	250
17	113	0.00913	0.0301	0.00768	220	230	250
18	19	0.01119	0.0493	0.01142	220	230	250
19	20	0.0252	0.117	0.0298	220	230	250
19	34	0.0752	0.247	0.0632	220	230	250
20	21	0.0183	0.0849	0.0216	220	230	250
21	22	0.0209	0.097	0.0246	220	230	250
22	23	0.0342	0.159	0.0404	220	230	250
23	24	0.0135	0.0492	0.0498	220	230	250
23	25	0.0156	0.08	0.0864	440	460	500
23	32	0.0317	0.1153	0.1173	220	230	250
24	70	0.00221	0.4115	0.10198	220	230	250

Table A3: Branch data for the IEEE 118-bus network

From	To	R	X	B	RateA	RateB	RateC
24	72	0.0488	0.196	0.0488	220	230	250
25	27	0.0318	0.163	0.1764	440	460	500
26	25	0	0.0382	0	220	230	250
26	30	0.00799	0.086	0.908	660	690	750
27	28	0.01913	0.0855	0.0216	220	230	250
27	32	0.0229	0.0755	0.01926	220	230	250
27	115	0.0164	0.0741	0.01972	220	230	250
28	31	0.0237	0.0943	0.0238	220	230	250
29	31	0.0108	0.0331	0.0083	220	230	250
30	17	0	0.0388	0	660	690	750
30	38	0.00464	0.054	0.422	220	230	250
31	32	0.0298	0.0985	0.0251	220	230	250
32	113	0.0615	0.203	0.0518	220	230	250
32	114	0.0135	0.0612	0.01628	220	230	250
33	37	0.0415	0.142	0.0366	220	230	250
34	36	0.00871	0.0268	0.00568	220	230	250
34	37	0.00256	0.0094	0.00984	440	460	500
34	43	0.0413	0.1681	0.04226	220	230	250
35	36	0.00224	0.0102	0.00268	220	230	250
35	37	0.011	0.0497	0.01318	220	230	250
37	39	0.0321	0.106	0.027	220	230	250
37	40	0.0593	0.168	0.042	220	230	250
38	37	0	0.0375	0	660	690	750
38	65	0.00901	0.0986	1.046	440	460	500
39	40	0.0184	0.0605	0.01552	220	230	250
40	41	0.0145	0.0487	0.01222	220	230	250
40	42	0.0555	0.183	0.0466	220	230	250
41	42	0.041	0.135	0.0344	220	230	250
42	49	0.0715	0.323	0.086	220	230	250
42	49	0.0715	0.323	0.086	220	230	250
43	44	0.0608	0.2454	0.06068	220	230	250
44	45	0.0224	0.0901	0.0224	220	230	250
45	46	0.04	0.1356	0.0332	220	230	250
45	49	0.0684	0.186	0.0444	220	230	250
46	47	0.038	0.127	0.0316	220	230	250
46	48	0.0601	0.189	0.0472	220	230	250
47	49	0.0191	0.0625	0.01604	220	230	250
47	69	0.0844	0.2778	0.07092	220	230	250
48	49	0.0179	0.0505	0.01258	220	230	250

Table A3 (continued)

From	To	R	X	B	RateA	RateB	RateC
49	50	0.0267	0.0752	0.01874	220	230	250
49	51	0.0486	0.137	0.0342	220	230	250
49	54	0.073	0.289	0.0738	220	230	250
49	54	0.0869	0.291	0.073	220	230	250
49	66	0.018	0.0919	0.0248	440	460	500
49	66	0.018	0.0919	0.0248	440	460	500
49	69	0.0985	0.324	0.0828	220	230	250
50	57	0.0474	0.134	0.0332	220	230	250
51	52	0.0203	0.0588	0.01396	220	230	250
51	58	0.0255	0.0719	0.01788	220	230	250
52	53	0.0405	0.1635	0.04058	220	230	250
53	54	0.0263	0.122	0.031	220	230	250
54	55	0.0169	0.0707	0.0202	220	230	250
54	56	0.00275	0.00955	0.00732	220	230	250
54	59	0.0503	0.2293	0.0598	220	230	250
55	56	0.00488	0.0151	0.00374	220	230	250
55	59	0.04739	0.2158	0.05646	220	230	250
56	57	0.0343	0.0966	0.0242	220	230	250
56	58	0.0343	0.0966	0.0242	220	230	250
56	59	0.0825	0.251	0.0569	220	230	250
56	59	0.0803	0.239	0.0536	220	230	250
59	60	0.0317	0.145	0.0376	220	230	250
59	61	0.0328	0.15	0.0388	220	230	250
60	61	0.00264	0.0135	0.01456	440	460	500
60	62	0.0123	0.0561	0.01468	220	230	250
61	62	0.00824	0.0376	0.0098	220	230	250
62	66	0.0482	0.218	0.0578	220	230	250
62	67	0.0258	0.117	0.031	220	230	250
63	59	0	0.0386	0	440	460	500
63	64	0.00172	0.02	0.216	440	460	500
64	61	0	0.0268	0	220	230	250
64	65	0.00269	0.0302	0.38	440	460	500
65	66	0	0.037	0	220	230	250
65	68	0.00138	0.016	0.638	220	230	250
66	67	0.0224	0.1015	0.02682	220	230	250
68	69	0	0.037	0	440	460	500
68	81	0.00175	0.0202	0.808	220	230	250
68	116	0.00034	0.00405	0.164	440	460	500
69	70	0.03	0.127	0.122	440	460	500

Table A3 (continued)

From	To	R	X	B	RateA	RateB	RateC
69	75	0.0405	0.122	0.124	440	460	500
69	77	0.0309	0.101	0.1038	220	230	250
70	71	0.00882	0.0355	0.00878	220	230	250
70	74	0.0401	0.1323	0.03368	220	230	250
70	75	0.0428	0.141	0.036	220	230	250
71	72	0.0446	0.18	0.04444	220	230	250
71	73	0.00866	0.0454	0.01178	220	230	250
74	75	0.0123	0.0406	0.01034	220	230	250
75	77	0.0601	0.1999	0.04978	220	230	250
75	118	0.0145	0.0481	0.01198	220	230	250
76	77	0.0444	0.148	0.0368	220	230	250
76	118	0.0164	0.0544	0.01356	220	230	250
77	78	0.00376	0.0124	0.01264	220	230	250
77	80	0.017	0.0485	0.0472	440	460	500
77	80	0.0294	0.105	0.0228	220	230	250
77	82	0.0298	0.0853	0.08174	220	230	250
78	79	0.00546	0.0244	0.00648	220	230	250
79	80	0.0156	0.0704	0.0187	220	230	250
80	96	0.0356	0.182	0.0494	220	230	250
80	97	0.0183	0.0934	0.0254	220	230	250
80	98	0.0238	0.108	0.0286	220	230	250
80	99	0.0454	0.206	0.0546	220	230	250
81	80	0	0.037	0	220	230	250
82	83	0.0112	0.03665	0.03796	220	230	250
82	96	0.0162	0.053	0.0544	220	230	250
83	84	0.0625	0.132	0.0258	220	230	250
83	85	0.043	0.148	0.0348	220	230	250
84	85	0.0302	0.0641	0.01234	220	230	250
85	86	0.035	0.123	0.0276	220	230	250
85	88	0.02	0.102	0.0276	220	230	250
85	89	0.0239	0.173	0.047	220	230	250
86	87	0.02828	0.2074	0.0445	220	230	250
88	89	0.0139	0.0712	0.01934	440	460	500
89	90	0.0518	0.032	0.032	660	230	250
89	91	0.0099	0.032	0.065	220	220	220
89	92	0.0099	0.0505	0.065	220	690	750
90	91	0.0254	0.0505	0.065	660	230	250
91	92	0.0387	0.1272	0.032	220	230	250
92	93	0.0258	0.032	0.0218	220	230	250

Table A3 (continued)

From	To	R	X	B	RateA	RateB	RateC
92	94	0.0481	0.158	0.0406	220	230	250
92	100	0.0648	0.295	0.0472	220	230	250
92	102	0.0123	0.0559	0.01464	220	230	250
93	94	0.0223	0.0732	0.01876	220	230	250
94	95	0.0132	0.0434	0.0111	220	230	250
94	96	0.0269	0.0869	0.023	220	230	250
94	100	0.0178	0.058	0.0604	220	230	250
95	96	0.0171	0.0547	0.01474	220	230	250
96	97	0.0173	0.0885	0.024	220	230	250
98	100	0.0397	0.179	0.0476	220	230	250
99	100	0.018	0.0813	0.0216	220	230	250
100	101	0.0277	0.1262	0.0328	220	230	250
100	103	0.016	0.0525	0.0536	440	460	500
100	104	0.0451	0.204	0.0541	220	230	250
100	106	0.0605	0.229	0.062	220	230	250
101	102	0.0246	0.112	0.0294	220	230	250
103	104	0.0466	0.1584	0.0407	220	230	250
103	105	0.0535	0.1625	0.0408	220	230	250
103	110	0.03906	0.1813	0.0461	220	230	250
104	105	0.00994	0.0378	0.00986	220	230	250
105	106	0.014	0.0547	0.01434	220	230	250
105	107	0.053	0.183	0.0472	220	230	250
105	108	0.0261	0.0703	0.01844	220	230	250
106	107	0.053	0.183	0.0472	220	230	250
108	109	0.0105	0.0288	0.0076	220	230	250
109	110	0.0278	0.0762	0.0202	220	230	250
110	111	0.022	0.0755	0.02	220	230	250
110	112	0.0247	0.064	0.062	220	230	250
114	115	0.0023	0.0104	0.00276	220	230	250

Table A3 (continued)

A4. Generator Marginal Cost Data

Generator marginal costs for the IEEE 118-bus test network are shown in Table A4. The linearized DC power flow used in Chapter 6 of this thesis assumes a constant marginal cost of generation. For simplicity, I assumed that there was no intercept term to the cost curve.

Generator bus	Marginal Cost ($/MWh)
10	0.217
12	1.052
25	0.434
26	0.308
31	5.882
46	3.448
49	0.467
54	1.724
59	0.606
61	0.588
65	0.2493
66	0.2487
69	0.1897
80	0.205
87	7.142
92	10
100	0.381
103	2
111	2.173

Table A4: Generator marginal costs in the IEEE 118-bus network

Appendix B: Matlab Code for the Wheatstone Network Search Algorithm

This appendix contains Matlab code to execute the Wheatstone search algorithm described in Chapter 5. The code has only been tested on Matlab version 7 for Windows; there are no guarantees that it will work on previous or even future versions of Matlab.

The code takes advantage of built-in functions of Matpower and Matgraph. Matpower is a set of m-files for power system simulation and analysis, available free of charge at http://www.pserc.cornell.edu/matpower/. Matgraph is a freely-available toolbox for working with undirected graphs; it can be downloaded from http://www.ams.jhu.edu/~ers/matgraph. Full functionality of both Matpower and Matgraph also requires Matlab's Optimization Toolbox.

```
%Wheatstone search algorithm -- Seth Blumsack, April 2006
%Make sure that you have Matpower and Matgraph directories added to
%your matlab path.  This algorithm will find embedded Wheatstones on a
%series-parallel reduced network

graph_init

%Step 1: Define the graph
%Load the branch data from a Matpower-formatted file

CaseData=fnUpdateCaseData('case13_red'); %Be sure to specify the case
here
elist=CaseData.branch(:,1:2);
g=graph;
add(g,elist);

%Step 2: Calculate the incidence matrices and matrix of geodesic paths
N=double(matrix(g));
N2=N^2;
N3=N^3;
triangles=0.5*diag(N3);
```

```
geodesic=dist(g);

%Step 3: Define T as the set of nodes that are part of at least one
%triangle
T=find(triangles);

%Step 4: Define D as the set of nodes that have degree greater than one
degree=deg(g)';
D=find(degree > 1)';

%Step 5: Define R2 as the set of all pairs of nodes that have geodesic
path
%length equal to two with path cardinality equal to two.

[u1,v1]=find(tril(geodesic)==2);
R1=[u1 v1];

[u2,v2]=find(tril(N2)==2);
R1_2=[u2 v2];

R2=intersect(R1,R1_2,'rows');

%Step 6: Define R3 as the set of all pairs of nodes connected by at
least
%two paths of length three

[u3,v3]=find(tril(N3)>=2);
R3=[u3 v3];

%Step 7: Define WS = R2 <intersect> R3 as the set of candidate
Wheatstone
%endpoints

WS = intersect(R2,R3,'rows');

%Step 8: For each pair of nodes in WS, find the set of neighbors shared
by
%each node in the pair

WS_neighbor=zeros(size(WS,1),2);

for i=1:size(WS,1)

WS_neighbor(i,:)=intersect(neighbors(g,WS(i,1)),neighbors(g,WS(i,2)));
end

WS_candidate=[WS WS_neighbor]; %Constructs the candidate four-node
Wheatstone networks

%Step 9: Calculate the clustering coefficient for all candidate
Wheatstone
%networks in WS_candidate

WS_cluster=zeros(size(WS_candidate,1),1);
WS_N=zeros(4);
c_avg=0;
N_k_morethanone=0;
```

```
for i=1:length(WS_cluster)
        for j=1:4
            for k=1:4
           WS_N(j,k)=N(WS_candidate(i,j),WS_candidate(i,k));
            end
        end

WS_N3=(WS_N)^3;
WS_triangles=0.5*diag(WS_N3);
m=sum(WS_N,2);

for j=1:4
    if m(j)>1
        c_avg=c_avg+2*WS_triangles(j)/(m(j)*(m(j)-1));
        N_k_morethanone=N_k_morethanone+1;
    end
end

c_avg=c_avg/N_k_morethanone;
WS_cluster(i)=c_avg;


end

%Step 10: The entries in WS_cluster equal to 5/6 represent Wheatstone
%sub-networks.

%First, we need to define the clustering coefficient for the Wheatstone

%Define the Wheatstone node-node adjacency matrix

WS_key_N = [0 1 1 0; 1 0 1 1; 1 1 0 1; 0 1 1 0];

%Calculate the clustering metric
WS_key_c_avg=0;
WS_key_N_k_morethanone=0;

WS_key_N3=(WS_key_N)^3;
WS_key_triangles=0.5*diag(WS_key_N3);
m=sum(WS_key_N,2);

for j=1:4
    if m(j)>1
        c_avg=c_avg+2*WS_key_triangles(j)/(m(j)*(m(j)-1));
        WS_key_N_k_morethanone=WS_key_N_k_morethanone+1;
    end
end

WS_key_c=WS_key_c_avg/WS_key_N_k_morethanone;


% Compare the candidate Wheatstone clustering metrics to the key
WS_candidate_cluster=[WS_cluster WS_candidate];

WS_find=find(WS_candidate_cluster(:,1) == WS_key_c);
```